



Rijkswaterstaat

Measured wind-wave climatology Lake IJssel (NL)

Main results for the period 1997-2006

Report RWS RIZA 2007.020





Rijkswaterstaat

Measured wind-wave climatology Lake IJssel (NL)

Main results for the period 1997-2006

Report RWS RIZA 2007.020

ERRATA

for:

**Measured wind-wave climatology Lake IJssel (NL); Main results for the period 1997-2006
Report 2007.020; Rijkswaterstaat RIZA; Lelystad (NL)
ISBN 978-90-369-1399-7**

- Equation (6.7a) and (6.7b) on page 148 both contain a printing error. The right hand side of the equations should start with $\beta_1 g^2$ and $\beta_2 g^2$ respectively, so that the full equations read:

$$(6.7a) \quad F_1(f) = \beta_1 g^2 (2\pi)^{-4} f_p^{-1} f^{-4} \left[\exp\left(\left(\frac{f}{f_p}\right)^{-4}\right) \right] \gamma \exp\left[\frac{-(f-f_p)^2}{2\sigma^2 f_p^2}\right]$$

$$(6.7b) \quad F_2(f) = \beta_2 g^2 (2\pi)^{-4} f_p^{3.35} f^{-8.35} \exp\left[\frac{-8.35}{4} \left(\frac{f}{f_p}\right)^{-4}\right]$$

- On the data DVD, the XTB-files for the location FL37 in the directory METINGEN_data\Xtabel need some revision. The files to be modified have names of the types:
 - 2506????cap.xtb.
 - 2506????LAL.xtb
 - 2507????cap.xtb
 - 2507????LAL.xtb

For all these files, the following should be modified:

- on the first line, the location name FL25 should be replaced by FL37
- in the 3rd and 4th column of the file, coordinates are given that belong to the FL25-location. They should be replaced by the coordinates of the FL37-location: x=155500, y=520000
- in the 8th column, the water depths should be increased by 0.49 m (the difference between the FL25 and FL37 lake bed position)

File names of the first months of 2006 contain no 'cap' or 'LAL' indication and should not be modified as they correspond to the FL25-location.

- Also on the data-DVD, the MATLAB-script *getpaalistr.m* contains a typing mismatch in the lake bed position of SL29: The statement 'NAPdepth = -2.22;' should read ': 'NAPdepth = -2.12;'
- As a result of the latter error, there is also an error in part of the SL29 XTB-files on the data-DVD: The files containing data from 2003 and more recent years (starting as '2903...', '2904...', '2905...', '2906...' or '2907...') contain an error in their 8th column: all water depths in this column are 0.1 m to high. All other variables, including the water level of the 7th column, are correct in these files.

Dr. M. Bottema, Rijkswaterstaat Centre for Water Management, May 2008

Colophon

Published by: Rijkswaterstaat RIZA; will merge into Rijkswaterstaat Water Management Department ('RWS Waterdienst') by 1/10/2007

Information: Phone: +31-320-298898/298411
Fax: +31-320-249218

Author: dr. M. Bottema

Date: 4 July 2007

Status: Report RWS RIZA 2007.020
ISBN 978-90-369-1399-7

Printed by: Drukkerij Artoos, Rijswijk

Contents

I.	Preface	5
II.	Summary	7
III.	Nederlandse samenvatting	9
IV.	Definitions, abbreviations and symbols	13
V.	List of Figures	19
VI.	List of Tables	27
1.	Introduction	29
1.1	General introduction	29
1.2	Relevance of the Lake IJssel wave measurements	29
1.3	Aims of this project and report	32
1.4	Project organisation	33
1.5	Relations with other projects	34
1.6	Brief overview of this report	35
2.	About the measurements and the data	37
2.1	Measuring locations	37
2.2	Instrumentation and maintenance	43
2.3	Acquisition and processing of data	50
2.4	Validation of measured data	57
3.	Availability and range of experimental data	65
3.1	Availability of experimental data	65
3.2	Range of experimental data	68
3.3	Measurements versus Hydraulic Boundary Conditions	71
4.	Wind and temperatures	73
4.1	Relevance of wind	73
4.2	Approximate overall climatology of wind	74
4.3	Climatology of extreme wind speeds	78
4.4	Spatial transformation of wind	81
4.4.1.	Model approaches for spatial wind transformation	82
4.4.2.	Wind speed ratios on open water	84
4.4.3.	Wind speed ratios – land and water stations	87
4.5	Turbulence and roughness data	93
4.6	Air and water temperatures	101
5.	Water levels, storm surge, seiches	107
5.1	Mean lake levels	107

5.2	Storm surge in stationary conditions	108
5.3	Time-dependent water level fluctuations	111
6.	Wave properties and wave climate	117
6.1	Overall wave height climatology	117
6.2	Wind-related wave height climatology	120
6.3	Wave periods	125
6.4	Wave steepnesses	129
6.5	Scaling of wave properties with the wind	132
6.6	Depth-limited waves	138
6.6.1.	Depth-limited wave growth	138
6.6.2.	Shoaling wave situations	141
6.7	Other wave-related issues	143
6.7.1.	Validity of effective fetch concept	143
6.7.2.	Wave spectra	148
6.7.3.	Wave height and wave period distributions	150
7.	Wave model calibration and test cases	157
7.1	Stationary calibration cases Lake Sloten	157
7.2	Stationary test cases Lake IJssel	160
7.3	Time-dependent test cases	172
8.	Wave run-up against dikes	177
8.1	Available data	177
8.2	Conceptual model framework	178
8.3	A few words about wave run up model applications	179
8.4	Effect of berms and oblique wave attack	180
9.	Conclusions and recommendations	183
9.1	Conclusions	183
9.2	Recommendations	196
	References	201
Appendix A	Alternatives for present instrumentation	211
Appendix B	Wave measuring errors	217
Appendix C	Intercomparison of wave instruments	237
Appendix D	Applied offsets and corrections	253
Appendix E	Alternatives for present instrumentation	263
Appendix F	Beaufort scale	271
Appendix G	Climate tables for information requests	273

I. Preface

In the last decade, Rijkswaterstaat IJsselmeergebied (who commissioned this work) and Rijkswaterstaat RIZA have put many joint efforts into obtaining a reliable data set of measured wind and wave data for Lake IJssel. At present, a number of changes is about to take place in both the present measuring campaign and the organisation of Rijkswaterstaat. As this process may involve some personnel changes as well, it was considered to be strongly desirable to document all results obtained so far within short notice. The present report is the main result of this documentary action.

Several people have contributed to this project, and thereby to this report. There are too many to specify them all, but the following people of Rijkswaterstaat IJsselmeergebied are to be mentioned in particular, not least of all because of their enthusiasm and their contributions (Photo 1-2 and 4-11; Figure 2.1) to this report:

- Ed van der Goes (until 2007), Hans Miedema and Harrie Oude Voshaar for data deliveries, and documentation.
- Remco Kleine and Arjan Ponger for instrumentation
- Charlotte Franken, Yasmine Panhuijsen and Nico Wijnstok (successive project leaders of operational part)
- Eric Regeling (overall project leader)

At Rijkswaterstaat RIZA, Dénes Beyer deserves special mention for his early contributions (1996-2000) to this project; he paved much of the way that allowed for doing the present work. Hans de Waal, Ellen Claessens, Yede Bruinsma and Herbert Berger are also mentioned for their advice and contributions.

II. Summary

In the period 1997-2007, an extensive wind and wave measuring campaign has been carried out on Lake IJssel and Lake Sloten in The Netherlands. The aim of this campaign was to gather and analyse well-documented wind and wave measurements of high quality, for a range of fetch, depth and (strong) wind conditions. The data should serve a number of purposes, and dike design in particular.

The campaign has resulted in a good indication of wind and wave climatology of both lakes, while enhancing the knowledge on various aspects of wind and waves. However, the gap between measured conditions (up to 9 Beaufort inclusive) and dike design conditions (with 12 Beaufort winds) has only slightly decreased due to an exceptionally long storm-free period from 1990 to at least mid 2007. Hence, it is recommended to continue (part of) the present measurements until at least one event with 10 Beaufort winds is suitably measured.

In the following, a brief overview of the contents of this report is given.

Chapters 1 and 2 give some introductory details like relevance and aim of the present project, the measuring locations, instrumentation, data processing and data validation. Detailed overviews of experimental techniques and measuring errors are given in Appendix A-B. Appendix C shows that step gauge, capa probe and log-a-level instruments all (can) agree excellently, but that the latter is sensitive to wind from 6 Beaufort (12 m/s) winds on.

In Chapter 3, the availability and range of the data is discussed. In the last 5 years, data availability during gales was excellent (Table 3.1). Some gales yielded wave periods that nearly equalled the (12 Beaufort) dike design values. However, water levels, wave heights and wave-run-up levels all remained well below the design values (section 3.3).

Chapter 4 is about wind and temperatures. A key result is the fact that during gales, wind speed differences between land and water largely disappear; a feature that can not yet be explained by any of the existing models and theories (section 4.4; Appendix E).

Chapter 5 is about water levels and its wind-induced set-up (storm surge). Rapid wind changes may also cause overshoots and oscillations up to a metre, larger than the stationary storm surge (section 5.3).

Chapter 6 discusses wave climatology and several features relevant to wave modelling. Key uncertainties in the latter are related to the way waves scale with the wind and to depth limited wave growth (section 6.5-6.6). Without these shallow water effects, design wave heights at Lake IJssel would have been order 60% higher.

Chapter 7 presents a number of test and calibration cases for wave models; time-dependent cases show that waves can grow very rapidly.

Chapter 8 discusses the present data of wave run-up against dikes. The main result is that run-up reduction by berms, dike roughness etc. (typically 50-75%) is wave height dependent. Finally, conclusions and recommendations are given in Chapter 9.

III. Nederlandse samenvatting

Managementsamenvatting

In het IJsselmeer en Slotermeer vindt sinds 1997 een uitgebreide golfmeetcampagne plaats waarbij Rijkswaterstaat IJsselmeergebied (RWS IJG) opdrachtgever en uitvoerder is, en Rijkswaterstaat RIZA (RWS RIZA) zorg draagt voor kwaliteitsborging, analyse en rapportage. Doel van de meetcampagne is het verkrijgen van goed gedocumenteerde wind- en golfmetingen voor een breed bereik aan strijklengte- en (harde) windcondities. Hoogwaterbescherming is daarbij het primaire toepassingsgebied; neventoepassingen zijn beschreven in par. 1.2.

In veel opzichten is het meetdoel nu gehaald: Er is nu inderdaad een set goed gedocumenteerde golf- en windmetingen voor een breed bereik aan windcondities (0-24 m/s; tot en met 9 Beaufort) en strijklengtecondities (1-30 km). Met name de in par. 6.1-6.3 beschreven golfklimatologie wordt door RWS IJG zeer bruikbaar bevonden. Ook bieden de huidige gegevens het nodige validatiemateriaal voor golfmodellen (Hoofdstuk 7), maar ook voor windmodellen, waterbewegingsmodellen en golfoploopmodellen (resp. Hoofdstuk 4, 5, 8). Een aandachtspunt is nog wel dat de metingen nog niet breed beschikbaar zijn gemaakt; het huidige rapport is hiertoe een eerste stap.

In één opzicht is het meetdoel *niet* gehaald: door een uitzonderlijk lange periode zonder zware stormen in het IJsselmeergebied (van maart 1990 tot heden) is het niet gelukt metingen te verkrijgen onder zware-storm-condities. Het gat tussen de zwaarst gemeten condities en de ontwerpcondities voor dijken is hierdoor maar weinig verkleind. Mede daardoor bestaat er nog altijd een meetbehoefte (zie par. 9.2), met als kernelementen het vaststellen:

- ..waarom het bij storm boven water vaak niet of amper harder waait dan op meer beschutte landstations, terwijl gangbare theoriën en modellen (par. 4.4 en Bijlage E) op orde 30% land-water-windsnelheidsverschil uitkomen;
- ..of golfcondities schalen met de *windsnelheid* of met de *windwrijvingskracht*. In termen van ontwerp golfhoogte kunnen beide benaderingen 50% verschillen (par. 6.5);
- ..wat de hoogte van de golfgroeilimiet op ondiep water is. Zonder die ondiepwatereffecten zou bij dijkontwerp met orde 60% hogere golven moeten worden gerekend, maar modellen lijken die effecten vaak te overschatten (par. 6.6.1).

Verder wordt aanbevolen via heranalyse van bestaande golfoploopdata te onderzoeken of gangbare formules de golfoploop op dijken in milde condities (langs rivieren?) overschatten. Bermen, taludruwheid en

schuine golfinval zorgen bij IJsselmeerdijken namelijk voor orde 50-75% golfploopreductie. Die reductie blijkt in milde condities sterker te zijn dan bij storm, terwijl modellen hier géén rekening mee houden.

Aanvullende details bij de managementsamenvatting

Hieronder worden enkele sleutelementen van elk hoofdstuk genoemd. Voor lezers-op-hoofdpijnen zijn Hoofdstuk 1-3 daarbij het meest interessant, samen met de conclusies en aanbevelingen in Hoofdstuk 9. In alle gevallen betreft het overigens uitsluitend conclusies op basis van de metingen; de validatie van specifieke modellen komt in dit rapport niet aan de orde om de scheiding tussen data(validatie) en modelvalidatie zuiver te houden.

Hoofdstuk 1 beschrijft het belang van de huidige metingen in relatie tot hoogwaterbescherming en andere informatiebehoeften zoals ecologie, scheepvaart, monitoringverplichtingen en niet in de laatste plaats informatieverstrekking aan derden. Ook wordt het hierboven al aangehaalde meetdoel beschreven, alsmede het doel van dit rapport: Het vastleggen van wind- en golfcondities in het IJsselgebied voor de kennis-, uitvoerings- en beleidwereld. De focus is daarbij niet alleen op gemiddelden maar ook op extremen en zaken die relevant zijn voor de validatie van wind-, waterbewegings- en golfmodellen.

Hoofdstuk 2 geeft een overzicht van de meetlocaties, de instrumentatie en de verwerking en validatie van meetgegevens. Bij het laatste moet worden opgemerkt dat de detectie maar vooral ook de *interpretatie* van verdachte trends in de metingen cruciaal is. Paragraaf 2.4 geeft hiertoe de nodige handvatten. Informatie over golfinstrumentatie is ook te vinden in de RWS Leidraad Monitoring (zie ook Bijlage A). In dit project zijn capstaven, stappenbaken en (akoestische) log-a-levels gebruikt. Veel voorkomende meetfouten worden uitgebreid besproken in Bijlage B. Uit een instrumentvergelijking (Bijlage C) blijkt ook dat stappenbaken en capstaven vooral gevoelig zijn voor algenaangroei en ijsschade, log-a-levels voor verwaaiing van de geluidbundel. Andere instrumenten missen vaak weer de hoogfrequente respons die nodig is om de korte IJsselmeergolven te bemeten.

Hoofdstuk 3 geeft een overzicht van de beschikbare metingen en de oorzaken van uitval. In de beginjaren was er veel uitval, maar sinds 2001 is meestal 75-90% van de data beschikbaar, ook tijdens storm. De hoogst gemeten (losse) golf mat 3.1 m van top tot dal. De hoogste waterstanden, significante golfhoogtes (H_{m0}) en golfploopniveaus waren resp. +0.8 m NAP, 1.4-1.8 m en +2.40 m NAP, alle ruim onder de waarden voor dijktoetsing (Tabel 3.2). De gemeten golfperiodes lagen echter vlak bij de toetswaarden, ook al zijn de metingen representatief voor gewone stormen en de toetswaarden voor *orkanen*.

Wind (Hoofdstuk 4) is cruciaal bij golfmodellering én dijktoetsing. Een indicatieve windklimatologie is gegeven in par. 4.2-4.3. De klimatologie kenmerkt zich door vrij kleine dag-nacht-verschillen, gemiddeldes rond 8 m/s, jaarextremen rond 18-24 m/s en pas vanaf windkracht 6 een duidelijke voorkeur voor zuidwestenwind. Voor betrouwbare extremenstatistieken blijkt vrijwel altijd een langjarige KNMI-windmeetreeks nodig, plus een vertaalslag van landstations naar open water. Zie par. 4.4 en Bijlage E. Bij storm blijken de land-water-windsnelheidsverschillen nihil te zijn terwijl gangbare theoriën en modellen op orde 30% verschil uitkomen. De reden van deze discrepantie tussen theorie en praktijk is vooralsnog onduidelijk. Buiten stormen hebben lucht-water-temperatuurverschillen vaak een significante invloed op het windveld, waarbij de lucht vaak kouder blijkt dan het water (par. 4.6). De aërodynamische ruwheid van wateroppervlakken is een sleutelparameter bij de modellering van wind, opwaaiing en golven (par. 4.7). Op basis van de huidige meetaanpak zijn over die ruwheid nog geen harde uitspraken te doen, al lijkt in milde condities (minder dan 8 Beaufort) de veel gebruikte parametrisatie van Wu (1982) het goed te doen.

Hoofdstuk 5 gaat in op gemiddelde meerpeilen, opwaaiing, en waterstandschommelingen. De opwaaiing in stationaire condities (par. 5.2) is goed voorspelbaar: deze neemt ruwweg kwadratisch toe met de windsnelheid en kan bij 18 m/s wind (8 Beaufort) langs de oevers van het IJsselmeer oplopen tot ongeveer een halve meter. Op tijdschalen van ca. ½ tot 3 uur is echter vaak sprake van een versterkte, resonante respons (par. 5.3). Hierdoor kunnen bij snelle windveranderingen oscillaties en 'doorschieters' tot een *meter* voorkomen, waarbij deze effecten soms domineren over de reguliere, stationaire opwaaiing.

Hoofdstuk 6 presenteert eerst een golfhoogte- en golfperiode-klimatologie (par. 6.1-6.3); één van de sleutelresultaten van deze meetcampagne. Twee resultaten springen er hier uit:

- wiskundige extrapolatie van golfklimatologie naar zeldzame extremen leidt makkelijk tot fysisch niet-plausibele resultaten
 - jonge golven (vlak uit de kust) blijken moeilijk voorspelbaar door een grote natuurlijke variabiliteit, vooral op ondiep water
- Golfsteilheden komen aan bod in par. 6.4. Geavanceerde golfmodellen vallen voor hun ijking vaak terug op semi-empirische golfgroeiparametrisaties. Vaak wordt daarbij onvoldoende aandacht gegeven aan twee zwakke punten in die parametrisaties: strijklengteaannames (par. 6.7.1) en vooral ook aannames over de *scaling* van golven met wind (par. 6.5). Ook dieptegelimiteerde golven (par. 6.6) zijn een aandachtspunt voor dijkontwerp in het IJsselmeergebied én de bijbehorende modellen. Bij gangbare golfmodellen komt de significante golfhoogte zonder extra afregeling namelijk niet hoger dan 38% van de waterdiepte, terwijl nu al waarden van 41-45% gemeten zijn, met een kans op nóg hogere

waarden bij écht zware storm. Tot slot wordt in par. 6.7 ingegaan op golfspectra, golfhoogte- en golfperiodeverdelingen.

Hoofdstuk 7 belicht nóg een sleutelresultaat van dit project: een set van 9 calibratie- en 12 testcases voor golfmodellen, met een windsnelheidsbereik van 10-24 m/s en een strijklengtebereik van 0.8 – 25 km. Uit tijdsafhankelijke cases (par. 7.3) blijkt verder dat de golven op het IJsselmeer binnen een uur nagenoeg volgroeid kunnen zijn.

Hoofdstuk 8 gaat in op de golfploopmetingen bij de Rotterdamse Hoek. Bermen, taludruwheid en schuine golfinval lijken op de meetlocatie (Rotterdamse Hoek) voor orde 50-75% golfploopreductie te zorgen. Volgens modellen is die reductie onafhankelijk van de golfhoogte; in de praktijk blijkt de reductie sterker in milde condities.

IV. Definitions, abbreviations and symbols

General note

As the group of readers of this report may be quite diverse, it is difficult to make lists of abbreviations, definitions and symbols that are suitable to all. Hence, the option of short lists with key items is chosen, rather than the option of complete but lengthy definition lists including items that are only mentioned once in this report. Descriptions of (wave) instruments are not given here, but in section 2.2 and Appendix A. Beaufort scale definitions (for wind) are given in Appendix F.

Abbreviations and acronyms

<i>ABL</i>	Atmospheric Boundary Layer: air layer that is directly influenced by the earth's surface, with typical depth of 0.1 - 2 km.
<i>ADCP</i>	Acoustic Doppler Current Profiler, see Appendix A.
<i>FFT</i>	Fast Fourier Transform to evaluate wave spectra (wave spectrum: distribution of wave energy over a given range of wave periods, lengths of frequencies).
<i>HBC's</i>	Hydraulic Boundary Conditions: Water levels, and sometimes also waves, used for periodic evaluations to test whether the dikes have sufficient height and strength in relation to their required safety level.
<i>HISWA</i>	Hindcasting Shallow water Waves, wave model that was frequently used until about 2000.
<i>KNMI</i>	Royal Netherlands Meteorological Institute
<i>MSW</i>	Monitoring system water (RWS monitoring network)
<i>NAP</i>	Dutch reference datum (~mean sea level)
<i>RDH</i>	'Rotterdamse Hoek': wave run-up measuring location
<i>RWS</i>	Rijkswaterstaat organisation (NL)
<i>RWS DWW</i>	Road and Hydraulic Engineering Institute; Special advisory institute of Rijkswaterstaat
<i>RWS IJG</i>	Regional RWS directorate of Lake IJssel area
<i>RWS RIKZ</i>	National Institute for Coastal and Marine Management; Special advisory institute of Rijkswaterstaat
<i>RWS RIZA</i>	Institute for Inland Water Management and Waste Water Treatment; Special advisory institute of Rijkswaterstaat
<i>SBW</i>	Strength and Loading of Water defences; large research project on flood protection in which several RWS institutes have a key role.
<i>SWAN</i>	Simulating WAVes Nearshore, advanced wave model

SWL	Still water level: average water level that remains after filtering out fluctuations by short, wind-induced, waves.
WDIJ	RWS Warning service for dikes in Lake IJssel region
WFD	European Water Framework Directive
WHD	Wave height distribution (frequency distribution of individual wave heights)
WOW	“Wet op de Waterkering”: Dutch Flood Defence Act (WOW, 1996)
WPD	Wave period (frequency) distribution

Definitions

General note: A '~' symbol indicates an approximate definition for laymen, rather than the exact definition, which for wave variables is often highly complex.

<i>Backing</i>	Anti-clockwise turning of wind direction
<i>Berm</i>	near-horizontal section that interrupts the dike slope
<i>Bias</i>	systematic deviation
<i>Calibration factor</i>	slope of calibration line (axis intercept is offset)
<i>Data block</i>	Series of samples, typically 20 minutes (for waves)
<i>Dike ring area</i>	Area, generally low-lying, surrounded by a closed chain of dikes and/or other water defences.
<i>Direction</i>	Wind and wave directions are indicated as the direction the wind and waves are coming from.
<i>Effective fetch</i>	Fetch parametrisation to translate complex coastline situation into equivalent situation with straight coast.
<i>Fetch</i>	Distance for which the wind blows over the water to generate waves and/or storm surge. For (small) lakes generally equivalent to the downwind distance from the coastline to the point of interest.
<i>Footprint</i>	Effective averaging area of measuring instrument
<i>Foreshore</i>	(edge of) nearshore shallow-water area
<i>Gale</i>	Wind of 8-9 Beaufort (Appendix F)
<i>Internal boundary layer</i>	Sub-layer within atmospheric boundary layer (the lowest 0.1-1 km under direct influence of the earth's surface) which is influenced by a new surface.
<i>Lake breeze</i>	Thermally driven circulation from cool lake to warmer nearby land, similar to sea breeze.

<i>Lake level</i>	Spatially averaged water level for lake under consideration.
<i>Macro transformation</i>	Spatial wind transformation method (section 4.4) in which the wind fully adapts to a new underlying surface.
<i>Meso transformation</i>	Spatial wind transformation method (section 4.4) with only <i>partial</i> wind adaptation as only the lowest 60 m adapts to a new underlying surface.
<i>Offset</i>	Correction to correct for bias
<i>Outlier</i>	Data point outside expected range of scatter
<i>Sample</i>	Individual measuring value
<i>Seiche</i>	Free and resonant oscillation of still water level, with typical time scales (for Lake IJssel) of 0.5 – 3 hours.
<i>Stability effects</i>	Effect of vertical temperature gradients in atmosphere (stable = warm air on top suppressing turbulence, unstable the opposite) on wind
<i>Stagger</i>	Series with subsequent identical measuring values
<i>Storm</i>	Wind of 10-11 Beaufort (Appendix F)
<i>Storm surge</i>	Wind-induced set-up of the time-averaged water level.
<i>Swell</i>	Waves generated elsewhere, propagating into area of interest.
<i>Validation</i>	(ideally) Integral approach to assure correctness of measured or model results
<i>Veering</i>	Clockwise turning of wind direction
<i>Wave height</i>	~ Vertical distance between wave crest and trough
<i>Wave length</i>	~ Horizontal distance between successive wave crests
<i>Wave period</i>	~ Time between passage of successive wave crests
<i>Wind sea</i>	Locally generated waves
<i>Wave shoaling</i>	~ Shortening and heightening of the waves due to reduction in wave propagation speed when waves enter shallow water

Symbols

- a Scale parameter in Weibull probability function (Eq. 4.1); unit of a equals unit of variable to be fitted.
- c_p Phase propagation speed of waves (m/s)
- d General indication for water depth; note that water depths are given in 'm' and lake bed levels in 'm NAP', i.e. with respect to the NAP datum

dir	Wind direction (from which wind is blowing, in degrees North)
ΔT	Temperature difference ($^{\circ}\text{C}$); generally $T_{\text{air}} - T_{\text{water}}$
Δz	Storm surge (m)
f	General indication for frequency (Hz)
f_{min}	Lower limit of spectral integration range to evaluate the spectral wave height and wave period measures H_{m0} , T_{m-10} , T_{m01} and T_{m02} (unity of $f_{\text{min}} = 1/T_{\text{min}}$: Hz)
f_{max}	As f_{min} but upper integration limit (Hz)
f_p	Peak frequency (in Hz ; $f_p = 1/T_p$)
g	gravitational acceleration (9.81 m/s^2)
GF	Gust factor (U_{max}/U_{10} , ratio of maximum gust and mean wind speed)
γ_i	Reduction factors in wave-run-up calculations (Chapter 8)
$h_{2\%}$	Absolute wave run-up height with respect to the NAP datum that is exceeded by 2% of the incoming waves (m NAP)
$H_{1/3}$	Significant wave height in time domain, average of the one-third fraction with highest waves (m)
$H_{1/10}$	As $H_{1/3}$, for highest one-tenth fraction (m)
$H_{1/50}$	(or $H_{2\%}$) As $H_{1/3}$ but for highest one-fiftieth fraction (m)
H_{m0}	Spectral significant wave height (m), evaluated from zero-th spectral moment, by $H_{m0} = 4\sqrt{m_0}$
H_i	Height of individual wave (m)
H_{max}	Maximum (trough-crest) wave height in a measuring series (m)
H_{RMS}	RMS wave height (m), defined as:
$H_{\text{RMS}} = \sqrt{\frac{\sum_{i=1}^N H_i^2}{N}}$ <p style="text-align: center;">with N the number of measured waves</p>	
k	Shape parameter in Weibull probability function (Eq. 4.1)
Ku	Kurtosis; in signal x : $\text{mean}[x^4] / \sigma_x^4$
κ	Von Kármán constant in logarithmic wind profile (0.4)
L	Wave length (m) or – in Appendix E – Monin-Obukhov length (m) which indicates atmospheric thermal stability conditions.
m_n	n-th spectral moment (m^2s^{-n}), defined as $M_n = \int f^n E(f) df$
R	Ratio of two variables (e.g, wind speeds)

s	General indication for wave steepness ($s=H/L$ with H = typical wave height and L typical wave length).
$s_{T_{m-10}}$	Wave steepness parameter evaluated from H_{m0} and T_{m-10} , using linear dispersion relation.
$s_{T_{m-10,o}}$	As $s_{T_{m-10}}$, but assuming deep water: $s_{T_{m-10,o}} = \frac{2\pi H_{m0}}{g T_{m-10}^2}$
s_{T_p}	As $s_{T_{m-10}}$, but using peak period T_p rather than T_{m-10} .
$s_{T_{p,o}}$	(or $s_{T_{p,o}}$) As $s_{T_{m-10,o}}$, but using peak period T_p rather than T_{m-10} .
$S(f)$	(or S_f) Wave spectrum (m^2/Hz)
Sk	Skewness; in signal x : $\text{mean}[x^3] / \sigma_x^3$
σ	General scatter indicator (one standard deviation)
t	Time (s)
T_{air}	Air temperature ($^{\circ}C$)
$T_{1/3}$	Average of the one-third fraction with longest waves (s)
$T_{H_{1/3}}$	Mean wave period of waves used in evaluation of $H_{1/3}$ (s)
T_i	Period of individual wave (s)
T_{m-10}	Spectral mean wave period ('energy period'), calculated from the spectral moments m_{-1} en m_0 : $T_{m-10} = m_{-1}/m_0$ (s)
T_{m01}	Spectral mean wave period ('mean period'), calculated from the spectral moments m_0 en m_1 : $T_{m01} = m_0/m_1$ (s).
T_{m02}	Spectral mean wave period ('zero-crossing period'), calculated from the spectral moments m_0 en m_2 : $T_{m02} = \sqrt{m_0/m_2}$ (s).
T_p	Peak period (s); wave period with highest energy level in wave spectrum.
$T_u(z)$	Turbulence intensity: $\sigma_u(z)/U(z)$, where σ_u is standard deviation in wind speed samples.
T_{water}	Water temperature ($^{\circ}C$)
u_*	Friction velocity (m/s); scale parameter in logarithmic wind profile which equals $(\tau/\rho)^{0.5}$ with τ the wind drag force per unit area and ρ the air density.
U	General indication for wind speed (m/s)
U_{10}	Measured wind speed (m/s) at 10 m height, generally averaged over (10 or) 60 minutes
U_3	As U_{10} , but measured at 3 m height (m/s)
U_{ow}	As U_{10} , but for specific open water (m/s)
U_p	(or U_{pot}): Potential wind speed (m/s) ; see section 4.4 and Wieringa, 1986: As U_{10} , but with partial exposure correction (Eq. 4.4).
U_{max}	Maximum wind gust (m/s), generally at 10 m height, averaged over 1 second, with a measuring interval of (10 or) 60 minutes.
x	Fetch or along-wind distance to upwind coast (m or km)

ξ_0	Wave breaking parameter in wave run-up formulas (Chapter 8); $\xi_0 = \frac{\tan(\alpha)}{\sqrt{s_0}}$, where $s_0 = \frac{H_{m0}}{1.56T_{m-10}^2}$ is a wave steepness parameter and α an effective dike slope.
z	General indication for (measuring) height (m)
z_{ABL}	Atmospheric boundary layer depth (m); Appendix E
z_d	Zero displacement height (m) in logarithmic wind profile
z_0	Aerodynamic roughness length (m); see (Tennekes, 1972; Wieringa, 1986)
z_{om}	Meso scale or landscape roughness (m), as z_0 but averaged over spatial scales of order 5-20 km.
$z_{2\%}$	Wave run-up height with respect to the still water level (SWL) that is exceeded by 2% of the incoming waves (m)

V. List of Figures

- Photo 1: FL2-location, view from North, April 2006
- Photo 2: Run-up-location during calm weather (2002)
- Photo 3: Run-up-location during 8 Beaufort winds (26/2/2002)
- Photo 4: FL5-location, view from S-SW, Oct 2006
- Photo 5: FL5-location, view from S-SW, Sept. 2004
- Photo 6: FL9-location, view from SE, Jan 2005
- Photo 7: FL25-location, view from E, 13/1/2006
- Photo 8: FL26-location, view from E, 13/1/2006
- Photo 9: SL29-location, view from SSW, 18/1/2006
- Photo 10: 3-metre-capacitance probes FL5 (right instrument, with some ice accretion) and FL9 (left), 23/1/2006
- Photo 11: Fist-size log-a-level, FL26, August 2006
-
- Figure 2.1: Measuring locations Lake IJssel and Lake Sloten, plus some (former) additional Rijkswaterstaat locations and some KNMI meteorological stations.
- Figure 2.2: Dike profile (cross section, view from North) at run-up location Rotterdamse Hoek.
- Figure 2.3: Illustration of the 7-step data processing procedure.
- Figure 2.4: Hierarchy of MATLAB-scripts; [H] indicates scripts which may use auxiliary scripts or functions.
- Figure 3.1: Percentage available wave data per month, from Jan. 1997 to Dec. 2006; the colour coding blue-yellow-red is an indicative quality measure: largely reliable, unreliable, strongly unreliable.
- Figure 3.2: Range of wind conditions as measured at FL2 from mid-1997 to 1/2/2007.
- Figure 3.3: Wave heights H_{m0} at FL2 as a function of still water level, as observed at FL2 from mid-1997 to 1/2/2007. Cyan, blue and red symbols denote peak periods T_p up to 4 s, from 4-5 s and from 5-6 s respectively.
- Figure 4.1: Percentage of FL2 wind data in a given wind direction class (of 20° width), for four different ranges of wind speed U_{10} .
- Figure 4.2: Percentage of FL2 data with 10-metre wind speeds above a threshold U , for winter (Dec-Feb), spring, summer and autumn.
- Figure 4.3: Percentage of SL29 data with 10-metre wind speeds above a threshold U , for winter (Dec-Feb) and summer (Jun-Aug), for daytime and nighttime hours.
- Figure 4.4: Wind speed U_{10} as a function of return time for FL2 and Stavoren-Haven-KNMI. The data points correspond to yearly wind maxima; the lines are Weibull fits.

-
- Figure 4.5: Potential wind speed U_{pot} as a function of return time for Amsterdam Airport (Schiphol-KNMI); for various periods of time.
- Figure 4.6: Evolution of 10-m wind speed (top panel) and wind direction (lower panel) for 8 different gales, based on FL2 data (except 18/1/07 when FL26 had to be used).
- Figure 4.7: Wind speed ratio $U_{10}(FL26)/U_{10}(FL2)$, as a function of FL2 wind speed $U_{10}(FL2)$, for a westerly wind direction sector of $240^\circ - 300^\circ$. Solid the average; dashed lines are 1 standard deviation off the mean value.
- Figure 4.8: Wind speed ratio $U_{10}(FL26)/U_{10}(FL2)$ for westerly winds ($240^\circ-300^\circ$), as a function of the air-water temperature difference, for 3 different wind speeds.
- Figure 4.9: Wind speed ratios for the present measuring locations as a function of wind direction (wind speeds above 6 m/s only).
- Figure 4.10: Wind speed ratio $U_{10}(FL2)/U_{pot}(Schiphol)$, as a function of the Schiphol potential wind speed $U_{pot}(Schiphol)$, for a WSW wind direction sector of $230^\circ - 270^\circ$. Solid line indicates mean values; dashed lines are 1 standard deviation off the mean value.
- Figure 4.11: Wind speed ratio $U_{10}(FL2)/U_{pot}(Schiphol)$, as a function of the air-water temperature difference, for 3 different potential wind speeds $U_{pot}(Schiphol)$.
- Figure 4.12: Measured wind speed ratio $U_{10}(FL2)/U_{pot}(Schiphol)$, as function of wind direction, for 3 different U_{pot} -values.
- Figure 4.13: As Figure 4.12, with potential wind speed of Berkhout-KNMI (top) and Stavoren-KNMI (below) as reference.
- Figure 4.14: Potential wind speed ratios between various KNMI-stations as a function of wind direction, with Schiphol as a reference and for $U_{pot}(Schiphol) \sim 12$ m/s.
- Figure 4.15 Gust factor GF as a function of wind direction for each of the measuring locations, for conditions with $U_{10} > 8$ m/s only.
- Figure 4.16 Average wind speed ratio U_3/U_{10} at FL2, as a function of wind direction, for $U_{10} > 8$ m/s.
- Figure 4.17 Average wind speed ratio U_3/U_{10} at FL2, as a function of wind speed U_{10} , for wind directions of $210-310^\circ$.
- Figure 4.18 Daily averaged water temperatures at FL26 as a function of Julian day number (Mar 2001- Jan 2007).
- Figure 4.19 Air-water temperature difference $T_{air}-T_{water}$ at FL26, as a function of wind direction, for day- and nighttime and summer and winter half year.
- Figure 4.20 Change in water temperature ($^\circ\text{C}$ per day) as a function of the wind speed U_{10} times the air-water temperature difference ΔT .
- Figure 5.1: Mean lake level (in cm NAP) of Lake IJssel as a function of day number (1-365), for the calendar years 1997-2006.
-

-
- Figure 5.2: Storm surge at the MSW-station Lemmer as a function of wind direction, for a wind speed of 11-13 m/s at FL2. All data are 2h-averages. Red points denote instationary data, blue points stationary data.
- Figure 5.3: Storm surge at the MSW-station Lemmer as a function of wind speed at FL2, for wind directions of 240°-280°. All data are 2h-averages. Red points denote instationary data, blue points stationary data.
- Figure 5.4: Water level registrations at the MSW-stations for 23-24 February 2002 (top), 2-3 May 2003 (middle) and 18-19 January 2007 (below).
- Figure 5.5: Response of Lake IJssel to wind for five locations: ratio of storm surge spectrum $S(\text{surge})$ [m^2/Hz] to spectrum of squared wind $S(U_{10}^2)$ [$(\text{m/s})^4/\text{Hz}$]. Based on 10-minute data from 27/1/2002 to 12/2/2002
- Figure 6.1: Approximate 4-year (2001-2005) climatology for the wave height H_{m0} (all locations, Nov.-April only).
- Figure 6.2: 20-Minute samples of wave height H_{m0} at FL2 (top) and FL25 (below) as a function of FL2 wind speed, for wind directions of 220-260° and the period 1997-2005. For FL2, still water levels (SWLs) above and below NAP have separate colours.
- Figure 6.3: Average H_{m0} at FL2 (top), FL5 (middle) and FL9 (below) for various wind speeds at FL2, as a function of wind direction.
- Figure 6.4: Average H_{m0} at FL25 (top), FL26 (middle) and SL29 (below) for various wind speeds at FL2 (for FL25/26) and SL29 (for SL29), as a function of wind direction.
- Figure 6.5: Average H_{m0} at FL2n (top) and FL37 (below), for various wind speeds at FL2n, as a function of wind direction.
- Figure 6.6: Average wave period T_{m01} for FL2 (top, FL5, FL9 and FL25 (below), for various wind speeds at FL2, as a function of wind direction.
- Figure 6.7: Average wave period T_{m01} for FL26 (top), SL29, FL2n and FL37 (below), for various wind speeds at FL2/SL29/FL2n/FL2n, as a function of wind direction.
- Figure 6.8: Peak period T_p at FL25 as a function of wind direction, for FL2 wind speeds of 11-13 m/s; cyan points denote 20-minute samples; line with squares denotes average.
- Figure 6.9: Deep water steepness $s_{Tm-10,o}$ (top) and real steepness s_{Tm-10} (below) as a function of wind speed, for the same averaged data as shown in Figure 6.3-6.5.
- Figure 6.10: Wave height H_{m0} (top) and peak period T_p (below) for deep water and 20 km of fetch, using parametric formulas of Kahma (1994) with U_{10} - and u^* -scaling.
- Figure 6.11: Wave height H_{m0} (top) and peak period T_p (below) for SW-winds at FL26. Shown are 20-minute samples (cyan points), average data (black line) and eye-fitted empirical scale relation (red line).
-

- Figure 6.12: Warm spring day with rather strong ESE-wind: Relative time evolution of wave height H_{m0} , mean wind speed U_{10} and wind standard deviation $\text{sig}(U)$ (σ_u) – all normalised with their daily average – as well as the wind speed ratio $U_{10}(\text{FL26})/U_{10}(\text{FL2})$. Top panel is 3/4/2002, lower panel is 7/5/2006.
- Figure 6.13: Wave height H_{m0} at FL26 as a function of air-water temperature difference, for NE-SE winds. $U_{10}(\text{FL26}) = 5\text{-}6$ m/s in top panel and 9-11 m/s in lower panel.
- Figure 6.14: Mean observed wave height H_{m0} , normalised with H_{m0} -value when still water level equals NAP. Top panel is FL2 (wind direction 240-300°), middle panel FL5 (subset from March 2006 on; 190-230°), lower panel is FL9 (180-240°). Reference line corresponds to fully depth-limited waves (H_{m0} proportional to depth).
- Figure 6.15: Wave-height-over-depth ratio H_{m0}/d as a function of dimensionless wind-and-depth parameter gd/U_{10}^2 . Experimental results from SL29 (left) and FL2 (right) are shown, for WSW-winds (220°-260°) of at least 12 m/s. SWAN-results are one-dimensional with infinite fetch.
- Figure 6.16: Ratio of FL5 and FL9 wave heights (H_{m0}) and peak periods (T_p), for SSW-winds, as a function over the wave-height-over-depth ratio H_{m0}/d at FL5.
- Figure 6.17: Wave period ratios T_{m01}/T_p and T_{m-10}/T_p for SSW-winds at FL5, as a function over the wave-height-over-depth ratio H_{m0}/d .
- Figure 6.18: Effective fetch x_H at FL2, as calculated by the inverse of Eq. (6.4a), as a function of wind direction for three different wind speeds..
- Figure 6.19: Effective fetches x_H and x_T as calculated by the inverse of Eq. (6.4) and geometrical fetch estimates, all as a function of wind direction. Top, middle and lower panel show results for FL2, FL2n (new FL2 location) and FL25, the latter on 0.3-30 km logarithmic scale.
- Figure 6.20: As Figure 6.19, for FL26, FL37 (0.3-30 km logarithmic scale) and SL29.
- Figure 6.21: Measured spectra and (drawn lines) parametrisations of Eq. (6.7), for SW winds of 12 m/s (6/12/06; blue line), 15 m/s (11/12/06, black line) and 22 m/s (18/1/07; red line). Top, middle and lower panel: FL2, FL5 and SL29.
- Figure 6.22: Ratio of individual wave height h divided by $H_{1/3}$, as a function of exceedance probability P , with x-axis transformed in such a way that Rayleigh distribution appears as a straight line. Top, middle and lower panel: FL2, FL5 and SL29, for various H_{m0}/d -values. The theoretical deep water Rayleigh distribution is plotted as a dashed black line.
- Figure 6.23: Ratio of individual wave period h divided by T_{m01} , as a function of exceedance probability P . Top, middle and

-
- lower panel: FL2, FL5 and SL29, for various H_{m0}/d -values. Only data with SW-winds of at least 6 m/s are included.
- Figure 6.24: Wave height as a function of wave period for individual waves; thick black line is theoretical deep water steepness limit (1/7, thin line is limit for actual water depth. Four cases are shown; all data are from 12-13h MET.
- Figure 7.1: Wave spectra (on double logarithmic scale) for the Lake Sloten calibration cases of Table 7.1. Top panel: case SLA-SLE, lower panel: case SLF-SLI
- Figure 7.2: Wave spectra (on double logarithmic scale) for the Lake IJssel test cases IJA (top), IJB (middle) and IJC (below).
- Figure 7.3: Wave spectra (on double logarithmic scale) for the Lake IJssel test cases IJD (top), IJE (middle) and IJF (below).
- Figure 7.4: Wave spectra (on double logarithmic scale) for the Lake IJssel test cases IJG (top), IJH (middle) and IJI (below).
- Figure 7.5: Wave spectra (on double logarithmic scale) for the Lake IJssel test cases IJJ (top), IJK (middle) and IJL (below). Please note change in locations and legend.
- Figure 7.6: Wind conditions, wave height and wave steepness for time-dependent test cases SL29. Green/red/blue/black lines correspond with 26/4/02, 2/5/03, 21/12/03 and 20/3/04. Main wind change starts at time = zero.
- Figure 7.7: Evolution of wave spectra (double logarithmic scale) at SL29 for the time-dependent test cases of 26/4/02 (top panel) and 21/12/03 (lower panel)
- Figure 7.8: Time evolution of wave height H_{m0} at the five Lake IJssel platforms, 26/4/2002
- Figure 8.1: Normalised relative wave run up $Z_{2\%}/H_{m0}$ at Rotterdamse Hoek as a function of still water level for westerly winds (240-300°), for two classes of FL2 wave height H_{m0} .
- Figure 8.2: Normalised relative wave run up $Z_{2\%}/H_{m0}$ at Rotterdamse Hoek as a function of FL2 wind direction at FL2, for still water levels greater than +0.25 m NAP. Results are shown for two classes of FL2 wave height H_{m0} .
- Figure B.1: Ratio of step gauge and real H_{m0} , as a function of H_{m0} and a number of sensor positions (sensor spacing 5 cm).
- Figure B.2: Example registration with soiling effects: SL29, 21/7/2005, 12h.
- Figure B.3: Wave height as a function of wind speed for WSW-winds, for summer and winter subsets of data. Top panel shows FL25-data with FL2-wind, lower panel SL29-data with SL29-wind. Both individual data and averages are shown, dashed lines indicate scatter (plus and minus one standard deviation) of the summer data.
- Figure B.4: Daily averaged kurtosis of raw wave signal, plotted as function Julian day number, for days with at least 4 Beaufort wind. Top and lower panel: FL26 and SL29.
- Figure B.5: Histogram of raw capa probe samples (FL2, 8/1/2005 from 13-14 h MET, with $H_{m0} \sim 1.4$ m).
-

-
- Figure B.6 Schematic example representation of calibration line (in millivolts) and slope of calibration line (mVolt per metre) as a function of relative water level.
- Figure B.7 Estimated ratio of capa probe H_{m0} divided by real H_{m0} (after Bottema, 2005), as a function of real H_{m0} for a number of capa probe support positions with respect to the still water level (SWL).
- Figure B.8 Skewness, kurtosis and T_{m-10} wave period as a function of still water level, for FL2-data of winter 2001-2002; only W-wind (240-300°) of 8-10 m/s)
- Figure B.9 Step gauge H_{m0} -values of FL2 (winter data of 1997-1999) and capa probe data of FL2 (winter 2001-2002) as a function of still water level, for westerly winds (240-300°) and wind speeds of 6, 9 and 12 m/s.
- Figure B.10 Deep water steepness $s_{T_{po}}$ at FL2 as a function of skewness and kurtosis (summer and winter data from 1997-2006, with winds from 210-300° above 8 m/s).
- Figure B.11 H_{m0} as measured by log-a-level as a function of capa probe H_{m0} ; all Lake IJssel locations, 16/10 - 15/12/06.
- Figure B.12 Raw signal (except for zero-offset correction) of capa probe and log-a-level, 1/11/2006, from 5h20 MET on.
- Figure B.13 Effect of a finite log-a-level footprint (20 cm diameter) on H_{m0} , T_{m-10} , T_{m01} and T_{m02} as a function of peak period T_p , together with an estimate of the deep water H_{m0} that would occur with this T_p .
- Figure B.14 Sketches illustrating wind deflection of sound beams.
- Figure C.1 Wave height H_{m0} (top panel) and wave period T_{m-10} (lower panel) at FL2 as a function of FL2 wind speed U_{10} , for westerly wind (240-300°), comparing winter half data of Oct97-Oct99 (step gauge) and Mar03-Apr05 (capa probe).
- Figure C.2 Comparison of step gauge and capa probe wave spectra, based on 1h of data with H_{m0} wave height of 1.25 and 0.15 m.
- Figure C.3 Step gauge and capa probe skewness at FL5 (all winter season data) as a function of wave height over depth ratio H_{m0}/d .
- Figure C.4 H_{m0} from uncorrected log-a-level data as a function of capa probe H_{m0} , Jan-Mar 2007, for FL2 (top), FL5, FL9, FL37 and SL29 (below). Black line indicates 1:1 relation (equal H_{m0} 's).
- Figure C.5 Ratio of log-a-level H_{m0} (after outlier filtering) and capa probe H_{m0} as a function of the latter; Jan-Mar 2007, for FL2 (top), FL5, FL9 and SL29 (below). Median of data is indicated by black squares and line.
- Figure C.6 As Figure C.5 but for T_{m-10} ratio and the locations FL2, FL5, FL37 and SL29.
- Figure C.7 As Figure C.6 but for T_{m02} ratio.
- Figure C.8 Capa probe and log-a-level skewness as a function of

capa probe H_{m0} ; Jan-Mar 2007, for FL5 (top) and SL29 (below).

Figure C.9 Comparison capa probe and log-a-level wave spectra. Top panel: Spectra during storm for FL2 ($H_{m0} \sim 1.7$ m) and SL29 ($H_{m0} \sim 0.6$ m). Spectrum during strong wind for FL5 ($H_{m0} \sim 1.0$ m) and during weak wind for FL37 ($H_{m0} \sim 0.1$ m).

Figure C.10 Instantaneous water level of capa probe and log-a-level during the storm of 18/1/07 (FL2 in top panel, SL29 in lowest panel) and the near-gale of 18/3/07 (FL5 and FL37, middle panels).

VI. List of Tables

Table 2.1	Coordinates of measuring locations, position of lake bed and global indication of instrumentation (see section 2.2 for details).
Table 2.2	Settings for processing of wave data.
Table 3.1	Available wave data for cases with at least 20 m/s wind (8-9 Beaufort); 'y' is available, '½' is partly available.
Table 3.2	Comparison of measured data with Hydraulic Boundary Conditions – for indicative comparisons only.
Table 4.1	Parameters of the Weibull fits for various selections of the present 1997-2006 data set. Notice that the real 10-metre wind is used for the open water locations, whereas exposure corrections are applied for Schiphol-KNMI (hence the use of U_{pot}).
Table 4.2	Ratio of $U_{10, open\ water} / U_{pot}$ as calculated with the macro-transformation method (assuming fully adapted open-water wind), for various terrain roughness z_o .
Table 4.3	Average turbulence parameters (with $1\ \sigma$ scatter) at FL2 (1997-2007) for SW-winds, with experimental and theoretical z_o and C_D .
Table 4.4	Wind speed ratios U_3/U_{10} (for 9/11/2006-31/1/2007 and wind directions of 230-330°), average water levels, calculated experimental z_o and C_D , as well as theoretical values.
Table 5.1	Estimated wind directions with near-zero storm surge, wind direction within 180°-360°-range with maximum storm surge, together with maximum surge (mean and standard deviation) for a FL2 wind speed of 17-19 m/s.
Table 6.1	Parameters characterising the climatology of wave height H_{m0} , as shown in Figure 6.1.
Table 7.1	Name, date and time (h MET) of Lake Sloten calibration cases, as well as water depth (water level = depth – 2.12 m), measured SL29-wind and main wave parameters (integration range: 0.03-1.5 Hz).
Table 7.2	Name, date, start time, mean lake water level, wind and air-water temperature difference for 1-hour test cases for Lake IJssel. Values between brackets are somewhat less accurate.
Table 7.3	Measured wind, approximate still water level (SWL) and measured wave conditions for test case IJA (2/10/1999, 3-4 h MET); spectral integration range for wave parameters: 0.03-1.5 Hz.
Table 7.4	As Table 7.3, for case IJB (22/2/2002, 4-5 h MET).

Table 7.5	As Table 7.3, for case IJC (27/10/2002, 14h20 h MET).
Table 7.6	As Table 7.3, for case IJD (12/11/2002, 13-14 h MET).
Table 7.7	As Table 7.3, for case IJE (2/4/2003, 14-15 h MET).
Table 7.8	As Table 7.3, for case IJF (18/4/2004, 14h20 MET).
Table 7.9	As Table 7.3, for case IJG (8/1/2005, 13-14 h MET).
Table 7.10	As Table 7.3, for case IJH (12/2/2005, 15-16 h MET).
Table 7.11	As Table 7.3, for case IJI (23/2/2005, 14-15 h MET).
Table 7.12	As Table 7.3, for case IJJ (1/11/2006, 7-8 h MET).
Table 7.13	As Table 7.3, for case IJK (18/1/2007, 12-13 h MET).
Table 7.14	As Table 7.3, for case IJL (18/1/2007, 19-20 h MET).
Table B.1	Estimate of required maximum integration frequency f_{max} (relative to peak frequency f_p), for a given wave parameter and a given error level
Table B.2	Estimate of minimum H_{m0} and T_p to guarantee a given accuracy in H_{m0} and the spectral wave periods, for $f_{max} = 1.0$ Hz and pure wind sea.
Table B.3	Wave overtopping over the instrument, typical errors as a function of Y_{top}/H_{m0} .
Table B.4	Errors when capa probe supports are at the still water level.
Table D.1	Corrections that should be applied to the raw wind speed data.
Table D.2	Cases where (unreliable) wind data should be replaced by exception values.
Table D.3	Corrections to be applied to raw wind direction data for FL2, FL26 and SL29, with start date of each correction period.
Table D.4	Preliminary offset corrections (m), to be applied to raw log-a-level signal.
Table D.5	Zero offset corrections (m), to be applied to raw step gauge signal, with start date of each sub-period in brackets.
Table D.6	Zero offset corrections (m), to be applied to raw capa probe signal, with start date of each sub-period; special cases are indicated as 'sc'.
Table D.7	List of the main periods with serious wave signal errors, other than the errors due to soiling and preferential values discussed in Appendix B.5-B.6.
Table F.1	Wind speed range for each of the Beaufort scale classes.

1. Introduction

1.1 General introduction

Since mid-1997, quasi-continuous wind and wave measurements have been carried out in Lake IJssel in the Netherlands; two years later later, measurements also started in Lake Sloten (see Chapter 2 for maps and further descriptions).

By now, the present extensive measuring campaign is close to its end, although not all measuring efforts will stop in the near future. Meanwhile nearly 10 years of wind and wave data have been gathered. Yet, much of this is only documented in preliminary internal reports (Beyer and Goes, 2000; Bottema, 2002ab, 2003ab, 2005, 2006ab; Jacobs and Vledder, 2003; Ruijter and Boomgaard, 2005). Besides these reports, a number of external publications is available (Bottema and Beyer, 2002; Waal, 2002; Bottema et al., 2003; Bottema, 2004a, Bottema and Regeling, 2005abc, Bottema and Vledder, 2005, 2006). However, these external publications are often rather fragmentary because of space considerations. In addition, many results of the publications issued before mid-2006 need some revision. For the description, detection and interpretation of suspect trends this applies to all results; for the data this especially applies to the wind speeds.

All in all, it is strongly desirable to present a complete, rather than fragmentary, overview of the Lake IJssel wave measurement results of the last 10 years. Moreover, there is a need to do this within short notice as a number of organisational (Rijkswaterstaat) and personnel changes will soon take place. Therefore, it was decided to present these results in the present technical report. This also allows to replace the preliminary (and sometimes inaccurate) results and interpretations of the previous publications by the present, final results.

1.2 Relevance of the Lake IJssel wave measurements

Safety against flooding

In an international context, the Netherlands is one of the few countries where flooding risks along the shores of some lakes receive as much attention as the flooding risks along the coast and along the major rivers. This is not surprising because for a fair number of Dutch lakes, the lake levels are at the same level as the surrounding polder land, or even higher. No wonder that the land surrounding such lakes has to be protected by dikes. The largest Dutch lakes are Lake Marken and Lake IJssel to the Northeast of the city of Amsterdam (see maps in Chapter 2). The sizes of these lakes are 696 km² and 1140 km² respectively;

their average depths are about 3.5 and 4.2 m. The size of both lakes is large enough to allow for significant wave generation by the wind, and for significant wind-induced set-up of the mean water level (storm surge). Together with the water volume of the lakes (roughly 2 and 5 billion m³) this may cause significant flooding damage if the surrounding dikes were to fail. Therefore, both lakes are mentioned in the Dutch Water Defences Law (“Wet op de Waterkering”, WOW, 1996).

The Dutch Water Defences Law has a number of features that are relevant to the monitoring of hydraulic conditions:

- It defines safety levels (in terms of maximum allowable water levels and/or flooding probabilities) for various dike ring areas along the main water bodies;
- It prescribes periodic assessment by the local water boards to check whether the height and strength of the dikes are still sufficient;
- It indicates that so-called Hydraulic Boundary Conditions (HBC's) should be made available to facilitate the above evaluation;
- It indicates when actual water levels should be passively made available and when – after exceeding certain safety thresholds – information should be actively given to local water managers.

For the present study, it is important to note that the safety standards in the Netherlands are quite high in comparison with abroad (RIVM, 2004), varying from an allowed flooding probability of 1/1250 per year along the major rivers (1/250 per year for a few special areas) to 1/10000 per year for densely populated areas along the coast. With such low failure probabilities, it is not a viable option to wait for suitable direct measurements of meteorological and hydraulic conditions for situations when the dikes are actually at risk. Hence, alternative strategies are needed:

- extrapolating extreme conditions from a sufficiently large and uniform experimental data set
- evaluate extreme conditions from hydraulic models

For wave measurements at Lake IJssel, the former is no suitable option because too many measuring locations are needed (too much spatial variation in the wave field) and because the data set is not statistically uniform because of physical reasons. As for the latter, small waves on Lake IJssel tend not to be hindered by the lake bottom but large waves are. In this context, researchers also refer to the ‘wave growth limit’ for shallow water (Waal, 2002): a situation where all wind energy input into the waves is compensated by various deep- and shallow-water dissipation processes.

All in all, it is inevitable to use hydraulic models to calculate the HBC's along Lake IJssel, irrespective of the question whether the actual HBC's are calculated in a probabilistic or deterministic way. However, these hydraulic models generally rely on tuneable model constants to reproduce the measured conditions. This is no problem if the model is to be applied within the range for which it is calibrated. For the HBC's

however, the present models are potentially inaccurate since they have to be applied far outside their calibrated range: that is for winds up to about 35 m/s (12 Beaufort; see Appendix F), rather than the present measurement range up to 24 m/s (9 Beaufort), which makes them potentially inaccurate. The present wave measuring campaign aims at (partly) solving this problem in two ways :

- doing a *long* measuring campaign to make sure that measurements are made during severe storms, and conditions as close to the HBC's as possible.
- assuring that the measurement range (in terms of wind, fetch, water depth, ...) is as varied as possible, because a model that is tuned on a diverse data set is likely to be more robust, suffering less from the above-mentioned extrapolation problem.

Ultimately, one may significantly improve the accuracy of the HBC's in this way. At present, the HBC's for Lake IJssel and Lake Marken are calculated with the HYDRA_M software (Westphal and Hartman, 1999; Blaakman and Lisman, 1999), which makes use of the WAQUA model (<http://www.netcoast.nl/tools/rikz/WAQUA.htm>) of Rijkswaterstaat to calculate storm surge, and the HISWA wave model (Holthuijsen et al., 1989) to calculate waves. However, HISWA has become outdated as support for HISWA stopped and nearly all researchers and consultants switched to the more advanced SWAN wave model (Booij et al., 1999), which has recently undergone some further model improvements (Westhuysen et al, 2007). It has yet to be tested whether these improvements are sufficient to predict the shallow-water wave growth limit (Waal, 2002) mentioned before; a situation which is expected to occur during the extreme winds associated with the design conditions for the Lake IJssel en Lake Marken dikes.

All in all, the present measurements are unlikely to directly influence the HBC's. Rather, the present measurements will extend our knowledge on wind, waves and storm surges; both in a local and general sense. The latter may lead to gradual improvements in both hydraulic and meteorological models. The overall effects of such improvements on the HBC's can yet hardly be assessed, partly because of mutual interactions of the models (and their tunings!), partly because the HBC's are not evaluated in a deterministic way, but in a probabilistic way involving thousands of combinations of wind and lake level.

Further applications

The present wave measurements mainly serve to improve the models used to evaluate the HBC's for the Lake IJssel dikes. Yet, there are also some further applications of interest.

The first of these applications is closely linked to the HBC's and the Law on the Water Defences (WOW, 1996): The Rijkswaterstaat RIZA Warning service for the Dikes in the Lake IJssel region (WDIJ) uses

at present the same (HYDRA_M) database as is used for the HBC's. However, an upgrade from the present system with schematised storms and a look-up database to a system with automatised on-line model calculations is planned for the near future.

Additional applications are possible in the fields of sediment transport and ecology (biological and chemical water quality, stability of vegetated shores). However, a much larger number of information requests of the past was related to construction projects in or near the water.

Wave information is also important for recreational navigation and professional ship traffic. For the latter, most years count a few wave-induced (near-)accidents on Lake IJssel, especially during 6-8 Beaufort winds; see (RVTV, 2001), and individual rescue reports on www.knrm.nl and www.kustwacht.nl. By using on-line wave information, the ship traffic control of Rijkswaterstaat IJsselmeergebied may be able to further improve the advise they provide to shipman travelling through Lake IJssel.

Wave climatology information is also highly relevant for ship traffic as some European regulations (ECE, 1997) prescribe which maximum wave height is allowable for which type of ship. Unfortunately, the regulation does not prescribe which probability of exceedance should be linked to the ECE wave height thresholds. As a result the regulation is not fully unambiguous; there is always a small probability on an extreme storm with exceptionally large waves.

Monitoring obligations

Finally, legal monitoring regulations must sometimes be taken into account.

For example, for the European Water Framework Directive (WFD, 2000) it is required to monitor a set of physical hydro-morphological parameters for every water system. For coastal waters and transitional (estuarine) areas, this parameter set also includes wave conditions; for Dutch inland lakes like Lake IJssel this appears not to be the case. Besides this, the Dutch Rijkswaterstaat Directive of 1971 (Stb, 1971) prescribes the gathering of data to monitor 'the hydraulic state of the country'. This is often interpreted as the monitoring of water levels (as is extensively done), but for locations where waves are relevant, one could argue that waves have to be monitored as well.

1.3 Aims of this project and report

The general aim of the present wave measuring campaign is :

- To gather and analyse well-documented wind and wave measurements of high quality, for various locations and various (strong wind) conditions, both for Lake IJssel and Lake Sloten.

In order to achieve sufficient variety in wave conditions, the following situations were to be measured :

1. waves for short fetches (< 2-5 km)
2. waves for long fetches (> 15 km)
3. waves on shallow foreshores
4. depth-limited wave growth; wave growth limit on shallow water (Waal, 2002)

The first three situations can be encountered on Lake IJssel, where it is the intention to measure both in mild and rough conditions (from a mild 5 Beaufort up to 9 Beaufort and more) to get as diverse a data set as possible.

However, Lake IJssel is too deep to investigate depth-limited waves growth for regularly occurring wind speeds (up to 9 Beaufort).

Therefore, the wave growth limit on shallow water is investigated separately on Lake Sloten.

Besides waves, two other issues are important:

- wave run-up against dikes
 - spatial distribution of wind on and near open water
- The former is investigated by a separate measuring location. The issue of wind is investigated by equipping part of the measuring locations with wind sensors, and by comparing our own results with those of the Royal Dutch Meteorological Office (the 'KNMI').

Finally, the main aims of this report are to document (where possible) :

- average wind and wave climate for Lake IJssel and Lake Sloten
- extremes in wind and wave climate
- specific features of wind and waves that are relevant to the tuning, validation and application of hydraulic and meteorological models

The above implies that the present report is aimed at three fairly different groups :

- scientists and engineers involved in the tuning, validation and application of hydraulic and meteorological models.
- people involved in similar measuring campaigns (by financing it or by carrying it out) who are interested in the do's, don'ts and results of the Lake IJssel experiments.
- and where possible also: policy makers, water managers and possibly even users of the water system, whenever they want to have a general impression of the hydraulic and meteorological and hydraulic conditions (climate, extremes) in the Lake IJssel region.

1.4 Project organisation

The measurements are commissioned by Ing. H.J. Regeling Rijkswaterstaat IJsselmeergebied (RWS IJG) and paid from the programme 'safety standards'. The measurements are carried out by the measuring department of RWS IJG (WSM, previously ANM / PAM), under responsibility of N.H.J. Wijnstok. The field work, data

management and primary documentation are mainly carried out by E.R.F. van der Goes (until 2006), Ing. R.S.E. Kleine, Ing. J.J. Miedema and Ing. A.J. Ponger.

The Rijkswaterstaat Institute of Inland Integral Water Management and Waste Water Treatment (RWS RIZA) is charged with the analysis of the data, with quality monitoring, and most of the publications. In the early years, this was done by Ir. D. Beyer. Since 2001, Dr. M. Bottema – the author of the present report – is responsible for this work.

It should be noted that the above reflects a project organisation that may soon undergo drastic changes. This is because most specialist (knowledge-intensive) hydraulic work from Rijkswaterstaat will probably be transferred to the Deltares, an Institute-in-formation that will contain parts of RWS, WL I Delft Hydraulics and TNO. Similarly, the measurements themselves may become the responsibility of RWS DID, the new Rijkswaterstaat organisation for Geo-Information.

1.5 Relations with other projects

Other measuring campaigns

Three (inter)national measuring campaigns are of relevance to the present project:

- Lake Tai-Hu, China, since 2006
- Scheldt areas, North Sea, Wadden Sea
- Lake George, Australia (until 1998)

Lake Tai-Hu is a measuring project initiated by Rijkswaterstaat (RWS RIZA and RWS IJG) in order to measure the shallow-water wave growth limit in more extreme conditions than usually encountered in the Netherlands. Lake Tai-Hu is larger than Lake IJssel, but with a depth of order 1.7 m, it is much shallower. The reason for the more extreme conditions at Lake Tai Hu is the possibility of occurrence of tropical typhoons.

Rijkswaterstaat is also responsible for a number of wave measuring projects in the Dutch Coastal Waters. Besides regular monitoring buoys, additional measurements have been carried out in – amongst others – the Western Scheldt area (RWS Zeeland) and in a special experimental ray near the village of Petten (RWS RIKZ). The last few years, additional data came available from the SBW-project (Strength & Loading of Water defences), run by various RWS institutes. SBW is a very large project which aims to reduce the uncertainties in the HBC's, and which includes a 15 year measuring campaign in the Wadden Sea (Groeneweg and Dongeren, 2002; Hoekstra and Hoitink, 2002; Stelwagen, 2002).

Finally, an extensive Australian wave measuring campaign was run by Swinburne University in Melbourne (Young and Verhagen, 1996; Young and Babanin, 2006). The campaign took place in Lake George, a lake of roughly 10x25 km with a depth of about 1.5 – 2 metres. The measurements lasted until the lake largely dried up, in 1999.

Wave model development

In the last 4 years, two PhD students at Delft University of Technology gave a major boost to the development of the SWAN wave model. One of them focussed on the modelling of non-linear three-wave interactions at shallow foreshores (Janssen, 2006); the other focussed on the general improvement of the SWAN wave model, both from numerical and physical viewpoints (Zijlema and Westhuysen, 2005; Westhuysen et al., 2007). In the latter case, RWS RIZA had a role in the user committee related to this PhD work. This also included the delivery of test case data based on the present Lake IJssel and Lake Sloten data.

The present wave measurements are also to be used in a wave model calibration and validation test bank tool (Wenneker, 2007).

Further relations

For a number of projects and activities, the link with the present measuring campaign is rather implicit, but often still important from a practical point of view. The main links that can be identified are:

- HBC-projects: improvement of underlying wind, wave, wave run-up and storm surge models; indicative comparison of measured conditions with design conditions
- WDIJ: Warning service for the Dikes in the Lake IJssel region: Like for the HBC's: improvement of underlying models. In some cases: contributing to verification of individual warnings.
- Dutch weather service KNMI: part of the present wind data is used to validate and improve the KNMI downscaling routine and its prediction of wind over open water. Some recent wind data – together with wind tunnel data reported in (Bottema, 1992, p. 77) – may also be used to evaluate exposure corrections for a dike-mounted KNMI wind measuring site near Trintelhaven, which was recently put into service.
- Any kind of project where wave data are essential as input information, for example in relation to ship traffic, morphology, ecology, etc.

1.6 Brief overview of this report

In the next chapters, the following issues will be discussed:

- The measuring locations, the instrumentation, and issues like maintenance, data acquisition, data processing and data validation: Chapter 2
- The global availability of data, together with an inventory of extreme events: Chapter 3
- Relevance of meteorological data (wind), wind climatology and wind extremes, spatial distribution of wind, aerodynamic roughness of the water surface, temperature data: Chapter 4
- Storm surge: Quasi-stationary results, analysis of natural scatter, time-dependent phenomena: Chapter 5

-
- Waves: scaling with the wind, absolute climatology, wave conditions as a function of wind conditions (stationary and time-dependent, with analysis natural scatter), depth-limited waves, wave spectra and wave height distributions: Chapter 6
 - Test and calibration cases for wave models: Chapter 7
 - Wave run-up against dikes: Chapter 8
 - Conclusions and recommendations: Chapter 9

For readers who prefer to have a brief glimpse on the main results only, it is recommended to focus on section 2.1, Chapter 3 and Chapter 9. The other sections and chapters generally require more background knowledge, while they contain a larger amount of details. This is even more true for the appendices, although Appendix F (Beaufort scale) is actually quite useful for non-specialists.

2. About the measurements and the data

2.1 Measuring locations

At the start of the project, there were three clusters of measuring locations, each with their own measuring aim. The name, aim and measuring locations of each cluster are given below, together with a picture of each location.

Photo 1 FL2-location, view from North, April 2006



.....
Photo 2 Run-up-location during calm weather (2002)



.....
Photo 3 Run-up-location during 8 Beaufort winds (26/2/2002)



Cluster 1: *Rotterdamse Hoek* ('Rotterdam corner', named after the debris of the 1940 bombings of Rotterdam city, that were used for the construction of the dike between the towns of Urk and Lemmer)

- main aim: measuring long-fetch wind and waves, together with wave run-up against dikes.
- locations: FL2 (waves) and RDH (run-up)

Cluster 2: *FRIGOL* near the South-Frisian coast and the region of Gaasterland (in use until early May 2007)

- main aim: measuring long-fetch waves and wave development on shallow foreshores.
- locations: FL5 (shallow foreshore) and FL9 (deep water)

.....
Photo 4 FL5-location, view from
S-SW, Oct 2006



.....
Photo 5 FL5-location, view from
S-SW, Sept. 2004



.....
Photo 6 FL9-location, view from
SE, Jan 2005



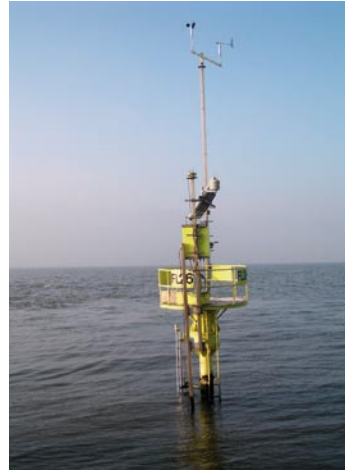
Cluster 3: *Enkhuizen* near the town of Enkhuizen

- main aim: measuring wind and waves for short and medium fetches.
- locations: FL25/FL37 (short fetches; FL37 replaces the FL25 from mid-2006 on) and FL26 (medium fetch)

.....
Photo 7 Left: FL25-location,
view from E, 13/1/2006



.....
Photo 8 Right: FL26-location,
view from E, 13/1/2006



Cluster 4: *Slotermeer*: the Frisian Lake Sloten

- main aim: measuring depth-limited wave growth and the wave growth limit on shallow water.
- location: SL29 (wind and waves)

.....
Photo 9 SL29-location, view
from SSW, 18/1/2006



The geographical positions of the above-mentioned locations are shown in Figure 2.1. They are also listed in Table 2.1, in which coordinates are given for each measuring location, together with the position of the lake bed and a global indication of the instrumentation. Further details about the instrumentation are given in section 2.2. The lake bed positions are derived from the available 40 m bottom grid for Lake IJssel (1999), and a recent 10 m bottom grid for Lake Sloten (2003). The actual water depths depend on the still water levels, which roughly vary from -50 to + 80 cm NAP (with an average near -25 cm NAP) for Lake IJssel and from -60 to -30 cm NAP for Lake Sloten (with an average of about -48 cm NAP).

It is important to mention some examples where locations were relocated or dismantled during the measuring campaign:

- FL2, 2/8/2005, because of digging of shipping lane near FL2; the new FL2-location is indicated as FL2n
- RDH, run-up gauge dismantled in 2003 because of planned dike reinforcement
- FL5, several location changes due to platform being washed away (1998) and after ice periods (2001/2003/2006); exact repositioning turned out to be difficult due to foreshore
- FL25, early 2006: repositioned and renamed to FL37, where there is less sheltering influence from the town of Enkhuisen.

As for the latter, photo 7 clearly illustrates that the upwind shore contains many trees that may contribute to undesired sheltering influences during offshore winds at FL25. A similar situation exists at the FL5-location (Photo 4). For FL5 however, the situation is even worse because a nearshore sand bar is likely to cause ill-defined fetches during offshore winds.

Table 2.1 Coordinates of measuring locations, position of lake bed and global indication of instrumentation (see section 2.2 for details)

location	start date	x-coord. (m)	y-coord. (m)	lake bed (m NAP)	main instrumentation
FL2	mid'97	167861	530005	-4.42	step gauge, wind
FL2	20/12/99	~167860	~530020	-4.43	capa probe, wind
FL2n	2/8/05	~166600	~529010	-4.41	capa probe, wind
RDH	<1997	~169000	~530000	not appl	run up gauge
FL5	mid'97	163395	538815	-1.63	step gauge
FL5	23/11/98	163458	538773	-1.69	step gauge
FL5	23/3/01	163391	538780	-1.89	capa probe
FL5	12/3/03	163978	538578	-1.45	capa probe
FL5	21/3/06	163973	538567	-1.50	capa probe
FL9	mid'97	161775	535920	-4.18	step gauge
FL9	16/3/01	~161770	~535920	-4.18	capa probe
FL25	mid'97	149000	526000	-2.62	capa probe
FL25	3/4/01	148997	525997	-2.82	capa probe
FL25	13/3/03	149006	526012	-2.91	capa probe
FL25	10/7/05	149006	526012	-2.91	capa probe, wind
FL26	mid'97	153000	526000	-5.50	step gauge, wind
FL26	13/3/01	~152990	~526000	-5.49	capa probe, wind
FL37	21/9/06	~155500	~520000	~-3.40	capa probe, wind
SL29	2/9/99	172496	548506	-2.11	capa probe, wind
SL29	15/3/03	172489	548502	-2.12	capa probe, wind

Sporadic early measurements are available for FL2/RDH (since 1991), FL9 (since 1994) and FL5 (FSW-platform at [159828,539553], since 1994). Further historical data of interest (see Wenneker, 2007) are:

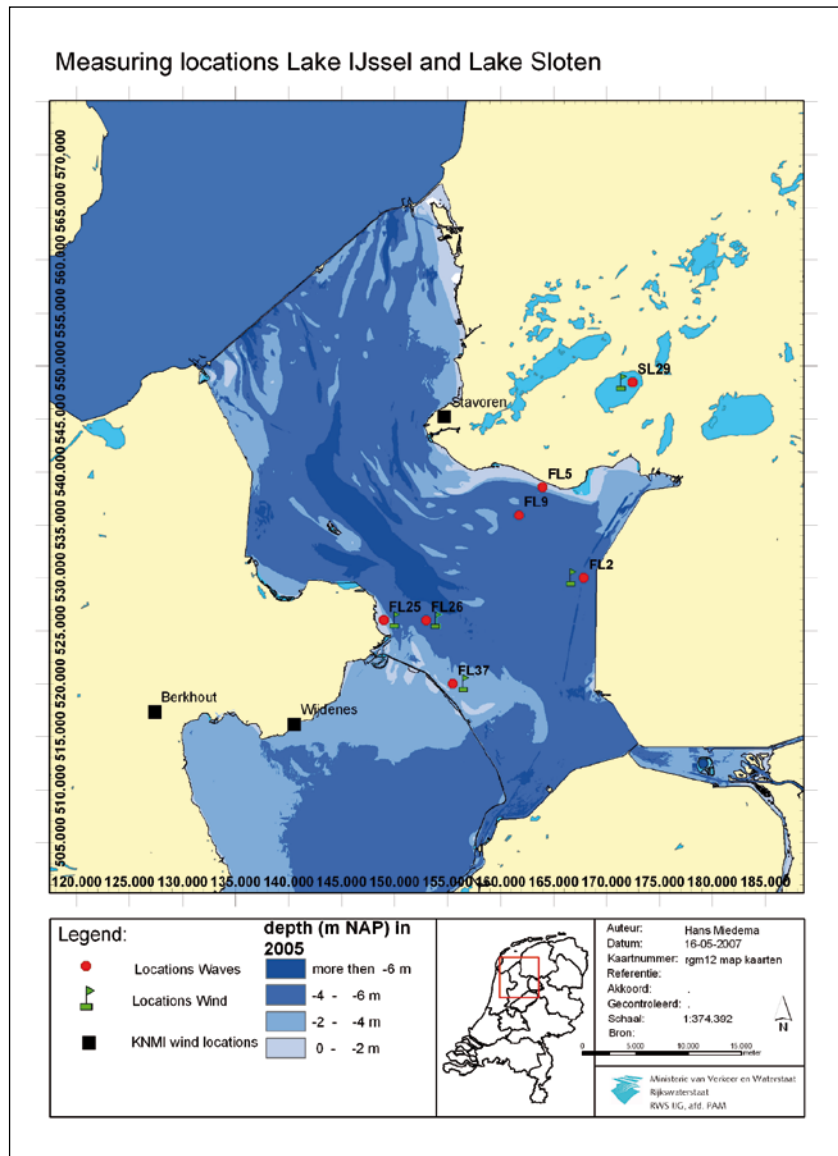
- wave data at HOZ ([158000,511000]; lake bed -4.2 m NAP) in Lake Marken during the winter of 1983-1984 (Bouws 1986)
- wind, wave and current data in Lake IJssel at Z1 and Z2 ([152000,529000] and [167000,516000], lake bed -6.2 and -5.2 m NAP), from Oct 1991 to Dec. 1992, no report available.
- sporadic wind and wave data in Lake Ketel at FL13 and FL20 ([181600,513475] and [177380,512397], lake bed -2.8 and -3.7 m NAP, during construction of sludge depot (1995/1996)

For wind reference data, the following KNMI-stations are useful:

- Schiphol / Amsterdam Airport, long-term statistics, since 1950
- Wijdenes, [140525, 516175], since 10/8/94
- Stavoren-Haven, [152850,544400], 18/6/1990-24/4/2002
- Berkhout, [127350,517350], since 22/3/1999
- Stavoren, [154725, 545250], since 23/12/1999

Wijdenes and Stavoren are the only stations with representative open water winds, at least for some wind directions (E-SSW and SSW-N respectively). During parts of 2006, KNMI-winds were also measured at a new location on the Houtrib dike, roughly at [155000 519000].

.....
Figure 2.1 Measuring locations Lake IJssel and Lake Sloten (in centre of red circles), plus some KNMI meteorological stations.



For internal purposes, RWS IJG also makes use of some additional wind and temperature measurements, for example at:

- FL33 in Lake Marken, roughly at [149000,517000], from June 2002 to mid-November 2004

- FL34 in Lake Veluwe, roughly at [486500,171000], from 4/1/05
- Besides this, RWS IJG has access to on-line data of the former KNMI Houtrib location (about [158300, 505600]). Measurements have been carried out since 1997, but stored data are only available until 1995 (see www.knmi.nl/samenw/hydra).

2.2 Instrumentation and maintenance

Energy supply

For each platform, the energy supply is provided by about three 12 Volt batteries. Without recharging, they typically can provide 12 Watt

for about three weeks. During summer, solar panels provide sufficient recharging; in winter frequent replacement of the batteries is advisable. The power consumption is typically 2-3 Watt for the wave gauges. For wind instrumentation, a similar rate applies; for lighting and data communication the required power is somewhat lower. In recent years, the amount of instrumentation on the platforms tended to increase. Therefore, some platforms are now provided with 5 batteries (instead of 3) and an additional wind generator (see Photo 1).

Wave instrumentation

Three types of instrument have been used for wave measurements:

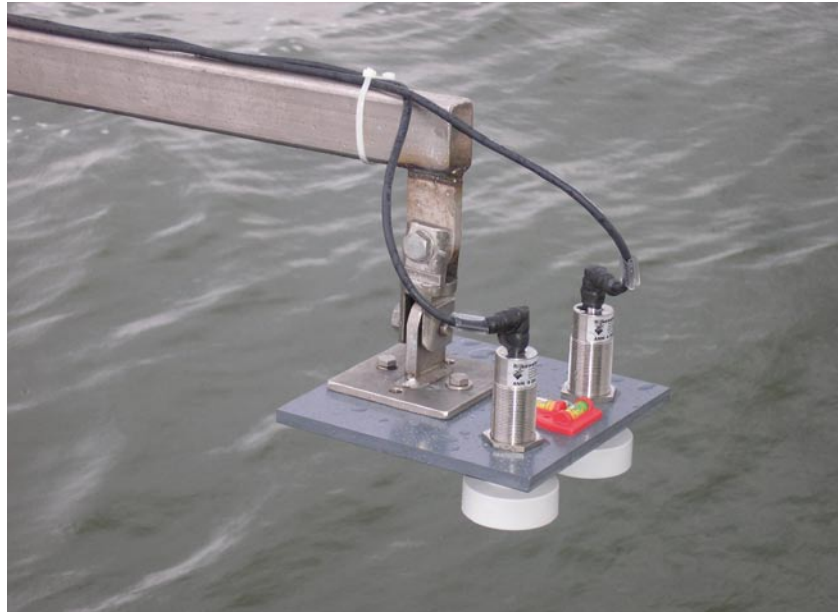
- step gauge (FL2 until Nov 1999, FL5/FL9/FL26 until Jan 2001)
- capacitance probe (FL25/FL37, SL29, elsewhere successor of step gauge), henceforth called capa probe
- Log-a-level (on pilot basis only, from Aug/Sep 2006 on)

The latter two are shown in Photo 10-11; no suitable step gauge pictures were available.

.....
Photo 10 3-metre-capacitance probes FL5 (right, with some ice accretion) and FL9 (left), 23/1/2006



.....
Photo 11 Fist-size log-a-level,
FL26, August 2006



Until early 2001, most of the present wave measurements were carried out with step gauges. Step gauges consist of a series of sensors which are short-circuited by submerging them into water. The highest 'wet' sensor is an estimator for the instantaneous water level. However, isolated wet sensors are rejected by the electronics because they are attributed to spray, rather than waves. The step gauges are of the 'Marine-300-11' type. They are 3 m long, and contained 60 sensors with 5 cm interspacing. The step gauges were sampled at 4 Hz.

The main errors of step gauges are related to:

- malfunctioning sensors and electronics
- soiling by algae (in the summer half year)
- the 5 cm spacing between individual sensors

Details are given in Appendix A and B.

RWS IJG not only has nearly two decades of experience with step gauges, but also with capacitance probes. The latter were first used for various experiments in Lake Ketel. In 1991-1992 they were also used in Lake IJssel (Z1/Z2). In the present measuring campaign they were first used at the FL25 (1997), next at the SL29 (1999), and finally (2001) at all other locations.

The present probes are of the 'Multicap DC11' type and have a length of 3 or 5 m, the latter at the FL2 since March 2001. They consist of a relatively thin teflon coated wire, connected by a number of supports (with a length and thickness of roughly 15 and 2 cm) with a thicker so-called mass tube (Photo 10). Together, they form a kind of electrical condensator, where the water serves as di-electricum which determines the electrical capacitance of the probe. In practice, the probe is fed by a fluctuating voltage, while the relation between water level and output voltage is measured beforehand by calibration. A linear fit of the calibration function is programmed into the data logger, so that its output is an instantaneous water level in centimetres. Like the

step gauges, the capacitance probes are usually sampled at 4 Hz. An exception is the FL25 where – except for a few periods in 1997-1999 – the waves were sampled at 8 Hz because of the short waves expected there (the fetch is less than 1 km).

The main errors of capacitance probes are related to:

- disturbance by the supports (for that reason, the supports near the still water line were generally partly or fully removed since late 2001)
- soiling by algae (in the summer half year)
- drift

Details are given in Appendix A and B.

One decade ago, step gauges and capacitance probes seemed the best alternative for the RWS IJG wave measurements. Especially for small lakes like Lake Ketel, buoys, pressure/current sensors and radar sensors seemed not to be a suitable alternative. Since then, it has become clear that step gauges and capacitance probe are not fully free from errors either. Therefore, a desk study (Ruijter et al., 2005) and wave flume study (Kuiper et al, 2005) were initiated to investigate a number of alternatives. From these studies, the acoustic Log-a-level appeared to be the most suitable option. In its present form (Photo 11), the log-a-level consists of two parallel downward-looking sensors, which emit a sound pulse count the time between emitting this pulse and receiving its reflection from the wavy water surface. The instrument requires little maintenance, but it also has some potential disadvantages:

- in very strong winds, the signal may be deflected to such an extent that signal loss occurs
- potential sensitivity to rain and spray
- because of the finite beam width (about 5°) and varying slope of the water surface, measurements do not relate to a single point but rather to so-called averaging footprint of a few decimetres diameter.

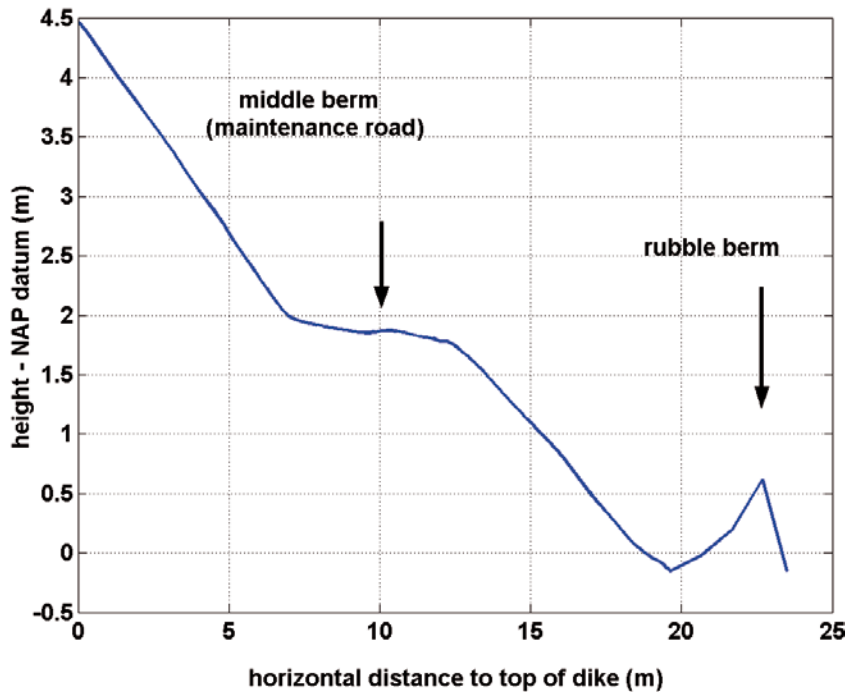
Further details are given in Appendices A-C. The above aspects are currently under investigation as part of a field pilot, which started in September 2006. Preliminary results of this pilot are discussed in Appendices B.8 and C.3. They suggest that the newest Log-a-level version (of early 2007) is quite suitable in mild conditions, but that it is perhaps too much of a fair-weather instrument as too many outliers occur for wind speeds above 12 m/s.

Instrumentation for wave run-up

Wave run-up against the dike at Rotterdamse Hoek was measured until the end of 2002. The run-up gauge used (Photo 2-3) has the same measuring principle as a step gauge, and is sampled at 4 Hz. It has 80 sensors with a horizontal distance of about 20 cm; the height of each sensor above the surface is about 7 cm. Because of its length, it is divided into two sections connected by a DATEC electronic unit. The dike profile is shown in Figure 2.2. The steeper dike sections have a slope of roughly 1:4. These are separated by a mildly sloping middle

berm (during some gales partly submerged, as in Photo 3). A rubble berm of – on average – nearly 0.5 m height is present in front of the dike (Photo 2). The run-up gauge closely follows the dike profile except for the rubble berm; the vertical position of sensor 1, 30, 51 and 80 is -0.07, +1.78, +1.99 and +4.45 m NAP respectively.

.....
Figure 2.2 Dike profile (cross section, view from North) at run-up location Rotterdamse Hoek.



Water level instrumentation

For the major inland water systems (like Lake IJssel), reference still-water levels are generally obtained from the standard Rijkswaterstaat MSW-network (Monitoring System Water; see www.waterbase.nl). Such data are not available for Lake Sloten. Therefore, reference still-water levels at SL29 are obtained from a separate 'Druck' pressure sensor of the PDCR910-type, with automatic compensation for the actual atmospheric pressure. Its accuracy is usually about 5 mm, but in rough weather (8 Beaufort winds and more) the still-water level from the pressure sensor can be up to about 10 cm lower than that of the capacitance probe and – as recently turned out – that of the Log-a-level. This suggests that the pressure sensor should be considered as fair weather instrument only, and should not be used with winds in excess of 7 Beaufort.

Wind instrumentation

The present instrumentation is primarily meant to measure the time-averaged wind, not the turbulence, although turbulence measurements can be definitely useful (see Chapter 4).

The wind direction is measured with a type 508 wind vane of Mierij Meteo. Its resolution is 1.4°; its response length is unknown. The wind speed is measured with type 403 (and sometimes type 018) cup anemometers of the same manufacturer. They each produce about 16

pulses for each metre of air passing by. The response length is specified to be about 2.9 m. The starting speed of the anemometers is less than 0.5 m/s, but due a slight non-linearity of their response, the calibration offset is often slightly negative (about -0.05 m/s).

Wind measurements were initially carried out at FL2, FL26 and SL29 only. From 10/7/2003 on, wind speeds were also measured at FL25 to investigate the wind development for short distances offshore. The latter measurements were continued at the successor of FL25, the FL37-location (in use since June 2006). The wind is sampled at 1 Hz, with a few exceptions at FL26 in the period 1997-1999. The data loggers store 10-minute wind maxima and 10-minute vectorial averages, except at FL25 where scalar averaging takes place by lack of a wind vane. At FL25, only averages are stored. Elsewhere, 1-second samples are stored since the second half of 1999.

The conventional measuring height for wind is 10 metres, but with a time-varying water level it is difficult to adhere exactly to this. Deviations of 0.2-0.3 m commonly occur, but the resulting errors are 2-3% in the worst case scenario, and more typically about 0.5%. At the FL2-location, wind speeds are also measured at 3 metres height. For this case, a similar mismatch in measuring height is likely to cause 2-3 times the above errors. More importantly, the platform has had a significant influence on the 3-metre-winds, as will be shown in Chapter 4. For that reason, RWS IJG started using a special extended boom (see Photo 1) by the autumn of 2004. In the raw wind direction measurements, a fixed bias is the most common error source. The underlying reason is that it is difficult to use compasses to orientate the vanes to the North because of all the iron in the platforms. In addition, biases sometimes develop spontaneously over time. In both cases, the remedy is to calibrate the measured wind directions with the wind direction of nearby official meteorological stations (of KNMI).

Temperature instrumentation

The vertical thermal stratification of the atmosphere can have a significant influence on the wave growth (see Young, 1998 and references therein). An easy practical way to get an impression of these thermal stability conditions is to measure the air-water temperature difference.

Air temperatures have been measured since mid-September 2002, initially only at the FL26, since mid-March 2005 also at the FL2. Temperatures are measured at about 5 m height, using a platinum PT-100-4-wire sensor with an anti-radiation shield (Photo 8, white box next to top of solar panel). The inaccuracy of the measurements is generally about 1°C , which is less accurate than desired. There were a number of reasons for this, such as insufficient calibration range ($10\text{-}20^{\circ}\text{C}$), incidental updating errors of the calibration data in the data logger software and on one occasion also the use of temperature-dependent electronics to connect the sensor to the data logger.

Water temperatures have been measured with a range of sensors:

- Campbell-107 at 1.2 m depth: at FL2 in second half of 2000 only, at FL26 since December 2000. The inaccuracy probably was 0.5°C, but in spring 2001 it was much larger due to drift.
- Endress and Hauser sensor at 0.4 m depth at FL25, from March 2003 – March 2005
- Yokogawa SC49-EP08 sensor for temperature and conductivity at 2 m depth, at FL2 since August 2002, at FL26 since March 2005.

The laboratory accuracy of the latter sensor is clearly better than of the former types, but there is one feature it does not account for: the fact that on calm and sunny summer days, the water temperatures in the first decimetres near the surface sometimes temporarily are up to 2-3°C higher than those at 2 m depth.

Maintenance

Maintenance of the present measuring network is crucial since one has to be sure that the rarest events (storms) during this measuring campaign are correctly measured. To assure the latter, regular maintenance of all the equipment is one of the required actions. As part of the regular maintenance, each location is visited about 10 times per year. Often, the maintenance during the winter months is intensified, whereas in the (relatively calm) summer months, maintenance is often stopped for 2-3 months. Most maintenance visits include the following actions:

- checking the energy supply (and replacing batteries if needed);
- checking electrical connections and data communication
- general checks on all measuring instruments;
- since Autumn 2001: temporary vertical displacement of capa probe to check for drift and other errors;
- ideally once per year: replacement of wind sensors at the end of their one-year calibration term;
- reparation or replacement of malfunctioning equipment.

In practice, the number of visits per season varies from 8 to 15, on one occasion (FL2, 2005-2006) even 25. Sometimes, maintenance is cancelled because of bad weather or long measuring interruptions (ice). On other occasions, extra visits are needed because of malfunctioning or damaged equipment.

It is of great importance that all actions (especially the unusual ones) during maintenance visits are properly documented. Therefore, since mid-1999, the maintaining engineers write down reports after each maintenance visit. In addition, during the last five years, Rijkswaterstaat IJsselmeergebied stores registration numbers of their instruments and other equipment in their instrument data base 'Ultimo', together with the period and location for/to which the instrument was borrowed from the central instrument storage. In this way, one can identify with reasonable (though not perfect) certainty which instruments are present on which location for a given date.

2.3 Acquisition and processing of data

Section 2.3 and 2.4 are mainly written for readers who are interested in procedures for acquisition, processing and validation of the data. Readers who wish to focus on the measurement results may prefer to start directly with Chapter 3, and skip the sections 2.3-2.4.

Data acquisition

For each location, the first step in the data acquisition is the local storage of the experimental data in a data logger. For the next steps, two options are available :

- *shore-station option*: Radio-transmitting the data to a nearby shore-based station several times a day, storing the data on the shore-station PC for some months, and retrieving the data by changing the hard disk of the shore station PC.
- *mobile phone option*: Establish telephone connections with the measuring location a few times per day, while directly transferring the data to the Rijkswaterstaat office in Lelystad.

Initially, the latter option was not available for all locations as the mobile phone network by that time (1997) only covered part of Lake IJssel. Further limitations of the mobile phone option are:

- sometimes data loss of a few days (mainly in weekends) due to interruptions of the PC-network in the Lelystad office
- need for larger data logger (Campbell CR10x instead of CR10)

On the other hand, the shore-station option also has its limitations:

- risk of data loss when hard disk crashes, or when it gets full before one expects it
- slow and cumbersome data retrieval by modem (~15 minutes per 24 h of data), which restricts possibilities for intermediate inspection after for example maintenance and reparations.
- in early years: risk that data of two locations get mixed up

For each measuring location, data acquisition took place as follows:

- run-up gauge Rotterdamse Hoek: direct connection to shore-station;
- FL2: shore station Rotterdamse Hoek until 4/11/2002 and from 17/3/2004 to 14/3/2005; else mobile phone;
- FL5: Frisian shore station until 25/10/2003, then shore station Rotterdamse Hoek until 6/9/2005, thereafter mobile phone;
- FL9: as FL5, but switch to mobile phone in March 2006;
- FL25: shore station Enkhuizen until 2001, then mobile phone;
- FL26: shore station Enkhuizen until 1998, then mobile phone;
- SL29: mobile phone.

.....
Figure 2.3 Illustration of the 7-step data processing procedure.

- (1) **ELECTRONIC CONVERSION OF MEASURED SIGNAL**
- (2) **CONVERSIONS BY DATA LOGGER SOFTWARE**
- (3) **MAKING ONE-DAY RAW DATA FILES**
- (4) **SPLITTING THE RAW DATA FILES**
- (5) **CORRECTIONS; STATISTICAL PROCESSING OF RAW SIGNAL**
- (6) **CREATING ONE-DAY TABULAR FILE OUTPUT**
- (7) **CREATING TABULAR OUTPUT FOR ONE/MORE YEARS**

Data processing - general

For the present measurements, data processing can be seen as a seven-step process, as illustrated in Figure 2.3. It is important to note that the first three, preparatory, steps are integral part of the data acquisition carried out by Rijkswaterstaat IJsselmeergebied. The analyses of Rijkswaterstaat RIZA only start at the fourth step. In the following, all data steps in data processing are briefly discussed.

Step 1 in data processing – electronic conversions

The output of a measuring instrument generally consists of an output current, voltage or pulse count. Often, this output does not match the input requirements for the data loggers. For example, for part of the wind measurements, an unspecified DA-converter is used to convert the discrete pulses to a continuous voltage. For the wave measurements, amplifiers are sometimes used to adjust the instrument output voltage to the range allowed by the data logger (0 – 2.5 Volt). Voltages outside this range often result in data logger exception values (e.g, -6999). For the temperature measurements, errors may result if – by mistake – temperature dependent resistances are used as amplifiers. All in all, it is critical that even for this stage of the measurements, the documentation is near-perfect. In practice however, this requirement is often overlooked.

Step 2 in data processing – conversions by data logger software

Generally, data loggers are not only used for pure data acquisition, but also as a means to convert voltages or pulse counts to a meaningful physical parameter like wind speed, temperature or water level. This step requires programming the calibration function of each instrument into the data logger. As the data logger does not store its input (voltages) but only its output variables, it is essential that the documentation of all (current and past) data logger software versions is near-perfect. Once again, this can be a significant error source in practice (see Appendices D.1 and D.4).

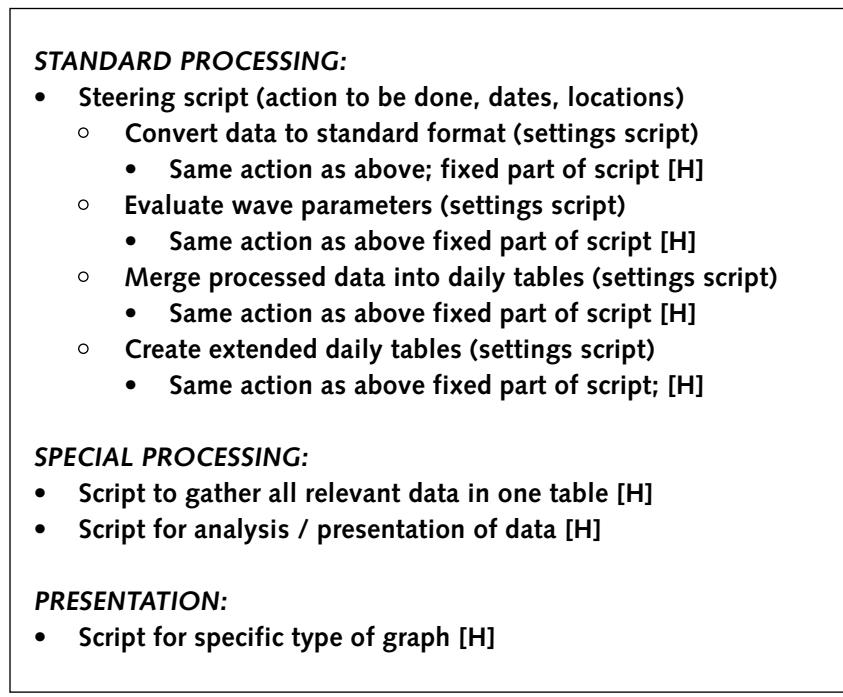
The main tasks of the PC's at the shore-station and RWS IJG office are to collect, (re)combine and store the raw data from the data loggers. With the old CR10 data loggers, data were often initially stored in a temporary file with a location-dependent name like FL2.DAT. Once per day, the latter file was renamed to a raw data file with a name of the type *ccyyymmdd.DAT* (initially also *.DDD) where *cc/yy/mm/dd* denote location code, year, month and day respectively. The latter file typically contained some data of the previous or following day(s); typically a few minutes, sometimes over an hour. In the latter case, the contents were often reshuffled to make sure that the contents of the DAT-file matched with its name.

In 2006, the switch to CR1000 loggers required a further preprocessing step as the new DAT-files contained too much text and symbols for easy processing. RWS IJG then facilitated further processing by also presenting the data in so-called Petten format, with one two-column file (time,variable) per variable per location per day.

Step 4-7 – data processing by RWS RIZA - general

After the aforementioned preprocessing steps by RWS IJG, RWS RIZA can start the actual processing and analysis of the data. To this end, a set of about 60 MATLAB scripts is used. This set of scripts is developed by RWS RIKZ and modified by D. Beyer of RWS RIZA; from late 2000 on, they were further adapted and extended by the present author. It is well beyond the scope of this report to fully document all these scripts; a concise description is given in (Bottema, 2006b). The hierarchy of the scripts is illustrated in Figure 2.4.

.....
Figure 2.4 Hierarchy of MATLAB-scripts; [H] indicates scripts which may use auxiliary scripts or functions.



As can be seen in Figure 2.4, scripts are needed for three purposes:

- standard processing
- special processing
- presentation (graphs)

For standard processing, there is a steering script to specify the processing step, date range, location, and processing options. For each processing step, first a script with adaptable settings is called for and next a script that normally should not be modified. The auxiliary scripts and functions either require no modification at all, or – by contrast – very frequent modification. The latter type typically contains instrument offsets/corrections and quality code settings. By and large, the same applies for special processing and presentation. Here, a simple structure of main script and help scripts often suffices.

Step 4 – converting data to standard format

The raw CR10 data logger files have an irregular structure, where lines with different variable types occur at different intervals. Therefore, RWS RIZA first converts the data to a standard format. With the CR1000 format and the Petten format, one could have skipped this step. However, this conversion is retained for the time being to make sure that all 1997-2007 data can be processed with one set of scripts.

The conversion of raw data to a standard format is done with a script named *funcmaakglwd... .m* with inputs like date and location code, and some flags to exclude or modify (if needed) the processing of wind and/or wave data. The conversion takes place as follows :

- check whether non-empty raw datafile exists
- define output directory for wave data
- define output files
- read line
- check whether 10- or 20-minute flag must be activated
 - if time is multiple of 20 minutes: write raw wave data
 - at multiple of 10 minutes: write 10-minute averages
- read next line; at end of file store last set of data.

For the new CR1000 and Petten formats, the procedure is similar, but the available time information allows to check for non-standard time intervals. Also, the Petten format allows to read all raw data at once rather than line-by-line. On the other hand, one must check whether all (up to 9) raw data files in Petten format are present.

In all cases, processing of one day of data for one location takes order 2 minutes on a PC with a Pentium 2 GHz processor.

The following files are generated during the process:

- Up to 72 one-column files per day, with up to 20 minutes **raw wave samples**. For example, the FL26 capa probe samples of 16-16h20 at 27/1/2007 are stored in the file *26070127.049* in the directory *.../FL26/070127/cap/*. Note that the instrument subdirectory 'cap' is only used from mid-2006 on.
- Optional, for locations/periods where **raw wind samples** are available: up to 144 three-column files (wind direction; U_{10} ; dummy or U_3) with up to 10 minutes raw wind samples. File name for FL26, 27/1/2007, 20h-20h10: *26070127wisa.121* in directory *../windsampl/FL26/26070127/*.
- For locations with wind instrumentation: Ten-minute **wind averages** for the above case are stored in a six-column file *26070127.wnd* in the subdirectory *wind/enkhui/2007/*. The columns include Julian day number, time (0-2400), mean wind direction, maximum gust, average wind speed and turbulence intensity (in %). Note that for FL2, the latter is on a 7th column as the 6th column contains the 3-metre-wind. Typical dummy values are -99 or -999, but for FL25/FL37, 0 may also be a dummy value. The WND files may contain some double lines because some DAT-files contain data of previous days. In rare cases, DAT-files may contain misdatings. In the WND-files, this may lead to undesired situations with different wind data having the same time stamp.
- Ten-minute **temperature** averages for the above location and date are stored in a general temperature directory in a four-column file *26070127.tmp*. The file properties are roughly as above, with Julian day number, time (0-2400), air and water temperature. Note that 0 is also a dummy value, and that internal logger temperatures are given if no suitable air temperature instrumentation is present.
- For SL29 only: **Still water levels (SWLs)** as measured by the **SL29 pressure sensor** (ideally in m NAP), for 27/1/2007 in a three-column file *29070127.drk* (day number, time, SWL) in a directory *../Waterstand/*.
- Characteristic values for all relevant variables (wind, waves, temperatures, SWL, battery voltage, etc., etc.) are stored at every multiple of 20 minutes, in a so-called **LOG-file** in a 'logfiles'-directory (file name example *26070127.log*). The logfiles contain 29 columns and – ideally – 72 lines with data.
- **Deviations from the standard file structure** are stored in the general wave data directory of each location, and in files with the above names but extensions like RGL, DXX, and MEL. These files contain non-recognised lines, data that could not be correctly stored due to these lines, and – for the latter cases – messages relating to incorrect time intervals and/or some specific cases with out-of-range values.

Step 5 – Processing of wave and run-up signal

The 20-minute raw data blocks of the previous step are the starting point for further wave (and wave run-up) data processing. For each day and location, the results are separately stored in a so-called GS-file: an irregularly structured file with 176 integers describing various wave parameters, wave spectra, as well as background information (time, date, location, settings). The gs-files are stored in a special gs-file directory, their name is for example *gs070125.FL2* or **.F26* (for FL2 and FL26 gs-file of 25 January 2007).

The data processing takes place with the scripts *funcgolfini....m* and *golven....m* and by and large, it takes place as follows:

The first step is to initialise some variables, to get some location-dependent meta-information and to open the 20-minute data block of interest. The next step is to call a script that applies offsets and – if necessary – corrections (see Appendix D for overview of offsets and corrections) to the raw signal. Cases with (near-)constant signal and cases with out-of-range values get a flag that aborts further processing because near-constant signals may cause the scripts to crash during further processing (e.g. percentile calculations).

Next the data (20 minutes, sometimes less) are split up in 100-second intervals. If there is more than 3 cm variation in the still-water levels (SWLs) of these intervals, the SWL *per interval* is subtracted from the raw signal instead of the overall SWL.

Then, zero-crossings are identified, and waves are defined from these zero-crossings. Only for waves longer than a minimum period T_{\min} (as given in Table 2.2) the period and height is used for further processing; short ‘ripples’ are neglected. From these individual waves, averages, extremes and percentile values are calculated, as well as the significant wave height and period.

Spectral wave height and period measures are also calculated as these are used for many applications. For each 100 s interval, a Discrete Fourier transformation (the MATLAB command “fft”) is applied. The wave spectrum then follows by averaging the spectra of each 100 s interval. The spectral moments m_{-1} , m_0 , m_1 and m_2 are defined from this averaged spectrum. In turn, these moments are used to calculate the spectral significant wave height H_{m0} and the wave periods T_{m-10} , T_{m01} and T_{m02} (see List of Symbols for explanation of each variable). Finally, the above is appended to a gs-file and shown in a plot as numeric data, together with graphs of the raw wave signal, the spectrum, and frequency distributions of wave heights and periods.

It is important to document the parameter settings of the above data processing; especially the wave periods T_{m01} and T_{m02} are very sensitive to these settings (see Appendix B.1 and Bottema, 2005). The main settings are given in Table 2.2. The maximum FFT frequency is always half the sample frequency. The interval length t and frequency resolution df are also directly related as $df = 1/t$.

The maximum and minimum frequency f_{\min} and f_{\max} define the spectral

integration range that is used for the evaluation of spectral moments m_n , and spectral wave height and wave period measures like H_{m0} and T_{m01} . However, in the *gs*-files, the file structure should not modify so here, the wave spectra are always given for the range of 0.01 to 1.0 Hz, with an interval of 0.01 Hz. Finally the choice of T_{min} (denoted "VGS" in the software) affects the time domain wave height and wave period measures like $H_{1/3}$ and $T_{1/3}$. Notice that the T_{min} of 1 s in table 2.2 is consistent with the f_{max} of 1 Hz.

.....
Table 2.2 Settings for processing of wave data.

	Standard value	Remarks
sample frequency	4 Hz	FL25: 8 Hz from Oct. 1997 – Jan. 2006
max. freq. from FFT	2 Hz	FL25: 4 Hz from Oct. 1997 – Jan. 2006
sample length T	20 min	or less for incomplete data block
interval length t	100 s	all cases
freq. resolution df	0.01 Hz	all cases
min. integr. freq. f_{min}	0.03 Hz	all cases
max. integr. freq. f_{max}	1.0 Hz	FL25, FL37 and SL29: 1.5 Hz
min. wave period T_{min}	1.0 s	FL25, FL37: 0.5 s

After the above processing, two final steps need to be made. Firstly, the *gs*-files must be moved from the main directory (where they can still be modified) to their final destination, the *gs*-files subdirectory.

If the latter action is done for FL2, the next step is to process the wave run-up data for the RDH-location (if present). First, the script *oplysm.m* links the sensor numbers of the run-up gauge to the dike profile. Next, sudden jumps in the signal (over 65 cm vertical run-up difference in 0.25 s) are filtered out, if they are present at all. After this, processing starts when there are at least 50 run-ups that exceed a level of +50 cm NAP. Then, average and maximum run-up heights are determined, as well as number of percentile values. Also, the data are shown in a plot which also contains a number of FL2 data. Finally, these data are stored in a file which resembles the above *gs*-files. If direct run-up processing is not possible, the above threshold (+50 cm NAP) is lowered by 10 cm and the whole process is repeated. If the threshold gets below +20 cm NAP, data processing stops. In that case, no data are stored as it is assumed that there was no measurable run-up.

Graphical presentation of the results during and after step 4-5
 During step 4 of the data processing, a plot with the raw wind data can be shown. During step 5, plots with the key results of the wave processing are shown for every 20-minute block. As in step 4, screen output is given if a file is not found or if its contents are suspect.

Furthermore, several dedicated scripts exist to :

- plot all raw 10-minute wind data for a given number of days
- plot all temperature data for a given number of days.
- plot time evolution and/or histograms of the raw wave signal for a given location and given data block(s).

- plot joint time evolution of raw wind and wave signal
- plot accu voltages (based on LOG-files)
- repeat step 5 for given date/location/data block to retrieve the graph that goes with it

The following plot types can only be made after completion of step 5:

- plot wave spectra of some successive data blocks (1 location)
- compare wave parameters of several locations (1 day)
- compare wave data, water levels and wind for a given number of days, for one location

Step 6 – Making one-day tabular file output

In this step, hydraulic and meteorological data are gathered in one table file per day and per location, with names like *26070125.tbx* (for FL26 table of 25 January 2007). The files are put in a separate Table-directory. Optionally, extended tables (*.XTB-files) can be made as well. These tables not only contain integral parameters but also percentile distributions and wave spectra. This allows an easier access to percentile values and wave spectra, with an extended spectral range up to 1.5 Hz. The integral wave parameters of the XTB-files are always evaluated with a fmax of 1.5 Hz. The XTB-files are extensively used for recent comparisons between the data of the capa probe and log-a-level instruments; note that for these cases, the file names have a suffix ('cap' or 'LAL') indicating the instrument type used.

Step 7 – Making tabular file output for one or more years

This step essentially consists gathering the TBX-files of step 6 into a single file. Similar aggregate files can be made for the WND- and TMP-files for wind and temperature respectively.

A further advisable step – although not part of the standard processing described above – is to use dedicated scripts to analyse and present the results of these season tables for wind, temperatures and waves. These scripts play an important role in the yearly validation of the data, in the yearly reports that are published, and in the analyses for the present report.

2.4 Validation of measured data

The classical validation approach, as used in software packages like WAVES2004 (XI, 2004), mainly focusses on verifying whether the data do not contain (too many) staggers, out-of-range values and outliers in the raw signal and its first derivative.

Such an approach is methodologically and mathematically sound, but experiences with the present project show that many errors are not detected in this way. This applies for gradually developing errors like drift and soiling, but also to incorrect (implementation of) calibration functions, malfunctioning or disturbing electronics and incorrect positioning or orientation of the measuring equipment. Moreover, natural scatter in the data is often order 15%, so that immediate detection of any error smaller than this is hardly possible.

Also, it is important to note that a mere detection of suspect data or suspect cases is not sufficient. The interpretation of such cases is crucial to identify measuring problems, to find their cause, and their solution. This interpretation requires a real experts' eye, a critical success factor for complex measuring projects like the present one.

For the above reasons, an integrated approach is strongly preferred. The aforementioned validation during – or directly after – data acquisition is only a part of this integral validation. To detect gradually developing errors or errors of order 20% or less, it is essential that not only 20-minute samples of the data are validated, but also aggregated data for a given set of ambient (wind) conditions. These subsets of aggregated data can cover anything from days to months. Jumps or drift in these subsets may be an indication for measuring errors, as well as data that deviate from a pre-defined set of reference results. An essential part of this validation approach is the documentation of maintenance actions in the field, as these actions typically mark the moment where problems either are solved or start to occur.

The validation (and monitoring) approach in general can be characterised by the following steps:

Explaining total absence of data

Total absence of data can have a range of causes like:

- temporary removal of platforms;
- no energy supply at platform (especially during winter nights);
- data logger or data transfer problems;
- data acquisition inactivated by purpose or inadvertently ('scheduler problem' of autumn 2000);
- corrupt or missing backups (until early 2000);
- problem with power, settings, or hard disk of shore-station PC;
- network problems at RWS IJG office;
- lost data files.

Partial absence of data

Whether data are partially absent can be judged from the reference files sizes given below.

Typical data file sizes for the DAT-files of the CR10 loggers are:

- about 2.0 MByte for 4 Hz step gauge data without wind samples (Run-up gauge RDH; FL2 until Nov. 1999, FL5/FL9 until Feb. 2001, FL26 until May 1999);
- about 3.4 MB for 4 Hz step gauge data with 1 Hz wind samples (FL26, June 1999 – Feb. 2001);
- about 3.0 MB for 4 Hz capa probe data without wind samples;
- about 4.4-4.8 MB for 4 Hz capa probe data with 1 Hz wind samples (SL29; FL2 from Dec. 1999 on, FL26 from Feb. 2001 on);
- about 6.0 MB for 8 Hz capa probe data without wind samples (FL25).

The CR1000 loggers, that were used since the summer of 2006, produce DAT-files of about 13.7-15.7 MB for the 4 Hz wave data, 3.6-4.1 MB for the 1 Hz wind data, and 8-14 kB for the 10-minute data; the exact file size depends on the number of variables included. The size of the files in Petten format is about 5.9-6.4 MB for the 4 Hz wave samples, about 1.5 Hz for the 1 Hz wind samples and order 2 kB for the 10-minute data.

Partial data absence can have a range of causes, for example:

- interruptions in data acquisition (see total absence);
- wrong sample frequency (FL25, 18/3-6/4/1999);
- data logger memory too small with respect to data retrieval intervals (FL25, summer 2001), causing order 1-hour interruptions at regular intervals of 4-8 hours;
- data logger disturbance related to data transfer (FL2, April 2003-2004): irregular interruptions at regular intervals;
- extra data processing for transfer of on-line wave parameters (FL2, summer 2005): small interruptions at regular small (seconds-minutes) intervals;
- synchronisation problems of the CR1000 loggers with acquisition of digital signal (from mid 2006 on): frequent interruptions of order 0.5 second;

Problems related to electronics, energy supply and data loggers

These problems can lead to loss of data (see above) and to disturbed data. In many cases, the problem cause is difficult to identify and is related to interference between the energy supply, the communication equipment, electronics and data logger (or interference within the data logger). Some examples of problems are:

- wrong time stamp of logger (check whether trends of different variables/locations are synchronous);
- exception values ($\pm 6999/7999$); either missing value or out-of-range input voltage for logger;
- overwhelming noise at start and end of 20-minute blocks (FL25, summer 2000): interference data logger and radio;
- several disturbed variables near/during GSM data transfer (FL2, April 2003-2004): interference data logger and GSM unit;
- 3-metre wind speed non-zero while disconnected from power (FL2, around Christmas 2004);
- capa probe signal on some (parts of) days decimetres too low (FL2/FL26/SL29 from mid 2006, with CR1000 loggers): some interference with wind vane;

Validation of wind direction

Before approving the data, one has to evaluate the correct offset (bias correction) for the wind direction; the vane is rarely exactly orientated to the North. This bias correction can be done by evaluating the sinus of the wind direction difference between the measuring location and a KNMI reference station. The sinus serves to avoid the 0°/360° discontinuity. The correction is preferably based on at least a month

of data; even day averages have a typical scatter (1σ) of order 5° . It is important to exclude weak winds (< 6 m/s) from this procedure as these are often associated with large directional variations, for example due to the passage of depression centres or due to local thermal (sea-breeze like) circulations.

One can check the raw and corrected data for the following

- fully invariant values: instrument removed/disconnected; problem with fuse or cable;
- negative value: same as above, temporary or permanent;
- preferential values at 180° distance: either logger software error (wrong conversion of cartesian to polar coordinates) or a wrong bit (0-1-value) in the raw instrument output;
- random values in comparison with nearby reference station, or scatter that is larger than 5° - 30° (both for samples and averages): logger software error, vane tail or vane interior damaged. Note that some real weak wind situations can also cause large scatter or seemingly random signals! ;
- (non-)agreement of trends in time with nearby reference station: either special situation (see item above), vane problem or wrong time stamp of data logger.
- time trend similar to nearby reference station, but fixed bias: wrong bias correction.

In the above, it is assumed that the data of the reference station are correct and representative. The KNMI reference data are generally reliable, but in the first half of 2000, the data of the new (inland) Stavoren station appear to have $+10^\circ$ wind direction bias. For the representativeness, it should be noted that near-surface wind directions are generally backed with respect to upper-level winds and that this effect is stronger over rougher terrain (e.g. Tennekes and Lumley, 1972). As a result, the wind directions over open-water are theoretically expected to be veered with respect to land-based winds, with average differences up to about 10 - 15° , provided the fetches are long enough (at least some tens of km). In practice however, no such differences were detected. In fact, a comparison between wind directions of the KNMI-stations of Wijdenes and Stavoren-Haven (Bottema, 2002a; Figure 4.2) yielded no average wind direction difference between upwind and downwind shores of Lake IJssel. As a result nearby onshore KNMI stations can be considered to be representative as a reference for the present data.

Validation of wind speed

Basic controls are easily done; advanced validation requires a lot of spatial wind modelling knowledge. The following problems may occur:

- invariant values: instrument removed/disconnected; problem with fuse or cable;
- negative value: zero wind or same problems as above, temporary or permanent;

-
- systematic occurrence of standard deviation more than 20-30% of mean or maximum gust above twice the mean (except in cases with showers, thunderstorms or weak winds): outliers;
 - sudden factor 2-3 jumps in raw signal: 'overflow' problem by double/triple counting of instrument pulses by electronic unit of FL2/FL26 wind set (until spring 2002);
 - periods with mean speed 2-3 times as high as elsewhere: same as above;
 - time trend dissimilar to that of other locations: natural causes, but possibly a wrong data logger time stamp or malfunctioning of the wind sensor;
 - 10-minute values scattering below expected value: wind vane problem yielding random directions, which cause reduced wind speeds because of vectorial averaging;
 - unexplained wind-speed dependent trend in wind speed ratio of two locations/levels: may point at a wrong zero-offset in one of the instrument calibrations (wrong FL2 offset from 2000 to April 2006; wrong FL26 offset from 2002 to April 2005).

All these checks are mainly suitable to detect large wind speed errors. Errors of order 25% and less can only be detected by examining spatial wind speed ratios (and their trends) for an extended period of time, together with an experts' estimate of the expected ratios. One can of course check for some basic rules:

- lower measuring levels yield reduced wind speeds
- rougher terrain yields reduced wind speeds
- wind speeds over open water generally stay constant or increase with fetch; wind speed may change over 20% in the first kilometre offshore, but generally changes 10% or less in the 5-20 km fetch range.

Once again however, there are several special cases (weak winds, small weather systems, large air-water temperature differences) where these basic rules do not hold.

Validation of temperature

For water temperatures, one could check whether:

- there are no exception values (0, $\pm 6999/7999$) or out-of-range values (in practice: outside the 0-25°C interval);
- the temperatures are not fully constant or scattering by more than order 0.3°C;
- there are no regularly occurring jumps during data transfer;
- there are no other sudden water temperature jumps (changes or more than 1°C are uncommon except on hot and calm summer days);
- water temperatures are within about 1°C of nearby measurements and within about 2°C of satellite data;
- water temperatures are within 5°C of climatology of the season.

For air temperatures, the first three checks would also be suitable, although scatter for the present FL2 and FL26 data can be order 1°C, with out-of-range values outside the interval –9°C to +34°C. Further indicative checks for the air temperature are:

- air temperature must be within 10°C of water temperature;
- day maximum should either remain below water temperature or below maximum of upwind land station;
- air temperature should remain above dew point temperature at nearby station (otherwise fog would develop);
- consistency of air-temperature difference: it is not very likely that FL2 air temperatures are above the water temperature while FL26 values are below it, or vice versa

Still water levels (from wave instrumentation or pressure sensor)

Still water levels (SWLs) can be considered for the validation of wave instrumentation and dedicated equipment like pressure sensors (at SL29). One could check the following:

- are the water levels (preferably day averages for calm days) consistent with reference data for Lake IJssel and Lake Sloten or do the offset corrections need to be adjusted;
- do the above adjustments have a water-level dependent trend? If so, the calibration factor (rather than just the offset) may be wrong;
- are the raw signal and calculated SWL realistic with respect to the instrument position and lake bed position?
- are the values and trends in raw signal and calculated SWL realistic with respect to neighbouring locations;
- do strong winds yield a spatially consistent storm surge distribution;
- are there any suspect trends? For example gradual increases due to soiling or due to an instrument sliding down, correlation with meteorological variables (early 1990 campaigns) or unexplained trends during calm weather (capa probe – wind vane interference with CR1000 data loggers used since 2006);
- for the present network, more than 2 cm change per minute is probably not realistic, so sudden jumps are suspect and possibly related to uploading of new/wrong logger software, inaccurate timing of corrections (in processed data) and instruments (temporarily) put at the wrong position during maintenance;
- oscillations with a period of 10-20 seconds to 20 minutes are probably also suspect as they are not related to wind waves or seiches on Lake IJssel and Lake Sloten.

Wave signal and wave parameters

For the wave signal and wave parameters, an important part of the validation is related to the known measuring errors described in Appendix B. The wave signal and wave parameters should be (and are) specifically screened for these errors, considering both the resulting effect of the errors and the error-prone conditions in which they are likely to occur. Of course, the same applies for wave run-up data.

For the remainder, a wide range of checks can be done on the wave signal and the wave parameters:

- out of range values or outliers in raw signal (less than zero, larger than instrument length, beyond lake bed level or beyond expected range of measurable values);
- staggers in raw signal (same value for two or more samples)
- biases and trends in measured wave parameters with respect to reference data (generally, the average wind to wave parameter relation for a few months of data is compared with a similar reference data subset);
 - bias or jump: wrong calibration factor?
 - trend: soiling, ageing, dependence on meteorological conditions?
- are the trends in wind, water levels and wave parameters consistent or are there different phenomena in place, like ship-induced waves (especially visible on calm days)
- are there any error indications in the experimental data, for example :
 - H_{\max} / H_{m0} systematically greater than 2 or less than about 1.5 for moderate/strong winds;
 - Wave period measures that differ more than a factor 2 or a T_{H13}/T_{m01} ratio in excess of 1.2-1.5 (both not suitable in mixed wave fields or during weak winds);
 - Wave steepnesses S_{Tm-10} (well) outside the range 0.04-0.08 (not in mixed wave fields and during/after quick wind changes; above 5-6 Beaufort winds only);
 - Steepness of steepest individual waves far below 1/7 (except during weak winds and decaying waves); or well above the theoretical (CERC, 1973) 1/7 steepness limit: raw signal too flat, or in second case: raw signal either too steep or too jagged (log-a-level signal before instrument adaptation of January 2007), or wrong calibration factor.
 - Wave heights H_{\max} and H_{m0} over about 0.9 and 0.6 times the water depth;
 - Wave height H_{m0} much larger than would be expected from deep water wind-fetch-wave height relation like (Kahma and Calkoen, 1992);
 - Non-smooth histogram of raw signal and/or its first derivative; their skewness Sk and kurtosis Ku outside the range of 0 to 1.3 and 3 to 4.5 respectively;
 - Ultra-smooth histograms and near-constant skewness and kurtosis: indication of too much preprocessing of raw signal;
 - Non-realistic wave spectra :
- low frequency energy as high as main spectral peak: noise or strong trend
- peak(s) at suspect position(s): noise or outlier(s) in raw signal

-
- high frequency slope above last spectral peak strongly deviates from theoretical f^{-4} relation (note: 'natural' deviations may be related to humps and peaks caused by higher harmonics and mixed wave fields): too steep a slope can be too slow an instrument response, too flat a slope can be noise;
 - spectral density in spectral tail strongly deviating more than factor 3 from expected $0.002 \text{ m}^2/\text{Hz}$ at 1 Hz frequency.
 - Suspect wave height distributions (WHDs) or wave period distributions (WPDs):
 - WHD during deep water conditions not consistent with Rayleigh distribution
 - WHD for extreme waves veers up instead of down (soiling, outliers?)
 - WHD for extreme waves veers down before waves become depth limited (instrument too short?)
 - steps between WPD values do not agree with sampling interval (FL26, Feb. 2007: 0.5 s intervals in period distribution with 0.25 s sampling interval) or (WHD) with instrument resolution

3. Availability and range of experimental data

3.1 Availability of experimental data

In nearly every field measuring campaign, part of the data is unsuitable for analysis, or even completely absent. In this section, the overall availability of wave data is discussed. The reliability of the data and the availability during strong winds also get some attention.

Figure 3.1 gives an impression of the overall availability of the data per month for the years 1997-2006, and of the quality of the data.

First of all, it can be noticed that the first systematically stored data become available by mid 1997 (and March 1998 for FL26). For SL29, the situation is slightly different as the Lake Sloten measurements only started in late August 1999. Secondly, there are a few major measuring interruptions during and after frosty periods, when all installations were removed. This was the cases in the winters of 1996-1997, 2000-2001, 2002-2003 and 2005-2006. Furthermore, there is a clear distinction between the period 1997-2000 and the period 2001-2006. In the former period, the data availability is below 40% (FL5/FL9) to 70% (FL2) for half of the months. From 2001 on, the majority of the months has a data availability of 75% for FL25 and SL29, to about 90% for the remaining locations. For both FL25 and SL29, many of the 'absent' data correspond to conditions with negligible wind and waves. In addition, FL25 had some modem and data logger problems in 2001 and 2002.

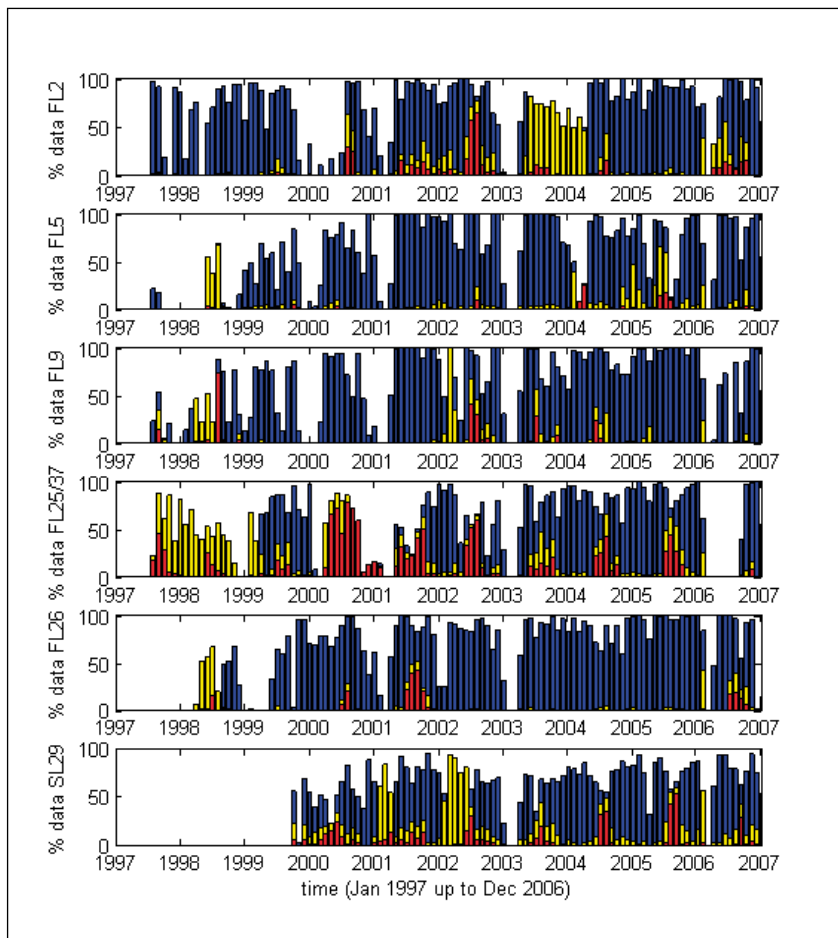
As for the reliability, two things can be noticed. Firstly, there are some extended periods with less reliable data, for example at FL2 and FL25. Secondly, there appear to be seasonal trends, especially for FL25 and SL29. These seasonal trends are related to soiling by algae, which can greatly deteriorate the quality of the data during the summer months.

Further details about the data reliability can be found in the yearly reports for the wave measurements, and in Appendices B-D. Most of the missing data are related to one of the following factors:

- Between mid-1998 and mid-2006, measuring interruptions due to (expected) ice are the largest source of missing data. In three winters, the equivalent of 40 months of data is lost, i.e. 7% of all potential data. Still worse is that fact that all data loss occurred in the winter, normally the windiest period of the year. Before 1998, the cold winters of 1996 and 1997 caused major measuring interruptions.
- Roughly 5% of all Lake IJssel data and slightly over 10% of all Lake Sloten data is not registered as available because data with negligible wind and waves less than a few centimetres are automatically discarded during the analysis.

- Until mid-2000, about 1 equivalent year of data got lost due to damaged or lost data backups. Before mid-1998, this problem was worst; from mid-2000 it is nearly absent.
- Communication problems (modems etc.) typically caused 6% of all data to get lost in the early years, and 2% after 2000.
- Similar rates of data loss were caused by problems with the shore-station PC. PC-network problems at the Lelystad-office led to additional data losses, but these were typically periods of only a couple of days, and only 1% of all data appear to be missing to these network problems.
- Absence of spare instruments only became a problem in 2006 (6 months of lost data), after two successive years with substantial ice damage.
- Malfunctioning wave instruments, energy supply problems and damaged installations (by vandalism or by ships on the wrong course) caused significant data loss during specific periods. A recent example is the first half of January 2007 at SL29, when most data were unreliable or absent due to empty batteries. Overall however, only 3-4% of all data is lost by one of the above factors. Once again, most data loss occurred during the early years of the measuring campaign.

Figure 3.1: Percentage available wave data per month, from Jan. 1997 to Dec. 2006; the colour coding blue-yellow-red is an indicative quality measure: largely reliable, unreliable, strongly unreliable.



On days with at least 15 m/s wind (7 Beaufort; see Appendix F for Beaufort scale), the availability of data is slightly better than usual. Before 2001, about 57% of the data was available on such days, from 2001 on this is nearly 90%. Yet the actual number of such strong wind days is highly variable. On average, one can count on 22 of such strong wind days per year. However, its actual range is from 8-10 days per season (for 2002-2003 and 2005-2006) up to 32-46 days per season (for 1998-1999 and 2001-2002); the season 2006-2007 will at least have 27 of such days.

For strong gales, it is worthwhile to consider the data availability for each separate gale. Table 3.1 lists all cases with sustained winds of 20-23 m/s. This corresponds to the upper range of 8 Beaufort and most of the 9 Beaufort range. Cases with a sustained 10 Beaufort on Lake IJssel have not occurred for a considerable period; the latest cases date from early 1990.

Table 3.1: Available wave data for cases with at least 20 m/s wind (8-9 Beaufort); 'y' is available, '½' is partly available.

date	FL2	FL5	FL9	FL25	FL26	SL29	gale characteristics
5/1/98	½			< ½			WSW, 8 Beaufort
4/3/98	y			y			SW, 8 Beaufort
28/2/99	y	y	y				SW, 8 Beaufort
3/12/99				y	½	½	SW, probably 9 Bft
28/5/00		y	y	y		½	9 Bft, veers S->W in 3 h
30/10/00	y	y				y	SW/S twin gale, 9 Bft
28/12/01	y	y	½	y		y	W-WNW 8 Bft, gusty
26/2/02	y	y	½	y	y	y	WSW 9 Bft, steady
9/3/02	y	y	½	y	y	y	~W 9 Bft, less steady
27/10/02	y	y	y	y	y	y	peak 23 m/s, SW->WNW
20/3/04		y	y	y	y	y	SW 8 Bft, sudden start
8/1/05	y	y	y	y	y	y	WSW 8 Bft
1/11/06	y	y	y	y	½	y	NNW 8 Bft
30/12/06	y	y	y	y	y	y	brief SW 8 Bft
11/1/07	y	y	y	y	y		SW 8 Bft
18/1/07	y	y	y	y	y	y	SW&W up to 23 m/s (9B)

As can be seen from Table 3.1, there are significant amounts of missing data for gales up to 2001 (especially for FL26), whereas the gale measurements from 2002 on were fairly complete. However, a few remarks have to be made :

- In nearly all cases with partly available data, the wind peak is partly or fully missing.
- For the first three gales, the 20 m/s limit was only reached at Stavoren-Haven; the FL2 wind speeds then typically were 2-4 m/s lower. The FL25-data of these gales are less reliable by lack of timely and accurate calibrations.
- For the gales of the winter 2001-2002, the FL9 data were less reliable due to wave overtopping over the instruments; for the same reason the FL5 water levels of 26/2/2002 are also unreliable. The SL29-reliability is slightly reduced in the first half of 2002

because of provisional ice damage repairs.

- During the gales of 27/10/02 and 20/3/04, the FL25-data seemed reliable but the wave heights were exceptionally low
- At 1/11/06, the FL26-probe gave up just after the wind peak. Also, it should be noted that by then, the FL25-location is replaced by the FL37.
- The cases of 30/12/06 and 11/1/07 only just reached 20 m/s. On the other hand, winds of 23-24 m/s were reached at 18/1/07, with both steady periods and sudden jumps. Unfortunately, some evening wind data of FL2 are missing.

In the seven years before the official start of this measuring campaign, from mid-1990 to mid-1997, gales seem to have occurred more often than in recent years. At the KNMI-station of Stavoren-Haven, 22 cases with 20 m/s winds occurred in that period. In 12 cases the winds reached into 9 Beaufort; in 4 cases (13/1/93, 24/1/93, 1/4/94, 17/2/95) the winds were even 23 to 24 m/s. Although Stavoren-Haven appears to be slightly more windy than the FL2, this is still a considerable number of gale cases. Unfortunately, measurements only seem to be available for four cases :

- 16/4/92, for Z2, 8 Beaufort from North, at Z2 nearly 9 Bft.
- 11/11/92, for Z2, brief gale, nearly 9 Bft from NW
- 17/2/95, FL2, brief gale, wind veering from SW to W
- 3/3/95, FL2, steady gale from WSW

Although there is no obvious reason to reject these wave data, one must also bear in mind that only processed data are available and that there is hardly documentation about these data and their validation. Hence, the reliability of these data is quite uncertain.

So far, the availability of wave run-up data at the RDH-location (Rotterdamse Hoek) has not been discussed. As wind speeds and water levels are too low for analysable run-up data during over 90-95% of the time, it makes little sense to discuss the overall availability. Instead, it is more useful to indicate periods with interesting run-up data. It turns out that two thirds of all analysable run-up data (about 2000 hours) are measured in the winter of 2001-2002, more specifically in the period of 26/1/02 to 10/3/02 (with a few more data in the month preceding that period). Most of the remainder is measured in 1998 and the first half of 1999. Unfortunately, the run-up gauge suffered from lightning damage in the period (October/November 1998) when the lake levels were at their highest. Outside the above-mentioned periods, hardly any suitable run-up data are available.

3.2 Range of experimental data

This section will give an indication of the range of wind speeds, water levels, wave conditions and wave run-up conditions that occurred during the measuring period of mid-1997 to the end of 2006. Further

climatology details will be given in Chapter 4 and 6. The present section intends to give a quick overview, which can be used for the following purposes:

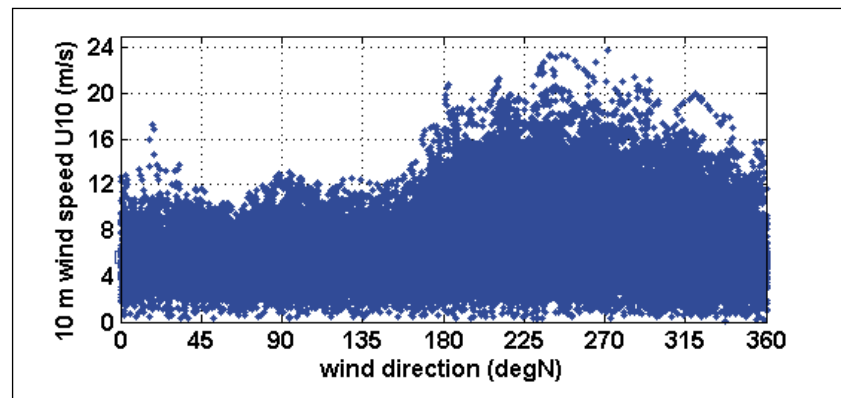
- comparison with other measuring campaigns;
- specification of range over which numerical models are - or can be – calibrated and validated;
- comparison with Hydraulic Boundary Conditions of nearby dikes.

First of all, the range of wind data is discussed.

As can be seen from Figure 3.2, the highest wind speeds of this measuring campaign strongly depend on wind direction. For FL2, the highest measured wind speeds for easterly wind directions are nearly always in the range of 10-14 m/s, which roughly corresponds to 6 Beaufort. The 15-17 m/s NNE-winds of 8/11/2001 were the only exception to this rule.

For westerly directions, the winds can be considerably stronger. Winds of 8 Beaufort (17.2-20.7 m/s) occur quite regularly if the wind direction is between South and NNW. Strong gales of 9 Beaufort seem to have preference for a fairly wide sector around WSW. Only a few of these gales have occurred in recent years (see Table 3.1). As a result, one can identify a number of individual 9-Beaufort cases from Figure 3.2.

.....
Figure 3.2: Range of wind conditions as measured at FL2 from mid-1997 to 1/2/2007.



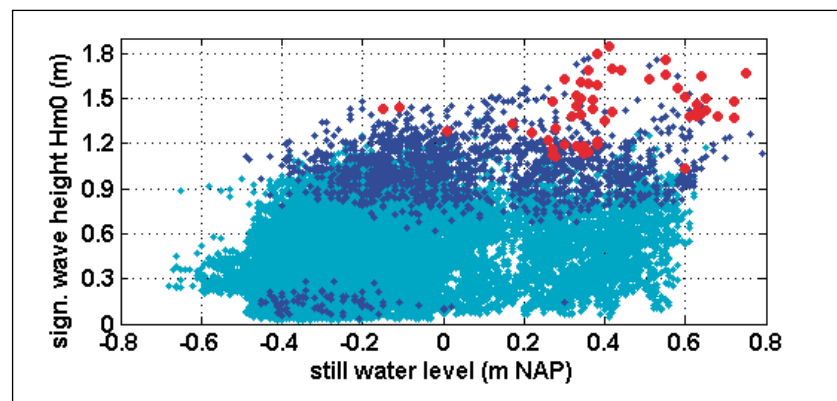
For FL26, the range of wind conditions is quite comparable with that in Figure 3.2. For the remaining wind locations, the highest wind speeds tend to be slightly lower due to the shorter measuring periods (especially for FL37); for FL25 and SL29 sheltering effects by nearby land also have some effect.

The present wind speed range is quite comparable with that of previous experiments of some length, such as the Lake Marken data of Bouws (1986) and the early unpublished data of Lake IJssel (as mentioned in section 3.1). It is unfortunate that the highest winds speeds that were measured along Lake IJssel (about 28 m/s, in 1978 and on 25/1/1990) occurred in periods when no wave measurements were done. Even the latter winds are far below the wind speeds used for probabilistic dike design, where wind speeds of 35-40 m/s (12 Beaufort) are commonly used (see Twuiver and Geerse, 1999). On the

other hand, the present data set may well be the best available. This is because alternative data sets for lakes tend to have a somewhat smaller wind speed range: for the extensive Lake George experiment, wind speeds range up to about 20 m/s (Young and Babanin, 2006).

The observed range of wave heights H_{m0} at FL2 is plotted as a function of the still water levels (with respect to the NAP datum) in Figure 3.3. The peak wave periods T_p are indicated with colour coding; the red symbols correspond to the largest T_p -values (5-6 s). Some elevated T_p -values (of 4-5 s) coincide with small H_{m0} and probably result from ship waves or swell like conditions during light winds. For the remaining cases, peak periods T_p in excess of 4 seconds generally occur for H_{m0} wave heights over 0.8 m, while cases with T_p between 5 and 6 seconds generally occur for H_{m0} -values in excess of one metre. The severest measured conditions so far (at FL2) have significant wave heights H_{m0} of 1.4-1.8 m, peak periods T_p of 5-6 seconds, and still water levels between -25 cm NAP (roughly the long-year average) and + 80 cm NAP. The highest individual waves (corresponding to H_{max}) then are in the range of 2.0-3.1 m.

.....
Figure 3.3: Wave heights H_{m0} at FL2 as a function of still water level, as observed at FL2 from mid-1997 to 1/2/2007. Cyan, blue and red symbols denote peak periods T_p up to 4 s, from 4-5 s and from 5-6 s respectively.



For FL9 and FL26, the measurement range is quite comparable to that of Figure 3.3, although the severest wave conditions at FL9 and FL26 occur with slightly lower still water levels (up to +50 cm NAP). In addition, the wave heights at FL26 tend to be somewhat lower with H_{m0} ranging up to 1.3-1.5 m.

At other locations, strong winds either coincide with short fetch or with depth-limited conditions. This significantly influences the data range:

- for FL5 (actually a series of different locations!), peak periods of 5-6 s do occur, but for still water levels of -20 cm to +60 cm NAP, wave heights H_{m0} remain below 1.0 m and 1.3 m respectively.
- For FL25, water levels up to +70 cm NAP occur in relatively calm conditions (as for FL26), but with more energetic waves (H_{m0} up to about 0.8-1.0 m and T_p up to 4-5 s), water levels range between -40 and +30 cm NAP.
- For FL37, few data are available, but the gale of 1/11/06 demonstrated that H_{m0} and T_p -values in excess of 1.1 m and 5.5 s

may occur, with still water levels of +10 cm NAP.

- For SL29, still water levels range between –70 and –28 cm NAP; during gales the lowest observed values are –45 cm NAP, together with H_{m0} up to 0.7 m and T_p up to 3.5 s.

One could make similar inventories for several additional hydraulic parameters. For most of these details, the reader is referred to Chapter 5-7. Details for wave run-up against dikes are given in Chapter 8. However, the range run-up data is also specified here because these data are directly relevant to dike design.

The highest run-up levels occurred during the gales of 26/2/02 and 9/3/02. The still-water level then was slightly above +60 cm NAP, while the so-called two-percent run-up level $h_{2\%}$ reached about +240 cm NAP. The highest individual waves even reached +270 cm NAP, about 70 cm above the middle berm of the dike. Photo 3 in section 2.1 shows the situation briefly after the highest run-up levels of 26/2/02.

3.3 Measurements versus Hydraulic Boundary Conditions

The design and evaluation conditions for the Lake IJssel dikes are determined in a probabilistic way. This implies that not a single hydraulic loading condition is used for dike evaluation and dike design, but a set of conditions which is weighed by their probabilities. This implies that a direct comparison between Hydraulic Boundary Conditions (HBC's) and measurements is not possible.

However, the HBC's are supplemented with so-called illustration points which correspond to the most probable hydraulic loading condition which the dike can just withstand (Rijkswaterstaat, 2002). With these illustration points, an indicative comparison with the present measurements is possible. The following illustration points are available from (Rijkswaterstaat, 2002) :

- F425, Marderhoek, facing SSW, close to the FL5
- N195, Westermeerdijk, facing W, 2 km South of FL2, 2.5 km SSW of RDH run-up site.
- H-IJM-202, Houtribdijk, about 2.5 km NW of FL37

.....
Table 3.2: Comparison of measured data with Hydraulic Boundary Conditions – for indicative comparisons only.

location	Hydraulic Boundary Condition (rounded)				measurement		
	water level (m NAP)	H_{m0} (m)	T_p (s)	wave dir. (degN)	water level (m NAP)	H_{m0} (m)	T_p (s)
F425 / FL5	1.0	2.0	6	240	+0.5	1.3	5.6
N195 / FL2	1.5	2.5	6	270	+0.8	1.6	5.8
H-IJM-202 / FL37	0.5	1.5	5	0	+0.1	1.1	5.6

Table 3.2 compares the severest conditions measured so far with the Hydraulic Boundary Conditions of nearby illustration points (see Rijkswaterstaat, 2002). In all cases, the measured still water levels are 0.4 to 0.7 m below the HBC-values. The measured wave heights are even about 30% below the HBC-values. For the wave periods, this is not true: the measured T_p -values are within 10% of the HBC-data; at FL37 the measured T_p is even slightly higher than the HBC-value. This may be reason for concern because the measurements were done in 8-9 Beaufort conditions, whereas the dike design conditions correspond to 12 Beaufort. Moreover, wave run-up against dikes is twice as sensitive to the wave periods as to the wave heights.

Despite all this, the measured wave run-up data at RDH suggest that there is quite some room between the maximum two-percent run-up level (+240 cm NAP) and the top of the dike (+450 cm NAP). It is worth investigating why one of the main measured run-up forcings (T_p) is close to its design value whereas this is not the case for the run-up itself.

So all in all, the conclusion should be :

The measured winds were up to 9 Beaufort, much weaker than is accounted for in dike design (12 Beaufort). Measured water levels and wave heights were therefore clearly lower than the Hydraulic Boundary Conditions (HBC's), while measured wave run-up levels remained well below the dike tops. However, care is needed in the prediction of wave periods as the measurements approach and sometimes even slightly exceed the HBC-illustration values.

Yet some care is needed if the above results should result in action.

This is because of two reasons :

- As the name indicates: 'illustration points' are only for illustration; one should not base hard conclusions on them
- Near FL37 and especially FL5, the waves are depth limited, which hampers a comparison with HBC illustration points if the latter do not coincide with the measuring locations.

4. Wind and temperatures

Wind data are crucial for the interpretation of wave data for lakes, as local winds are the primary forcing of the waves. In the following sections, first the relevance of wind will be discussed. Next an approximate wind climatology will be presented. Thereafter, methods and data for spatial wind transformation will be discussed. The next issue is the aerodynamic roughness of (wavy) water surfaces, a crucial parameter in various hydraulic models. Finally, air and water temperatures will be discussed.

4.1 Relevance of wind

General considerations about the relevance of wind for the purpose of flood protection are given in (Lammers and Kok, 2006), together with an inventory of wind-related knowledge gaps. For forecasts with wave models, the findings of Bidlot and Holt (1999) are relevant: *'Especially in [wave] forecasting, errors in predicted wind fields soon dominate the other error sources (internal [wave model] errors)'*.

Besides this, wind is a crucial element of the framework for interpretation that is required to make use of the present wave measurements. For example, the single fact that 'the Lake Sloten location SL29 might have wave heights over 0.6 m' is of little use if one can not assign a *probability* to such an event. A direct calculation of the probability of a given wave event requires a continuous series of data. In practice, it is nearly impossible to obtain a quasi-continuous series of data, either because of equipment failure or because of interruptions due to the lakes freezing over. Hence, the best alternative is to describe the waves as a function of their main forcing, the wind. The advantage of this approach is the fact that missing wind data of the present network may be replaced by continuous data series of nearby meteorological stations, even though this requires some transformations (see later in this chapter).

However, if the wind becomes the main reference parameter for the waves, each error in the wind data influences the interpretation and use of the wave data. For example, too high a wind in a wave model calibration may lead to a calibration where wave growth parameters become too small, which leads to model underestimations in calculations where the correct wind is used.

In the following, it will be specified what wind accuracy is needed to keep the errors in the hydraulic parameters below 10%. Besides wave heights and wave periods, storm surge effects and run-up levels will be considered as well.

For the time-averaged wind speed U_{10} , the following approximate scaling relations apply :

- wave height: $H_{m0} \sim U_{10}^{1.2}$ to $U_{10}^{1.5}$ (see SWAN-study of Bottema, 2006c, as well as Kahma and Calkoen, 1992)
- peak period: $T_p \sim U_{10}^{0.5}$ to $U_{10}^{0.6}$ (same references)
- storm surge: $\Delta z \sim U_{10}^2$ to $U_{10}^{2.5}$ (derived from Chapter 5 and from Waal, 2003)
- required dike height for a 1:4 dike without berms / absolute wave run-up: $h_{2\%} \sim U_{10}^{1.3}$ (Waal, 2003)

To avoid 10% storm surge height errors, the accuracy in U_{10} must be 4%; for the same error in H_{m0} , a U_{10} -error of 7% may be acceptable, for T_p this would be 17%. Because generally, storm surge in the present data is of somewhat lesser importance (it tends to be less than 0.5 m for U_{10} up to 18 m/s), the required U_{10} accuracy is mainly determined by the wave heights and run-up levels. This implies that the U_{10} -accuracy should be better than 7% to avoid over 10% interpretation error in the wave height (and run-up) data. For moderate winds ($U_{10} \sim 10$ m/s), this is a maximum allowed absolute error of only 0.7 m/s.

The relation between wind direction and the above hydraulic parameters is less straightforward than for wind speed. For storm surge and wave heights, the following facts must be taken into account:

- A 30° change in wind direction may result in a storm surge increase from zero to half the maximum attainable value for that wind speed (see Chapter 5).
- For wind blowing obliquely offshore, and measuring locations less than 1-3 km offshore, wave height may change by 10% by wind direction changes as small as 6°. In most other cases, the sensitivity to wind direction is much smaller.

All in all, wind direction errors in excess of 5° clearly seem undesirable.

4.2 Approximate overall climatology of wind

In the following, an overall wind climatology for moderate wind conditions is presented for the locations FL2, FL26, SL29 and Schiphol / Amsterdam Airport. For the present measuring locations, the measured 10-metre wind speeds are used, for Schiphol the so-called potential wind speeds, a 10-metre wind-speed which is partially exposure corrected (see section 5.4).

Data were available (and used) for the following periods:

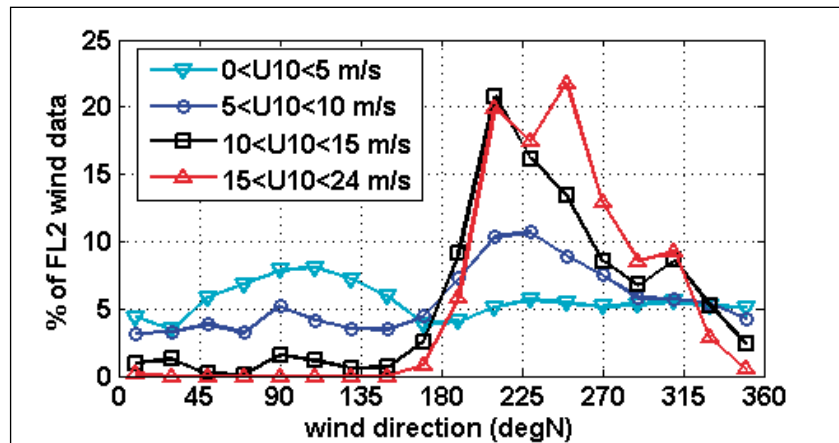
- FL2: mid-1997 to end of 2006
- FL26: March 1998 to end of 2006
- SL29: September 1999 to end of 2006
- Schiphol-KNMI: mid-1997 to mid-2006

It is important to note that order 30-40% of all FL2/FL26/SL29 data was either missing, or excluded because of instrument failure. To avoid biases, yearly averages were not evaluated directly from the data;

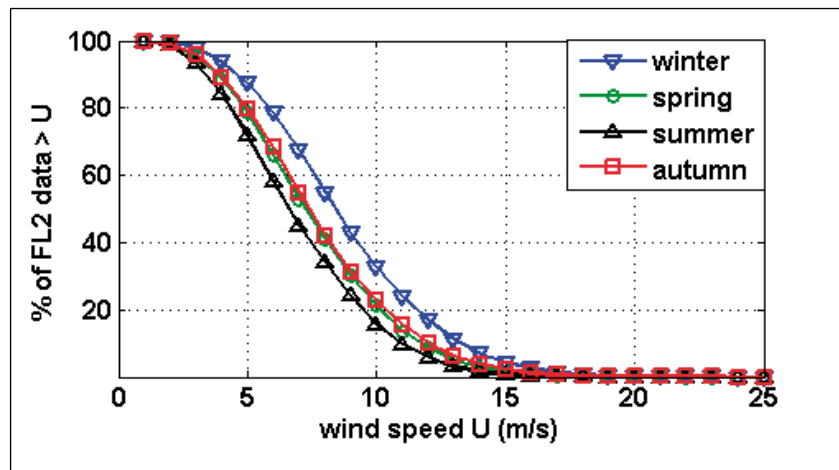
instead they were calculated as a four-season average. Otherwise, no attempts were made to account for the missing data. That implies that the present climatology is highly approximate. Nevertheless, the data show some interesting trends.

The first of these trends is shown in Figure 4.1. The graph shows the relative contribution of each 20° wind direction sector to the FL2 wind statistics, for four different wind speed classes. It is commonly assumed that Holland has prevailing south-westerly winds. Figure 4.1 shows that this assumption only holds for strong winds. For weak winds, there seems to be no prevailing wind direction. Actually, Figure 4.1 suggests even a slight preference for easterly directions during weak winds. Both results, for strong and for weak winds, are in accordance with the trends in the long-term wind statistics reported in Wieringa and Rijkoort (1983).

.....
Figure 4.1: Percentage of FL2 wind data in a given wind direction class (of 20° width), for four different ranges of wind speed U_{10} .



.....
Figure 4.2: Percentage of FL2 data with 10-metre wind speeds above a threshold U , for winter (Dec-Feb), spring, summer and autumn.

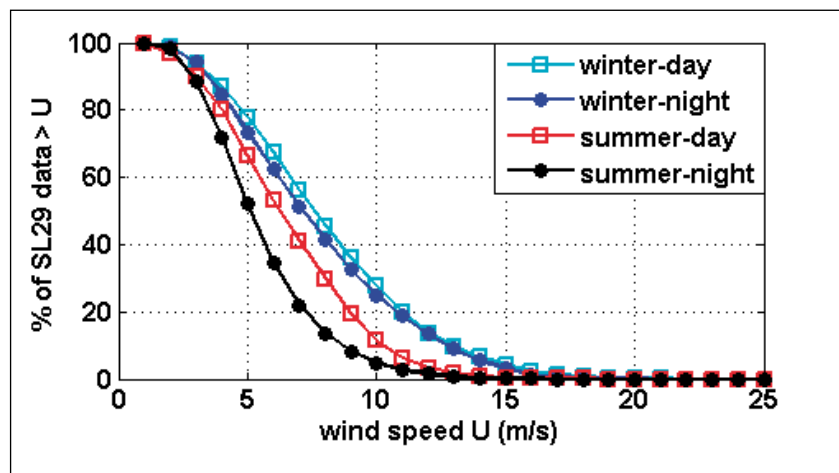


For the present campaign, missing data and instrument failure tend to have a slight preference for winter and summer respectively. Missing winter data are often related to ice periods, unreliable summer data often to lightning damage. Figure 4.2 shows that seasonal trends in the wind climate of FL2 are present, but that the trends are relatively limited. Typically, the wind speeds during winter are about 20%

higher. In reality the difference may even be slightly smaller as winters with ice periods (and increased amounts of missing data) tend to be more anticyclonic and less windy than mild winters.

Figure 4.3 shows the wind statistics of SL29. In this case, only summer and winter data are shown as each of these is divided into daytime and nighttime hours, the latter being from 19h-7h MET. During winter, there is little difference between daytime and night-time winds. During summer, this also applies for FL2. At SL29 however, summer night-time winds are significantly weaker than the daytime winds. In that respect, SL29 (unlike FL2) behaves as a typical land station.

.....
Figure 4.3: Percentage of SL29 data with 10-metre wind speeds above a threshold U , for winter (Dec-Feb) and summer (Jun-Aug), for daytime and nighttime hours.



Climate statistics as presented in Figure 4.2-4.3 are often parameterised with a Weibull function :

$$(4.1) \quad P(U_{10} > U) = \exp\left(-\left(\frac{U}{a}\right)^k\right)$$

where P is the probability that the wind speed U_{10} exceeds a limit U , while 'a' is a scaling parameter and k a shape parameter. If $k=2$, formula (4.1) reduces to a so-called Rayleigh distribution. Smaller k -values typically correspond to a calm wind climate with a few very high extremes; the opposite is true for a large k -value. For the a -parameter, it must be noted that in practice, 'a' is close to 1.1 the average of all fitted wind speeds.

Wieringa and Rijkoort (1983) state that the above formula provides good fits for a wind speed range of 4-16 m/s, so they recommended to exclude wind speeds outside this range for the Weibull fit. For the present fits, the same procedure is used while – in line with the above – calms were excluded as well. Visual inspection suggested that the fits were of good quality.

The results of the Weibull fits are presented in Table 4.1. The wind speed scale 'a', is largest for the open water stations FL2/FL26 and in winter, when it attains values of 9.9 m/s. The lowest values occur for night-time summer data for land-based or land-influenced stations:

Schiphol (Amsterdam Airport) and SL29 then have 'a'-values of 5.5-6.1 m/s. For Schiphol, the yearly averaged 'a'-value is 7.3 m/s, which corresponds to a yearly averaged potential wind speed of about 6.6 m/s, about 20% higher than the 'a'-value for 1951-1976 of Wieringa and Rijkoort (1983).

The shape parameter k tends to be about 2.6 for the open water locations FL2/FL26, and about 2.3 over land. The only other trend is that for land stations, where the nighttime k-value can drop to 2.0. Both k-trends are similar to the trends reported by Wieringa and Rijkoort (1983). Surprisingly, all k-values are significantly larger than the recommended values of Wieringa and Rijkoort (1983), which are 1.7 for land stations and 2.2 for marine stations. This trend also applies for the Schiphol-KNMI-data of 1997-2006. Hence, it is unlikely that the differences are solely caused by bias in the FL2/FL26/SL29-data. Rather, it appears that the wind conditions in 1997-2006 were different from those in the 1951-1976 period of Wieringa and Rijkoort (1983). The higher a- and k-values of the present analysis suggest that the 1997-2006 period differs from the previous period by a stronger prevalence of moderate winds, at the cost of both very light and very strong winds.

Table 4.1: Parameters of the Weibull fits for various selections of the present 1997-2006 data set. Notice that the real 10-metre wind is used for the open water locations, whereas exposure corrections are applied for Schiphol-KNMI (hence the use of U_{pot}).

	FL2 (U_{10})		FL26 (U_{10})		SL29 (U_{10})		Schiphol (U_{pot})	
	a	k	a	k	a	k	a	k
winter	9.9	2.9	9.9	2.8	8.8	2.3	8.3	2.4
spring	8.5	2.6	8.5	2.6	7.7	2.4	7.4	2.4
summer	7.8	2.5	7.7	2.7	6.7	2.3	6.5	2.4
autumn	8.8	2.6	8.6	2.7	7.7	2.3	7.1	2.3
daytime	8.8	2.6	8.7	2.5	8.2	2.4	7.9	2.6
nighttime	8.7	2.6	8.8	2.7	7.3	2.1	6.7	2.0
all data	8.8	2.6	8.7	2.6	7.7	2.2	7.3	2.3

Two features of interest remain to be discussed.

Firstly, the Weibull fit parameters of Table 4.1 are based on wind speeds only, whereas in reality, they depend strongly on wind direction. This issue is further investigated for the FL2 data. It turns out that the scale parameter 'a' ranges from 6.9 m/s for easterly winds to 9.9 m/s for south-westerly winds; both these data are yearly averages. The shape parameter ranges from 2.6 to 2.9 for north-westerly and south-westerly wind respectively.

Secondly, it should be noted that extrapolation of the Weibull fits to high wind speeds may lead to implausible situations in which very strong winds seem the most likely in the least expected situation (land station, night-time data). For SL29 such implausible situations may occur for wind speeds over 19 m/s, for Schiphol this may be the case beyond 16 m/s. Therefore, it is recommended to use Table 4.1 only for the recommended wind speed range of 4-16 m/s.

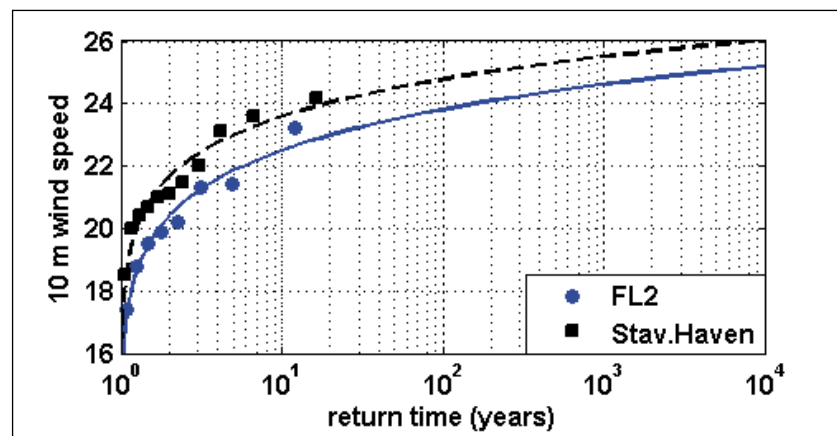
All in all, it can be concluded that the trends in Table 4.1 are in accordance with Wieringa and Rijkoort (1983). However, this is not true for the values of the Weibull fit parameters. Therefore, caution is needed when applying the present results.

4.3 Climatology of extreme wind speeds

For dike design, hydraulic conditions are needed with probabilities down to 0.0001 per year, in other words with average return times up to order once per 10000 years. As the hydraulic conditions for Lake IJssel are strongly wind-dependent, one also needs to know wind extremes with similar return times. However, the longest available homogeneous records (such as for Amsterdam Airport / Schiphol-KNMI) have a length of 50 years and are for land stations. This homogeneity is essential as inhomogeneous records tend to result in overestimations of extreme wind speeds (Wieringa, 1996; an example for Lelystad-airport is given in Taminiau, 2004).

Near Lake IJssel, Houtrib has a rather inhomogeneous record of 18 years (Taminiau, 2004); the best alternative then is Stavoren-Haven with a record length of 11 years. The best location for the present network is FL2, with an equivalent record length of 8 years.

Figure 4.4: Wind speed U_{10} as a function of return time for FL2 and Stavoren-Haven-KNMI. The data points correspond to yearly wind maxima; the lines are Weibull fits.



The above record lengths are far too short for reliable estimates of a 1/10000 year wind speed. Actually, the records are even too short to reliably determine the function by which the data should be extrapolated, so that any extrapolation is highly arbitrary. Hence, one should only consider the trends in the data discussed below, and not the values of the extreme wind speeds themselves.

As an example, Figure 4.4 shows the available yearly wind maxima for Stavoren-Haven (KNMI; 1991-2001) and FL2 (1995 + 2000-2006), together with fitted probability distributions based on Weibull functions. It should be noted that the choice for a Weibull fit is highly arbitrary, even though fits of several functions by Taminiau (2004) suggest that wind extremes obtained from Weibull-fits are rarely

outliers (in comparison with other fits). Also, it should be noted that the plotted probabilities are not simply estimated as r/N (rank r over number of data N), but as $(r-0.3)/(N+0.4)$, in accordance with Wieringa and Rijkoort (1983).

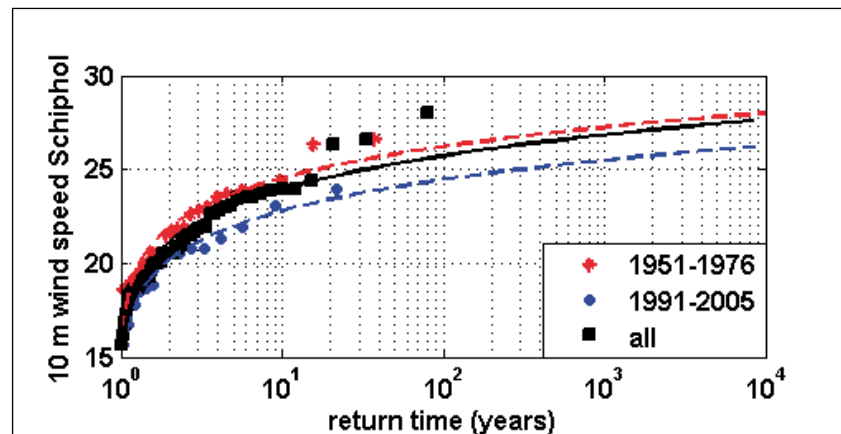
The main results of the present analysis were :

- The extreme wind climates of FL2 and Stavoren-Haven appear to be highly similar, although wind speeds for the latter station are about 1 m/s higher.
- The effect of replacing calendar years by 12-month seasons starting at 1 July is remarkably small, with less than 0.5 m/s difference in the 1/10000 year wind speeds (extra analysis, data not shown in graph).
- The actual wind extremes are less than 26 m/s. This seems unrealistically low: in the last decades, there were *five* storms where KNMI *land* stations had wind speeds of 26-28 m/s.

The latter would imply that storm winds over land would be stronger than over open water. This seems unrealistic because surface friction over land surfaces is relatively large; in addition deep depressions preferably form over sea.

For comparison, the above analysis was repeated for the potential (partly exposure corrected) wind data of the KNMI station at Amsterdam Airport (Schiphol); see Figure 4.5.

.....
Figure 4.5: Potential wind speed U_{pot} as a function of return time for Amsterdam Airport (Schiphol-KNMI); for various periods of time.



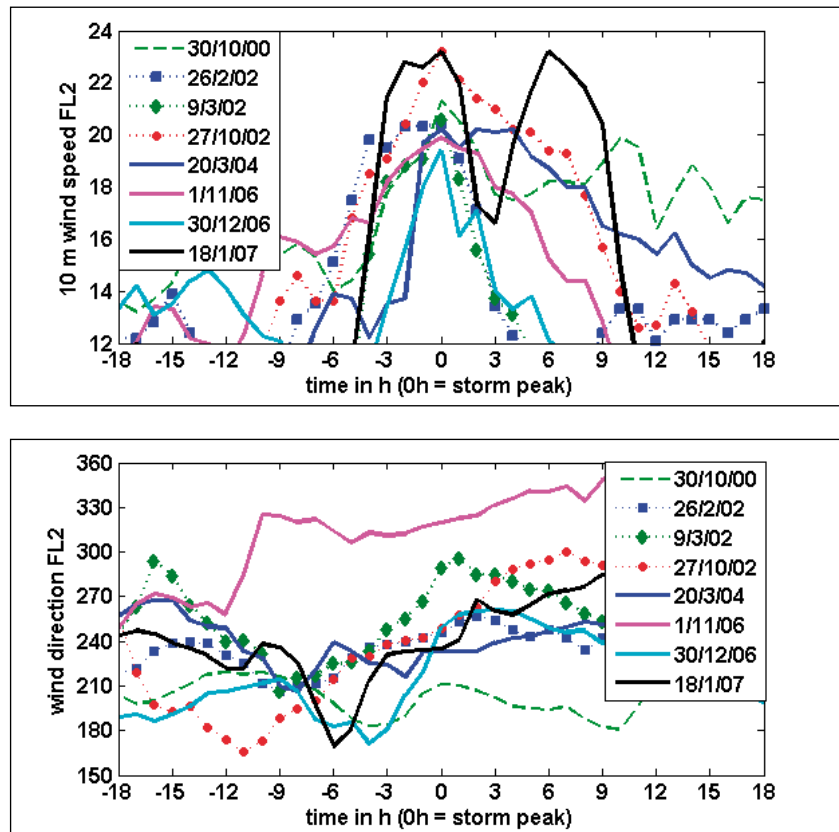
The main results for Schiphol are as follows :

- Both the measured wind speeds and the extrapolated extremes are higher than for the open-water-stations of Figure 4.4; whereas the opposite would be expected.
- The extremes of Figure 4.5 are order 10-30% lower than previously published values (Wieringa and Rijkoort, 1983; Verkaik et al., 2003). This suggests that the extremes from the present analysis tend to be too low. At least, the present extrapolation is a poor fit to the three highest data points in Figure 4.5.
- The 1951-1976 results (the same period as in Wieringa and Rijkoort, 1983) nearly give the same results as the complete data set.

- The period 1991-2005 (the period to which the data in Figure 4.4 relate) has significantly weaker storms and a lower 1/10000 year-value.

The latter observation has two important implications. Firstly, the timing of the present measuring period was unlucky by the absence of severe storms. Secondly, a record length of 15 years definitely appears to be insufficient to remove statistical variability due climate oscillations on time scales of order 5-20 years.

Figure 4.6: Evolution of 10-m wind speed (top panel) and wind direction (lower panel) for 8 different gales, based on FL2 data (except 18/1/07 when FL26 had to be used).



For dike design, one not only needs knowledge on peak wind speeds, but also on storm duration and wind directions during storms. At present, the number of storms is far too small to derive such multi-parameter statistics. Therefore, only some examples of the wind speed and wind direction evolution during gales are given, see Figure 4.6.

The upper panel of Figure 4.6 shows that storm durations are quite variable. The gales of 30/10/2000 and 18/1/2007 had the longest duration, but in the past (e.g., 1953) some storms lasted much longer. The quickest rate of wind speed increase was 6 m/s per hour at 20/3/2004 and 18/1/2007. The quickest decrease, 5 m/s per hour, also occurred at 18/1/2007. However, the average gale seems to have a typical rate of wind speed change of order 1.5 m/s per hour. The lower panel shows the evolution of wind direction. Most storms had directions between South and West-North-West, the main

exception being the NNW-storm of 1/11/2006. On average the wind veers at a rate of roughly 5° per hour, in the hours just before the peak of the storm; after the peak the veering appears to be somewhat slower. However, the storm of 9/3/2002 had a veering rate of 12° per hour. During the passage of small and intense depressions over the area of interest, the veering rate can be much larger, as was demonstrated during the 8-Beaufort case of 30/12/2006 when the veering rate even was about 25° per hour. On the other hand, the storm of 30/10/2000 passed without wind veering. Actually, some cases (after frontal passages of 8/11/2001 and 28/12/2004) even have backing 7-8 Beaufort winds.

All in all, the key results of this section can be summarised as follows: *The present estimates of extreme (1/10000 year) winds lead to the implausible result that wind extremes on land are higher than over Lake IJssel. This is despite the fact that the present method seems to underestimate wind extremes over water and over land. Besides this general result, the period 1991-2005 has a remarkable absence of severe storms, which significantly influences the extremes derived from this period.*

The duration of observed storms at FL2 is quite variable. The rate of wind speed change is typically order 1.5 m/s per hour, but can be up to 6 m/s per hour. The rate of wind veering during storms is typically 5° per hour, but both smaller and much larger values are possible.

4.4 Spatial transformation of wind

In the previous section, it was demonstrated that the measurement series for stations at or near open water are too short for an accurate evaluation of extreme wind speeds. In practice, one therefore has to use the long term statistics of a land-based (KNMI-) meteorological station, while transforming the measured wind speeds over land to an assumed wind speed over open water. This transformation can be written as:

$$(4.2) \quad U_{10,ow} = R * U_{pot,KNMI}$$

where $U_{10,ow}$ is the open water wind at 10 metre height which is to be calculated, R a transformation factor, and U_{pot} the so-called potential wind speed (Wieringa, 1986; Verkaik et al., 2003), a 10 metre wind speed which is partly corrected for exposure effects.

The transformation factor or wind speed ratio R depends on a number of factors :

- The spatially varying landscape roughness or mesoscale terrain roughness (on scales of say 5-20 km), around the KNMI-station where long-term wind statistics are taken from;
- The aerodynamic roughness of the water surface at the location where wind is to be predicted;

- Sheltering effects by nearby shores and nearby land;
- Wind speed (as it affects the roughness of water surfaces);
- Vertical temperature stratification, which determines whether or not (stronger) upper level winds can easily mix down to the surface;
- Geographical distance in relation to the typical size (generally hundreds of km but sometimes smaller) of storm fields and weather systems.

In this section, some simple model estimates for the wind speed ratio R will be considered, together with a number of measured wind speed ratios. The analysis will focus on fetch and roughness effects as temperature effects are not included in these models, while information on weather systems is often lacking. Finally, some estimates of the aerodynamic roughness of water surface will be discussed in a later section.

4.4.1. Model approaches for spatial wind transformation

In appendix E, the cornerstones for spatial wind transformation models are discussed. One of these cornerstones is the logarithmic wind profile (Tennekes, 1973):

$$(4.3) \quad U(z) = \frac{u_*}{\kappa} \ln \left(\frac{z}{z_0} \right)$$

where z is the measuring height, u_* the so-called friction velocity, κ the Von Kármán constant (~ 0.4) and z_0 the so-called roughness length. Details about these parameters, and about the range of validity of (4.2), are given in Appendix E.

An important parameter is the so-called potential wind speed U_{pot} (Wieringa, 1986; Verkaik et al., 2003). It is defined as:

$$(4.4) \quad U_{\text{pot}} = U_{10} \frac{\ln(60/z_0) \ln(10/0.03)}{\ln(10/z_0) \ln(60/0.03)}$$

where U_{10} is the (real) wind speed at 10 m height and z_0 the local terrain roughness for the first kilometre(s) near the site. In fact, replacing U_{10} by U_{pot} is equivalent to replacing the logarithmic wind profile section for 10-60 m height and the *real* roughness length z_0 by a fictitious profile with a reference roughness length of $z_0=0.03$ for open grass land. Implicitly, the approach also assumes that sheltering effects only occur in the lowest 60 metres, whereas the actual surface influences typically extend upwards to order 0.2 – 2 km. For that reason, the name 'potential wind speed' is somewhat misleading as the name suggests that all exposure effects are accounted for. Maps of the annually averaged U_{pot} (Wieringa and Rijkoort, 1983; Wieringa, 1986) show that the latter is far from true. In fact, rougher regions of order 5-10 km (like major cities and forest areas) clearly show up in these maps.

Some decades ago, some hydraulic model calculations may well have been based on a wind field where the open water wind is assumed equal to either the measured or the potential wind speed on a nearby land station. This approach clearly is not valid and a first improvement for Rijkswaterstaat RIZA was proposed by Bak and Vlag (1999). They linearly interpolated potential wind speeds from various KNMI-stations, and then applied the inverse of Equation (4.4) to evaluate their open-water wind speed estimator $U_{10,owBV}$ from the interpolated U_{pot} . Except for climate differences, this essentially is an approach with a spatially constant U_{pot} , where for the lowest 60 m, the land-roughness based wind profile section is replaced by a profile section based on an open water roughness. In this way, it is assured that the wind over open water is larger than over land. However, the adapted layer is only 60 m in height, which is generally far too shallow (see Appendix E). The above approach is called *meso transformation*, as Wieringa (1986) calls the wind at 60 m height the meso wind. In this report, the term *partially adapted open-water wind* will also be used to indicate results of this method.

As for the climate differences, Wieringa (1986) shows that after correction of all roughness effects, the average wind near Lake IJssel increases roughly 10% for each 40 km one moves to the Northwest.

An alternative for the meso transformation is the *macro transformation*, an approach based on *fully adapted open-water wind*. This approach assumes that the winds above 60 m are also fully adapted to the underlying terrain; KNMI uses a so-called meso roughness for 5x5 km blocks to describe this terrain. The present calculations according to this approach are done as follows. Firstly, the wind speeds below 60 m are calculated in the way described above. What remains to be done is to calculate the ratio of the 60 m wind speed $R_{60} = U_{60,2}/U_{60,1}$ at the two locations to be considered. Note that by definition, $U_{60} = 1.308 * U_{pot}$ (Wieringa and Rijkoort, 1983), as can be seen by applying Equation (4.3) with $z_0=0.03$ m. The ratio R_{60} is evaluated with so-called resistance laws as described in Appendix E:

$$(4.5) \quad R_{60} = \frac{U_{60|z_{o,2}}}{U_{60|z_{o,1}}} = \frac{\ln(60/z_{o,2})}{\ln(60/z_{o,1})} \left(\frac{z_{o,2}}{z_{o,1}} \right)^{0,0706}$$

where the suffixes 1 and 2 indicate the properties for location 1 and 2. The meso roughness for the KNMI-station under consideration can be looked up in the KNMI-documentation (www.knmi.nl/samenw/hydra). For open water, a Charnock formula in accordance with (Wu, 1982) is used to calculate the roughness length z_0 :

$$(4.6) \quad z_0(\text{open water}) = 0.0185 * u_*^2 / g$$

where $g = 9.81 \text{ m/s}^2$ and u_* is already introduced.

For partially adapted open-water winds (meso-transformation) and (4.6), the results are easy to summarise. For U_{pot} -values of 5, 10, 15 and 20 m/s, the ratio $U_{10,open_water} / U_{pot}$ equals 1.14, 1.11, 1.10 and 1.08 respectively. This implies that the wind differences between land and water slightly decrease with increasing wind speed because the roughness of the water surface then increases.

With *fully* adapted open-water winds (*macro transformation*), the wind speed differences between land and water increase considerably. Table 4.2 gives some typical results, where it should be noted that $z_o = 0.03$ corresponds to perfectly flat grass land that hardly occurs in practice. A $z_o = 0.1-0.2$ corresponds to a more typical open polder landscape, and $z_o = 0.4$ m to a fairly rough landscape with orchards, villages etc. (see Wieringa, 1993).

Table 4.2 Ratio of $U_{10, open water} / U_{pot}$ as calculated with the macro-transformation method (assuming fully adapted open-water wind), for various terrain roughness z_o .

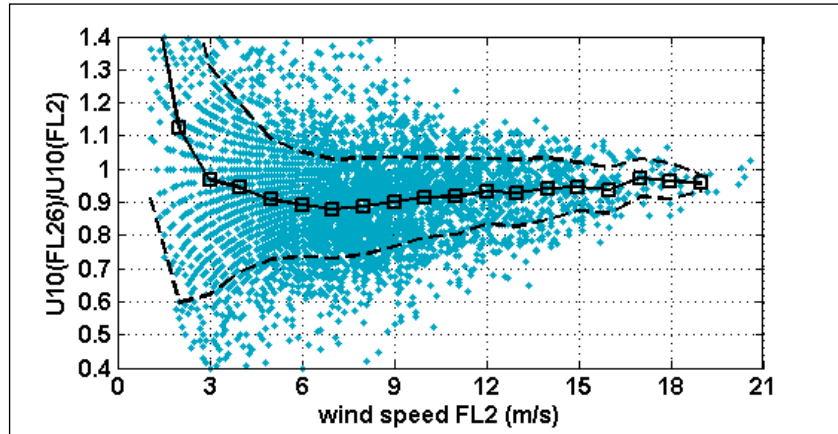
z_o (m) ->	0.03	0.1	0.2	0.3	0.4
U_{pot} (m/s)					
5	1.32	1.44	1.53	1.60	1.66
10	1.28	1.38	1.47	1.53	1.58
15	1.23	1.34	1.42	1.47	1.52
20	1.20	1.29	1.37	1.42	1.47

It should be noted that the above numbers are only valid if the wind is fully adapted to open water. Although much of this adaptation takes place in the first kilometres, a full adaptation requires some 20-50 km of fetch. To adequately account for finite fetch effects one should use a far more advanced model. In a simplified approach, one can modify the level to which the wind is adapted, or modify the effective roughness for the location under consideration. The latter approaches are used in so-called internal boundary-layer models and two-layer models respectively; see Appendix E. As opposed to the meso- and macro-transformation methods described above, such models are difficult to validate with the present data. The only exception is the application of the two-layer model to KNMI-stations near lake IJssel, as for these stations, all required roughness information can be obtained from www.knmi.nl/samenw/hydra.

4.4.2. Wind speed ratios on open water

By mutually comparing the wind speeds of the present measuring platforms, one can investigate how the wind develops over open water. In addition, such comparisons are useful when the quality and consistency of the data must be checked. However, the present network does not include land-based stations. As a result, one needs additional data before one can transform open-water-winds to a land-based site with long-term wind statistics.

Figure 4.7: Wind speed ratio $U_{10}(\text{FL26})/U_{10}(\text{FL2})$, as a function of FL2 wind speed $U_{10}(\text{FL2})$, for a westerly wind direction sector of $240^\circ - 300^\circ$. Solid the average; dashed lines are 1 standard deviation off the mean value.



Before evaluating these ratios, one first must have an indication of the scatter and trends in the underlying data. Because the roughness of a water surface depends on wind speed, it is – for given wind direction – useful to start investigating any wind-speed dependent trends.

Figure 4.7 shows that for a data subset with westerly winds, the wind speed ratio $U_{10}(\text{FL26})/U_{10}(\text{FL2})$ only weakly depends on wind speed, except for very weak winds, for U_{10} below 3 m/s. In all other cases, the wind speed ratio is between 0.9 and 1.0 with a weakly increasing trend. The relative scatter in the underlying data decreases from 40% via 20% to 10% for wind speeds of 3, 6 and 15 m/s respectively. Actually, summer observations indicate that during conditions with strong solar radiation and weak winds, a complex local lake breeze system may even develop.

Further analyses suggest that a significant part of the scatter in Figure 4.7 is not random, but correlated to the air-water temperature difference at FL26. Figure 4.8 shows the wind speed ratio $U_{10}(\text{FL26})/U_{10}(\text{FL2})$, for given wind speed and wind direction, as a function of the air-water temperature difference at FL26. It should be noted that the above is a simplified presentation for layman, and that the so-called bulk Richardson number $Ri_b = 0.5 \cdot (g/T_{air}) \cdot \Delta T / (U_{10}/10)^2$ (Kaimal and Finnigan, 1994, p. 15) represents a more correct physical scaling. In accordance with this scaling, the sensitivity of the wind speed ratio to the air-water temperature difference ΔT in Figure 4.8 is smallest for the highest wind speed class.

In reality, the situation is even more complex as turbulent exchange and wind speeds over water are not only influenced by ΔT . Water vapour also significantly influences the air density and as a result, the above stability effects are also influenced by evaporation and (sometimes) condensation. This implies that a thermally neutral atmosphere (as assumed in most wave models) not necessarily corresponds to $\Delta T = 0$, and vice versa. In fact, Oost et al (2000) present several cases where the air at some distance from the water surface is warmer than the water, while due to evaporation, the atmosphere still behaves in an unstable way.

.....
Figure 4.8: Wind speed ratio $U_{10}(\text{FL26})/U_{10}(\text{FL2})$ for westerly winds ($240^\circ\text{--}300^\circ$), as a function of the air-water temperature difference, for 3 different wind speeds.

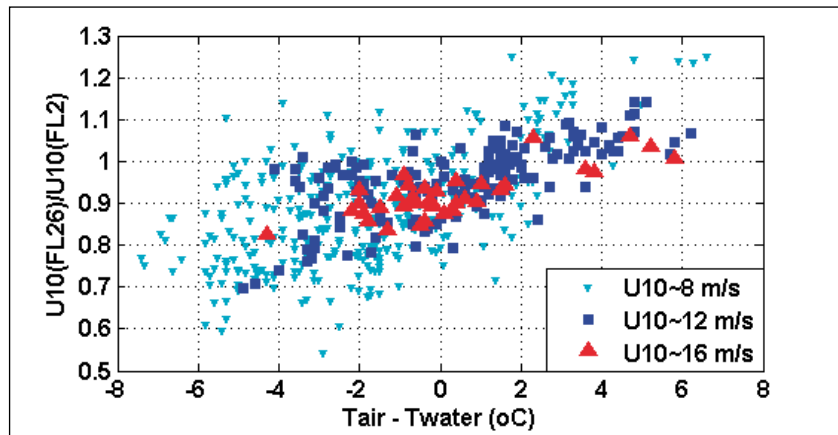


Figure 4.8 shows that for westerly winds, the FL26-winds are clearly smaller than the FL2-winds for unstable conditions (air colder than water), slightly smaller in neutral conditions, and slightly larger in stable conditions. The latter is remarkable because in stable conditions, the wind apparently overshoots for short fetches, before it decreases to its equilibrium value for long fetches.

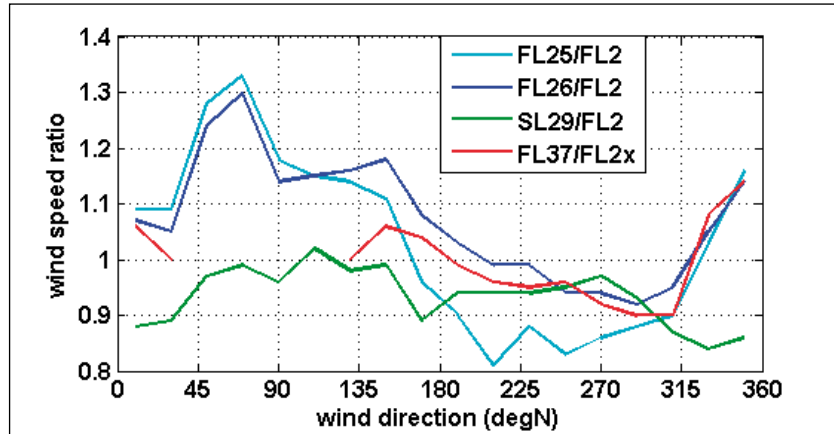
The above effects are not limited to weak winds. The above thermal stability effects may still cause 10% bias if the wind is as strong as 7 Beaufort, provided that the absolute value of ΔT is larger than 5°C . Such conditions did occur on:

- 8/4/2005, 4/7/2005, 20/5/2006 (unstable atmosphere), and
- 23/12/2004, 7/1/2005, 12/2/2005, 27/3/2006 and probably also on 26+28 January 2002, 11+12+26 February 2002 and 4 February 2004.

For the above strong-wind cases, there seems to be little random scatter. The opposite is true for moderate winds. The systematic stability trends then are larger than for strong winds, but the scatter increases even more.

For further analyses, it is assumed that the above thermal effects average out for climatic data. This assumption seems justified in moderate to strong winds. In weak to moderate winds, unstable conditions (air colder than water) tend to dominate, see Figure 4.8. For that reason, a lower wind speed limit of 6 m/s is chosen for further analyses: high enough to strongly reduce biases and scatter, low enough to be able to include easterly winds as well. The resulting wind speed ratios are shown in Figure 4.9.

.....
Figure 4.9: Wind speed ratios for the present measuring locations as a function of wind direction (wind speeds above 6 m/s only).



The comparison of the models of section 4.4.1 with Figure 4.9 is not straightforward as accurate information about effective roughnesses and fetches is not readily available. The only exception is the meso transformation method mentioned in section 4.4.1, which effectively assumes uniform wind speeds over open water. Figure 4.9 clearly shows that this is not the case, and that deviations as large as 20-30% may occur.

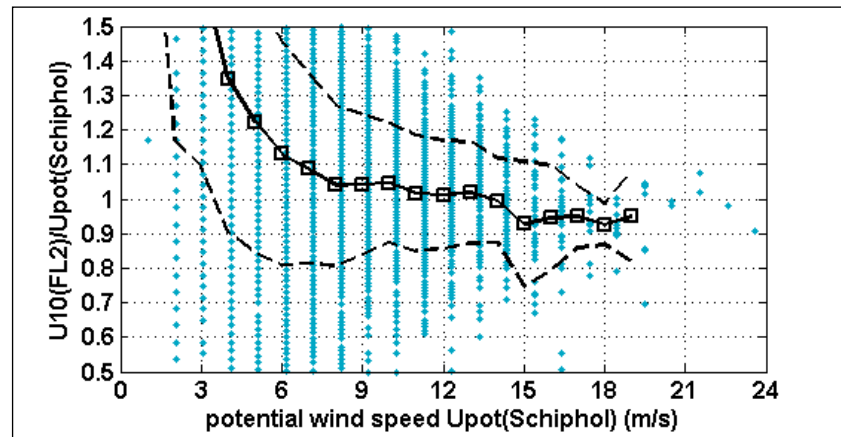
It is instructive to consider Figure 4.9 for a number of wind directions. For all wind directions, the SL29-fetches are shorter than the FL2-fetches, least so for easterly winds, most so for NW-winds. This is clearly reflected in the wind speed ratios of Figure 4.9. The large FL25- and FL26-fetches for NE-winds also clearly show up in the wind ratios, as does the strongly reduced FL25-fetch for SW-winds. However, for FL26, the situation is more ambiguous because for SW-wind, the FL26-wind is as strong as at FL2, despite the fetch difference. Apparently, some wind-direction dependent climate gradients also play a role. For FL37, only half a year of data is yet available, with the FL2 at its new (2006) position. To avoid false trends, only data points with less than 2% uncertainty are shown (this is also the maximum uncertainty in the other data). For W-NW-winds, upwind land masses seem to cause some sheltering. On the other hand, the effect of the FL2-sheltering for easterly winds seems to be unexpectedly weak. The effect of moving the FL2 1.5 km to the SW (due to digging of shipping lane in 2005, see section 2.1 and Table 2.1) is difficult to quantify exactly because no simultaneous measurements are done for the old and new location. By using FL26 as a reference for both FL2-locations, it is estimated that the new FL2 (FL2n) has about 6% larger wind speeds for easterly winds, and – somewhat unexpectedly given the fetch differences – 3% stronger winds for SW-directions, while the winds for NW-directions are 3% weaker.

4.4.3. Wind speed ratios – land and water stations

The conversion of land-based long-term wind statistics to an open-water location of interest is an essential element of the Hydraulic Boundary conditions. Because of the length of its records, the KNMI-station of Schiphol is often taken as a reference. Note that the so-

called potential (partly exposure corrected) wind speed U_{pot} is taken as a reference, not the raw U_{10} -measurements. Figure 4.10 shows the ratio $U_{10}(FL2)/U_{pot}(Schiphol)$ as a function of U_{pot} , for WSW-winds.

Figure 4.10: Wind speed ratio $U_{10}(FL2)/U_{pot}(Schiphol)$, as a function of the Schiphol potential wind speed $U_{pot}(Schiphol)$, for a WSW wind direction sector of $230^\circ - 270^\circ$. Solid line indicates mean values; dashed lines are 1 standard deviation off the mean value.



Two differences with respect to Figure 4.7 can be directly noticed:

- The discrete steps in the x-variables (as the available KNMI-data were first rounded and then corrected for exposure).
- The stronger trend in the wind speed ratio

The decreasing trend in Figure 4.10 is in accordance with both wind transformation models of section 4.4.1, but the values are not. With the meso transformation (assuming *partly* adapted open-water winds), $U_{10}(FL2)/U_{pot}$ should decrease from 1.15 at $U_{pot} = 5$ m/s to 1.08 at 20 m/s. The experimental trend in Figure 4.10 seems over *three* times as strong, but the wind speed ratios themselves seem to be 5-15% lower.

For the macro transformation (assuming *fully* adapted open-water winds), a meso-scale roughness of $z_0 \sim 0.2$ m is assumed for Schiphol (see www.knmi.nl/samenw/hydra). The resulting $U_{10}-U_{pot}$ -ratios then should be in the range of 1.53-1.37. These values are order 40% too high, but except for weak winds (< 6 m/s), the magnitude of the trend is predicted quite correctly.

Further inspection of Figure 4.10 shows that a considerable amount of data corresponds to a situation where there is more wind over land than over open water. These data seem unrealistic, unless they correspond to one of the following situations:

- passage of sharp wind variations of short duration (< 2 hour)
- small scale wind fields
- climate gradients
- thermal stability effects

The first item only occurs a few percent of time, and for strong winds, this also applies to the second item. In fact, only two recent cases are known with near-gale winds at Schiphol, and only moderate winds at FL2 (27/10/1998 and 25/11/2005). All in all, the above two phenomena do not explain more than one third of the suspect strong wind cases with $U_{10}(FL2)$ smaller than $U_{pot}(Schiphol)$. By the way, part

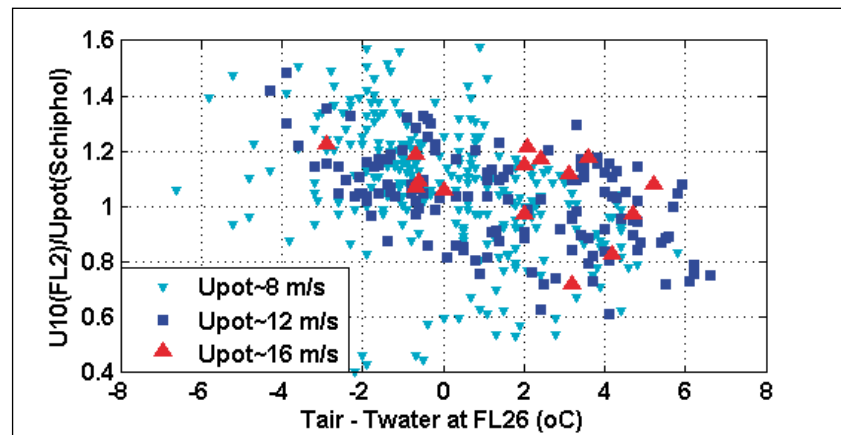
of the suspect cases is related to the strongest southwesterly gales measured so far: 27/10/2002 and 18/1/2007.

Time-averaged or climatic wind gradients do exist, but they are not expected to cause over 5% (or possibly 10%) increase of the Schiphol winds with respect to FL2 (Wieringa and Rijkoort, 1983; p. 83).

As for thermal stability effects, two strong wind cases (28/1 and 11/2/2002) have strongly stable atmospheres over Lake IJssel.

Finally, some meteorologists consider yet another possible cause of the reduced spatial wind differences during storms. Right behind intense depressions, deep mixing throughout the troposphere is a fairly common phenomenon, causing severe wind gusts. In their view, this deep mixing may also lead to situations where land-water differences in the wind are smaller than usual.

Figure 4.11: Wind speed ratio $U_{10}(\text{FL2})/U_{\text{pot}}(\text{Schiphol})$, as a function of the air-water temperature difference, for 3 different potential wind speeds $U_{\text{pot}}(\text{Schiphol})$.



Some further indications of thermal stability effects are given in Figure 4.11. Figure 4.11 suggests that wind speeds over open water tend to be weaker than those over land if there are strongly stable conditions over open water (air warmer than water); the opposite is true in unstable conditions. This even applies in relatively strong wind speeds of 12-16 m/s. Hence, it seems likely that many cases with wind speed ratios below 1 in Figure 4.10 correspond to cases with stable atmospheric conditions over water. This conclusion only applies for SW-winds at FL2. The same trend did not occur for FL26, which indicates that the above trends mainly occur for fetches larger than a few kilometres. Yet, there are also some common features for FL2 and FL26:

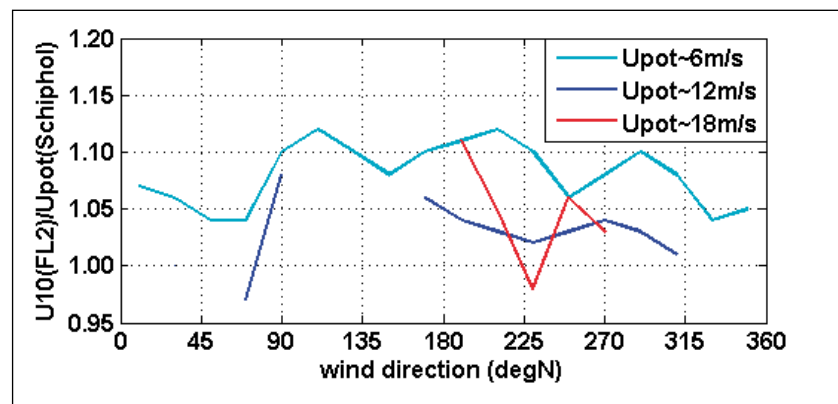
- during weak winds over land (small U_{pot}), conditions over water are often unstable, whereas they are often stable during moderately strong U_{pot} -values over land;
- The scatter is clearly larger than for the $U_{10}(\text{FL26})/U_{10}(\text{FL2})$ ratio of Figure 4.8.

Both features are related to the (unknown) stability conditions over land. These are mainly relevant for wind speeds below 6 m/s (Wieringa and Rijkoort, 1983) to 11 m/s (Bottema, 1993). During clear and calm nights, the land surface cools and this cool air is transported over the water, causing a preference for unstable conditions during weak winds.

During sunny days, the opposite is true: surface heating enhances turbulent mixing and tends to bring down the relatively high upper-layer wind speeds down to the land surface. Moderately high U_{pot} values then coincide with stable conditions over water, due to warm air being transported from the warm land surface towards (and over) cooler water. The above phenomena explain the first item mentioned above; variations in the thermal stability over land explain the larger scatter.

In practice, the above-presented temperature information is often not available, so that wind speed ratios must be evaluated from wind and terrain data alone. Figure 4.12 shows the $U_{10}(FL2)/U_{pot}(Schiphol)$ -ratio as a function of wind direction for three different U_{pot} -values: 6, 12 and 18 m/s.

.....
Figure 4.12: Measured wind speed ratio $U_{10}(FL2)/U_{pot}(Schiphol)$, as function of wind direction, for 3 different (U_{pot} -values).



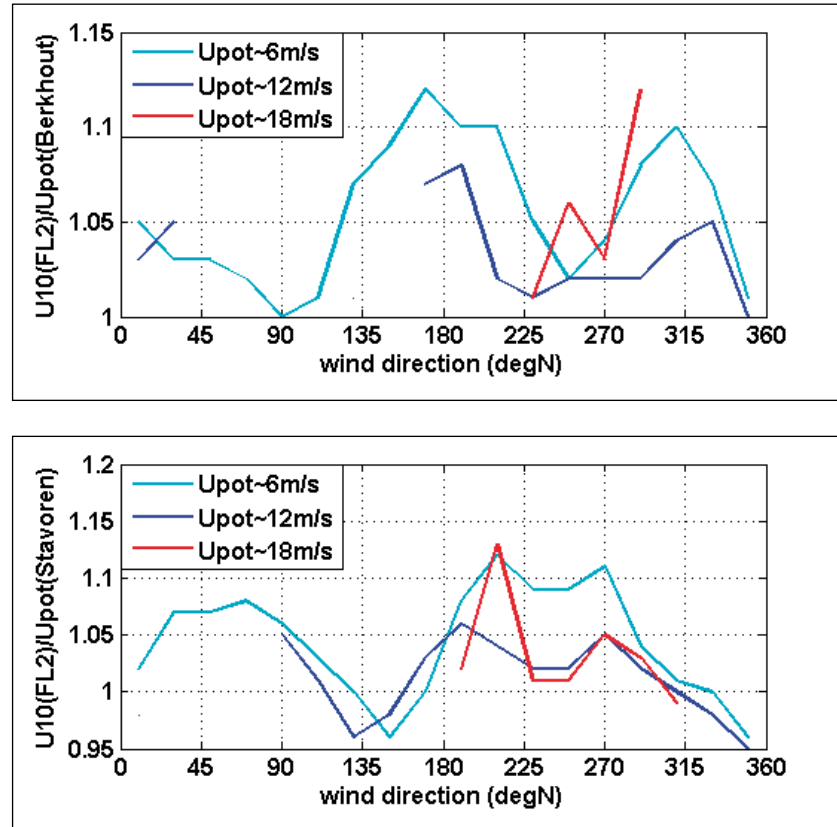
With the meso-transformation method (assuming partially adapted open-water winds) of section 4.1.1, the calculated wind speed ratio $U_{10}(FL2)/U_{pot}(Schiphol)$ should be independent of wind direction, while it varies between 1.13 and 1.09 for U_{pot} values of 6 and 18 m/s respectively.

For the macro-transformation method, the landscape roughness (z_{om}) should also be taken into account. For Schiphol, z_{om} is about 0.2 m for wind directions between 130° and 290°. For the remaining directions, z_{om} increases to a maximum of 0.4 m at about 20°. The resulting wind speed ratios are 1.52-1.64 for $U_{pot} = 6 \text{ m/s}$ and 1.39-1.49 for $U_{pot} = 18 \text{ m/s}$.

The experimental wind speed ratios are nearly all below the model values mentioned above. Contrary to expectations, the meso transformation (without theoretical basis, assuming an arbitrary degree of partially adapted open-water winds) often yields results close to the measurements. By contrast, the macro transformation typically yields wind speed ratios that are order 40% too high, even though its theoretical basis is sound. In fact, the only weak point in the latter approach is the assumption that winds are *fully* adapted to open-water conditions, whereas in practice, they are rather *nearly* adapted.

As the above results are quite unexpected, similar comparisons were made between FL2 and the U_{pot} of the land-based KNMI stations Stavoren and Berkhout. Their main advantage is their proximity to FL2: 20 and 40 km only. Their disadvantage is their limited record length: only about 7 years. The results are shown in Figure 4.13; by and large, the results are quite similar to those of Figure 4.12.

Figure 4.13: As Figure 4.12, with potential wind speed of Berkhout-KNMI (top) and Stavoren-KNMI (below) as reference.



Although Figure 4.12-4.13 may suggest differently, the above does not imply that the meso-transformation method of section 4.1.1 is correct in general. Besides the fact that a theoretical basis is lacking (see Appendix E), there is a non-negligible number of situations where this method is empirically incorrect:

- Cases where a land-based U_{pot} exceeds U_{10} over open water (at FL2), as shown in Figure 4.12-4.13.
- Similar cases for FL26 and FL37, where U_{10} for westerly winds is often *below* U_{pot} and about 7% below the U_{10} of FL2 (Figure 4.9). For FL25 (SW-winds) and SL29 (NNW-winds) the reductions can be even stronger, but in those cases the fetch is less than 1 km, too short for real open water conditions.
- Easterly wind cases for FL25 and FL26: in those cases, U_{10} is 10-30% larger than at FL2 and up to 40% larger than U_{pot} (instead of the assumed maximum of 1.12).

Despite the above problem cases, the meso transformation still seems to perform somewhat better than the macro transformation, despite

the far better theoretical basis of the latter. However, if the meso transformation is to be used, it should be valid for more than just a set of KNMI-stations with near-ideal smooth terrain (like Schiphol, Berkhout and Stavoren), and its underlying assumptions should be valid as well. The latter implies that there should be no spatial variation of U_{pot} , at least not over short distances.

Figure 4.14: Potential wind speed ratios between various KNMI-stations as a function of wind direction, with Schiphol as a reference and for U_{pot} (Schiphol) ~ 12 m/s.

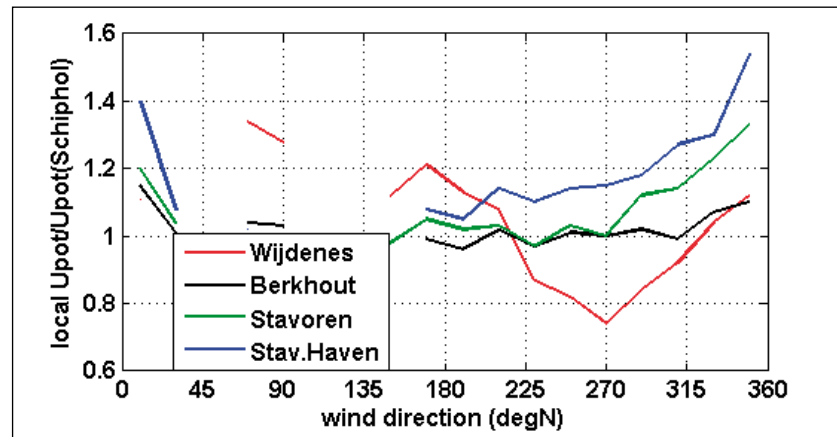


Figure 4.14 shows the potential wind speed ratios for various KNMI-stations. The meso transformation method assumes these ratios to be 1, unless there is influence of large-scale climate gradients. Although part of the data is uncertain by lack of underlying data (from NNW-winds through NE to SSE), it is still possible to identify some trends :

- For northerly winds, all ratios tend to be greater than 1, apparently due to a rougher landscape North of Schiphol.
- For westerly winds, the Wijdenes ratio drops below 0.8 due to rough terrain upwind of that location (orchards, poplar shelterbelts)
- Stavoren-Haven has increased ratios for nearly all westerly winds, presumably due to its position on the shore of Lake IJssel.
- For NW-winds, the short fetch from Lake IJssel also becomes noticeable in the Stavoren data.
- Otherwise, Stavoren and Berkhout seem to be as good a location as Schiphol, as their U_{pot} ratios are nearly 1.0.

The latter point explains why the trends in Figure 4.13 were similar to those in Figure 4.12. In a more general sense however, the underlying assumptions of the meso-transformation method can imply a wind speed mismatch of over 20%.

If the macro transformation is to be valid, then Eq. (4.5) must be valid with the meso roughnesses z_{om} of www.knmi.nl/samenw/hydra . The following results were found:

- For N-NNE-wind, z_{om} is 0.005 m (Stavoren-Haven) to 0.1 m (Berkhout) near Lake IJssel, and 0.4 m at Schiphol. The U_{pot} ratios then should be 1.16-1.37, which is in accordance with Figure 4.14.
- For S-SW-wind, z_{om} at Wijdenes increases from 0.001 to 0.03 m; at Schiphol it is 0.2 m. The U_{pot} ratios then should decrease from 1.33

to 1.17; the ratios in Figure 4.14 are 10-25% lower.

- For winds of South to West, the z_{om} and U_{pot} ratio of Berkhout and Schiphol are both nearly 1.0, in accordance with Eq. (4.5).
- For wind directions around WNW, the z_{om} values at Wijdenes and Schiphol are 0.3 and 0.2 m respectively; the U_{pot} -ratio then should be 0.95. The real sheltering is at least 10% stronger (Figure 4.14).
- Last but not least, Stavoren-Haven faces open water for westerly winds, with z_{om} between 0.004 m (SW) and 0.0001 m (NW). The corresponding z_{om} 's of Schiphol are 0.2 and 0.3 m, which yields U_{pot} -ratios of 1.28 to 1.43. However, the ratios of Figure 4.14 are 10-15% lower.

All in all, the macro-transformation method seems to perform quite well, unless the terrain is much rougher or smoother than of Schiphol. Unfortunately, the latter is generally the case. A point of lesser importance is the fact that the above z_{om} -values for open water are often a few times larger than those of Eq. (4.6). However, the effect of this on the U_{pot} -ratios is 5% or less. Still, it is worthwhile to consider to actual open-water-roughnesses, as will be done in the next section.

Finally, the main conclusions of this section can be summarised as:
In some, but not all, cases the wind speeds over open water are unexpectedly low. As a result, there is no single wind transformation method that has proven to be satisfactory for all cases. A complicating factor is the fact that in most of the experimental data range, air-water temperature differences significantly influence the wind speeds over land and especially over open water.

4.5 Turbulence and roughness data

The aerodynamic roughness of the wavy water surface of Lake IJssel is a key parameter in the underlying models to evaluate dike design conditions. This not only applies to models for spatial wind transformation, but also to wave models and models that calculate wind-induced currents and wind-induced set-up of the mean water level (storm surge). It is important to measure the above roughness since most literature expressions for roughness parameters are valid for long fetches, deep water and moderate wind (up to 10 Beaufort) only. Situations with 'slow' waves due to short fetch may significantly increase the roughness. In shallow water, modified wave steepnesses may also play a role. Finally, the trend of increasing roughness with stronger wind may reverse if spray generation by wave breaking is so intense that the wind 'loses its grip' on the water surface (Makin, 2003). The following issues will be discussed in this section:

- Definition of roughness parameters and role in the modelling chain for dike design conditions
- Methods to evaluate roughness parameters for the present data set, and their accuracy

- Turbulence data and resulting roughness parameters
- Roughness parameters from wind profile analysis

Definition of roughness parameters; relevance for dike design

The roughness length z_0 is an integration constant in the logarithmic wind profile that is discussed in section 4.4 and Appendix E. In physical terms, it represents a turbulence scale near the surface rather than a surface property itself. For many land surfaces, z_0 is roughly order 10% of the obstacle height. However, for water surfaces, the ratio of z_0 to the water wave height is generally much smaller. For many engineering applications, the surface roughness is expressed in terms of a drag coefficient $C_D = (U(z)/u_*)^2$, where $U(z)$ is the mean wind speed at level z , and u_* the so-called friction velocity, where ρu_*^2 (with ρ the air density) represents the surface drag force per unit area that is exerted by the wind. Typical expressions for C_D (Wu, 1982) and z_0 (Charnock, 1955) for open water are :

$$(4.7) \quad C_D(z=10\text{ m}) = 0.001 \cdot (0.8 + 0.065 \cdot U_{10})^2 ; z_0 = 0.0185 u_*^2 / g$$

with g the gravity acceleration (9.81 m/s^2).

For the evaluation of dike design conditions, C_D is a vital parameter as it not only plays a role in spatial wind modelling, but also in the modelling of storm surge effects and of wind waves.

The importance of accurate C_D -estimates for dike design is illustrated in (Waal, 2003). His lowest z_0 -value of 0.0002 m corresponds to the open water z_0 recommended by Wieringa (1993), while his 'central' z_0 -value of 0.0008 m is consistent with the above Eq. (4.7) with a U_{10} of 15 m/s. The corresponding C_D -values are 0.00137 and 0.00180. Note that the z_0 -values differ by a factor 4, and the C_D values only by a factor 1.31. Figure 10.18 in (Waal, 2003) can be used to demonstrate the effect of the above z_0 - and C_D -difference in typical dike design conditions for Lake IJssel, with an open water U_{10} of about 35 m/s, and a fetch and water depth of 20 km and 5 m respectively. For a dike with 1:4 slope without berms, the wave run-up ($h_{2\%}$) and the required dike height for those conditions are about 4-5 m. The above z_0 - and C_D -differences of a factor 4 and 1.31 yield 6% difference in required dike height, or about 24-30 cm in absolute terms. This is quite a relevant uncertainty, as is illustrated by the following. The RWS Warning service for the Dikes near Lake IJssel (WDIJ) uses alarm levels which are defined as follows: If the probability for (storm) events where wave run-up reaches the crest of the dike is denoted as P , then the alarm level corresponds to the wave run-up height of events with a probability of *ten* times P (Reitsma, 1997). At the RDH site, the alarm level is about 1 m below the dike top. The 24-30 cm dike height differences resulting from the above C_D and z_0 -uncertainties therefore correspond to an uncertainty in (flooding) probability of about a factor 2. This implies that the roughness parameters C_D and z_0 are definitely

relevant in the modelling chain for dike design conditions.

Roughness parameter evaluation methods, and their accuracy
The conventional method to derive z_o is to fit the measured wind at different levels to the logarithmic wind profile. In the present case, none of the locations has sufficient levels for real wind profile fits. However, for FL2, the roughness length z_o can be directly evaluated from the ratio of the 3-metre and 10-metre wind by:

$$(4.8) \quad U_3/U_{10} = \ln(z_3/z_o) / \ln(z_{10}/z_o)$$

where z_3 and z_{10} are the heights of the 3- and 10-metre sensors above the *actual* water level. It should be noted that Eq. (4.8) is only valid if thermal stability effects on the U_3/U_{10} -ratio are negligible. Common error sources in this way of estimating z_o are related to disturbances (obstacle effects or thermal stability effects) affecting U_3/U_{10} , inaccuracies in (the assumed) actual water level and inaccuracies in each of the measuring heights with respect to the NAP datum. With an assumed reference z_o -value of 0.001 m, the effect of these error sources is as follows:

- A deviation of just 1% in U_3/U_{10} causes a factor 1.81 difference in z_o and 14% difference in C_D ;
- A 20 cm inaccuracy in height of the 3m-sensor yields a factor 1.64 difference in z_o and 11% difference in C_D .
- A 20 cm inaccuracy in height of the 10m-sensor yields a factor 1.14 difference in z_o and 3% difference in C_D .
- A 20 cm water level inaccuracy yields a factor 1.41 difference in z_o and 8% difference in C_D .

If z_o - and C_D -inaccuracies greater than a factor 4 and 1.31 are no longer accepted, the above results imply the following:

- Deviations in U_3/U_{10} (from obstacle or stability effects) should be 2% or less.
- Deviations in the 10m mounting height play a minor role, even if they are 50 cm.
- Deviations in water levels and the 3m mounting height do not seem as critical as the U_3/U_{10} -deviations, but preferably, they are reduced as much as possible.

If the above wind profile approach is not preferred, or if only one wind sensor is available, roughness parameters can also be derived from the turbulence intensity T_u :

$$(4.9) \quad T_u(z) = \sigma_u/U(z) = (\sigma_u/u^*)\kappa / \ln(z/z_o) \sim 0.96 / \ln(z/z_o)$$

where σ_u is the standard deviation in the sampled wind speed, and κ the Von Kármán constant (~ 0.4). Note that T_u is often expressed as a percentage, e.g. $T_u = 10\%$ instead of 0.1. The main error sources are due to deviations in the T_u -value (due to thermal stability or obstacle effects), in the mounting height and/or water level, in the Von Kármán

constant κ , or in the σ_u/u^* ratio. The examples below demonstrate that the main focus should be on deviations in T_u , κ or σ_u/u^* :

- A 20 cm mounting height or water level inaccuracy yields 2% error in measuring height and z_0 ; the C_D error then is 0.4%;
- A factor 1.1 deviation in T_u , κ or σ_u/u^* yields a factor 2.3 error in z_0 and a 21% error in C_D .

The actual deviations in T_u , κ or σ_u/u^* for a given case are hard to assess as they depend on averaging time (in this case: 1 hour) and on obstacle effects, thermal stability and the presence or absence of turbulence that is not generated near the earth's surface. Some examples are given below:

- The range of published Von Kármán constant values κ is 0.35-0.44, well above the above-mentioned range of a factor 1.1. However, the most common κ -values are 0.40 and 0.41 (2.5% difference).
- For an ideal thermally neutral atmosphere, most published σ_u/u^* -values are about 2.4 (Panofsky and Dutton, 1984, as adopted here) or 2.5, a 4% difference. However, these values can become twice as large (Panofsky and Dutton, 1984) if extra turbulence is present due to thermal convection, upstream hills and/or upper-air turbulence.
- The T_u -values can also be modified by flow distortion due to the measuring platform and due to averaging time effects. The latter can cause a factor 1.1 difference in T_u ; see the gust factor discussion below. At the 10 m level, no flow distortion effects were detected in the mean wind and turbulence, which was to be expected as the relative distance between the wind sensors and the main obstacle (the solar panels) was about 5 obstacle diameters; see Photo 1.

In many routine measurements, T_u is not measured but maximum gusts are. Wieringa (1986) presents a rather complex formula that allows to calculate z_0 from so-called gust factor measurements:

$$(4.10) \quad GF = \frac{U_{\max}}{U_{10}} = A_{AT} \frac{1 + [1.42 + 0.3 \cdot \ln((1000U_{10}t) - 4)]}{\ln(z/z_0)}$$

where GF is the gust factor, U_{\max} the maximum gust of duration t and A_{AT} a constant that depends on averaging time; A_{AT} is 1.0 for 10-minute values and 1.1 for the hourly values used here. For further explanations, the reader is referred to Wieringa (1973, 1986). The error propagation arguments are essentially the same as for T_u . However, it should be noted that not the effect of GF are similar to T_u , but the effects of $(GF-1)$. In practice, a given relative GF-variation has less effect than the same relative variation in $(GF-1)$ as the former is typically about 1.35 and the latter about 0.35.

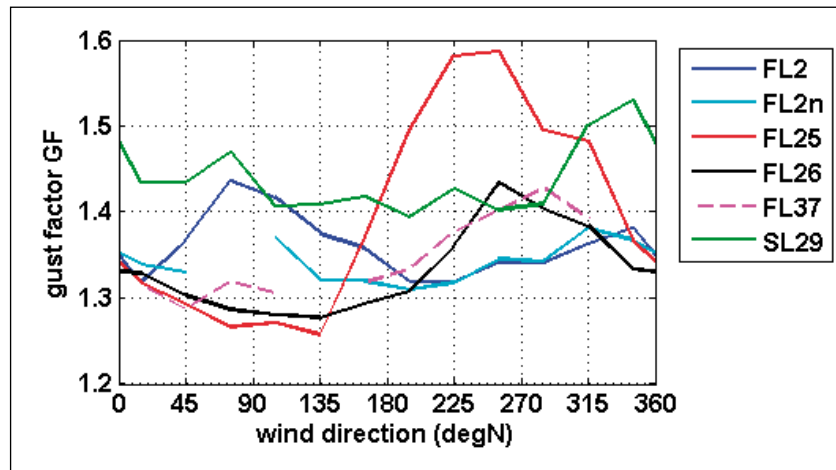
Finally, it is important to note that T_u , σ_u/u^* and GF all need several kilometres to fully adapt to a new underlying surface, whereas the wind profile in the lowest 10 metres only needs order 0.2-1.0 km for

full adaptation. Hence, the above turbulence-based methods are only suitable for fetches in excess of 5-20 km.

Turbulence data and resulting roughness parameters

In previous publications like (Bottema, 2006b), it was demonstrated that flow distortion by the measuring platform typically affected the U_3/U_{10} -ratio by 4-10%. Since the U_3/U_{10} -errors were considered to be too large, the analysis of turbulence data was considered to be an interesting alternative. Figure 4.15 gives an impression of the main trends in the gust factor GF for cases with at least 5 Beaufort winds.

.....
Figure 4.15 Gust factor GF as a function of wind direction for each of the measuring locations, for conditions with $U_{10} > 8$ m/s only.



In most cases with onshore winds and at least 10 km of fetch, the average gust factor is 1.35 or less. On the other hand, GF can strongly increase for cases with offshore winds and short fetches. Offshore winds at FL2, FL26 and even FL37 can lead to gust factors of about 1.43. On Lake Sloten, gust factors are elevated for all wind directions due to the short fetch. With wind along the lake, the SL29 gust factors are slightly above 1.4, but for the short fetches associated with NNW-winds, the average gust factor even exceeds a value of 1.5. However, the highest gust factors occur at FL25 during offshore winds: the town of Enkhuizen and upstream trees then lead to an average gust factor of nearly 1.6.

No separate turbulence intensity graphs is shown as the trends are nearly identical due to the excellent (linear) correlation between GF and T_u . Typical T_u -values are 9.2%, 11.5% and 13.8% for GF values of 1.3, 1.4 and 1.5 respectively. Note that these measurements are in accordance with Wieringa and Rijkoort (1983), who give typical T_u -values for open water and open terrain which are 8% and 16% respectively.

Because roughness estimates are most interesting and most accurate during strong winds (because of smaller thermal stability effects), it makes sense to focus on cases where strong winds are most likely, i.e. SW-winds. Since FL2(n) has the best exposure for these SW-winds, only FL2(n) data will be considered from here. As the roughness

parameters in Eq. (4.7) are U_{10} -dependent, we will first investigate the U_{10} -trends. The results are shown in Table 4.3.

Table 4.3 Average turbulence parameters (with 1σ scatter) at FL2 (1997-2007) for SW-winds, with experimental and theoretical z_0 and C_D .

U_{10} (m/s)	9-11	14-16	17-23
GF (-)	1.314 ± 0.103	1.366 ± 0.078	1.399 ± 0.068
T_u (%)	9.4 ± 2.8	10.6 ± 1.7	11.5 ± 1.1
$z_{0,GF}$ (m)	$5.93 * 10^{-6}$	$1.66 * 10^{-4}$	$7.87 * 10^{-4}$
z_{0,T_u} (m)	$3.67 * 10^{-4}$	$1.17 * 10^{-3}$	$2.37 * 10^{-3}$
$z_{0,Eq.47}$ (m)	$2.74 * 10^{-4}$	$7.53 * 10^{-4}$	$1.62 * 10^{-3}$
$1000 * C_{D,GF}$	0.78 ± 0.93	1.32 ± 0.89	1.79 ± 0.91
$1000 * C_{D,T_u}$	1.53 ± 0.13	1.95 ± 0.68	2.30 ± 0.45
$1000 * C_{D,Eq.47}$	1.45	1.78	2.10

First of all, it turns out that all turbulence and roughness parameters have an increasing trend with U_{10} . However, there is significant scatter in the underlying data. For the gust factor GF, the relative scatter (1 standard deviation divided by mean value) is 8% for moderate wind to 5% for strong winds. For T_u , these figures are 30% and 10%. The resulting scatter in the non-averaged z_0 -data is so large it could not be included in the table: it is a factor 6-100 when derived from GF and a factor 2-6 when derived from T_u . The trends in the relative C_D -scatter are less straightforward: they are 51-120% when C_D is derived from GF and 8-35% when derived from T_u . This large scatter implies that a single storm rarely provides enough data for suitable estimates of roughness parameters. Furthermore, it should be noted that roughness estimates from gust factors GF are relatively uncertain, even though the scatter in GF itself is relatively small.

Comparison with literature and theoretical values also yields some interesting results:

- The C_D -estimates from T_u agree excellently with Wu's (1982) parametrisation (Eq. (4.7)), although the present C_D -estimates are consistently 5-10% higher.
- For moderate wind speeds, many gust factor estimates of z_0 are physically unrealistic as they are below the theoretical lower z_0 -limit for a perfectly smooth surface (Tennekes and Lumley, 1972), which is slightly lower than 10^{-5} m for moderate winds.

For the latter reason, and because of the far greater amount of scatter, the gust-factor method is preferably not to be used if roughness parameters can also be derived from turbulence intensity data. Besides this, there are also some theoretical objections against the gust factor method (Verkaik, 2000).

Roughness parameters from wind profile analysis

The above turbulence-based roughness analysis assumes that the turbulence is fully adapted to the open-water-conditions. Typically, the complete atmospheric boundary layer needs at least order 20 km for full adaptation (Jensen, 1978). So even for long-fetch conditions with onshore winds at FL2, it is not fully certain whether the turbulence

is fully representative for open water conditions. For reliable wind profile analysis, the required fetch is only order 100 times the highest measuring height. At present the upper level is at 10 m height which yields a required fetch of order 1 km. On the other hand, the lower 3m-level at FL2 is significantly disturbed by the measuring platform, as is illustrated in Figure 4.16.

.....
Figure 4.16 Average wind speed ratio U_3/U_{10} at FL2, as a function of wind direction, for $U_{10} > 8$ m/s.

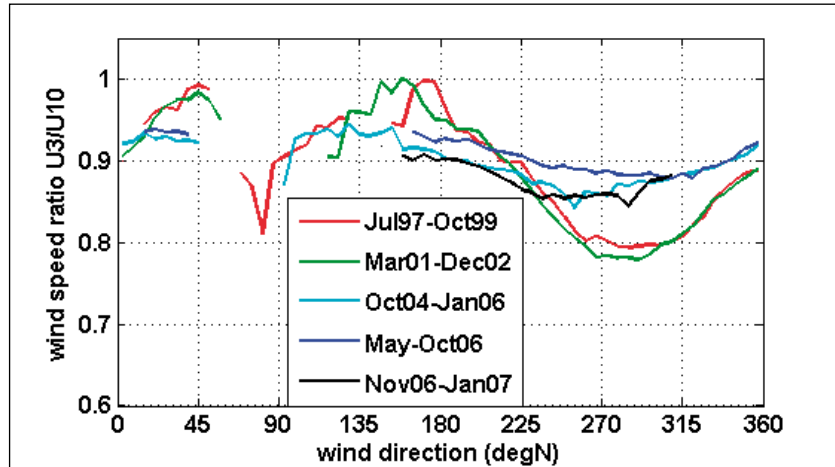
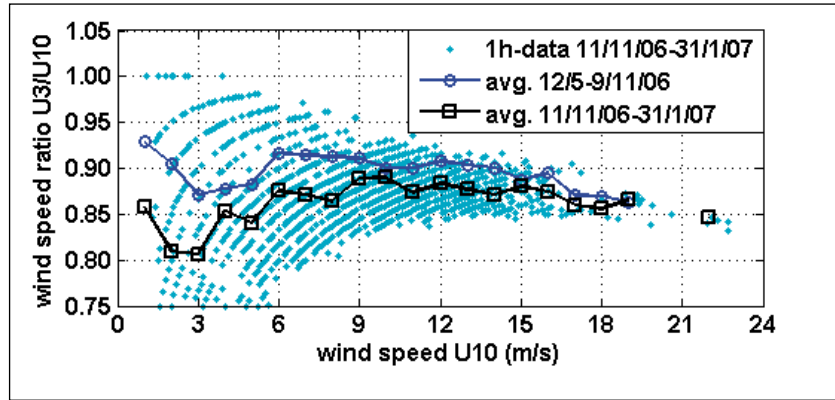


Figure 4.16 shows the wind speed ratio U_3/U_{10} at FL2 as a function of wind direction. Until October 2004, the 3-metre-boom only extended about 1.5 m westward from the platform. This resulted in significant disturbance of the 3-metre-winds (U_3) at FL2. For NE- and SSE-winds, U_3 increased about 10% as the wind 'squeezed' along the sides of the platform. For W-WNW winds, U_3 was reduced by about 10% because of flow blockage in front of the platform. For easterly winds, U_3 was reduced even more as the sensor then was in the wake of the platform.

Wind profile analyses with the desired 1-2% accuracy in U_3/U_{10} are clearly impossible with the type of error. Therefore, the 3-metre-boom was extended by another 2 metres during September 2004. Figure 4.16 shows that the resulting platform disturbance is much smaller indeed. When the wind is along the boom axis and towards the platform, the U_3 -reduction is about 2%. The actual reduction depends on the period under consideration because some modifications to the platform position and orientation were made in March, May and November 2006. However, most sub-periods have either a lack of strong wind conditions, or they lack an accurate specification of the actual height of the 3-m wind sensors. The only period that is suitable for in-depth analyses starts at 11/11/2006; the actual height of the 3-m sensor then is +3.55 m NAP. Before starting the actual roughness analysis, it is useful to investigate the U_3/U_{10} -trends as a function of wind speed. See Figure 4.17.

Figure 4.17 Average wind speed ratio U_3/U_{10} at FL2, as a function of wind speed U_{10} , for wind directions of 210° - 310° .



The cyan points in Figure 4.17 represent hourly data for the period 9/11/2006 to 31/1/2007; the black line with squares represents the average of these data. The blue line with circles represents the average for the period of 12 May – 8 November 2006, with a slightly different wind direction range of 230° - 330° .

For weak winds, the U_3/U_{10} -trends are rather ambiguous as the scatter in the underlying data is very large. For winds above 5-6 Beaufort, the scatter becomes relatively small while the U_3/U_{10} -ratio tends to decrease with wind speed. Much of this scatter correlates with the air-water temperature difference. Typically, 2°C change in the air-water temperature difference yields order 3-4% change in the U_3/U_{10} -ratio for $U_{10} \sim 8$ m/s, and order 1.5-2% change for $U_{10} \sim 16$ m/s. In all cases, stable atmospheres (air warmer than water) yield the lowest U_3/U_{10} ratios.

The resulting roughness parameters are given in Table 4.5, where it should be noted that a +2% obstacle correction is applied on the U_3/U_{10} -ratio.

Table 4.4 Wind speed ratios U_3/U_{10} (for 9/11/2006-31/1/2007 and wind directions of 230° - 330°), average water levels, calculated experimental z_0 and C_D , as well as theoretical values.

U_{10} (m/s)	10	15	19	22
Meas. U_3/U_{10}	0.89	0.88	0.865	0.846
Corrected U_3/U_{10}	0.908	0.898	0.882	0.863
Avg. water level (m NAP)	-0.06	0.16	0.28	0.28
$z_{0,prof}$ (m)	$1.1 \cdot 10^{-4}$	$5.2 \cdot 10^{-4}$	$2.39 \cdot 10^{-3}$	$7.63 \cdot 10^{-3}$
$z_{0,Eq.47}$ (m)	$2.74 \cdot 10^{-4}$	$7.53 \cdot 10^{-4}$	$1.41 \cdot 10^{-3}$	$2.1 \cdot 10^{-3}$
$1000 \cdot C_{D,prof}$ (m)	1.23	1.64	2.30	3.11
$1000 \cdot C_{D,Eq.47}$ (m)	1.45	1.78	2.04	2.23

The resulting C_D -values for moderate wind speed tend to be 8-15% below the theoretical Wu (1982) values, and 15-20% below the earlier discussed C_D -estimates from the turbulence intensity T_u . Given the uncertainties in the profile-derived C_D -values (1% error in U_3/U_{10} yields 14% error in C_D), this agreement is quite good. During storms, the profile-derived C_D tends to be higher than Wu's (1982) C_D , with a difference as large as 39% for a 22 m/s wind speed. Although this evidence is only based on one storm case (18/1/2007), it is still interesting as 39% C_D -increase over water will reduce the land-water

speed difference by order 8%. In this way, it might help to explain why most land-water wind speed differences disappear during storms (see Section 4.4).

Aerodynamic roughness and water waves

On a final note, it is interesting to consider the relation between water waves and the aerodynamic roughness parameters z_o and C_D .

In many applications, z_o is roughly proportional to the height of obstacles at the earth's surface. Hence, the ratio z_o/H_{m0} (with H_{m0} the significant wave height) is considered first. For westerly winds of 10, 15 and 20 m/s, FL2 has a H_{m0} of about 0.65, 1.0 and 1.4 m respectively (see Chapter 6), i.e. a factor 2.2 H_{m0} -increase for the wind speed range of 10-20 m/s. For same wind speed range however, the z_o -increase is between a factor 6 (turbulence intensity method) and a factor 30 (profile method). This implies that other factors are at least as significant as the z_o/H_{m0} -ratio.

Possibly the most important of these other factors is the wave age parameter U_{10}/c_p , where c_p is the phase speed of the waves. Typically, situations with large U_{10}/c_p -values tend to produce larger roughnesses. These 'slow wave' situations may be related to shallow water effects (as in the long-wavelength cases of Oost, 1998), or to short fetches. The measured peak periods T_p at FL2 are typically 3.3 and 5.2 for onshore wind speeds of 10 and 20 m/s respectively. For deep water, this would yield U_{10}/c_p -values of 2.0 and 2.4. For FL2 however, shallow water effects become significant above 5 Beaufort, and the real U_{10}/c_p -values are 2.0 and 3.4 respectively. This increasing U_{10}/c_p -trend is consistent with the observed increase of z_o/H_{m0} with wind speed. For depth-limited conditions however, the effects on z_o of slower waves on one hand, and wave breaking on the other hand, may well be counteracting. Hence, reliable z_o -measurements seem to be essential if z_o is to be known in depth-limited conditions.

All in all, the above at least provides some insight in the relation between wind waves and aerodynamic roughness of the water surface. For practical purposes, it is important to know whether the drag parametrisation of Eq. (4.7) holds for Lake IJssel. The present data are obtained without dedicated instrumentation (for this purpose) and are too inaccurate for definite conclusions. By and large, they suggest that Eq. (4.7) may be a good approximation in mild conditions. For storms, too few data are yet available, but it appears that caution is needed when applying Eq. (4.7) in these conditions.

4.6 Air and water temperatures

A thermally neutral atmosphere is a key assumption in many hydraulic models, especially in relation to the air-water exchange of momentum. When the effects of water vapour on the air density are neglected, such a neutral atmosphere occurs when air and water temperatures

are equal. Besides this, water temperatures are highly relevant. From a broad operational viewpoint, it is important to know how quick and how often Lake IJssel freezes over. From an ecological (and recreational and water consumer's) viewpoint, episodes with high temperatures are relevant as they may affect the water quality. In winter the water quality effect is mainly indirect through the shellfish filtering the water, in summer the effects are rather direct through growth of bacteria and algae, and decrease of oxygen levels.

Figure 4.18 Daily averaged water temperatures at FL26 as a function of Julian day number (Mar 2001- Jan 2007).

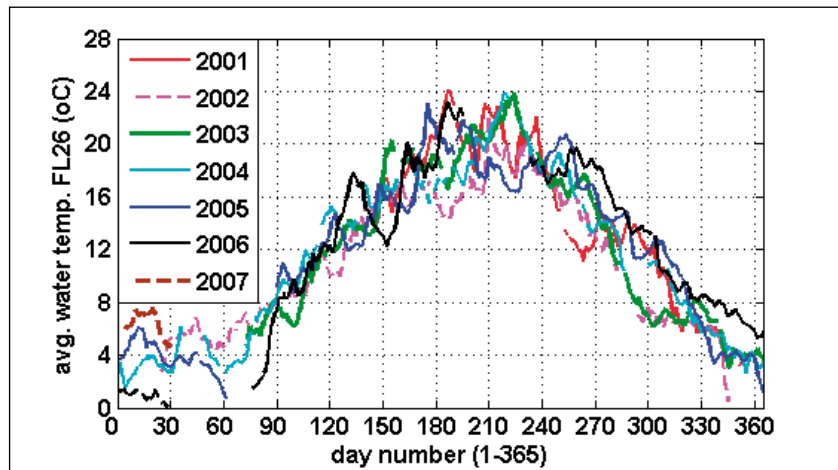


Figure 4.18 shows the measured water temperatures at FL26 during the last six years. Note that from December to March, significant parts of 2001, 2002 (Dec.), 2003, 2005 (Mar.) and 2006 (Feb.) are missing because of measuring interruptions due to ice. For the remainder, typical water temperatures range from 16-24°C in summer to 0-8°C in winter. On average (and year-round), the present FL26 temperatures are $1.5 \pm 0.7^\circ\text{C}$ higher than those of the Breezand series (1959-1992) for the North of Lake IJssel (see www.waterbase.nl). As spatial temperature differences in Lake IJssel generally appear to be small, it is likely that this temperature difference is related to a run of exceptionally mild years that started in 1988. Some further features of interest are :

- For about 75% of the years, Breezand reaches a water temperature peak of 20°C during summer. For FL26, the years 2001-2006 have all reached $22-24^\circ\text{C}$.
- From the second half of May to the end of September, water temperatures are generally above 16°C . This is also the period where instrument soiling due to algae tends to occur.
- For most days from early July to mid-December, the highest daily temperatures originate from the present FL26 data set rather than the Breezand data. This is mainly due to the hot summers of 2003 and 2006, and the exceptionally mild autumns of 2005 and 2006.
- For about 75% of the years, Breezand had water temperatures of 0°C .
- These freezing temperatures may occur from the last week of November (1965) to the last week of March (1969), with the

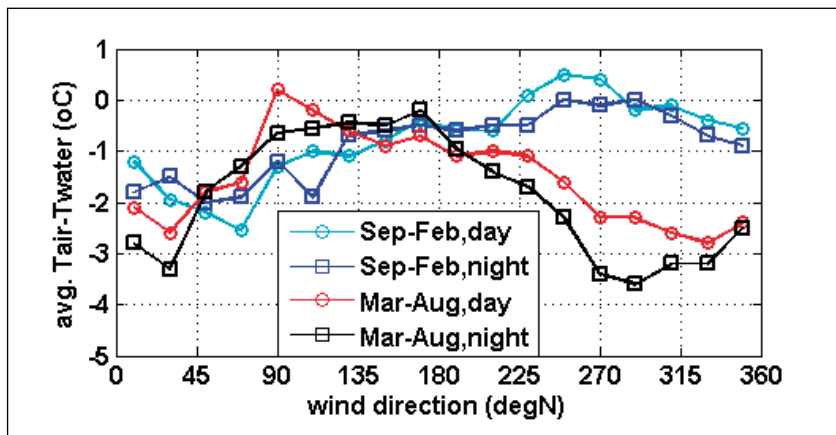
highest probabilities (order 25% for a given day) between Mid January and the end of February.

- Occasions where the lowest temperatures for a given day originated from the FL26 data were rare: a few days in mid-September 2001 and the second last week of October 2002.

The difference between air and water temperature ($\Delta T = T_{\text{air}} - T_{\text{water}}$) at FL26 can be up to 4-9°C to either side, with a typical scatter (1σ) of about 2°C. The trends in ΔT are assumed to depend mainly on:

- time of day
- season
- wind direction
- wind speed

Figure 4.19 Air-water temperature difference $T_{\text{air}} - T_{\text{water}}$ at FL26, as a function of wind direction, for day- and nighttime and summer and winter half year.



The dependence of ΔT (mean and scatter) on wind speed appears to be weak. The only clear trend is that above 6-7 Beaufort, air-temperature differences tend to be slightly smaller than in moderate wind cases.

The trends for the other parameters are summarised in Figure 4.19. A remarkable feature in Figure 4.19 is the fact that the average air temperatures are systematically lower than the water temperatures. Note the average ΔT is also slightly below zero for (southerly) wind directions which usually yield above-seasonal temperatures. Probably, evaporation effects tend to bias T_{air} over Lake IJssel downwards with respect to the air temperatures over land.

Also, it is remarkable that the lowest ΔT -values tend to occur in the months when Lake IJssel is warming, rather than cooling. This suggests that the water temperatures are not only strongly influenced by the air-water temperature difference, but also by radiation effects.

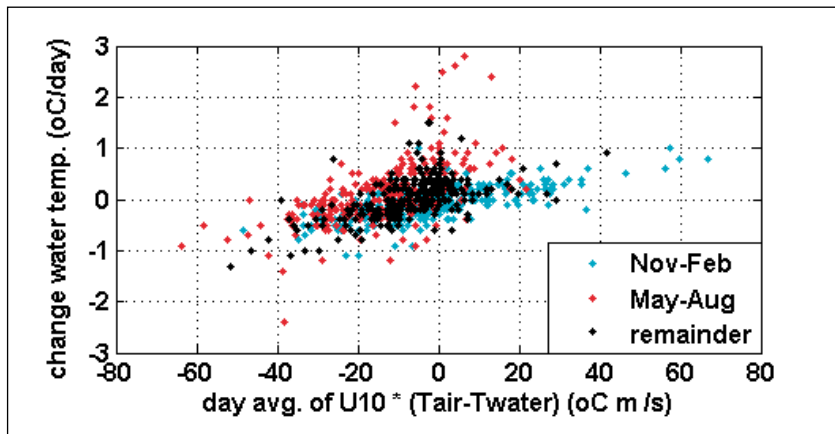
Further inspection of Figure 4.19 reveals the following trends:

- On average, there is hardly any difference between daytime (7-19 h MET) and nighttime values of ΔT . Inspection of the underlying data shows that several days indeed have a very small daily amplitude of T_{air} , even in the summer half year.
- In spring and summer, small air-water temperature differences are

most likely to occur for Southeasterly winds. However, ΔT may still strongly differ from zero for individual cases.

- In autumn and winter, the above applies for a broad sector centered about (south)westerly wind directions.
- Unstable atmospheres ($T_{\text{air}} < T_{\text{water}}$) in autumn and winter are most likely during northeasterly winds. In spring and summer, this is the case for westerly and northerly winds, especially during nighttime.

Figure 4.20 Change in water temperature ($^{\circ}\text{C}$ per day) as a function of the wind speed U^{10} times the air-water temperature difference ΔT .



For operational purposes like ice prediction (and for ecological purposes), knowledge about the change in water temperature may be useful. In Figure 4.20, the water temperature change at FL26 (in degrees per day) is correlated with the wind speed U_{10} times the air-water temperature difference ΔT . For a 1°C water temperature increase per day and a wind speed of 10 m/s , the air must be order 7°C warmer than the water. Note that the water warming in stable atmospheres (with limited turbulent mixing in the atmosphere) tends to be slower than the cooling in unstable atmospheres (with enhanced turbulent mixing). In the latter case, for a 1°C T_{water} change with 10 m/s wind, the air only needs to be $4\text{-}5^{\circ}\text{C}$ cooler than the water.

Note that such a $1^{\circ}\text{C}/\text{day}$ cooling for a 4.5 m deep lake corresponds to a heat flux of order $220\text{ W}/\text{m}^2$, which is fairly large in meteorological terms. If it is assumed that all this is used for evaporation (in reality, a smaller but significant fraction consists of exchange of sensible heat), this would result in order 7.5 mm evaporation per day. In the specific situation of Lake IJssel, roughly $75\text{ m}^3/\text{s}$ of river discharge would be needed to compensate for this.

Figure 4.20 also suggests that in summer, rapid warming can occur *without* a combination of strong wind and large ΔT . This is another indication that at least during summer, radiation plays an important role in the water temperature budget.

If one is interested in investigating some cases with rapid warming or rapid cooling in detail, it is worthwhile to consider some of the following cases: 2/2/2002, 13/12/2003, 4/2/2004, 22/5/2004, 23/5/2004, 12/10/2004, 23/12/2004 and 12/2/2005. All cases

have at least 13 m/s wind and an absolute air-water temperature difference of at least 5°C. Only the May 2004 cases have an unstable atmosphere; in all other cases, the air is warmer than the water. The most extreme cases with a stable atmosphere probably are 12/2/2005 ($U_{10} \sim 17$ m/s and $\Delta T \sim +5^\circ\text{C}$) and 4/2/2004 ($U_{10} \sim 15$ m/s and $\Delta T \sim +7^\circ\text{C}$). For the latter case, it is unfortunate that the FL26 wind data are missing, as are most FL2-data.

For wind and hydraulic modelling applications, it is important to verify the assumption of a thermally neutral atmosphere. One could use the above cases for this, but the disadvantage is that many of the above cases have no clear reference situation with near-neutral atmospheric conditions.

If one considers similar situations as above, but with constant ambient conditions and a strong day-night differences in air temperature and ΔT , one is likely to find strong-wind cases with both large and small ΔT -values, where the latter can serve as a near-neutral reference. In addition, this daily thermal stability variation allows to monitor stability-related trends in the spatial wind field, and in the scaling of waves with the wind. The most suitable cases for this type of study are 16-17 October 2005 with an unstable atmosphere and 7-8 May 2006 with a stable atmosphere. The cases of 14/5/1998 and 3/4/2002 are similar to the latter case, but they lack reliable air temperature data and part of the other required data.

All in all, a summary of water temperature climatology is given, as well as some trends in air-water temperature differences. As mentioned above, radiation seems to be a key factor in water temperature modelling. For wind and hydraulic modelling, it is important to note that significant air-water-temperature differences (and heat fluxes) to either side can occur, but that there is a preference for situations where the air is cooler than the water, especially during NW-winds in spring and summer.

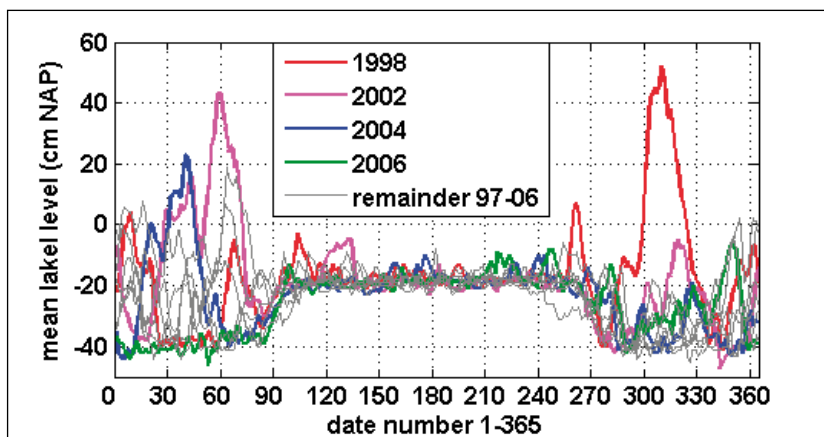
5. Water levels, storm surge, seiches

In the present chapter, spatially averaged lake levels will be briefly discussed, as well as storm surge effects and time-dependent water level fluctuations like seiches.

5.1 Mean lake levels

If wave hindcasts are to be done for situations with depth-limited wave growth over lakes, it is essential to know the spatially averaged water levels for the lake under consideration. For brevity, the latter is henceforth referred to as 'mean lake levels'. In the present section, some climatological properties of the mean lake levels of Lake IJssel and Lake Sloten will be discussed.

Figure 5.1: Mean lake level (in cm NAP) of Lake IJssel as a function of day number (1-365), for the calendar years 1997-2006.



For Lake IJssel, lake levels are kept as close as possible to a target level, which is 20 cm under the NAP datum from mid-April to end-September, and -40 cm NAP for the remaining months. The actual lake levels may be slightly lower than the targets during severe summer droughts, and up to about a metre higher during periods with a high discharge of the Rhine and IJssel rivers. The latter is especially the case if strong (north-)westerly winds inhibit a free water discharge from Lake IJssel to the Wadden Sea. As illustrated in Figure 5.1, the main periods with strongly elevated lake levels were during October/November 1998, February/March 2002 and February 2004. By contrast, most of the year 2006 showed exceptionally small deviations from the target water levels. The 10 year averages of the lake levels vary little throughout the year: in summer they are about -19 cm NAP, in late autumn about -30 cm NAP. However, the standard deviations around the mean are strongly variable. In summer they are only a few centimetres, but in late winter, standard deviations around the mean can be as large as 20 cm.

For Lake Sloten, regular water level measurements are only available for the SL29-location in the north-eastern half of the lake. Because of the small size of Lake Sloten, the SL29-data probably approximate the mean lake levels within five centimetres as long as winds do not exceed 6 Beaufort. The average observed lake levels for Lake Sloten (SL29) typically vary from about –47 cm NAP in winter to a slightly lower average of about – 53 cm NAP in summer, with a typical data range of plus or minus 8 centimetres around these averages. Measured water levels outside this range were often either due to experimental errors (ice, algae, ...) or to storm surge effects in strong winds. Only two periods could be identified in which water levels really appeared to be strongly elevated: 11-12 September 2001 and 26 February to 2 March 2002. In the former period, lake levels rose up to –20 cm NAP; in the latter period they were about –35 cm NAP.

5.2 Storm surge in stationary conditions

Wind-induced set-up of the mean water level, henceforth indicated as *storm surge*, plays a significant role in the hydraulic loading of the dikes of Lake IJssel. In addition, storm surge effects play a significant role in the daily water management of Lake IJssel and Lake Marken because storm surge effects have great influence on the amount of water that can be discharged from these lakes to the Wadden Sea.

The present measuring network was optimised for wave measurements rather than storm surge measurements. As a result, there are some limitations in using the present data for storm surge estimates:

- storm surge effects at the present locations are relatively small as all locations are relatively close to the centre of Lake IJssel.
- Algae (in summer) and drift (for capacitance probes) make the present water levels relatively inaccurate, especially for storm surges smaller than about 0.3 m.

For the above reasons, routine data of the MSW-network (Monitoring System Water) are also included in the present analysis. The following stations are considered :

- HOUN (158190,504550) : Houtrib-Noord, in south corner of Lake IJssel;
- LEMM (177000,539000) : Lemmer, in Lemster Bay, 40 km NNE of Houtrib;
- KORN (151650,564680) : Kornwerderzand-binnen, NNE-corner of Lake IJssel, near Wadden Sea;
- DOEV (132160,549290) : Den Oever binnen, NNW-corner of Lake IJssel, near Wadden Sea;
- KRAB (148000,523000) : Krabbersgat-noord, SW-side of Lake IJssel, near town of Enkhuiizen and near FL25-location.

Only data from October 2000 on were considered, because from then on, MSW-data were in an easy-to-use format. However, further data are available on www.waterbase.nl.

All storm-surge related data that are to be presented are based on 2-hour averages. This is done to diminish the influence of resonant oscillations in Lake IJssel, and to make sure that the presented storm surge data are largely in equilibrium with the wind. For further details about non-stationary response, the reader is referred to section 5.3; this section will only present quasi-stationary storm surge data.

Figure 5.2: Storm surge at the MSW-station Lemmer as a function of wind direction, for a wind speed of 11-13 m/s at FL2. All data are 2h-averages. Red points denote instationary data, blue points stationary data.

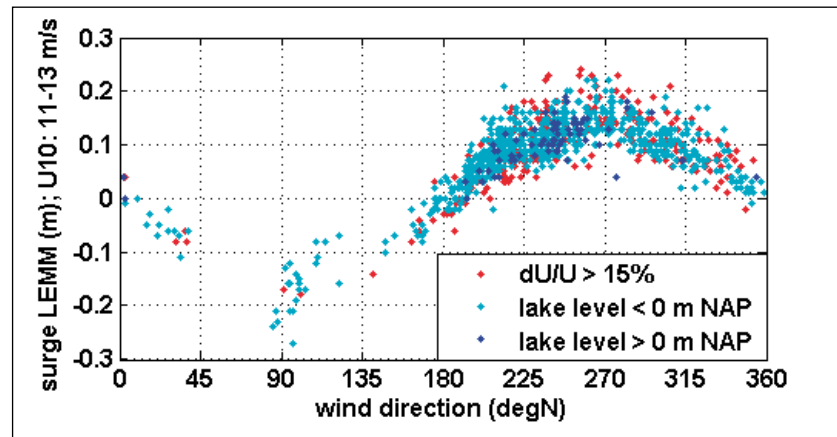
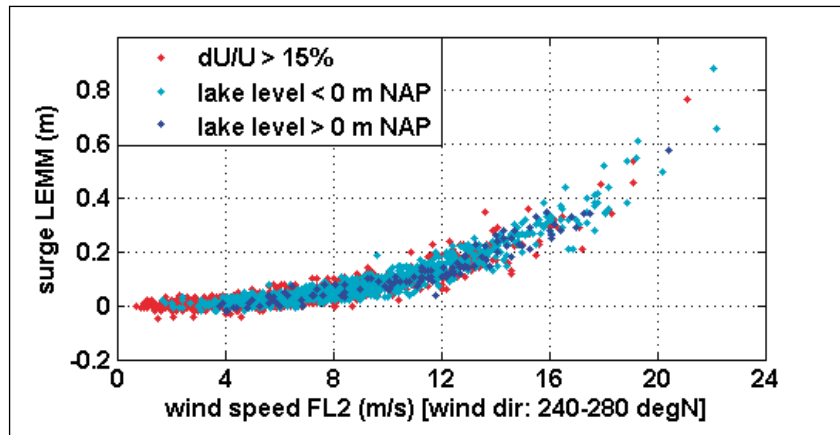


Figure 5.2 present storm surge data for the MSW-station Lemmer as a function of wind direction, for a wind speed (at FL2) of 11-13 m/s. All data are two-hour averages.

It can be seen that water levels at Lemmer tend to be above the mean lake level for westerly winds, and below it for easterly winds. The blue points indicate quasi-stationary data, the red points data for which the wind vector changed by more than 15% per hour. Remarkably, the scatter in the red points is hardly larger than for the blue points.

Figure 5.3 again shows some data for Lemmer, but this time as a function of wind speed, for a more or less westerly wind direction sector of 240°-280°. In accordance with theoretical expectations, the storm surge Δz is roughly proportional to the squared wind speed U_{10}^2 . Closer inspection suggests that the surge even increases slightly quicker, as $\Delta z \sim U_{10}^{2.2}$. This probably can be attributed to the fact that the drag coefficient also slightly increases with wind speed; see section 4.5. Also, it can be noted that at least 8 Beaufort (17 m/s wind) is needed for storm surges in excess of 0.4 m. As a result, the amount of data with significant storm surges is quite limited, and only includes a wind direction range of S to NNW (180°-330°; see Figure 3.2).

Figure 5.3: Storm surge at the MSW-station Lemmer as a function of wind speed at FL2, for wind directions of 240°-280°. All data are 2h-averages. Red points denote instationary data, blue points stationary data.



By analysing graphs like Figure 5.2-5.3, wind directions with minimum storm surge effects could be identified for each location. The results of this approximate analysis are given in Table 5.1. Table 5.1 also gives a maximum storm surge that is expected to occur for a FL2 wind speed of 17-19 m/s, and the mean wind direction of the data that are used to estimate this maximum surge.

Table 5.1: Estimated wind directions with near-zero storm surge, wind direction within 180°-360°-range with maximum storm surge, together with maximum surge (mean and standard deviation) for a FL2 wind speed of 17-19 m/s.

location	near-zero storm surge		near-maximum surge	
	1 st wind dir.	2 nd wind dir	wind dir	surge (m)
FL2	~50°	~200°	~270°	+0.31±0.09
FL5	~170°	~360°	~250°	+0.22±0.07
FL9	~170°	~360°	~250°	+0.14±0.04
FL25	~100°	~270°	~210°	-0.17±0.04
FL26	~100°	~270°	~210°	-0.19±0.04
HOUN	~90°	~270°	~190°	-0.51±0.06
LEMM	~180°	~360°	~250°	+0.36±0.07
KORN	~100°	~260°	~190°	+0.52±0.06
DOEV	~30°	~220°	~290°	-0.41±0.12
KRAB	~110°	~290°	~190°	-0.31±0.05

A final point of interest is the scatter in the experimental data, as shown in Figure Figure 5.2 and 5.3. Remarkably, most of the scatter seems unrelated to expected sources of scatter such as:

- instationarity of the wind (as indicated by the red points)
- larger storm surges in shallower water (as theoretically expected, and as indicated by the cyan points)
- lower drag coefficients and storm surge in stably stratified atmospheres (air warmer than water), and vice versa; not shown in Figure 5.2-5.3.

Closer inspection of the data suggest that the scatter occurs both within and between cases. For example, the cases of 28/1/2002 and 24/6/2004 both have wind speeds and directions of 17.5 m/s and 245° during 10 hours, but the storm surges are 36±4 and 32±4 cm respectively. Similar cases with stronger wind fluctuations (as on 28/12/2001), may have 2-hour storm surges that are up to 50% different from than the 32-36 cm mentioned just before, even

when the two-hour averages of the wind remain stationary. These instationary cases will be further investigated in section 5.3.

5.3 Time-dependent water level fluctuations

In practice, time-dependent storm surges can significantly deviate from the stationary estimates of the previous section. First of all, the actual storm surges during storms with rapidly changing winds may not have reached their equilibrium with the wind. Secondly, the water levels may oscillate on time scales of order one hour, either due to wind forcing or due to near-resonant phenomena.

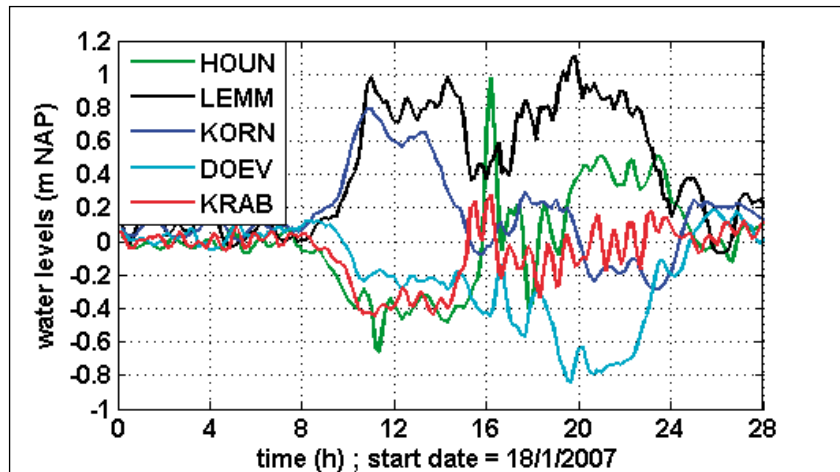
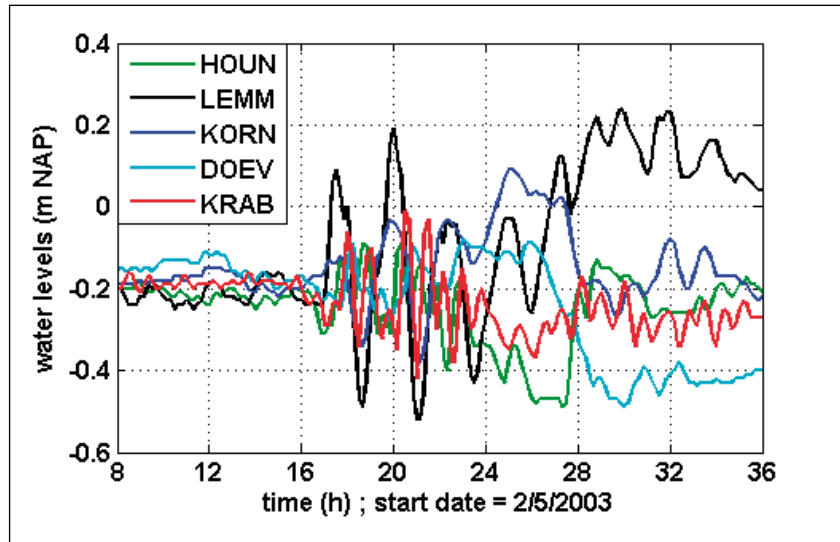
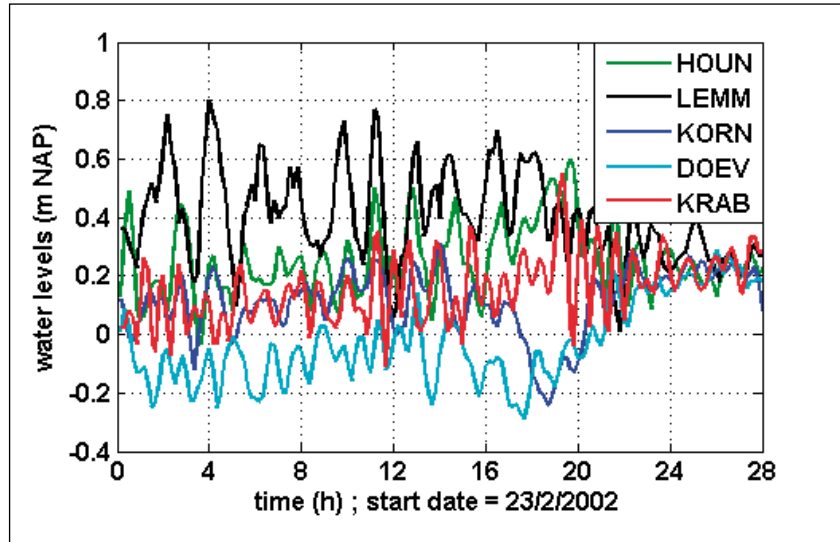
The issue of non-equilibrium storm surges during rapidly changing storm winds is closely related to the response time of Lake IJssel : after a step change in wind conditions, the storm surge needs a certain amount of time before it is in equilibrium with the new wind conditions. In practice, it is hardly possible to directly estimate response times from the analysis of individual cases. This is because almost no cases can be found where the wind is sufficiently strong (at least 8 Beaufort) for significant storm surge, and where the wind change is quick enough to approximate a step change.

In practice, it is more convenient to assume that the storm surge is in equilibrium after a time which roughly equals the time that a long wave needs to travel from one side of Lake IJssel to the other. Such long waves propagate at a speed $c = (gd)^{0.5}$, where g is the gravity (9.81 m/s^2) and d the water depth (typically 4.5 m). For SW-NE travelling waves, the one-way travel time across Lake IJssel is somewhat under 1 hour. For NW-SE travelling waves, the travel time is slightly over 2 hours. Hence, the two-hour averaging period for the previous section seems to be reasonable.

A first guess of the period of resonant oscillations can be obtained from the two-way travel time, i.e. twice the travel times mentioned above. A more advanced analysis (Jong et al., 2006) suggests that several standing wave patterns can develop in Lake IJssel, where some of the main modes have periods of 4.4 hours (with the highest amplitudes near the NW and SE shores) and 1.3 – 2.3 hours (with the highest amplitudes near the SW and NE shores). This also implies that these oscillations are not purely local, but that they are part of a larger spatial pattern.

Some example registrations with fluctuating water levels are given in Figure 5.4.

Figure 5.4: Water level registrations at the MSW-stations for 23-24 February 2002 (top), 2-3 May 2003 (middle) and 18-19 January 2007 (below).



The top panel of Figure 5.4 shows the water level registrations for the five MSW-stations of section 5.2, for 23 February 2002. Until 16h MET, there was a westerly wind of 15 m/s on average, but the wind was extremely gusty. As a result, the 10-minute averages of the wind ranged from 8 to 19 m/s. As a result, large water level oscillations occurred; at Lemmer, Krabbersgat and Houtrib, the largest crest-trough distance of these oscillations was 70, 50 and 40 cm respectively. This is of the same order as the largest stationary storm surges as observed in Figure 5.3 and Table 5.1. Another feature of Figure 5.4a is the fact that the oscillations are often non-coherent: both the oscillation periods and the amplitude development (through time) differ strongly between each of the locations. For example, the dominant periods in Lemmer are about 2 hours, whereas they are less than 1 hour in Krabbersgat.

The middle panel of Figure 5.4 shows the registrations of 2-3 May 2003. On 2 May, two thunderstorm gust fronts pass at about 17h and 19h30 h MET respectively, with wind suddenly changing from SE 3-4 Beaufort to a WSW 6-7 Beaufort which in both cases lasts for 10-15 minutes. In the night, the wind increases to a steady westerly wind of 16 m/s in the morning of the 3rd May. The latter case yields quite a coherent pattern with a positive storm surge of a few decimetres at Lemmer, and a negative surge of similar size at Den Oever. On 2 May however, the passage of the gust fronts once again produces incoherent patterns where each location has its own preferred oscillation period. Here too, the oscillations in Lemmer are quite large, with a size of up to 70 cm and a period of about 2.5 hours.

The lower panel of Figure 5.4 shows the registrations of 18-19 January 2007. The wind increases from South 8 m/s at 7h to SW 22 m/s from 10-15 h MET, then sharply drops to West 15 m/s at 16 h, while a second peak of W-WNW 23 m/s is reached between 18 and 22 h MET.

Water level overshoots and oscillations of a few decimetres are quite common, but the main feature to be noticed is the +98 cm NAP peak at the Houtrib location around 16 h. The westerly wind direction around that time yields negligible steady storm surge effects (Table 5.1). Therefore, it must be concluded that this nearly 1 metre overshoot with respect to the mean lake level is almost entirely due to unsteady and (possibly) resonant phenomena.

The above cases demonstrate that at least at Lemmer and Houtrib, the amplitude of apparently resonant water oscillations can be as large as the largest storm surges observed in the present data series of 2000-2006. Most cases with (resonant) water oscillations seem to occur during passages of thunderstorm fronts or during very gusty winds. In one case (18/1/2007) however, such oscillations were related to a 9 Beaufort gale with rapid wind changes. This shows that for storms with quickly changing wind, (resonant) water oscillations may be a significant phenomenon.

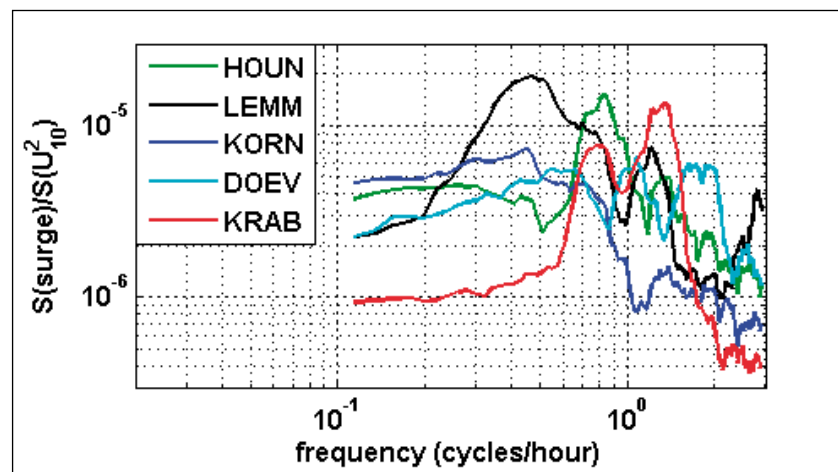
It is important to be able to distinguish between quasi-stationary and near-resonant response of the water levels for a number of reasons :

- to decide upon modelling approach (steady or non-steady)
- to evaluate the optimum averaging time for data
- because of potential effects on dike design

To identify resonant response, a special spectral analysis was carried out. Firstly, a continuous subset of data with persistent strong winds was looked for, preferably with small day-to-day variations of the average lake level. Few of such subsets were available; the best one turned out to be 27/1/2002 to 12/2/2002. For this subset, storm surges were calculated for all available 10-minute water levels of the Lake IJssel MSW stations mentioned in section 5.2. Note that that only MSW-stations were considered; the storm surges of the present wave measuring locations were considered to be too small for a reliable analysis.

A further step was to couple the storm surges to a forcing that is *linearly* proportional to the storm surge: the component of the squared wind speed that was along the wind direction with maximum storm surge (see Table 5.1), $U_{10}^2 \sin(\theta)$. In this case, the FL26 wind was used as the FL2 wind was not reliable for all days. The next step was to calculate the spectra for the 10-minute wind forcing, and spectra for the 10-minute storm surge data. The ratio of these spectra is the response function shown in Figure 5.5. It is important to note that spectral densities, like those in Figure 5.5, are proportional to squared amplitudes. As a result, a factor 10 difference in Figure 5.5 corresponds to a factor 3 difference in $\Delta z/U_{10}^2$ ratio, where Δz is the storm surge.

.....
Figure 5.5: Response of Lake IJssel to wind for five locations: ratio of storm surge spectrum $S(\text{surge})$ [m^2/Hz] to spectrum of squared wind $S(U_{10}^2)$ [$(\text{m}/\text{s})^4/\text{Hz}$]. Based on 10-minute data from 27/1/2002 to 12/2/2002



In a general sense, the curves in Figure 5.5 can be characterised by a near-horizontal low-frequency section with quasi-steady response (left side of graph), one or more peaks with resonant water level response to the wind, and a high-frequency section (lower-side of graph) with decreasing response, where the wind fluctuations are too quick to be followed by a suitable storm surge response.

The following conclusions can be drawn from Figure 5.5 :

- For most locations, the storm surge response is steady for time scales over 2 hours, but for Lemmer, this appears to be 5 hours.
- Resonant peaks with at least a factor 2 amplification in $\Delta z/U_{10}^2$ occur at Lemmer (broad peak, period ~ 2 h), Krabbersgat (periods of order 0.7 and 1.3 h) and to a lesser extent at Houtrib (period ~ 1.2 h).
- Smaller resonant peaks occur at Lemmer (about 0.4 and 0.8 h), and at Den Oever (about 0.6, 1 and 1.8 h).
- Most, but not all, of the above resonant peaks were also identified in the analysis of (Jong et al., 2006). The reverse also applies: most, but not all peaks of (Jong et al., 2006) are identified in Figure 5.5.
- Kornwerderzand is the only MSW-location in Figure 5.5 that is free of significant resonance peaks.
- For Kornwerderzand, the storm surge no longer fully responds to the wind for time scales less than two hours. This may be due to the finite spatial size of wind fluctuations of this time scale, but also to the finite response times of Lake IJssel. For wind across the lake, like in Lemmer, the response time may be shorter, but because of the presence of resonance peaks, Figure 5.5 does not allow to verify this for the other locations.

All in all, the present analysis suggests that time-dependent storm surge phenomena should be accounted for in the data analysis and in modelling approaches if the time scale of wind variations is less than 2 hours. Partly this is because storm surge then no longer fully responds to the wind, partly this is because of the occurrence of strong resonance phenomena. However, for the location of Lemmer, a minimum time scale of 5 hours is more appropriate.

The above conclusions only apply for the main body of Lake IJssel. If Lake Ketel is to be included in a model simulation, or the Zwartemeer lake to the Northeast of Lake Ketel, considerably longer periods of stationary wind are needed to justify a stationary model approach. This is because the narrow channels between Lake IJssel, Lake Ketel and the Zwartemeer lake each cause significant time lags in the storm surge response, which greatly increases the effective response times to wind in these backwaters. Ultimately, this also implies that model calibrations for these backwaters should not be used for Lake IJssel without prior verification, and vice versa.

6. Wave properties and wave climate

In this chapter, the wave climate of Lake IJssel and Lake Sloten will be discussed. A number of (trends in) relevant stationary wave properties will also be discussed. The time-dependent wave behaviour is too complex to discuss in this chapter, but some interesting cases will be highlighted in Chapter 7 (section 7.3).

In section 6.1, a global description of wave height climate for Lake IJssel and Lake Sloten will be given. As too many data are missing for a direct evaluation of wave climate, section 6.2 will highlight an important component in the indirect evaluation of wave height climate at each of the measuring locations: the relation between wind conditions and wave height. Next, wave periods and wave steepnesses are discussed in section 6.3 and 6.4.

From section 6.5 on, some specific issues will be highlighted such as:

- the scaling of wave heights with the wind speed (section 6.5)
- depth-limited waves (section 6.6)
- validity of the effective fetch concept (section 6.7.1)
- wave spectra and distribution functions for the heights and periods of individual waves (section 6.7.2 and 6.7.3).

6.1 Overall wave height climatology

Knowledge of the wave climate – and more specifically the wave height climate – is important for several applications, for example :

- dike design, and flooding protection in general
- serviceability for various activities (recreation, shipping, ...) and maintenance works on Lake IJssel
- ecological modelling

If continuous and reliable measurements are available, the local wave height climatology can be calculated directly. However, with many long-term wind-wave measuring campaigns, the aim of continuous and continuously reliable measurements is extremely hard to achieve. For the present data, this is illustrated in Figure 3.1 in Chapter 3.

The present climatology will focus on the months November to April (inclusive), for the period of autumn 2001 to spring 2005. There are a number of reasons to consider this period only:

- during the summer half year (May-October) the measurements are likely to be biased due to soiling by algae;
- before spring 2001, the number of unreliable and/or missing data generally exceeded the number of reliable data;
- between August 2005 and June 2006, the FL2 and FL25 platforms were moved to a new location.

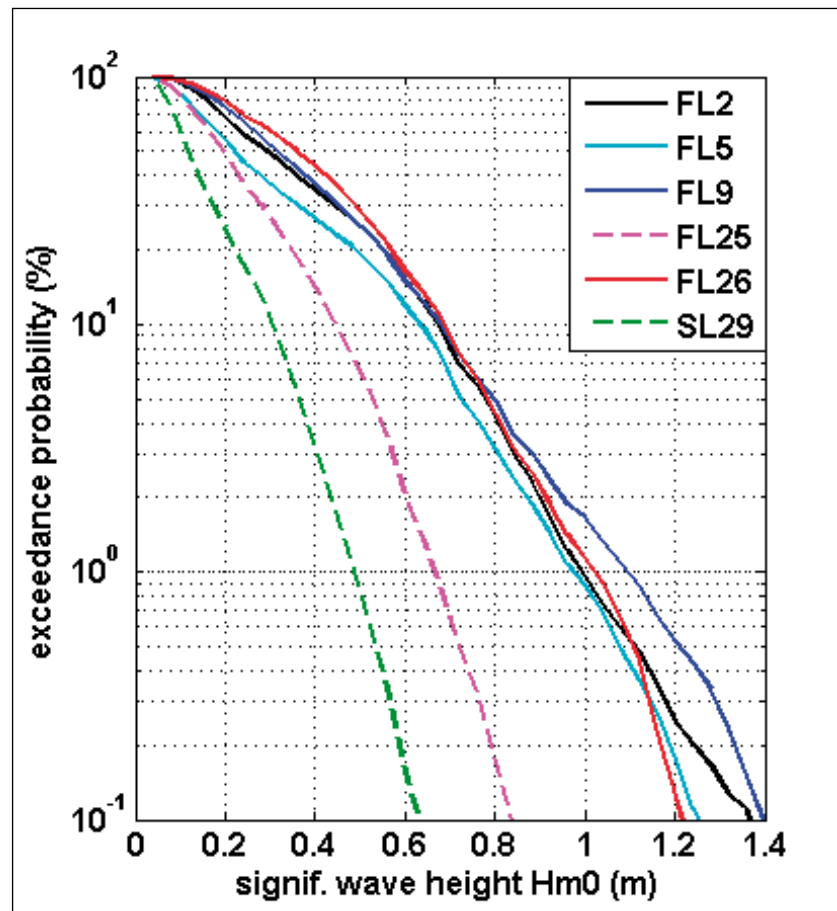
With the above precautions, a reasonable estimate of local wave climatology can be made. Still, there remain some limitations to the accuracy of the data to be presented. This is because:

- Wind speeds for November-April are order 5% above the yearly average, as are probably the wave heights;
- Yearly wind speed (and probably also wave height) averages have a scatter (1σ) of about 5-10% around the long-term climate average;
- Roughly one-third (FL26, FL9, FL25) to about one-half (SL29, FL2, FL5) of the data is either missing or unreliable.

The latter implies that a special approach is needed to deal with missing and unreliable data. Most of these data occur for winds around 3 Beaufort, so neglecting these data would weigh the average towards strong wind cases. Therefore, each unreliable or missing sample is replaced by the average wave height that is associated with the wind conditions related to that particular sample. Note that with this, the effect of ice cover is neglected. This may especially be relevant for SL29, as Lake Sloten may have been fully frozen over for about 9 weeks (2+6+0+1) in the 4-year period under consideration. Lake IJssel probably only had order two weeks of floating ice fields and a few days of closed ice cover.

The resulting approximate climatology is shown in Figure 6.1.

.....
Figure 6.1: Approximate 4-year (2001-2005) climatology for the wave height H_{m0} (all locations, Nov.-April only).



Note that the exceedance probabilities for a given wave height H_{m0} are plotted on a logarithmic scale in order to show both the average values (near the top of the graph, slightly below the 50% level) and the values occurring for about 10 hours per year (0.11%, near lower end of graph). For a more quantitative evaluation, Weibull fits are made for the 0.5-90% probability interval; Table 6.1 gives the results.

Table 6.1: Parameters characterising the climatology of wave height H_{m0} , as shown in Figure 6.1.

	FL2	FL5	FL9	FL25	FL26	SL29
long term mean of H_{m0} (m)	0.35	0.30	0.37	0.23	0.39	0.15
standard deviation H_{m0} (m)	0.22	0.22	0.22	0.15	0.21	0.10
Weibull scale parameter a (m)	0.38	0.32	0.41	0.25	0.44	0.16
Weibull shape parameter k	1.57	1.31	1.64	1.55	1.87	1.42

It should be noted that the (winter half) year average of H_{m0} is much smaller than the highest H_{m0} -values measured so far. The latter are typically a factor five larger than the long-term averages.

As for the Weibull fit parameters, the scale parameter 'a' is typically order 10% above the long term mean of H_{m0} (see Table 6.1), in accordance with similar wind climate fits of Wieringa and Rijkoort (1983). The fits themselves are quite good as for a given exceedance probability, the fitted H_{m0} -values are within a few percent of the original ones of Figure 6.1.

Still, caution is needed. The reason for this lies in the different shape parameters 'k' of the fits. High k-values typically occur if the extremes are close to the average; low k-values if the average values are low but the extremes high. The former tends to occur on locations where the fetch varies little with wind direction, like FL26. The latter occurs on locations with large directional fetch variations. This applies especially for FL5, where effective fetches range from 0.5 km for NNE winds to about 20 km for SW-winds. The result of these difference in k-values is that the *fitted* values (not the original ones of Figure 6.1) for FL5 and FL26 cross at $H_{m0} \sim 0.9$ m. According to the fits, FL5 has even the highest probabilities of *all* locations when H_{m0} is above 1.1 m. As FL5 is the location that has by far the lowest water depth and strongest depth-limitation of the waves, this result is clearly implausible.

The above result also yields an important conclusion for dike design purposes :

- fitting a mathematical distribution to a data set of measured wave heights does not necessarily produce physically realistic wave heights for extreme conditions.

The above conclusion is illustrated by the result of some additional fits in which the probability interval to be fitted is extended from 0.5-90% to 0.05-90%. For FL2, this hardly changes anything. For FL5 however, the Weibull 'k' increases from 1.31 tot 1.35. This change is plausible because for FL5, the severest (and rarest) conditions are typically depth-limited conditions where the wave heights are smaller than they would be in deeper water.

A final point is the application of the above to ship design and ship routing. European regulations (ECE, 1997) describe the design standards for ships in relation to a maximum allowable wave height parameter $H_{1/10}$. Although the regulation contains only $H_{1/10}$ thresholds and (apparently) no maximum allowable exceedance probability, it can still be useful to describe the wave climate in terms of $H_{1/10}$. Given the approximate character of Figure 6.1, the most convenient option is to use a conversion ratio $H_{1/10}/H_{m0}$. This conversion ratio typically is about 1.19 ± 0.05 to 1.25 ± 0.05 , with the highest values occurring during moderate conditions (H_{m0} order 0.5 m) at FL2, FL5 and FL9.

6.2 Wind-related wave height climatology

Ideally, the wave statistics of section 6.1 require nearly continuous measurements. Generally, the fraction of missing data is 20% or more (see Chapter 3), which is quite significant. Moreover, the climatology of section 6.1 is only valid for the winter half year as summer wave data are likely to be biased due to algae.

All this implies that in practice, one often needs a near-continuous wind data set as a starting point for wave climatology, and that the next step is to quantify the relation between wind conditions and wave heights. This latter step will be dealt with in the present section. These wind-wave transformation relations are also useful in another context, which is to supplement the wave model test cases to be discussed in Chapter 7 with a much larger set of wind-related wave data. A 'climatological' data set of this type has the additional advantage of averaging out random case-to-case variations that may bias individual cases.

The basis of the wind-to-wave transformation relations to be developed is the type of scatter plot shown in Figure 6.2, where the wave height H_{m0} (winter half year data only) is plotted as a function of wind speed for southwesterly wind directions.

Figure 6.2a shows the FL2 results. For given wind speed, the relative scatter in H_{m0} (based on 1σ) typically is 10-15% for moderate winds and order 5% for very strong winds. The total range of H_{m0} -samples for given wind is typically about a factor 1.5. For cases with strongly fluctuating wind (like 22/2/2002), the scatter may occur between consecutive 20-minute samples, but generally the scatter reflects case-to-case variability. For example, all data of 29/10/1998 are in the upper part of the scatter cloud. A first sight, the elevated still water levels for this day (+40 cm NAP) seem a plausible explanation for this deviation. Surprisingly, the scatter clouds for data with normal and elevated water levels (below and above NAP) show no systematic bias, although elevated water levels seem to dominate for winds above 17 m/s. The latter is plausible because FL2 will then have significant storm surge effects.

The results for the short-fetch location FL25 are shown because they

differ markedly from those of the other locations. Figure 6.2b shows that the scatter for FL25 is much larger, and that for very strong winds, the scatter cloud has a bimodal character. For the latter, no explanation is yet available. As yet, one can only describe what happens: during some cases with very strong winds (like 27/10/2002 and 21/3/2004) the waves at FL25 seem to be blown flat, while energy levels are depleted for the full wave spectrum (see Figure 7.2c in Chapter 7). Yet nothing noticeable happens in many other stormy situations with similar conditions and instruments. In moderate conditions, FL25 also has a fairly large amount of H_{m0} -scatter. Part of this seems to be inherent to situations with short fetch and weak to moderate winds. However, atmospheric conditions also explain part of the scatter. For example, the case of 7/1/2005 had a stable atmosphere and a wind speed ratio $U_{10}(\text{FL25})/U_{10}(\text{FL2})$ that was larger than usual. As a result, these data end up in the upper part of the scatter cloud. Finally, it should be noted that for given fetch and wind speed, experimental scatter tends to be somewhat larger during easterly winds than during westerly winds. This is probably linked to atmospheric (stability) conditions as spatial wind speed ratios also tend to have more scatter during easterly winds.

Figure 6.2: 20-Minute samples of wave height H_{m0} at FL2 (top) and FL25 (below) as a function of FL2 wind speed, for wind directions of 220-260° and the period 1997-2005. For FL2, still water levels (SWLs) above and below NAP have separate colours.

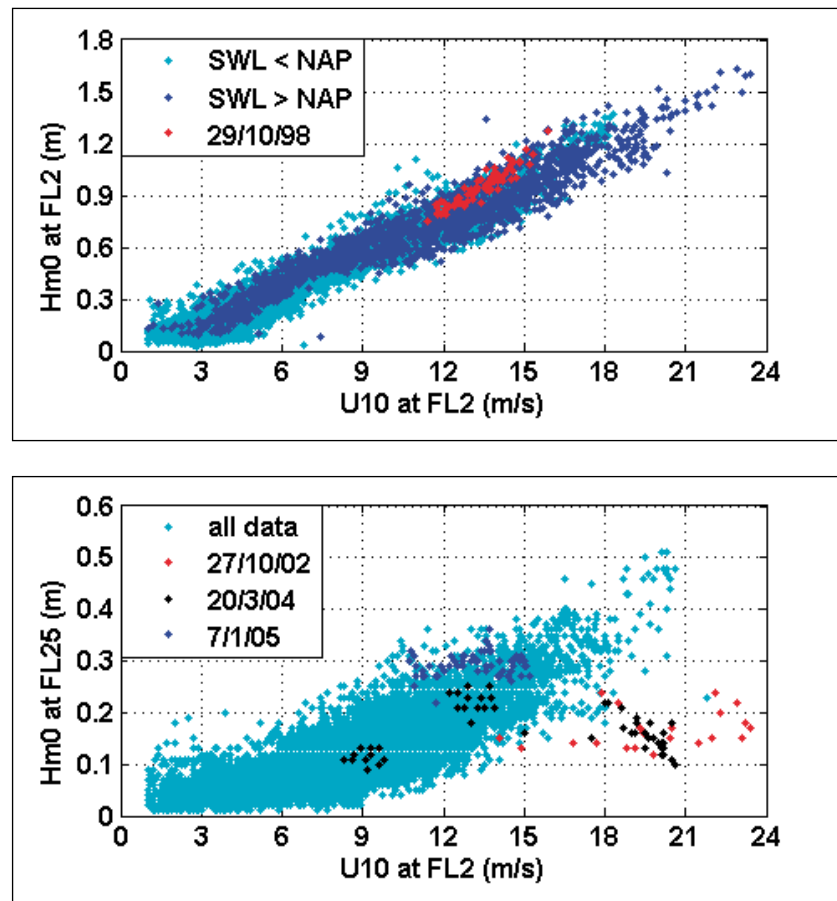
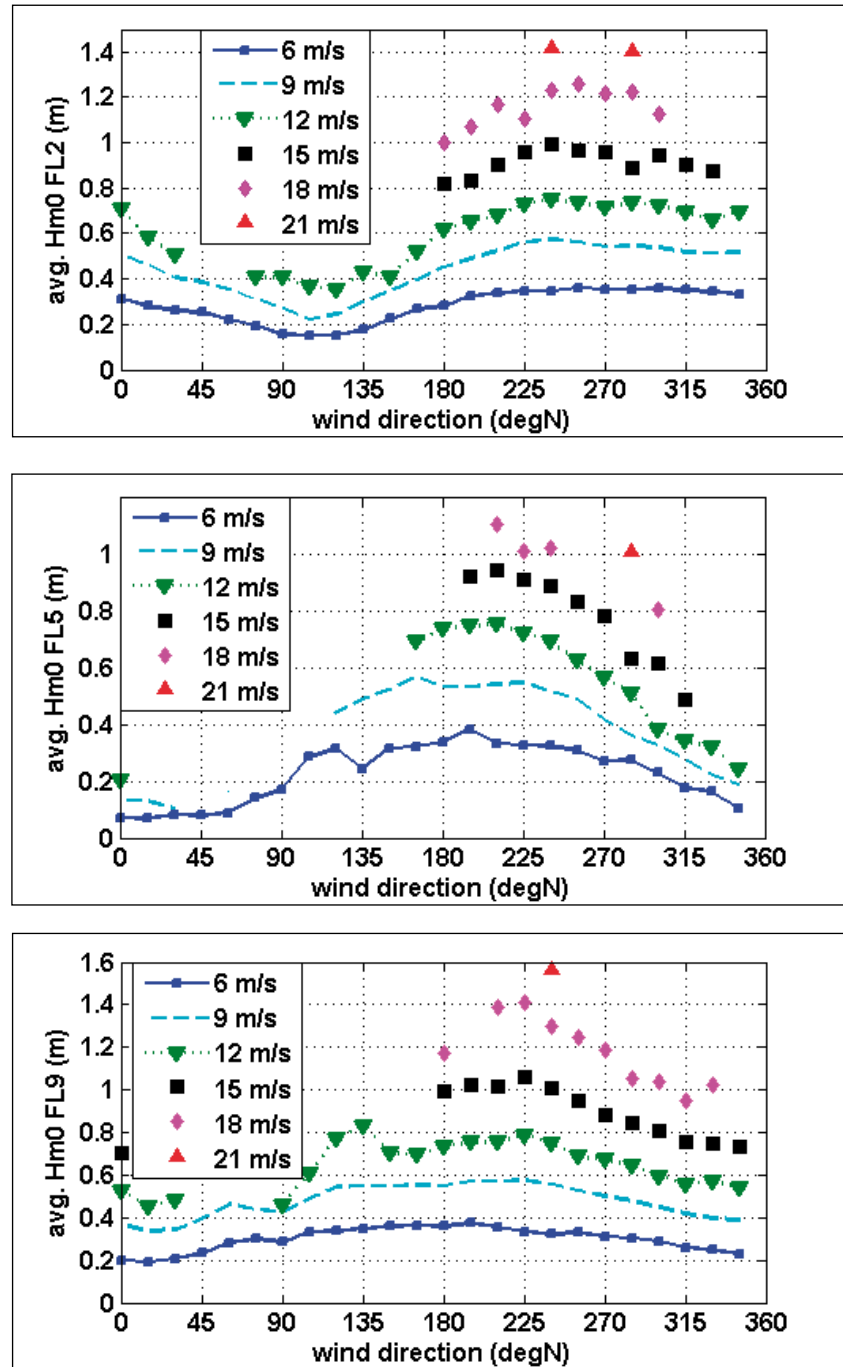


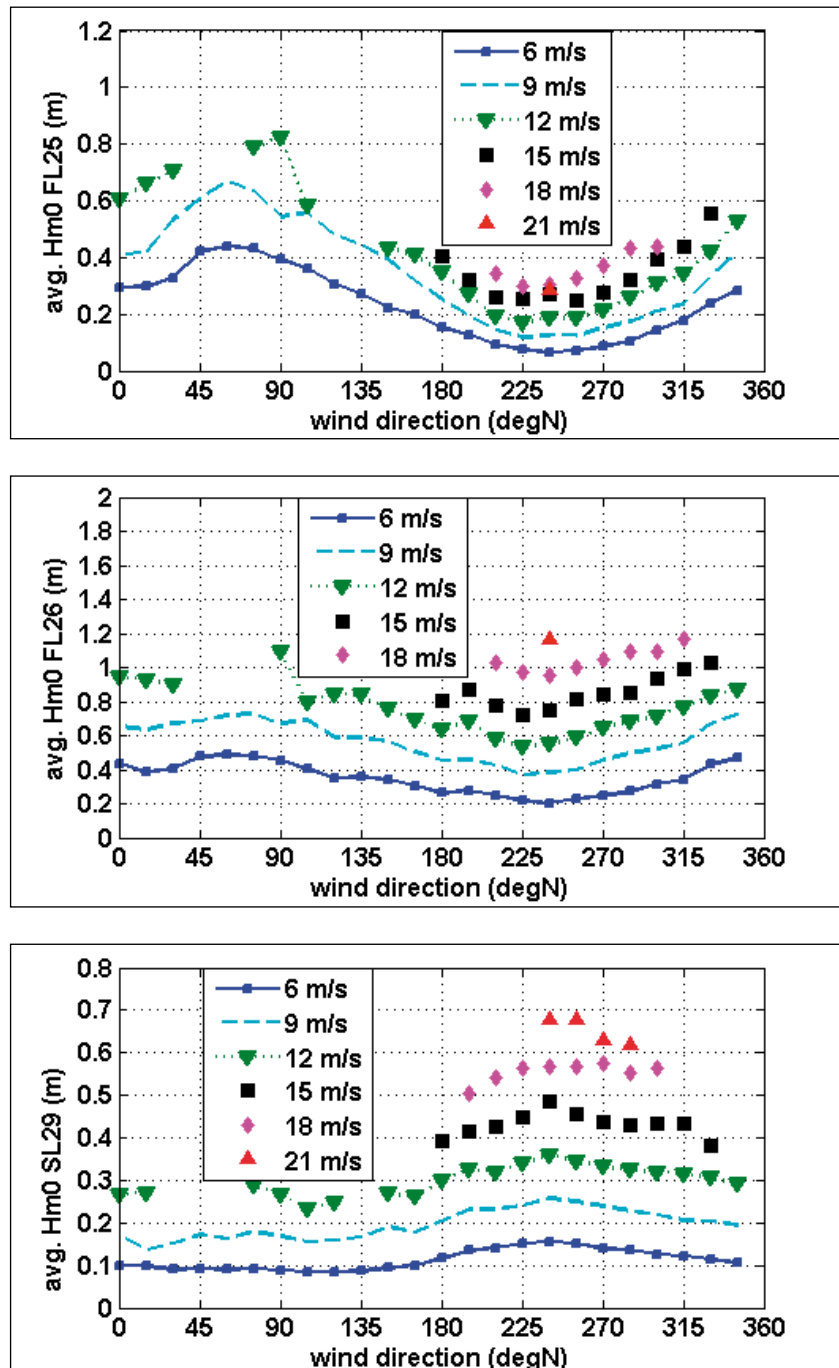
Figure 6.3 shows the average H_{m0} as a function of wind direction for a number of wind speeds, and the locations FL2, FL5 and FL9. From the underlying data, summer data (May-September) were rejected due to the risk of soiling. In addition, the FL5 data set was limited to 2001-2003 as FL5 was relocated more than once, and other subsets of data were smaller. Finally, only data with still water levels (SWLs) between -60 and +20 cm NAP were considered. Average water levels were typically near -25 cm NAP, but close to NAP for 7-8 Beaufort westerly winds, and +10 to +40 cm NAP (for FL5 and FL2) for the 21 m/s data, where SWLs between +0 and +60 cm NAP were allowed.

.....
Figure 6.3: Average H_{m0} at FL2 (top), FL5 (middle) and FL9 (below) for various wind speeds at FL2, as a function of wind direction.



Each data point in Figure 4.3 is based on order 10-500 twenty minute values. The former applies for the highest wind speed plotted for given wind direction, the latter for moderate (south)westerly winds. For the plotted points with few underlying data, 2-5% of H_{m0} -variability may occur. Indeed, some of this variability shows up in the plots of FL2 and FL9 (For FL2, see the WNW and SW-winds of 15 and 18 m/s; for FL9, see the SE-winds of 12 m/s).

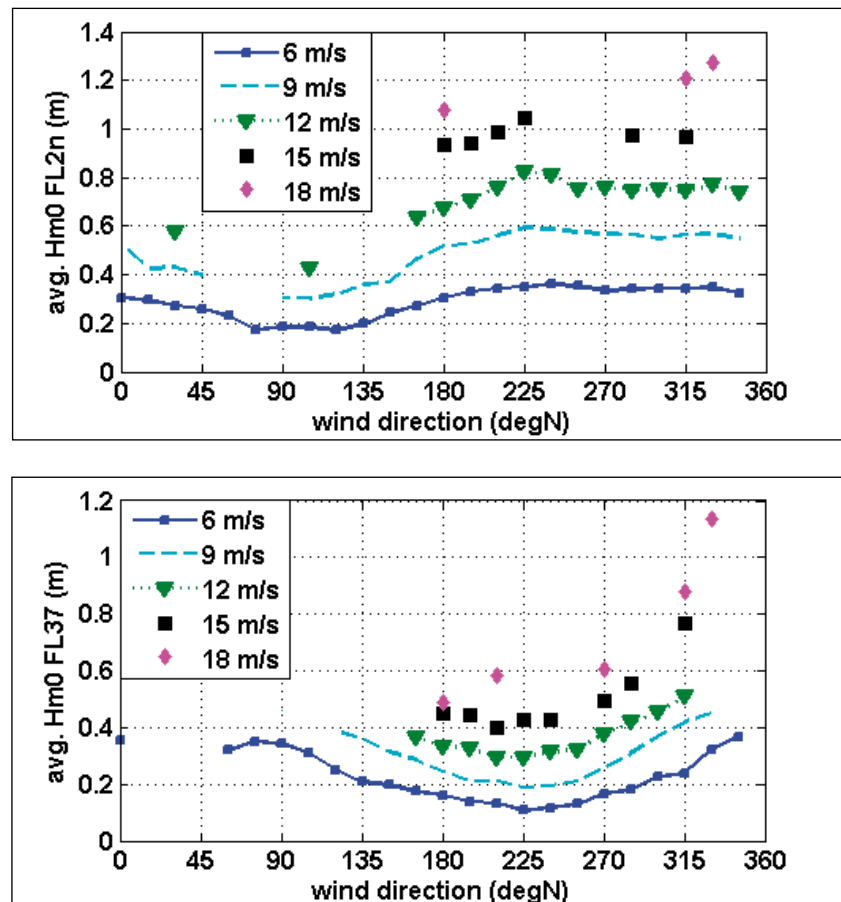
.....
Figure 6.4: Average H_{m0} at FL25 (top), FL26 (middle) and SL29 (below) for various wind speeds at FL2 (for FL25/26) and SL29 (for SL29), as a function of wind direction.



The results of FL25, FL26 and SL29 are shown in Figure 6.4, for which similar remarks apply. The underlying still water levels (SWLs) for SL29 are generally close to -48 cm NAP, but they tend to about -60 cm and -40 cm NAP for very strong southerly and westerly winds respectively. For FL25 and FL26, average SWLs are roughly -20 cm NAP. For FL25, the H_{m0} data points (Figure 6.4a) for 15, 18 and 21 m/s hardly differ due to the bimodal scatter cloud shown in Figure 6.2b. For easterly winds, the H_{m0} of FL25 and FL26 seems to be unexpectedly high, but the number of underlying data is small.

Finally, the results of the FL2n (since mid-2005) and the FL37 (since mid-2006) are shown in Figure 6.5. The trends for easterly winds and very strong winds are still somewhat ambiguous as the data sets for FL2n and FL37 are 5-10 times smaller than for FL2-SL29. The underlying SWLs levels of the FL2n are similar to those of the FL2. For FL37, SWLs scatter around -25 cm NAP, but they are about NAP and -50 cm NAP for very strong (north)westerly and southerly winds respectively.

.....
Figure 6.5: Average H_{m0} at FL2n (top) and FL37 (below), for various wind speeds at FL2n, as a function of wind direction.



For all cases of Figure 6.3-6.5, the wave heights H_{m0} have a clear correlation with wind speed and fetch. As will be shown in Section 6.6, the effect of water depth on H_{m0} is often rather ambiguous.

Although the scaling of H_{m0} with wind will be discussed in a later section, one can already state that in general, H_{m0} is roughly proportional to wind speed. The main exceptions are FL5 (depth-limited wave breaking during storms) and FL25 (unexplained and unreproducible wave flattening during some storms).

The scaling of H_{m0} with fetch is hard to discuss without presenting lots of details. Qualitatively however, one can easily see that fetch variations are reflected in the wind direction dependence of H_{m0} . This not only applies to the wind directions with largest and smallest H_{m0} (for given wind speed), but also to the relative variations of both fetch and H_{m0} as a function of wind direction. These variations are much smaller for locations with relatively uniform fetch, like SL29, FL26 and FL9.

6.3 Wave periods

For the wave periods, a wind-related climatology can be derived that is similar to the one for the wave heights discussed in the previous section. The results for the wave period measure T_{m01} are shown in Figure 6.6 and 6.7.

By and large, the trends in T_{m01} are the same as those previously shown for the wave height H_{m0} . However, two additional things are worth mentioning:

- Except for a few exceptions (mixed wave fields at the edges of sheltered direction sectors), the relative scatter in the underlying T_{m01} data is generally smaller than for H_{m0} . As a result, the curves of Figure 6.6-6.7 tend to be slightly smoother than those of Figure 6.3-6.5.
- The examples of H_{m0} -variability of the previous section (strong winds FL2, SE-winds FL9, E-winds FL25/FL26) also show up in the T_{m01} graphs. This suggests that the variability is rather linked to the (wind) forcing of the waves than to the (steepness of) the waves themselves.

Because of space considerations, other (spectral) wave period measures are not discussed as extensively as T_{m01} . Still, it is interesting to highlight some features of the peak period T_p . Figure 6.8 shows that if conditions are favorable for mixed wave fields, T_p -values for given ambient (wind) conditions may cluster around two or even three different values. Such mixed wave fields and ambiguous T_p -behaviour mainly tend to occur along the edges of sheltered wind direction sectors, like SSW and WNW winds for the FL25.

.....
Figure 6.6: Average wave period T_{m01} for FL2 (top), FL5, FL9 and FL25 (below), for various wind speeds at FL2, as a function of wind direction.

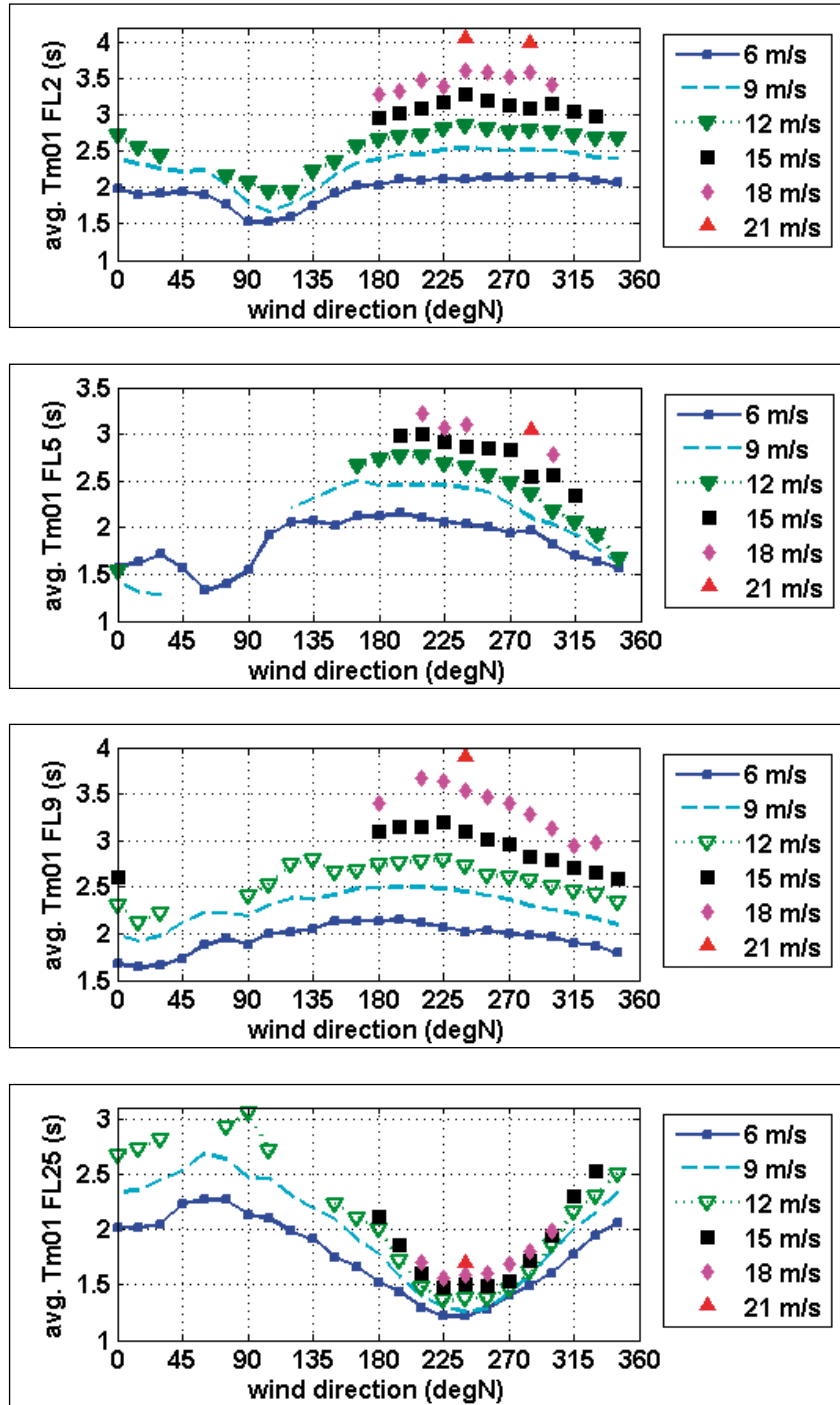
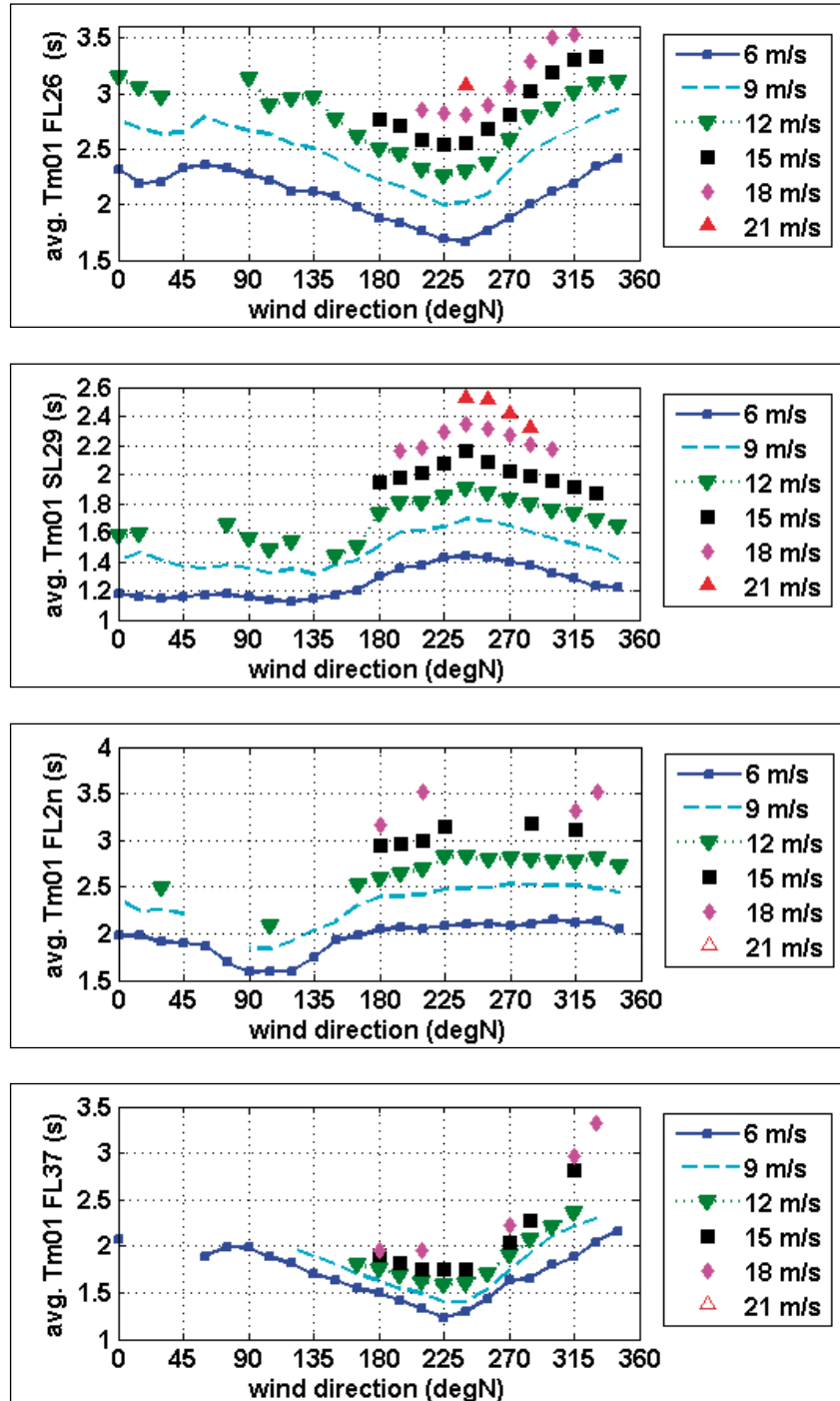
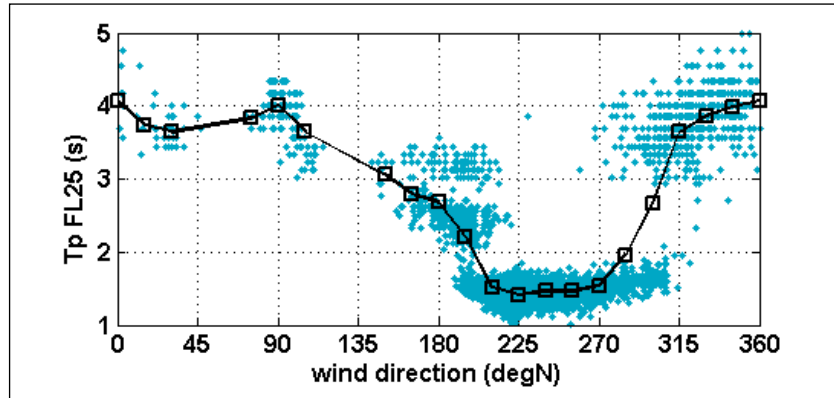


Figure 6.7: Average wave period T_{m01} for FL26 (top), SL29, FL2n and FL37 (below), for various wind speeds at FL2/SL29/FL2n/FL2n, as a function of wind direction.



.....
Figure 6.8: Peak period T_p at FL25 as a function of wind direction, for FL2 wind speeds of 11-13 m/s; cyan points denote 20-minute samples; line with squares denotes average.



In graphs like Figure 6.6-6.7, the use of T_p or T_{m-10} instead of T_{m01} has another disadvantage: the behaviour of T_p and T_{m-10} in situations with very low waves (H_{m0} order 0.1 m or less). Both parameters then tend to be biased by residual low frequency wave energy, so that T_{m-10} and T_p during weak winds are often higher (!) than during moderate winds. The trends in the zero-crossing period T_{m02} are much less ambiguous, but there is a reason to reject this parameter too: its extreme sensitivity to the spectral integration range used (see Appendix B.1). As a result, T_{m01} remains as the most suitable parameter to be presented.

Despite the complex trends in T_p and T_{m-10} , it is still useful to highlight some of the main trends during strong winds (at least 5 Beaufort). In many situations, T_p and T_{m-10} can be related to T_{m01} by:

- $T_p / T_{m01} \sim 1.13 - 1.33$
- $T_{m-10} / T_{m01} \sim 1.07 - 1.17$

The standard JONSWAP spectrum (p. 187 in Komen et al., 1994) yields T_p/T_{m01} and T_{m-10}/T_{m01} ratios of about 1.11-1.19 and 1.04-1.08 respectively. If the upper end of the spectral integration range is denoted as f_{max} (see Table 2.2), the lowest value of each pair (1.11, 1.04) corresponds to cases with $T_p \sim 6f_{max}$; for the highest values of each pair $T_p \sim 2f_{max}$. All in all, the above wave period ratios seem to be slightly larger than for standard spectra.

Even more important are the exceptions to the above wave period ranges, as these are the situations where simple parametrisations and simple modelling approaches fail. The main exceptions to the above are:

- FL2 – offshore winds: $T_p/T_{m01} \sim 1.05$ for ESE winds
- FL5 – offshore winds: T_p/T_{m01} is order 1 for NE winds
- FL5 – onshore winds: T_p/T_{m01} may increase to 1.5 and T_{m-10}/T_{m01} to 1.22 during 8 Beaufort winds from SW, probably due to shoaling and breaking of the waves on the FL5 foreshore.
- FL9 – oblique onshore winds: T_p/T_{m01} may be up to 1.4 for 7-8 Beaufort westerly winds; the reason for this increase is not clear.
- FL25 – offshore winds (SSW-WNW): $T_p/T_{m01} \sim 1.05$; for winds up to 7 Beaufort (and occasionally above it), T_{m-10}/T_{m01} may be up to 1.3-1.8.

- FL25 – wind nearly parallel to shore (NW-N): $T_p/T_{m01} \sim 1.5-1.75$;
 $T_{m-10}/T_{m01} \sim 1.25$.
- FL26: For T_p/T_{m01} same trends as for FL25, but much weaker and just within the interval of 1.13 to 1.33.
- SL29 – offshore winds (N-SE): in moderate winds, T_{m-10}/T_{m01} can be well above 1.17, generally when wave heights are order 0.1 m or less.
- FL2n : same remarks for new FL2-location as for the old FL2.
- FL37: For SSW-WSW and for NW-N winds similar trends as FL25, but slightly weaker.

All in all, the above exception situations are most likely to occur:

- during offshore winds, especially when the fetch is order 1 kilometre or less.
- for wind roughly parallel to the shore (FL25, FL37)
- shoaling and breaking waves on foreshore (FL5)

6.4 Wave steepnesses

The wave steepness is a very useful parameter as its natural variations are small. Therefore, wave steepnesses can be a useful benchmark to validate both experimental data, wave model results, and statistical extrapolations to estimate dike or platform design conditions from given wave data sets.

For the present study, the overall wave steepness 's' is simply defined as $s = H/L$, where H is a wave height and L a characteristic wave length. L can be implicitly evaluated from a measured wave period measure T, using the so-called dispersion relation:

$$(6.1) \quad L(T) = (g T^2 / 2\pi) * \tanh(2\pi d / L(T))$$

where d is the water depth. In section 6.7.3, we will briefly discuss the steepness of individual waves, but here, we will focus on two integral wave steepness parameters:

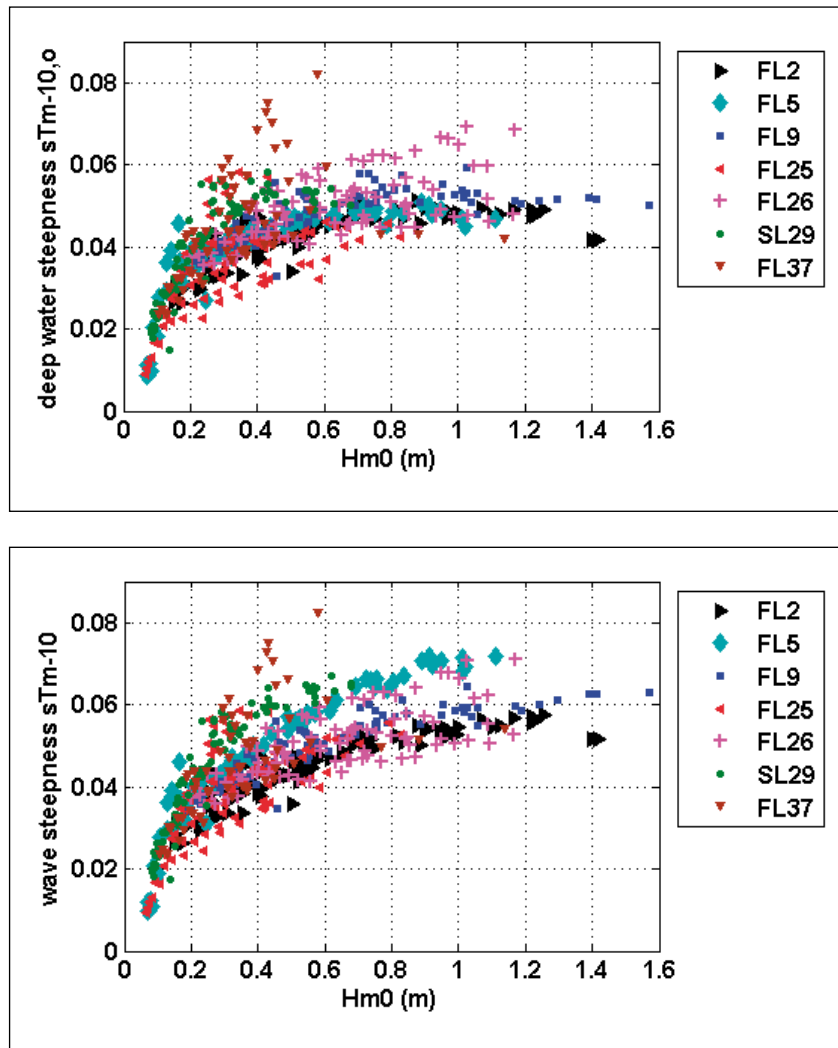
$$(6.2a) \quad s_{T_{m-10}} = H_{m0} / L(T_{m-10})$$

$$(6.2b) \quad s_{T_{m-10,o}} = 2\pi * H_{m0} / (g T_{m-10}^2)$$

Both parameters are based on the wave period measure T_{m-10} . The former is the real wave steepness, the latter is the so-called deep water steepness $s_{T_{m-10,o}}$. The latter is much simpler to calculate as one has not got to deal with the implicit tangens hyperbolicus term.

Figure 6.9 shows the wave steepnesses related to all data points shown in Figure 6.3-6.5, plotted as a function of the wave height H_{m0} .

.....
Figure 6.9 Deep water steepness $s_{Tm-10,o}$ (top) and real steepness s_{Tm-10} (below) as a function of wind speed, for the same averaged data as shown in Figure 6.3-6.5



The deep water steepness $s_{Tm-10,o}$ (Figure 6.9a) initially has a strong increase with H_{m0} , followed by near constant values around 0.05 for H_{m0} greater than 0.6 m. Much of the former trend is artificial as for small and short waves, the finite spectral integration range tends to increase T_{m-10} and to reduce H_{m0} , resulting in an even stronger steepness reduction. As a result, the steepnesses of Figure 6.9a are about 15% too low for $H_{m0} \sim 0.4$ m and over 30% too low for $H_{m0} \sim 0.2$ m; see Appendix B for full error estimates.

After correction for the aforementioned errors, the deep water steepnesses $s_{Tm-10,o}$ are nearly always in the range of 0.04 to 0.06. Still, there are a few exceptions to this rule:

- FL25 appears to have low steepness values in conditions with mixed wave fields (SSE and WNW winds), as some non-locally generated 'swell' tends to be present in those conditions
- Short fetch locations with pure wind sea, like FL26 and especially FL37 tend to have higher steepnesses than 0.06, especially in strong winds.

Finally, the two FL2 data points at $H_{m0} \sim 1.4$ m seem rather low, possibly due to a capa probe calibration drift of order -10% in the second half of 2002 (from which these points mainly originate).

The trends in the real steepnesses are largely the same, except for FL2, FL5, FL9 and SL29. For FL2 and FL9, the real steepnesses are about 20% higher during strong winds, but they are still near the central axis of the scatter cloud. At SL29 and FL5, the highest waves are also strongly depth-limited, and as a result, the real steepnesses are clearly larger than the deep-water steepnesses $s_{Tm-10,o}$. However, it must be noted that FL5 is situated on a shallow foreshore with significant wave shoaling, so that FL5 wave steepnesses may be different from the result of other locations.

Because of the smaller variations in parametrisations of the present data, the deep-water steepness $s_{Tm-10,o}$ may be slightly preferable over the deep water steepness s_{Tm-10} . The wave steepnesses based on the T_{m01} and T_{m02} have not been considered in detail because their errors due to the finite spectral integration range are much worse than those in Figure 6.9. This type of error is much smaller for a steepness based on the peak period T_p , but a disadvantage of s_{Tp} is its sensitivity to jumpy T_p behaviour in mixed wave fields. Therefore, s_{Tp} will only be discussed briefly. In fact, the main reason to consider s_{Tp} is linked to the fact that for deep water conditions, a simple relation can be derived from the empirical wave growth curves of Kahma and Calkoen (1992), see also (Bottema and van Vledder, 2006):

$$(6.3) \quad s_{Tp} \approx 0.086 \left(\frac{gx}{U_{10}^2} \right)^{-0.07}$$

With assumed fetches x between 1 and 20 km, and assumed wind speeds U_{10} between 10 and 20 m/s, this theoretical wave steepness ranges from 0.043 for long fetch and moderate winds to 0.056 for short fetch and gale-force winds. The observed values range from about 0.04 for moderate winds at FL2 and FL9, to about 0.05-0.06 for strong winds at FL26, and about 0.07 for strong offshore winds at the short-fetch locations FL25 and FL37. Note that this s_{Tp} trend is similar to the $s_{Tm-10,o}$ trend of Figure 6.9a.

Overall, the present wave steepness data seem to agree quite well with the steepness parametrisation (6.3) that was derived from Kahma and Calkoen (1992). However, the observed wave steepnesses s_{Tp} in conditions with strong wind forcing and very short fetch (order 1 km or less) can be somewhat larger, reaching s_{Tp} values of about 0.07 and occasionally even 0.08.

6.5 Scaling of wave properties with the wind

Knowledge of the physical scaling behaviour of the waves is essential for any type of wave forecasting, whether it is by simple parametric growth curves or by advanced numerical models like the spectral wave models SWAN (Booij et al., 1999). Actually, the latter category of models contains a range of tuneable parameters, and simple (semi-empirical) parametric wave growth curves are commonly used to tune these complex models.

Moreover, there has been a scientific debate about the way waves should be scaled with the wind during the last decades. The main issue of this debate is the question whether wave properties should be scaled with:

- the 10-metre wind speed U_{10} (or another wind speed at fixed or variable level)
- the so-called friction velocity u^* (see Chapter 4)

As the latter is directly related to the wind drag force per unit area τ (with $\tau = \rho u^{*2}$ where ρ is the air density), the above essentially boils down to the question whether wave properties should be scaled by a wind *speed* or by a wind *force*. As the wind speed U_{10} is essentially taken from an arbitrary (though internationally agreed) level and u^* is directly related to the air-water momentum exchange, wave scaling with u^* seems most plausible from a physical point of view. However, a combination of wave measurements and direct u^* measurements is rarely, if ever (Kahma and Calkoen, 1992) available. Therefore, and for convenience, the waves are often scaled with directly measured wind parameters, like U_{10} .

For deep water, Kahma and Calkoen (1992) propose the following U_{10} -based parametric wave growth formulas for their composite data set:

$$(6.4a) \quad H_{m0} = 4.0 \sqrt{0.00000052 \frac{U_{10}^4}{g^2} \left(\frac{gx}{U_{10}^2}\right)^{0.9}}$$

$$(6.4b) \quad T_p = \frac{2\pi}{13.7} \frac{U_{10}}{g} \left(\frac{gx}{U_{10}^2}\right)^{0.27}$$

where x is the fetch and g the gravity acceleration.

In a later publication (Kahma and Calkoen, 1994), they present a version with u^* -scaling:

$$(6.5a) \quad H_{m0} = 4.0 \sqrt{0.00065 \frac{u_*^4}{g^2} \left(\frac{gx}{u_*^2}\right)^{0.9}}$$

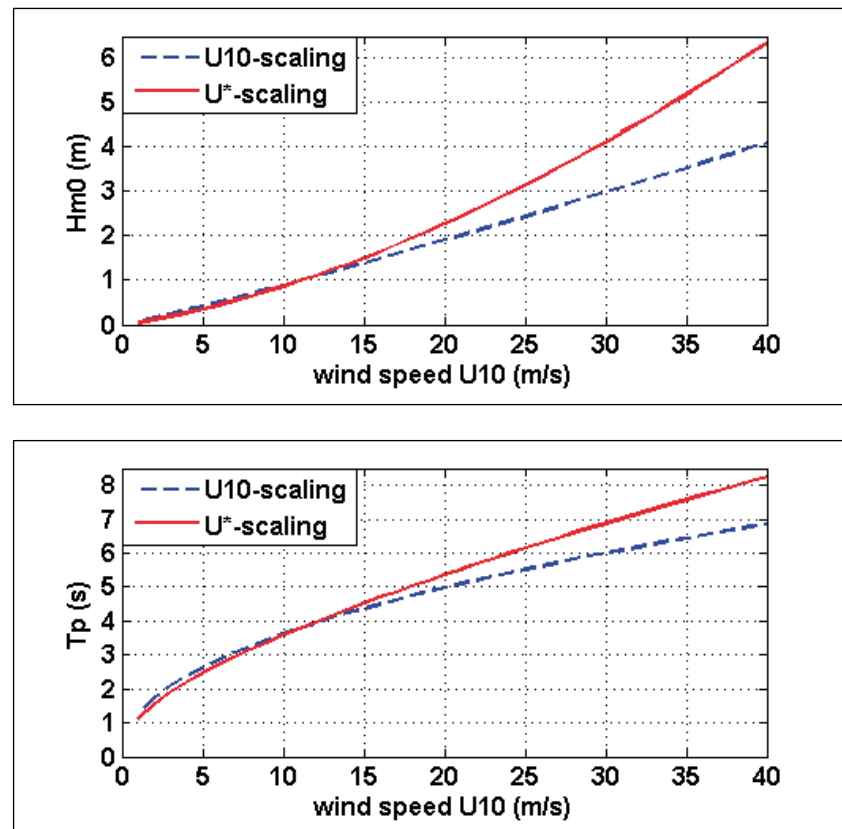
$$(6.5b) \quad T_p = \frac{2\pi}{3.08} \frac{U_*}{g} \left(\frac{gx}{u_*^2}\right)^{0.27}$$

The latter formulas are used to tune the wave model SWAN (Booij et al., 1999).

In Figure 6.10, the H_{m0} - and T_p -values as calculated with Eq. (6.4) and (6.5) are plotted as a function of mean wind speed U_{10} , for deep water and a typical Lake IJssel fetch x of 20 km. In Figure 6.10, u_* is converted to U_{10} using Eq. (6.6), i.e. with the C_D - or drag coefficient formula of Wu (1982). This approach is equivalent to the approach as reported in Kahma and Calhoun (1992), who also used (Wu, 1982) to convert U into (an assumed) u_* .

$$(6.6) \quad C_D = (u_* / U_{10})^2 = 0.001 * (0.8 + 0.065 * U_{10})$$

.....
Figure 6.10 Wave height H_{m0} (top) and peak period T_p (below) for deep water and 20 km of fetch, using parametric formulas of Kahma (1994) with U_{10} - and u_* -scaling.



Some key results of Figure 6.10 are:

- With u^* -scaling (Eq. 6.5), H_{m0} and T_p tend to be lower than predicted with Eq. (6.4) for wind speeds below 11 m/s, higher for winds above 11 m/s, and much higher for dike design conditions with winds of order 35 m/s.
- The H_{m0} -difference between Eq. (6.5) and (6.4) is about -10% for $U_{10} \sim 7$ m/s, $+20\%$ for 21 m/s and as much as $+50\%$ for $U_{10} \sim 37$ m/s.
- The T_p -differences are roughly twice as small as the H_{m0} -differences.
- The above trends apply for all fetches as the scaling power between H_{m0} , T_p and the fetch remains the same in Eq. (6.4) and (6.5).
- For dike design conditions with $U_{10} \sim 35$ m/s, deep water H_{m0} -values of 3.5 – 5 m are predicted and deep water T_p -values of about 7 sec. In the actual design conditions (Rijkswaterstaat, 2002), especially H_{m0} is significantly lower. In fact, H_{m0} is about 2.5 m for the most exposed locations. This suggests that shallow water effects yield 30-50% wave height reduction. These effects will be further investigated in the next section.

The differences shown in Figure 6.10 can be a significant source of uncertainty if wave-based design conditions must be evaluated for locations where the waves are not strongly depth-limited.

In fact, there is yet another potential error source for the SWAN wave model (Booij, 1999), and possibly also for other models. In SWAN, Eq. (6.5) is used for model tuning while assuming that the real dependence between wind, fetch and deep water waves can be described by Eq. (6.5). In reality, Eq. (6.5) is based on a number of assumptions, which are not applied in a fully consistent way. Firstly, Kahma and Calkoen (1992) note that no direct u^* measurements are available. Hence, they used Eq. (6.6) to convert their U_{10} (or $U(z)$ -) scaled data set to a u^* scaled data set. For this step, it is important to note that with Eq. (6.6), u^* roughly scales as $U_{10}^{1.25}$ to 1.3 . As a result, H_{m0} must scale with different powers of U_{10} and u^* respectively; the same applies for T_p . However, the powers in the U_{10} - and u^* -based scaling relations of Eq. (6.4) and (6.5) are identical. This implies that Eq. (6.5), the (Kahma and Calkoen, 1994) scaling relation used to tune the SWAN wave model, is inconsistent with the underlying equations (6.4) and (6.6).

Figure 6.11, shows how H_{m0} and T_p scale with the locally measured U_{10} . Only results for SW-winds at FL26 are shown as this assures a relatively homogeneous fetch of 4-5 km, and the best approximation of deep water conditions that is available in the present data set; even for $U_{10} = 20$ m/s, H_{m0} is less than 20% of the water depth.

.....
Figure 6.11 Wave height H_{m0} (top) and peak period T_p (below) for SW-winds at FL26. Shown are 20-minute samples (cyan points), average data (black line) and eye-fitted empirical scale relation (red line).

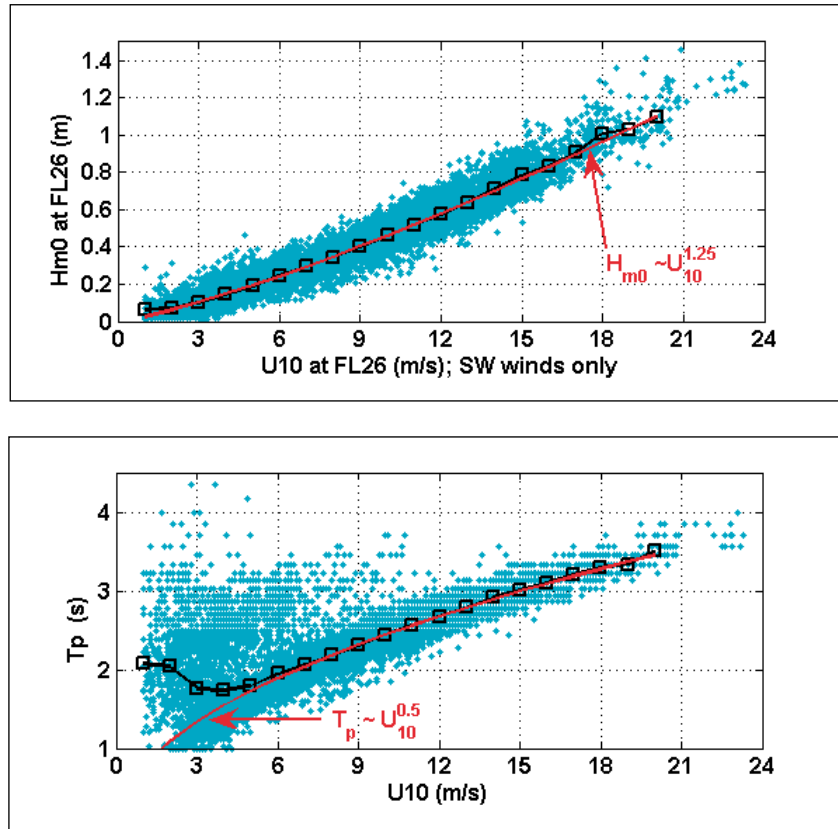


Figure 6.11 shows that for approximate deep water conditions in the present data set, the wave properties scale as follows with the mean wind speed U_{10} :

- $H_{m0} \sim U_{10}^{1.25}$
- $T_p \sim U_{10}^{0.5}$

If Eq. (6.6) is assumed to be a reasonable approximation (in accordance with section 4.5), the present u^* -based scaling relations are in first approximation:

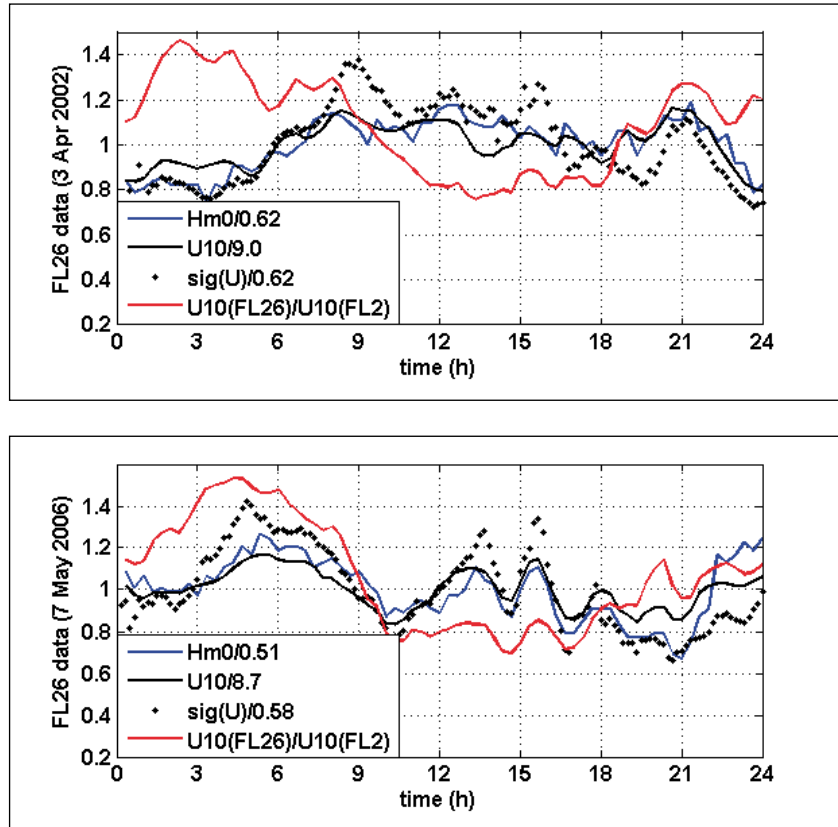
- $H_{m0} \sim u_*$
- $T_p \sim u_*^{0.4}$

The results for Kahma and Calkoen (1994) formulas, Eq. (6.4)-(6.5), are:

- Eq. (6.4); U_{10} -scaling: $H_{m0} \sim U_{10}^{1.1}$; $T_p \sim U_{10}^{0.46}$
- Eq. (6.5); u_* -scaling: $H_{m0} \sim u_*^{1.1}$; $T_p \sim u_*^{0.46}$

This implies that the U_{10} -dependence of the present data is slightly steeper than Kahma and Calkoen's (1994) U_{10} -scaling (despite the fact that for strong winds, no perfect deep water conditions exist for the present data), while the present u^* -scaling is slightly flatter than their u^* -scaling. This would suggest that the best way to scale the present data is somewhere between U_{10} - and u^* -scaling.

Figure 6.12 Warm spring day with rather strong ESE-wind: Relative time evolution of wave height H_{m0} , mean wind speed U_{10} and wind standard deviation $\text{sig}(U)$ (σ_u) – all normalised with their daily average – as well as the wind speed ratio $U_{10}(\text{FL26})/U_{10}(\text{FL2})$. Top panel is 3/4/2002, lower panel is 7/5/2006.



In order to get more clarity about this scaling question, direct measurements of u^* are crucial. Unfortunately, u^* has not yet been measured over Lake IJssel. However, there are some special conditions (long fetch, neutral or stable atmosphere) where the standard deviation in the wind speed samples σ_u is a fixed multiple of u^* : $\sigma_u \sim (2.2-2.5)u^*$.

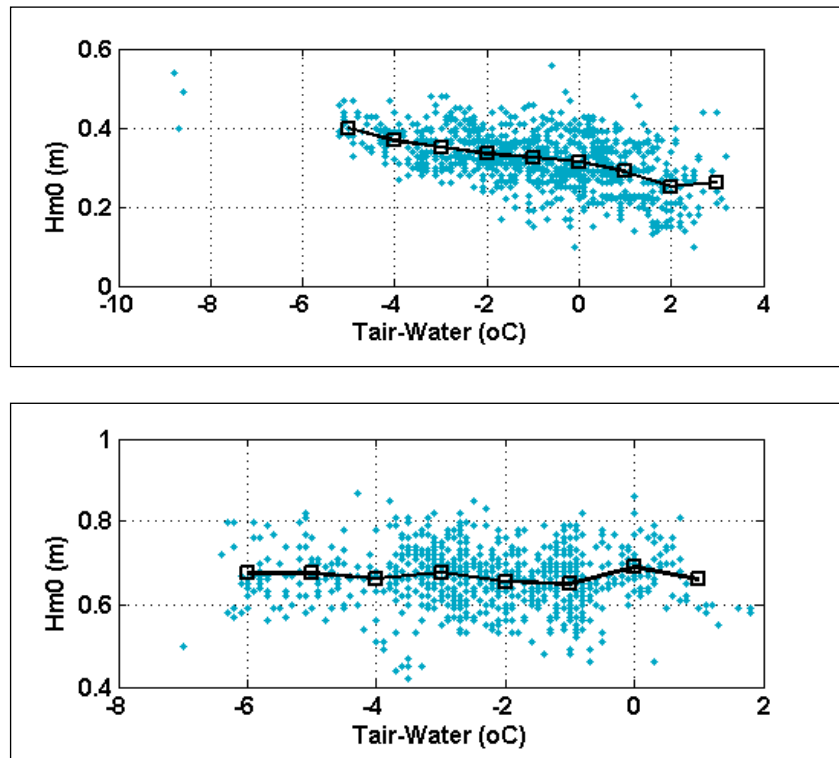
The results of two potentially interesting days (3/4/2002 and 7/5/2006) are shown in Figure 6.12. Both days are warm spring days with an ESE wind of about 5 Beaufort. Near sunrise, air-water-temperature differences are near-zero; in the afternoon the air is about 5°C warmer than the water.

As the primary focus is on scaling relations, all variables (H_{m0} , U_{10} , u^*) are normalised with their 24h-average. For each variable, this average is indicated in the legend. For 3/4/2002, the 24h averages in H_{m0} , U_{10} and σ_u are 0.62 m, 9.0 m/s and 0.62 m/s respectively. The red line in each graph corresponds to the U_{10} wind speed ratio between FL26 and FL2. During the afternoons, the atmosphere is so stable that wind speeds decrease with increasing fetch: FL26 then has 20% less wind than FL2.

As it turns out, the relative time trends of H_{m0} , U_{10} and σ_u are all quite similar. Closer inspection suggests that H_{m0} and U_{10} correlate slightly better than H_{m0} and σ_u . This would lead to the surprising result that U_{10} -scaling would perform slightly better than the (theoretically more plausible) u^* -scaling. However, this result should be used with caution

as the present analysis is based on u^* -approximations rather than u^* -measurements.

.....
Figure 6.13: Wave height H_{m0} at FL26 as a function of air-water temperature difference, for NE-SE winds. $U_{10}(\text{FL26}) = 5\text{-}6$ m/s in top panel and 9-11 m/s in lower panel.



An issue that is related to the above scaling questions is the influence of atmospheric thermal stability on wave growth. Previous research (Young et al., 1998) suggests that these influences can be quite important.

Figure 6.13 shows H_{m0} at FL26 as a function of air-water temperature difference, for easterly winds of 5-6 m/s (top panel) and 9-11 m/s (lower panel). For weak winds, there are indeed significant stability-related trends, with lower H_{m0} in stable conditions and higher H_{m0} in unstable conditions. This is not surprising because for given U_{10} , the wind drag (like u^*) is smaller for stable conditions and larger for unstable conditions. For short fetches and SW-winds (not shown), the above trends weaken somewhat, for 5 Beaufort winds (lower panel) they disappear altogether. The latter also explains why Figure 6.12 shows no clear stability- and daytime-related trends in the H_{m0}/U_{10} -ratio.

All in all, the present data set does not clarify whether U_{10} - or u^* -scaling is preferable. This inconclusive result is not surprising as no direct u^* -measurements are available. However, some conclusion can be made about atmospheric thermal stability effects on wave growth. Direct thermal stability effects on wave growth were only detected for weak to moderate winds. For strong winds, the effect is mainly *indirect*, through the spatial wind field. Yet even this indirect effect is often far from negligible, see section 4.4.2.

6.6 Depth-limited waves

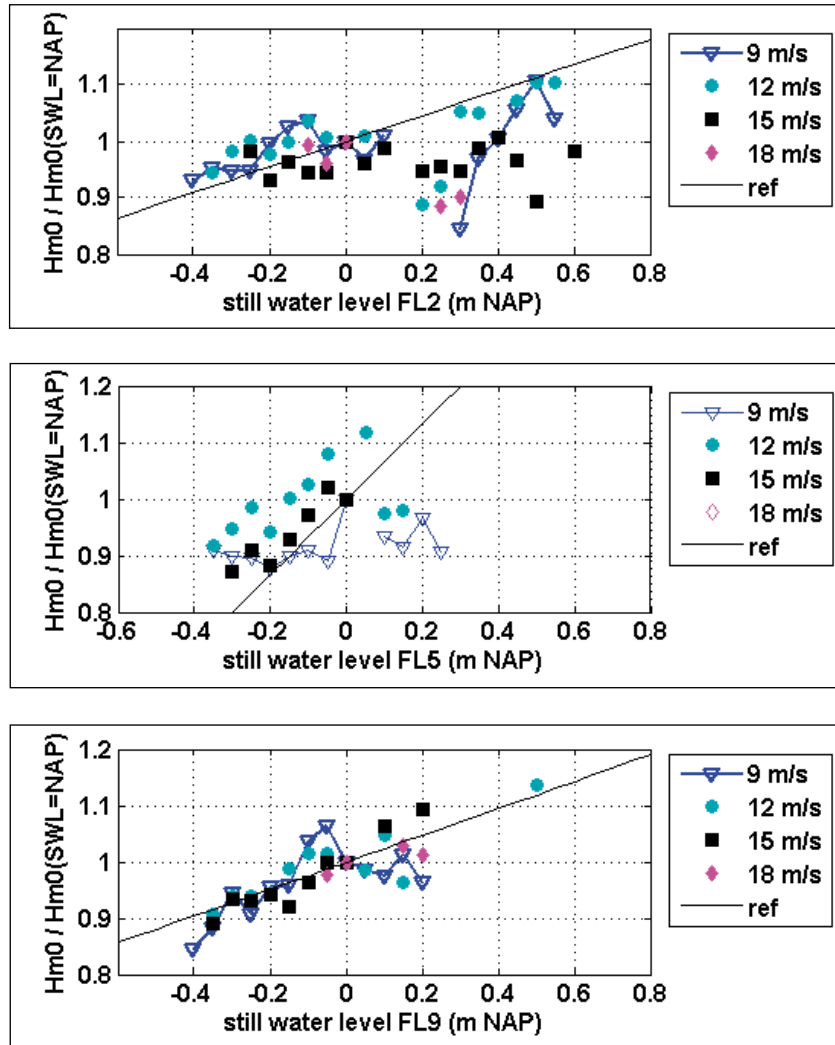
In the previous section, it was concluded that the present design wave heights for (water defences around) Lake IJssel are about 30-50% lower than they would have been for infinitely deep water. This implies that the design waves for Lake IJssel are strongly depth-limited, and that it is important to accurately predict the effects of finite water depth on the waves of Lake IJssel. For most of Lake IJssel, the bottom is relatively flat so that depth-limited wave growth over flat bottoms is the issue of interest. This issue will be investigated in section 6.6.1. Some parts of Lake IJssel (near Enkhuizen and the Frisian shores) have shallow foreshores. Measurements related to these conditions will be discussed in section 6.6.2.

6.6.1. Depth-limited wave growth

One way of validating wave models for depth-limited wave growth, or any other phenomenon of interest, is to select representative cases and to validate the model for these cases. This approach will be considered in Chapter 7.

In this section, the focus will be on trends related to depth-limited wave growth. For sake of brevity, only trends in the wave height H_{m0} will be considered. The basis of the present analysis is the type of 'wave climate' plots like Figure 6.3-6.5, but with results plotted as a function of still water level (SWL) rather than wind direction. Next, all results were normalised with the H_{m0} associated with the wind speed class under consideration, and an SWL equal to NAP. In this way, all results for one location could be presented in a single graph. This is done in Figure 6.14, where the results of FL2, FL5 and FL9 are shown. The results of FL2 and FL9 will be discussed below; the FL5 results will be considered in section 6.6.2.

Figure 6.14: Mean observed wave height H_{m0} , normalised with H_{m0} -value when still water level equals NAP. Top panel is FL2 (wind direction 240-300°), middle panel FL5 (subset from March 2006 on; 190-230°), lower panel is FL9 (180-240°). Reference line corresponds to fully depth-limited waves (H_{m0} proportional to depth).

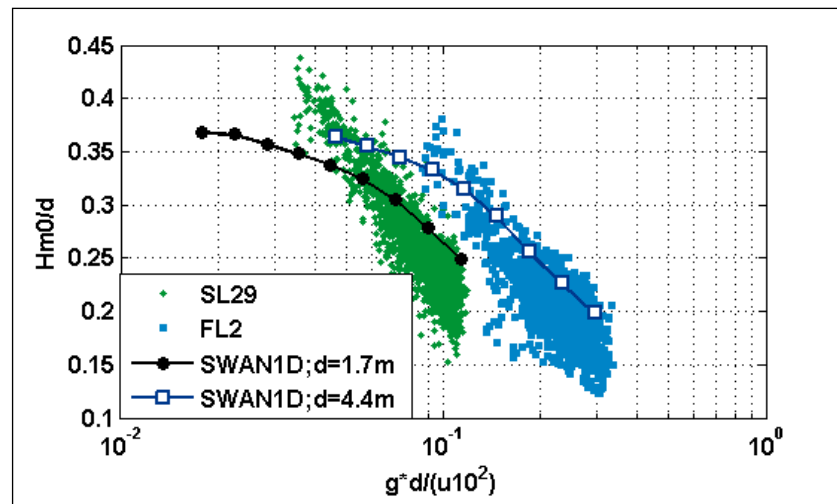


The top panel shows the aggregated results of FL2, for four different wind speed classes (each 2 m/s wide) and an onshore and long-fetch wind direction sector from the west: 240-300°. The black drawn line equals the relative depth change as a function of SWL. It also depicts the trend that would occur if the depths were fully depth limited, with a H_{m0} proportional to the water depth. For FL2, this reference trend line has a slope of 10% H_{m0} change for every 44 cm change in SWL. Surprisingly, the results for the lowest wind speed classes are close to the fully depth-limited reference line, whereas H_{m0} has no depth-dependent trend or even a slightly decreasing trend for large wind speeds.

Apparently, there are too many 'disturbing' factors to accurately detect the real depth-limited trend in the FL2 data. Natural scatter is one cause of these disturbances. Natural variations are often case-to-case variations (section 6.2), rather than variations within a case. This may well cause scatter in Figure 6.14 as the number of underlying data for each data point in Figure 6.14 is small, while each case typically has its own SWL value. Experimental errors may also play a role. The response of the upper third of the capa probe FL2 is order 7% weaker than for

the middle part of the probe (fig. 3.5 in Bottema, 2005) and this may help to explain the weaker depth-limited trends for strong winds. In addition, many underlying data (2000-2002) with SWLs of about +20 cm NAP have too low a H_{m0} due to disturbances by the capa probe supports (see Appendix B.6 for background information). The dip in the data of Figure 6.14a (for SWLs of about +0.1 m NAP) suggest that most of these data were successfully filtered out, but not all of them. The results for FL9 (for SSW-winds of 180-240°) are shown in Figure 6.14c. Only results with H_{m0} smaller than 1.1 times the distance between the SWL and instrument top were included, to avoid biases by wave overtopping over the FL9 capa probe (see section B.3). The results of Figure 6.14c suggest that the waves are close to fully depth-limited for large and *small* wind speeds. This apparent depth-limitation is highly surprising because H_{m0}/d for weak winds is simply too small to expect any significant depth-limitation. In fact, the FL9 H_{m0}/d -ratios at wind speeds of 9, 12, 15 and 18 m/s are 0.14, 0.18, 0.25 and 0.31 respectively, all when the SWL equals the NAP datum. For the FL2, these numbers are typically 7% (in absolute terms: 0.01-0.02) smaller.

Figure 6.15: Wave-height-over-depth ratio H_{m0}/d as a function of dimensionless wind-and-depth parameter gd/U_{10}^2 . Experimental results from SL29 (left) and FL2 (right) are shown, for WSW-winds (220°-260°) of at least 12 m/s. SWAN-results are one-dimensional with infinite fetch.



An alternative way of investigating depth limitation is to explore the trends in H_{m0}/d as a function of the dimensionless depth parameter gd/U_{10}^2 , as is done by (Waal, 2002). Figure 6.15 shows a selection of FL2- and SL29-data, together with one-dimensional SWAN-model results with default physical settings and infinite fetch. Note that the data selection is such (WSW-winds with long fetch, at least 12 m/s wind speed) that fetch-limited data (rather than depth-limited data) are eliminated as much as possible. Some finite fetch effects may remain, but model estimates of these finite fetch effects range from anything between 2% and 40% (Waal, 2002). Hence, caution is needed in the interpretation of Figure 6.15, but some general conclusions can be made.

This is certainly true for the SWAN results, which have no finite fetch effects as they are for quasi infinite fetch. For low wind speeds (in the right of the graph), both SWAN curves are relatively steep. For

H_{m0}/d greater than 0.32 however, both SWAN-lines curve downwards, indicating enhanced depth limitation. Ultimately, the SWAN results have an upper limit of $H_{m0}/d \sim 0.38$, no matter how high the wind speed is.

Unlike SWAN, the experimental data show no kink near $H_{m0}/d = 0.32$ and both experimental data sets exceed SWAN when H_{m0}/d is larger than 0.32. This is all the more remarkable as the experimental data have finite fetch, and the SWAN results not. In fact, the FL2 results of 18/1/2007 approximate the highest possible SWAN-value of H_{m0}/d over horizontal bottoms (0.38), whereas the SL29-results have clearly exceeded it during several storms.

For the SL29-data, two things are interesting to note:

- Young and Babanin (2006) report H_{m0}/d and gd/U_{10}^2 values for Lake George that range to 0.45 and 0.028 respectively, values that correspond well with the present SL29-data.
- The two windiest SL29-cases so far have fairly different H_{m0}/d values: 0.41-0.44 at 27/10/2002, about 0.37 at 18/1/2007. There is a small chance that this is an indication for an absolute H_{m0}/d -limit of order 0.45, but several more severe storm data are needed to find out whether this is indeed the case. Still, the Lake Sloten data obtained so far have a clear asset: they support the Lake George data and provide well-documented test cases (Chapter 7) in which H_{m0}/d for flat bottoms is well above the model limit of 0.38.

6.6.2. Shoaling wave situations

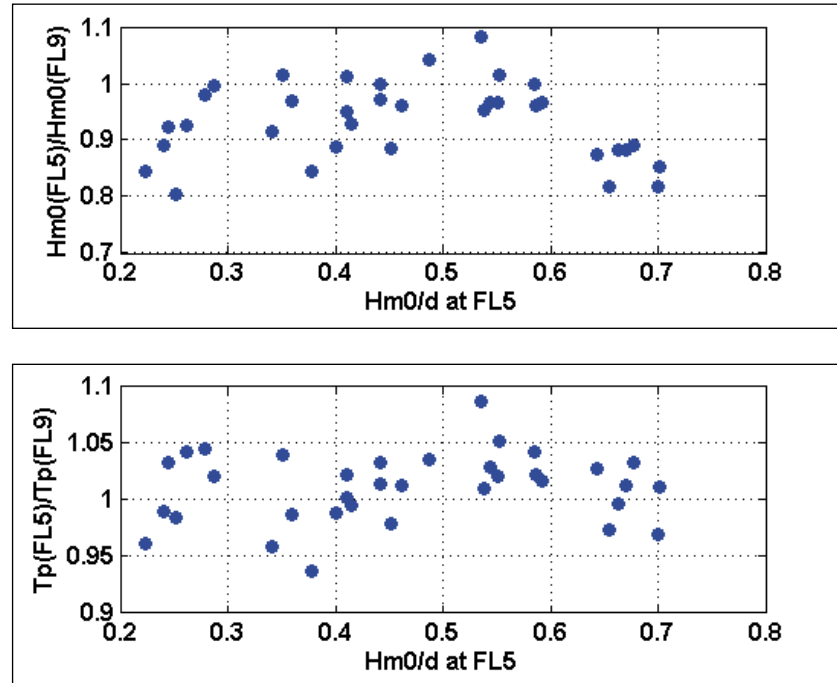
Knowledge of shoaling and breaking waves on foreshores is of great importance for flood protection along Lake IJssel. Most of the Frisian coast and part of the coast near Enkhuisen have shallow foreshores, where wave heights and wave periods may be reduced significantly. Even without foreshores, significant wave transformation may occur when the waves propagate from Lake IJssel over the lower (underwater) slopes of the dike.

The most suitable location to investigate situations with shoaling and breaking waves is FL5. Unfortunately, FL5 has had many location changes. For the present analysis, the subset of data starting in March 2006 (excluding summer data) was least biased by experimental errors. This data subset is further restricted because only wind directions of 190-230° are considered to guarantee near-normal incidence of the waves to the foreshore, and a near-constant fetch ratio of FL5 and FL9.

In Figure 6.14b, the H_{m0} -trends of FL5 are shown as a function of still water level (SWL). For SWLs equal to the NAP datum, the actual H_{m0} values are 0.62, 0.74 and 0.96 m for wind speeds of 9, 12 and 15 m/s respectively. This corresponds to H_{m0}/d values of 0.41, 0.49 and 0.64. For moderate winds and low waves, the H_{m0} -trend hardly depends on the SWL, whereas the trends are close to the fully depth-limited

reference line for strong (7 Beaufort) winds and high waves. These trends definitely seem to be physically plausible. What is puzzling however, is the fact that the FL9-trends in Figure 6.14c are all close to fully depth-limited, even though the H_{m0}/d values of FL9 are as small as 0.14 to 0.31.

Figure 6.16: Ratio of FL5 and FL9 wave heights (H_{m0}) and peak periods (T_p), for SSW-winds, as a function over the wave-height-over-depth ratio H_{m0}/d at FL5.

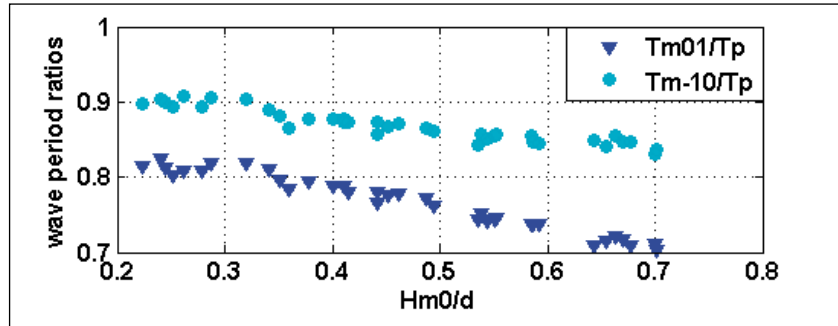


In Figure 6.16, the ratio of FL5 to FL9 wave heights (H_{m0}) and peak periods (T_p) is plotted as a function of the H_{m0}/d parameter at FL5, considering SSW-winds only. Note that no individual samples are plotted, but rather the averages for 5 cm wide SWL classes, defined for wind speed classes of 8-10, 11-13 and 14-16 m/s.

Because of the slightly longer fetch at FL5, H_{m0} and T_p can potentially be about 6% and 3% higher than at FL9. Figure 6.16a shows that the actual H_{m0} -ratio is about 0.9 for mild conditions, increasing to about 1.0 for $H_{m0}/d \sim 0.5$, after which it decreases to about 0.85 for $H_{m0}/d \sim 0.7$. This implies that despite the slightly longer fetch, FL5 generally has lower waves than FL9, even in mild conditions. The largest FL5-to-FL9 H_{m0} ratios occur when H_{m0}/d at FL5 is about 0.5, possibly as a result of wave shoaling. For H_{m0}/d -values larger than 0.5, the H_{m0} -ratio drops, presumably as a result of (enhanced) wave breaking at FL5. Besides this, it is interesting to note that H_{m0}/d at FL5 can reach values as high as 0.7 anyway.

The peak periods at FL5 tend to be equal to those of FL9, or a fraction larger, in accordance with the larger fetch. The absence of T_p -trends as a function of H_{m0}/d probably reflects the fact that wave shoaling and mild wave breaking both have little effect on T_p .

Figure 6.17: Wave period ratios T_{m01}/T_p and T_{m-10}/T_p for SSW-winds at FL5, as a function over the wave-height-over-depth ratio H_{m0}/d .



Other wave period measures are not as insensitive to depth-limitation as the peak period T_p . Figure 6.17 clearly indicates that the ratio of T_p to T_{m-10} and especially T_{m01} starts to decrease as soon as H_{m0}/d exceeds a value of about 0.32. This decrease is related to the transfer of wave energy from the spectral peak to higher harmonics, as can be seen for various depth-limited spectra shown in section 6.7.2 and Chapter 7.

Results like the above are quite important since the knowledge about wave periods over shallow foreshores is even more limited than the knowledge of wave heights for these locations. On the other hand, it is important to note that the above trends are location-specific. Especially far up the flat part of a foreshore, the wave properties may be quite different from those of the FL5, which is rather more typical for the upper half of a *sloping* foreshore.

6.7 Other wave-related issues

In this section, some remaining issues are discussed, like the concept of effective fetch (section 6.7.1), the frequency spectra of wind waves (section 6.7.2) and the frequency distributions for the heights and periods of individual waves (section 6.7.3).

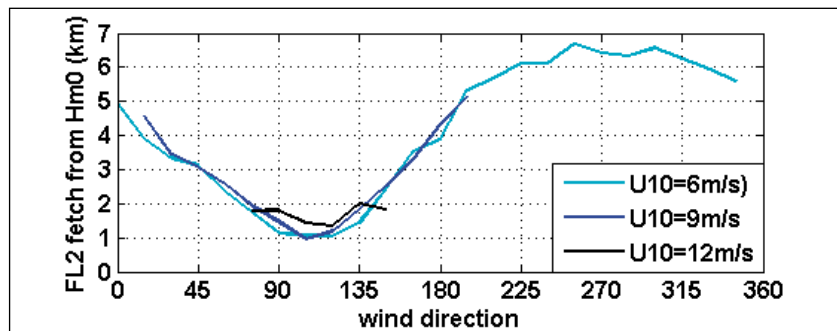
6.7.1. Validity of effective fetch concept

Parametric wave growth curves are extremely useful for a quick first guess of wave conditions at a particular location, for which one hardly needs more than a simple pocket calculator. Examples of these curves are those of Kahma and Calkoen (1992, 1994), Bretschneider (CERC, 1973) and Young and Verhagen (1996); see also Holthuijsen (1980) for a summary of wave growth curves. In practice, one nearly always has to deal with complex coast lines and wind that is not perpendicularly blowing offshore. For those situations, the concept of effective fetch is crucial: the assumption that for a given location and wind direction, a single effective fetch is sufficient to calculate the wave height and wave period with a given set of parametric growth curves.

The parametric formulas of Kahma and Calkoen (1992) are very useful to investigate the validity of the effective fetch concept because of

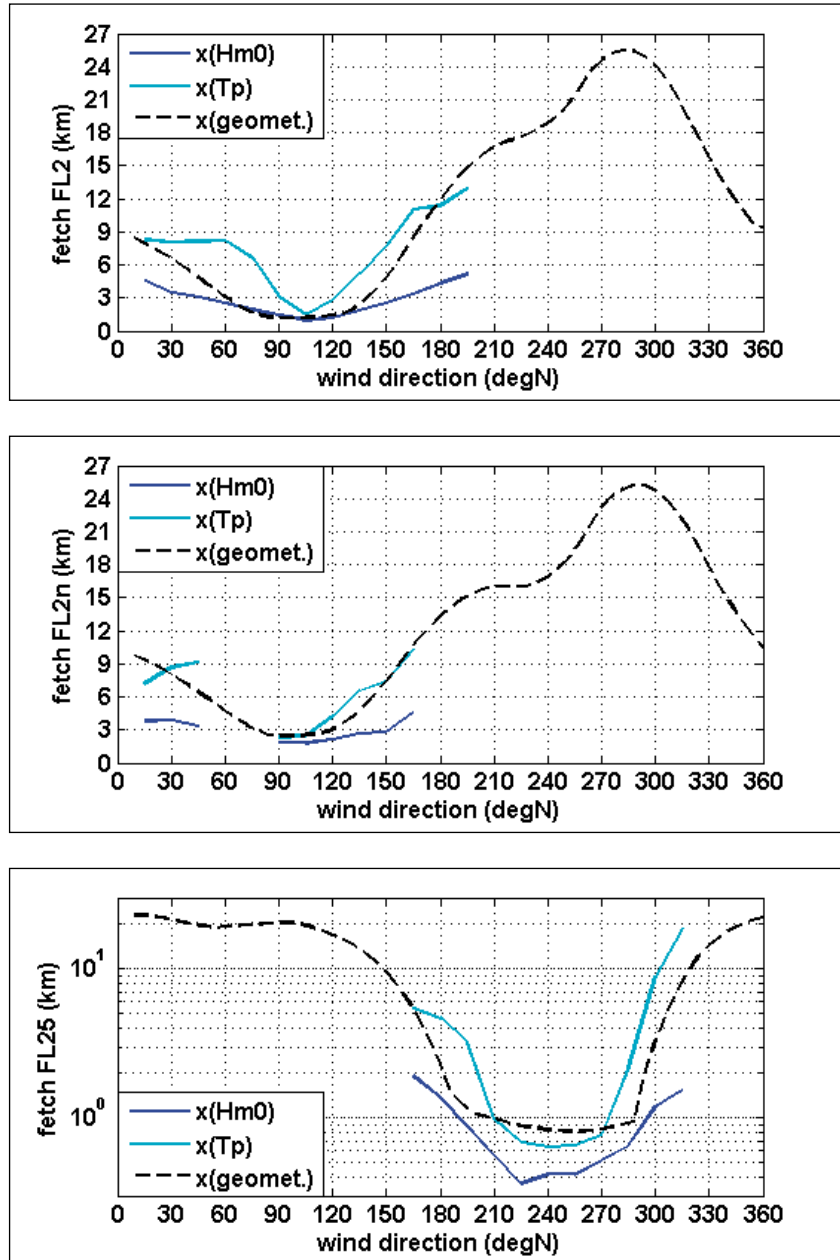
their simplicity; see Eq. (6.4). A drawback of these formulas is that they are only valid for deep water. SWAN model data (Bottema and Vledder, 2006) suggest that bottom friction effects become noticeable for H_{m0} -values above 0.5 m (12% of the water depth). Hence, the application of Eq. (6.4) is limited to cases where $H_{m0}/d < 0.12$. Another limitation is linked to the fact that the present waves do not scale exactly according to Eq. (6.4); see section 6.5. For the latter reason, the inverse of Eq. (6.4a) was applied to the H_{m0} -data of FL2 that were plotted in Figure 6.3. The subset of these data where H_{m0}/d did not exceed the above threshold of 0.12 is plotted in Figure 6.18. The results for wind speeds of 6 and 9 m/s agree excellently. The results for $U_{10}=12\text{m/s}$ deviate somewhat, but it should be noted that the number of underlying data for this wind speed is small, while the scatter is large.

.....
Figure 6.18: Effective fetch x_H at FL2, as calculated by the inverse of Eq. (6.4a), as a function of wind direction for three different wind speeds.



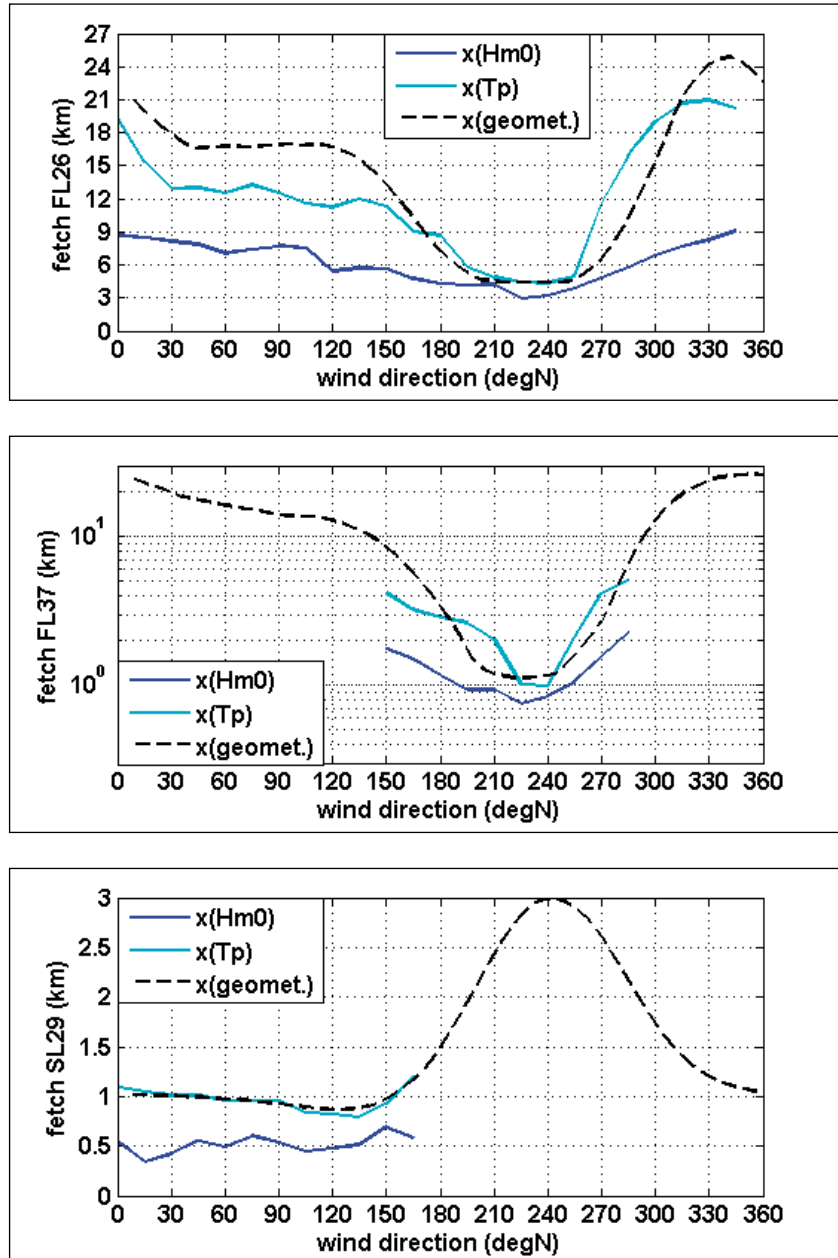
The validity of the effective fetch concept is investigated by mutually comparing the H_{m0} - and T_p -fetches x_H and x_T from Eq. (6.4a) and (6.4b). In all cases, only data were considered where the local U_{10} was in the range of 8-10 m/s. For lower wind speeds, the risk on biases by thermal stability effects and experimental errors was considered to be too large. For higher wind speeds, there generally were insufficient data with H_{m0}/d values of 0.12 or less. In addition to this, geometrical fetch estimates were considered. These fetches were provided by JP de Waal of RWS RIZA, and they are evaluated by weighting the actual fetches in a $[-45^\circ, +45^\circ]$ sector around the wind direction with a \cos^2 weighting factor, in accordance with Holthuijsen (1980).

.....
Figure 6.19: Effective fetches x_H and x_T as calculated by the inverse of Eq. (6.4) and geometrical fetch estimates, all as a function of wind direction. Top, middle and lower panel show results for FL2, FL2n (new FL2 location) and FL25, the latter on 0.3-30 km logarithmic scale.



Fetches were calculated for all locations where local wind data are available; the results are given in Figure 6.19-6.20. Note that some plots are given on a logarithmic scale of 0.3-30 km to facilitate inspection of the results for very short fetches.

Figure 6.20: As Figure 6.19, for FL26, FL37 (0.3-30 km logarithmic scale) and SL29.



From Figure 6.19 and 6.20, the following main features can be noted:

- In nearly all cases, the fetch as calculated from T_p is larger than from H_{m0} . This implies that the measured steepness differs from Kahma and Calkoen's (1992) steepness of Eq. (6.3)-(6.4), even though the general steepness range is correct (section 6.4).
- The H_{m0} - and T_p fetches agree relatively well in the centre of sheltered sectors, especially when H_{m0} is not larger than about 5% of the water depth
- The largest differences in H_{m0} - and T_p -fetch tend to occur along the edges of sheltered sectors, for slanting fetch. For onshore winds the differences seem to be close to a factor 2.
- The geometrical fetches appear to agree best with the fetches as estimated from the peak period T_p . This is somewhat surprising,

because for low wave heights and very short fetches, T_p easily gets positively biased by 'swells', ship waves, etc.. The fact that the H_{m0} -fetches are quite systematically well below the geometrical fetch are an indication that Eq. (6.4a) tends to overestimate H_{m0} for these cases. Perhaps, this is also an indication that there is even noticeable depth-limitation on the H_{m0} wave heights when H_{m0} is only about 10% of the water depth.

From the above, one is tempted to conclude that the effective fetch concept is generally a poor approximation, except perhaps in the centre of sheltered sectors. On the other hand, it should be noted that both the H_{m0} - and T_p -based fetch estimates are sensitive to biases in the underlying data. In fact, in Figure 6.19-6.20, a relatively small 10% error in H_{m0} and T_p will show up as fetch errors of about 20% and 40% respectively. The above is not only relevant in relation to the underlying H_{m0} - and T_p -measurements, but also to the general accuracy of the parametric wave growth formulas used.

It is because of the latter issue that Bottema and Vledder (2006) not only based their analysis on Eq. (6.4), but also on the 1984 parametric formulas of Bretschneider (in Young and Verhagen, 1996) and Young and Verhagen (1996), and on a comparison of one- and two-dimensional SWAN-simulations. Their analysis led them to the conclusion that generally, the effective fetch concept is least accurate in the first kilometres offshore, and for slanting fetches. They also found two other results of interest:

- The T_p -fetches as calculated by Bretschneider for shore-parallel and onshore winds are *larger* than the distance to the nearest shore which implies that Bretschneider underestimates the measured T_p -values. No further conclusions can yet be drawn about Bretschneider as (Bottema and Vledder, 2006) intended to verify the effective fetch concept. The validation of individual parametric wave growth formulas is outside the scope of (Bottema and Vledder, 2006) and also of this report.
- The H_{m0} - and T_p -fetches as derived from Young and Verhagen's (1996) formulas agreed best during slanting fetches, where other formulas had their poorest performance. Possibly this is because their underlying Lake George data are also biased towards slanting to parallel fetch conditions.

All in all, caution is required in more than one way. First of all, one can not always count on the validity of the effective fetch concept. Secondly, it seems that parametric wave growth formulas can be significantly biased towards the properties of their underlying data, and due to their hidden fetch assumptions. Therefore, it is strongly recommended to validate parametric wave growth curves with wave measurements that are representative for the locations at which these formulas are to be applied. As many advanced wave models rely on parametric wave growth curves for their tuning, the same also applies to more advanced wave models.

6.7.2. Wave spectra

If one is to discuss the phenomenology of wave frequency spectra, one sub-section will not be sufficient. This is certainly so if not only wave spectra are considered in pure wave growth situations, but also in situations with mixed wave fields. In Chapter 7, which discusses test and calibration cases for wave models, a considerable amount of attention will be given to the phenomenology of wave spectra. In the present section, only the wave spectra in some standard situations will be considered, as these are the situations that are most suitable for parametrisations. We will focus on situations with depth-limited conditions as the SWAN model then seems to have more difficulty in reproducing the present data than during deep water conditions (Bottema, 2006c). Cases with complex upwind coastlines will not be considered in this section as such cases are hard to parameterise anyway.

As for the depth-limited wave spectra, a parametrisation based on Lake George is recently published by Young and Babanin (2006). This parametrisation may be suitable to model the measured wave spectra of Lake IJssel and Lake Sloten as well. Therefore, the evaluation of Young and Babanin's (2006) parametrisation will be the main topic of this section. Their parametrisation is in fact the sum of a conventional deep water spectrum F_1 and a second harmonic spectrum F_2 , where the formulas for F_1 and F_2 read:

$$(6.7a) \quad F_1(f) = \beta_1 g^2 (2\pi)^{-4} f_p^{-1} f^{-4} \left[\exp\left(\left(\frac{f}{f_p}\right)^{-4}\right) \right]^\gamma \exp\left[\frac{-(f-f_p)^2}{2\sigma^2 f_p^2}\right]$$

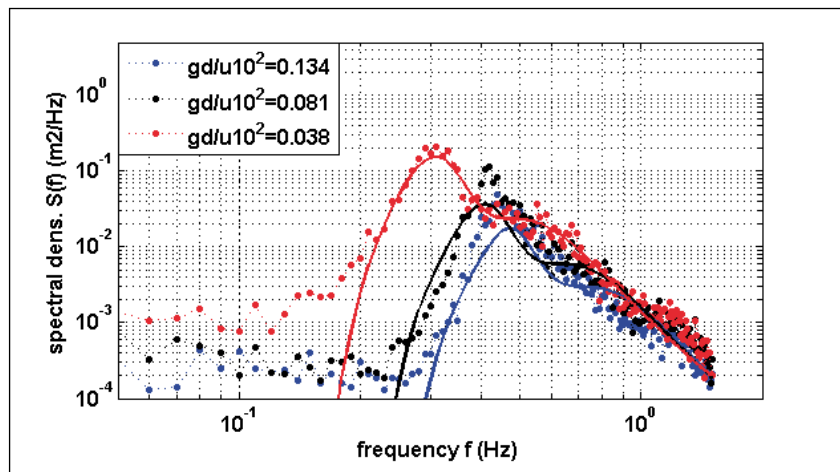
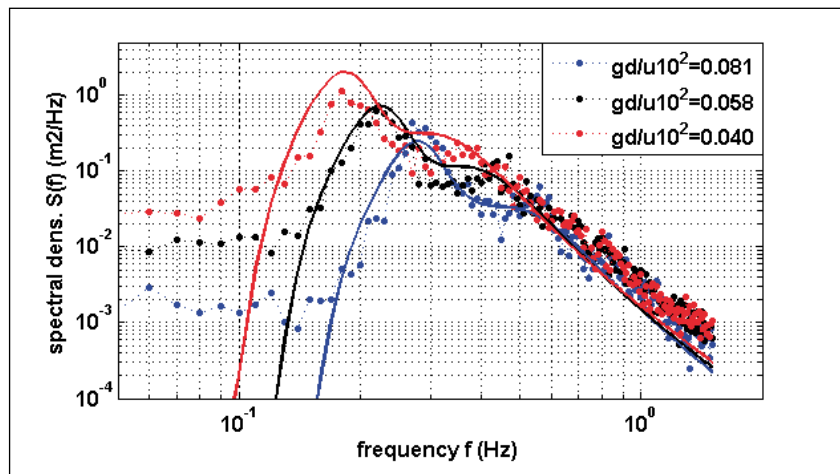
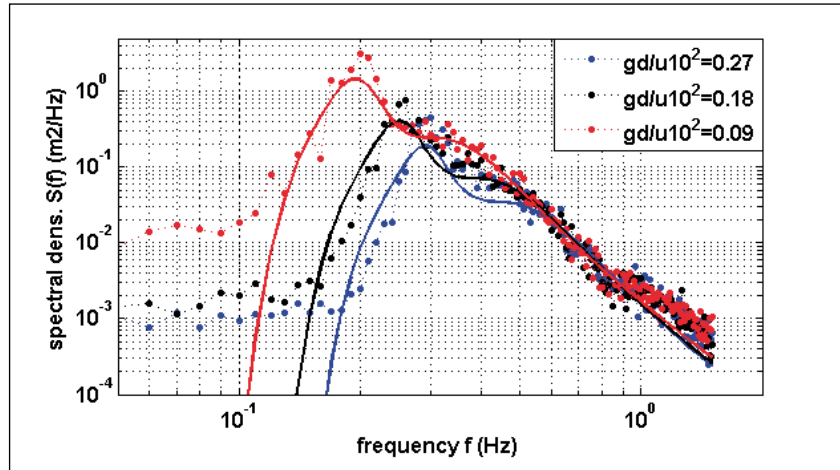
$$(6.7b) \quad F_2(f) = \beta_2 g^2 (2\pi)^{-4} f_{p2}^{3.35} f^{-8.35} \exp\left[\frac{-8.38}{4} \left(\frac{f}{f_{p2}}\right)^{-4}\right]$$

where (see the original publication for extensive explanations):

- β_1 is parametrised as $0.00589 * (gd/u_{10}^2)^{0.085}$ with g the gravity acceleration (9.81 m/s^2) and d the water depth;
- f_p is the peak frequency ($1/T_p$);
- γ is the peak enhancement factor, parametrised as $\gamma = 0.00297\beta_1^{-1.34}$;
- σ is a shape factor, parameterised as $\gamma = 2 * 10^{-6} \beta_1^{-2.09}$;
- β_2 is 0.074;
- f_{p2} (second harmonic) is 1.76 times the peak frequency f_p ;

This parametrisation is tested for three locations (FL2, FL5, SL29) and three cases: 6/12/2006 (2-8 h MET), 11/12/2006 (2-8 h MET) and 18/1/2007 (11-14h MET). All cases have wind directions close to SW, wind speeds are about 12, 15 and 21 m/s respectively. The resulting spectra are shown in Figure 6.21.

.....
Figure 6.21: Measured spectra and (drawn lines) parametrisations of Eq. (6.7), for SW winds of 12 m/s (6/12/06; blue line), 15 m/s (11/12/06, black line) and 22 m/s (18/1/07; red line). Top, middle and lower panel: FL2, FL5 and SL29.



For FL2, the parametrisation performs quite well, although for all wind speeds, the height of the spectral peak seems somewhat underestimated, while the hump near twice the peak frequency is somewhat overestimated. At frequencies near 1 Hz, the measured spectral energy is perhaps somewhat high, but besides this, the measurements and parametrisations in the spectral tail nearly collapse on a single line. Finally, it can be noted that the present

parametrisation even seems to give a better spectral fit than the SWAN wave model results as presented in (Bottema, 2006c). The gd/u_{10}^2 -values are given in the legend of Figure 6.21a. The corresponding H_{m0} values are 0.80, 1.03 and 1.74 m; the H_{m0}/d values 0.19, 0.24 and 0.37.

For FL5, the parametrisation performs quite well for the first case, where H_{m0} is 0.71m and H_{m0}/d is 0.58. For the strong wind cases however, the measured secondary maximum is rather predicted as a broad hump; and for the case of 18/1/2007, there is also a mismatch (overestimation) in the spectral peak. For these two cases, H_{m0} is 1.05 and 1.28 m, with H_{m0}/d values of 0.75 and (with wave breaking) 0.65. However, if we take into account that the conditions are quite different from those from which the parametrisation was derived (a sloping bottom in reality instead of the assumed flat bottom, with H_{m0}/d up to 0.75 instead of 0.45), the results are still quite reasonable.

Figure 6.21 c gives the results for the SL29. The parametrisation seems excellent for the severe conditions of 18/1/2007, but it underestimates the spectral peak and overestimates the hump for the other cases. The H_{m0} -values for all three cases are 0.28, 0.40 and 0.65 m, the H_{m0}/d values 0.16, 0.23 and 0.37.

Finally, one can do a cross-comparison for the three cases where $gd/u_{10}^2 \sim 0.08$ (storm case FL2, mild case FL5, mid-case SL29). The parametrisations for these three cases are of course quite similar in shape. For FL2 and FL5, the parametrisations also agree well with the measured spectra. For SL29 however, the predicted hump is not yet present.

All in all, Young's and Babanin's (2006) spectral parametrisation (Eq. 6.7) is a reasonable first estimate. For H_{m0}/d -ratios of 0.3-0.6, the parametrisation actually performs quite good. However, the cross-comparison of cases with $gd/u_{10}^2 \sim 0.08$ suggests that for equal gd/u_{10}^2 -values, the spectral shape may still vary significantly.

6.7.3. Wave height and wave period distributions

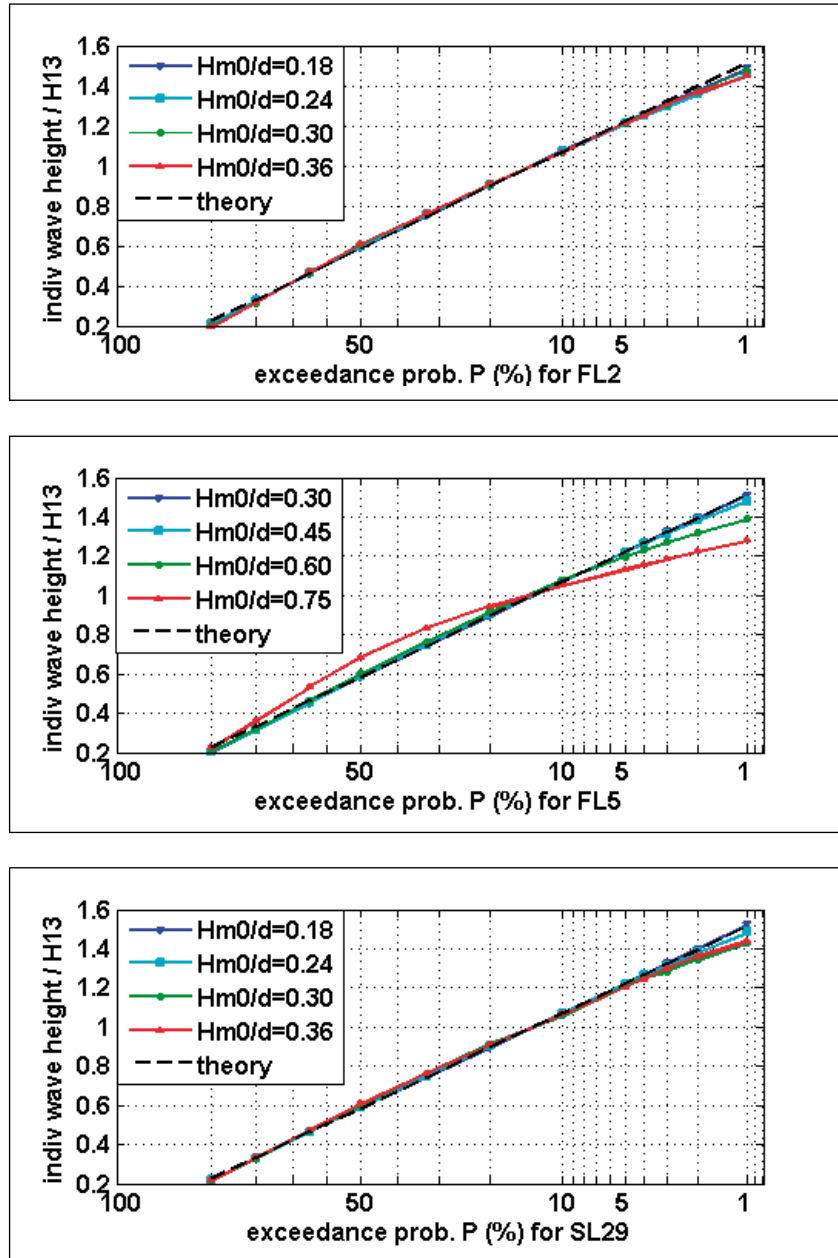
So far, we have mainly considered integral wave parameters like the spectral significant wave height H_{m0} , the peak period T_p and the mean spectral period T_{m01} . In reality, wave samples have a whole range of wave heights and wave periods around the above integral values. Each of these individual wave heights and wave periods has its own probability.

For deep water, the cumulative wave height probability is commonly described with a Rayleigh distribution :

$$(6.8) \quad P(H_i > H) = \exp\left(-\left(\frac{H}{H_{rms}}\right)^2\right)$$

where P is the probability that an individual wave height H_i exceeds the level H , and H_{rms} the so-called RMS wave height (see symbol list).

Figure 6.22: Ratio of individual wave height h divided by $H_{1/3}$, as a function of exceedance probability P , with x-axis transformed in such a way that Rayleigh distribution appears as a straight line. Top, middle and lower panel: FL2, FL5 and SL29, for various H_{m0}/d -values. The theoretical deep water Rayleigh distribution is plotted as a dashed black line.



Some example wave height distributions for FL2, FL5 and SL29 are shown in Figure 6.22. The underlying data are from the period November 2006 – January 2007. In each case, four different classes of wave height-over-depth ratio H_{m0}/d are considered, for example 0.17-0.19, 0.23-0.25, 0.285-0.315, 0.345-0.375. All data within such a class are aggregated to the average $H_p/H_{1/3}$ -ratios shown in Figure 6.22, where H_p is a given wave height percentile. In addition, a black dashed 'theory'-line is plotted. In fact, this is the deep water benchmark of Eq. (6.8), with the additional assumption that $H_{1/3} = 0.707 * H_{rms}$. Finally, it should be noted that all x-axes are converted in such a way that the Rayleigh distribution of Eq. (6.8) appears as a straight line in the graphs.

For FL2 (top panel of Figure 6.22), all actual wave height distributions are very close to the deep water Rayleigh distribution. Only for H_{m0}/d -values of 0.3 and more, a slight flattening of the curves can be seen for the highest wave heights, and the lowest probabilities (2% and less).

For FL5, the wave height distribution remains close to the Rayleigh distribution for H_{m0}/d up to 0.45. For $H_{m0}/d = 0.6$, the curve flattens off for $H/H_{1/3}$ greater than 1.2; for even larger H_{m0}/d -values, the whole distribution is distorted.

Finally, the results for SL29 are fairly similar to those of FL2, although for H_{m0}/d -values of 0.3 and more, the curves flatten off slightly more. In fact, $H(1\%)/H_{1/3}$ in depth-limited conditions can be nearly 10% lower than for deep water.

Two things are especially worth noting here:

- the wave height distributions only appear to have significant distortions over sloping bottoms (at FL5), not (yet) for depth-limited wave growth over flat bottoms (FL2, SL29);
- it is surprising that depth-limitation on H_{m0} appears to be significant for H_{m0}/d values as low as order 0.1 (section 6.7.1), whereas the frequency distribution for individual wave heights only shows noticeable finite-depth effects for H_{m0}/d -values of 0.3 and more. This combination of effects seems only possible if small and large waves are damped to the same extent in situations with *weakly* depth-limited waves.

For individual 20-minute-blocks, a few exceptionally high waves may easily distort the low-probability end of the wave height distribution. As a few of such high waves also have strong influence on the kurtosis of the raw measured signal, it is not surprising that Witteveen and Bos (2006) found a strong correlation between the wave height distribution and the kurtosis. However, this correlation rather describes the variability than the systematic depth-limited trends that are interesting for this study. Witteveen en Bos (2006) present several theoretical distributions that can be fitted to the data, to investigate such trends.

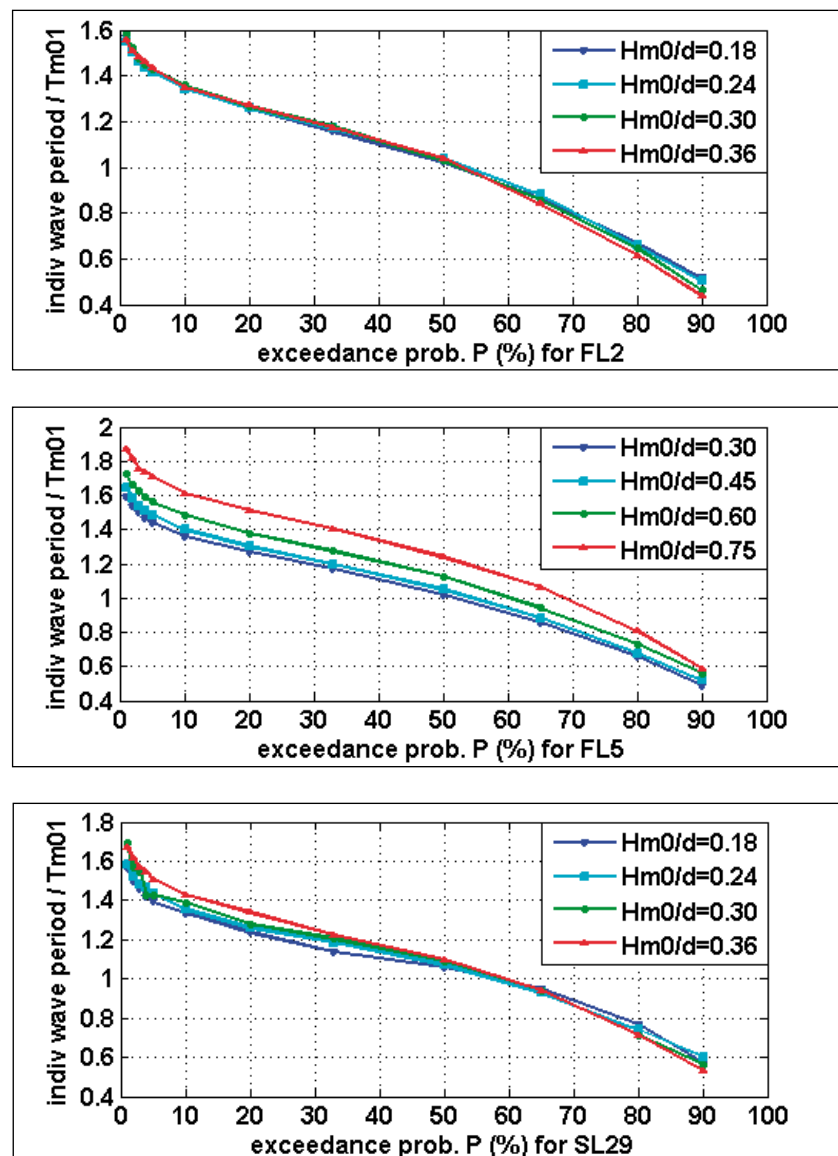
Most of these distributions are rather complex; for this study, only a simple Weibull fit (Eq. 4.1) is considered. For all curves in Figure 6.22, the Weibull scale parameter a (for the $H/H_{1/3}$ -ratio) is between 0.69 and 0.71. The highest a -value (0.71) occurs for the FL5-curve with $H_{m0}/d = 0.75$. The Weibull power k generally is between 1.89 and 2.00, with FL2 values around 1.95 (due to slight non-linearity of capa probe?) and SL29-values around 1.99. Only FL5 has a clear trend, with k increasing from 1.89 for $H_{m0}/d = 0.3$ to $k=2.21$ for $H_{m0}/d = 0.75$.

For the wave periods, theoretical expressions are not as simple as for the wave heights (Witteveen and Bos, 2006). Moreover, mixed wave conditions during offshore winds may greatly affect these distributions.

Therefore, only situations with southwesterly winds of at least 6 m/s were considered for the FL2, FL5 and SL29. The results are shown in Figure 6.23. Note that no x-axis transformation is applied by absence of a theoretical distribution requiring such a transformation.

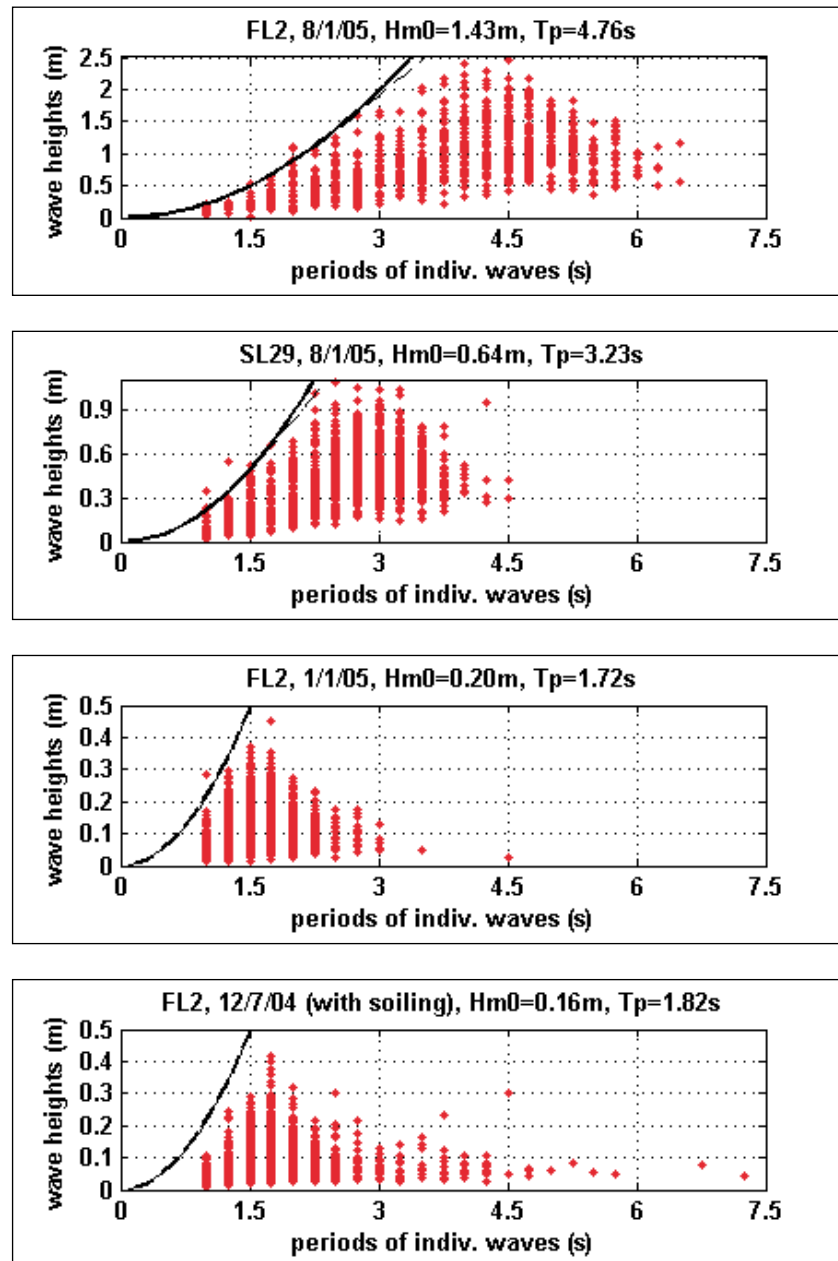
Figure 6.23 shows that all FL2-results are very similar. To a somewhat lesser extent, this also applies to the SL29-results. However, the main feature to be noticed is in the FL5-results. For H_{m0}/d up to 0.45, there is hardly any difference with the other locations. For H_{m0}/d -values of 0.6 and more however, the total curve is 10-30% higher than in milder conditions. This probably is related to the asymmetry of the waves in the latter conditions. This asymmetry shows up as a regular pattern of broad and shallow troughs with short and comparatively high wave crests. In this situation, the regular wave pattern tends to yield large time domain periods for the individual waves, which are normalised with a spectral T_{m01} -period which is relatively low because of the higher harmonic associated with the wave asymmetry.

Figure 6.23: Ratio of individual wave period h divided by T_{m01} , as a function of exceedance probability P . Top, middle and lower panel: FL2, FL5 and SL29, for various H_{m0}/d -values. Only data with SW-winds of at least 6 m/s are included.



Like for the wave heights, the wave period distributions of Figure 6.23 are fitted with a Weibull distribution (Eq. 4.1). The scale parameter a for the T_i / T_{m01} -ratio is 1.02-1.05 for FL2, 1.05-1.26 for FL5 (with the highest value for $H_{m0}/d=0.75$) and 1.09-1.12 for SL29. The Weibull-power k has quite a lot of variation, which is not yet explained. Typical k -values are 3.0-3.5 for FL2, 3.2-3.4 for FL5 and 3.4-4.0 at SL29. At FL2 and SL29, the highest k -values tend to occur for mild conditions.

.....
Figure 6.24: Wave height as a function of wave period for individual waves; thick black line is theoretical deep water steepness limit (1/7, thin line is limit for actual water depth. Four cases are shown; all data are from 12-13h MET.



Finally, it is interesting to plot the wave height as function of the wave period, for each of the individual waves in a sample. Figure 6.24 shows four example plots of this type. The thick black lines indicate the 1-to-7 theoretical steepness limit for deep water. In the top part of the first two subplots, the 1-to-7 steepness limits (dashed lines) based on the

actual water depth can also be seen; elsewhere, they coincide with the deep water steepness.

A common feature of nearly all plots is the fact that nearly always, the steepness of some of the shorter waves is very close to the theoretical steepness limit. In this context, shorter waves are typically waves with periods that are at least 30% smaller than the peak period. The highest individual waves typically occur near the peak period, which is not surprising as this is the period with most wave energy. For still larger periods, wave heights and wave steepnesses quickly decrease.

Graphs like Figure 6.24 can be quite useful for data validation. For example, the last subplot of Figure 6.24 shows a sample where the capa probe is strongly soiled with algae. The maximum steepness of the short waves is for this case only about 50% of its normal value. However, it must be noted that in very weak winds, the maximum steepness can also remain below the 1-to-7 limit. On the other hand, there are no such physical explanations for cases where many waves are above the theoretical 1-to-7-limit; for such cases, it is likely that the data are biased by experimental errors.

7. Wave model calibration and test cases

In the present chapter, a number of model calibration and model test cases will be discussed, both for stationary and time-dependent cases.

7.1 Stationary calibration cases Lake Sloten

Dike design conditions for the eastern shores of Lake IJssel are typically associated with hurricane-force winds, fetches of order 20 km and a water depth of order 5 metres. The waves in these design conditions are expected to be strongly depth-limited, much more so than in the storms measured so far. However, there are still significant wave model uncertainties in such strongly depth-limited conditions (Waal, 2002; Bottema, 2006c).

As depth-limited conditions are much more common at the shallow Lake Sloten than at the deeper Lake IJssel, it makes sense to use the Lake Sloten data set as a basis for wave model *calibration* cases. The Lake IJssel data set can then be used to derive an independent set of test cases for wave models.

In (Bottema, 2006c), three selection criteria were used for the selection of calibration cases:

- stationarity
- representativeness
- absence of experimental errors

As for *stationarity*, all selected cases have less than a few percent wind speed change per hour, and less than a few degrees wind direction change. Also, all cases were checked for representativeness. That implies that for given wind conditions, the measured wave conditions should be no outlier with respect to other cases, but rather a central estimate. This is quite important because the random scatter in H_{m0} is typically 15%.

Furthermore, all potential calibration cases were thoroughly screened for experimental errors, of which the main sources are discussed below. *Soiling* by algae can cause errors far over 20% during the summer half year, but by restricting the selection to October-April and thoroughly screening the data of October, November and April, most errors can be avoided.

Although *instrumental drift* is regularly checked for, it is hard to detect drift effects of less than 5-10% from field data. Hence, errors of up to 5-10% in the wave heights and steepnesses can not be fully excluded. The (unavoidable) use of a finite spectral integration range yields errors in H_{m0} , T_{m-10} , T_{m01} and T_{m02} of up to -4%, +4%, +9% and +16% in the cases to be presented. The latter is a worst case scenario for T_p

~1.7 s; for a T_p of order 3.5 s (twice as large as the previous T_p -value), the errors are a factor 3-5 smaller (Bottema, 2005; see also Appendix B.1).

In model calibration, not only the above experimental errors need to be considered but also modelling errors related to the model numerics, the model physics, and the model input in terms of lake bed level (typically with a few cm uncertainty), water levels, currents and wind. As for the latter, using the measured SL29-wind for all of Lake Sloten (i.e. using uniform winds by lack of suitable spatial wind model which would take into account nearshore sheltering) typically yields +7% and +4% overestimation in the model estimates of H_{m0} and the wave periods respectively (Bottema, 2006c).

All in all, the following calibration cases were selected:

.....
Table 7.1: Name, date and time (h MET) of Lake Sloten calibration cases, as well as water depth (water level = depth – 2.12 m), measured SL29-wind and main wave parameters (integration range: 0.03-1.5 Hz).

name	date	time	depth	U_{10}	dir	H_{m0}	T_p	T_{m-10}	T_{m01}	T_{m02}
		h	m	m/s	degN	m	s	s	s	s
SLA	10/2/02	4-5	1.65	11.0	245	0.34	2.27	2.01	1.82	1.73
SLB	12/2/02	13-14	1.69	15.0	253	0.47	2.86	2.53	2.09	1.95
SLC	26/2/02	14-15	1.83	20.8	243	0.70	3.45	2.98	2.61	2.39
SLD	10/10/02	12-13	1.65	10.6	88	0.23	1.67	1.66	1.47	1.42
SLE	27/10/02	15-16	1.67	21.4	252	0.71	3.23	2.96	2.53	2.30
SLF	20/3/04	20-21	1.66	19.4	241	0.66	3.13	2.85	2.48	2.27
SLG	1/11/06	5-6	1.70	17.1	314	0.45	2.52	2.32	2.05	1.90
SLH	18/1/07	12-13	1.66	21.9	234	0.66	3.23	2.92	2.50	2.27
SLI	18/1/07	19-20	1.68	22.6	276	0.67	3.26	2.87	2.43	2.20

The cases were selected for the following reasons :

- SLA: benchmark with little depth-limitation of waves
- SLB: typical intermediate case (some depth-limitation)
- SLC: highest water level for near-9 Beaufort winds
- SLD: as SLA but with 1 km instead of 3 km effective fetch
- SLE: strongest depth-limitation measured so far
- SLF: case to support high H_{m0}/d value of case SLE
- SLG: strongest wind case with fetch below 1.5 km
- SLH: strongest wind case with wind along long axis of lake
- SLI: strongest wind case for full data set

If a model calibration is to be performed on only a few cases, it recommended to retain at least SLB, either SLA or SLD, and two cases out of the set SLC, SLE, SLH and SLI. For case SLG, it should be noted that the accuracy for this case is slightly less than for the other cases because a small amount of soiling was still present in early November 2006. Finally, some of the most interesting cases actually occurred after the set of calibration cases reported in (Bottema, 2006c) was submitted to RWS RIKZ for the SWAN Test Bed. For that reason, the old cases were retained and simply supplemented with case SLG-SLI.

Although the validation of wave models is not within the scope of this report, it is still useful to highlight some results of a recent

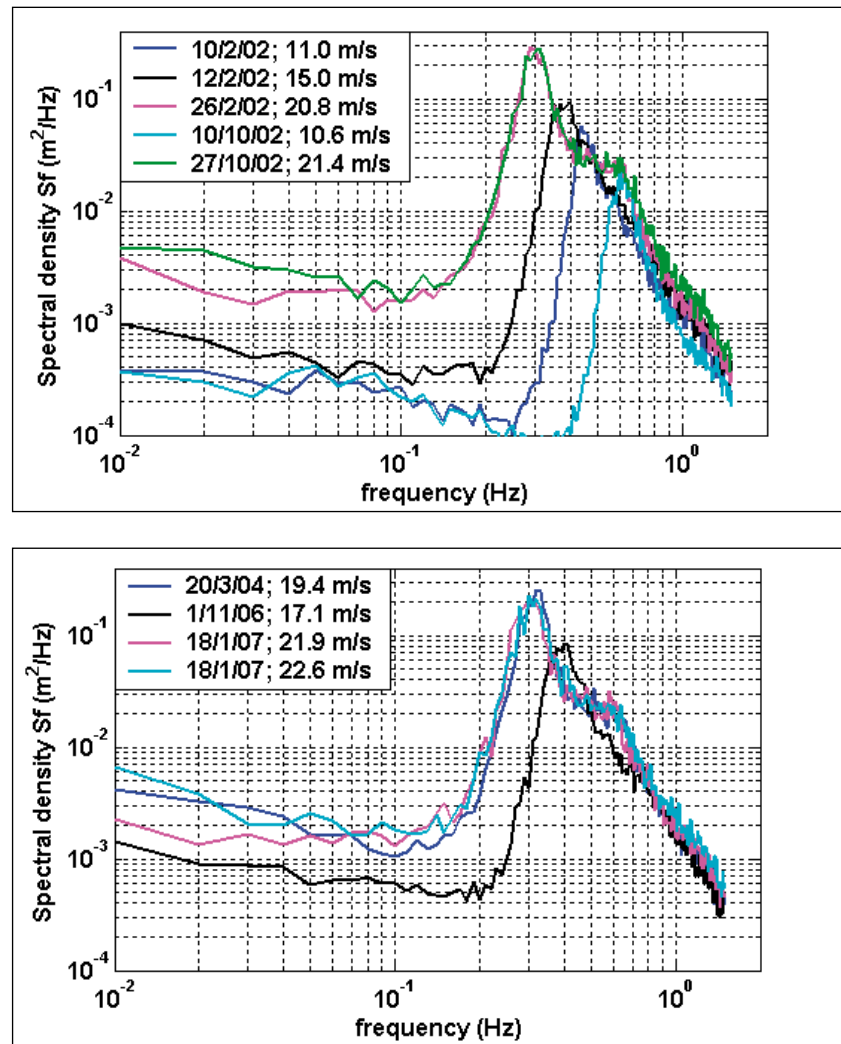
validation (Bottema, 2006c) of case SLA-SLF with the SWAN spectral wave model (Booij et al., 1999), both with improved model physics (Westhuysen et al., 2007) and default physics. The key settings were:

- 40 m spatial resolution (and 10 m bottom grid)
- no current, uniform wind, uniform water level

Some of the above settings may slightly bias the results if the waves are not fully depth-limited. For H_{m0} , the uniform wind field assumption may cause up to +7% bias for all cases, while discretisation errors may cause up to +5% bias for case SLD and SLG. For both error sources, wave period errors are typically twice as small.

The total SWAN errors (SWAN minus experimental data) with default settings were 0 to -20% for H_{m0} , -13 to -22% for T_p and -15 to -35% for the other spectral wave period measures. The underestimations were largest for strong winds and depth-limited conditions. With improved (Westhuysen et al., 2007) SWAN physics, errors in depth-limited conditions were by and large a factor 1.5-2 smaller.

Figure 7.1: Wave spectra (on double logarithmic scale) for the Lake Sloten calibration cases of Table 7.1. Top panel: case SLA-SLE, lower panel: case SLF-SLI



As SWAN is a spectral wave model, it makes sense to consider the wave spectra as well. The measured spectra are shown in Figure 7.1. The main trends in the measured spectra (Figure 7.1) and modelled spectra (Bottema, 2006c) are:

- The SWAN errors in the position of the spectral peak are directly related to the aforementioned SWAN errors in T_p . With default SWAN-physics the position of the spectral peak is consistently too far to the right; with improved physics the bias is much smaller.
- For the cases with strong wind and strong depth limitation (SLC, SLE, SLF, SLH, SLI), the spectral peak looks very pronounced. For such cases, SWAN underestimates the energy levels in the peak by a factor 3. In milder conditions, this underestimation is rather a factor 1.5-2.
- In the measurements, a distinct spectral hump occurs at about twice the peak frequency for the above strong-wind cases. The hump is hardly reproduced with the default SWAN physics, and not at all with the improved physics.
- The high-frequency spectral tail looks nearly identical for all cases, with slightly lower energy levels for the cases with the mildest conditions. For all cases, the SWAN energy levels in the tail appear to be order 50% higher than in the measurements.

A feature that only occurs in the measurements is the increase of low-frequency energy during stormy conditions, as can be seen in Figure 7.1. The raw measurements also reveal a feature that can only be predicted with phase-resolving models: the asymmetry of the waves. The latter can be described by the skewness Sk of the surface elevation signal, where Sk for SL29 varies from about 0.5 in mild conditions to nearly 1.0 in stormy conditions. Some wave experts are also interested in the skewness of the vertical velocity signal of the waves, Sk_w . During stormy weather at the SL29 site, Sk_w may significantly deviate from zero, and it may even reach values of 0.2 to 0.3.

7.2 Stationary test cases Lake IJssel

A recent set of stationary wave model test cases for Lake IJssel is reported in (Bottema, 2006c). This set will be supplemented with a few recent test cases.

In (Bottema, 2006c), the following test case selection criteria were used:

- stationary conditions
- at least 80% of the data is available and reliable
- the FL2 and FL26 wind speeds differ less than 5-10%

As for the stationary conditions, no cases are selected with more than 10° wind direction change and/or 10% wind speed change in the preceding two hours.

The second criterion is related to the wish to compare different measuring locations during a storm.

The third criterion is perhaps the most important. Since there is no validated and widely accepted spatial wind model, one has to rely on the assumption that the wind field is nearly uniform over Lake IJssel, at least for the central part containing the measuring locations.

Some additional criteria can only be applied on recent data. Therefore, the following criteria were used for screening rather selecting cases:

- less than 5-10% difference between the FL25/FL37-wind with the FL2 and FL26 wind
- representativeness of test case data
- limited thermal effects (small air-water temperature differences)

.....
Table 7.2: Name, date, start time, mean lake water level, wind and air-water temperature difference for 1-hour test cases for Lake IJssel. Values between brackets are somewhat less accurate.

name	date	time (h)	lake level (m NAP)	wind dir. (degN)	U ₁₀ (m/s)	T _{air} -T _{water} (°C)
IJA	2/10/99	3h	-0.20	215°	15.2	(~ zero?)
IJB	22/2/02	4h	+0.08	215°	18.8	(~ zero?)
IJC	27/10/02	14h20	-0.26	249°	23.2	(+4°C ?)
IJD	12/11/02	13h	-0.14	193°	9.7	(~ zero?)
IJE	2/4/03	14h	-0.29	328°	14.6	(~ zero?)
IJF	18/4/04	14h20	-0.18	169°	11.9	0°C
IJG	8/1/05	13h	-0.20	246°	19.9	+4°C
IJH	12/2/05	15h	-0.39	286°	18.3	+2°C
IJI	13/2/05	14h	-0.33	314°	11.9	0°C
IJJ	1/11/06	7h	-0.33	322°	19.8	-2°C
IJK	18/1/07	12h	+0.06	237°	22.4	+4°C
IJL	18/1/07	19h	+0.10	267°	23.5	+2°C

The selected test cases are specified in Table 7.2. Note that the wind speed in Table 7.2 is representative for at least 10 km of fetch since an arithmetic average of all U₁₀-data would be biased towards the more sheltered locations. A brief description of each test case follows below.

Case IJA (Table 7.3) ; 2/10/1999, 3-4 h MET (SSW 7 Beaufort)

An exceptionally stationary case with wind speed and direction trends as small as 1.5% and 1° per hour, and one of the two benchmark cases for intermediate (7 Beaufort) wind conditions. The uniformity of the wind field is not perfect as FL26 has 10% less wind than FL2. For FL25 the additional wind reduction (not measured) probably is of the order of another 10%. The representativeness is not fully optimal either; the H_{m0} for FL25 is 20% less than the long-term average for similar wind conditions. For FL26 this difference is 10%.

The wave spectra are shown in Figure 7.2 (to be shown). For FL5, which is on a foreshore, the second harmonic on twice the peak frequency can be seen, and possibly even the third harmonic. For FL25, the steep spectral tail and especially the presence of low-frequency humps may be an indication of mixed wave fields instead of a pure locally generated wind sea.

.....
Table 7.3: Measured wind, approximate still water level (SWL) and measured wave conditions for test case IJA (2/10/1999, 3-4 h MET); spectral integration range for wave parameters: 0.03-1.5 Hz.

loc.	wind_dir. (degN)	U ₁₀ m/s	SWL m_NAP	H _{m0} m	T _p s	T _{m-10} s	T _{m01} s	T _{m02} s
FL2	214°	15.1	-0.22	0.89	3.95	3.35	2.97	2.71
FL5	-	-	-0.17	0.95	4.35	3.65	2.99	2.64
FL9	-	-	-0.23	1.09	4.06	3.61	3.23	2.95
FL25	-	-	-0.28	0.21	1.59	1.72	1.54	1.48
FL26	210°	13.6	-0.33	0.69	2.97	2.78	2.46	2.27

Case IJB (Table 7.4) ; 22/2/2002, 4-5 h MET (SSW 8 Beaufort)

Until recently, this was the only available test case with strongly elevated water levels. Now, case IJK may well be a better alternative. Case IJB is nearly as stationary as case IJA, with much smaller wind speed differences between FL2 and FL26 (Table 7.4). The reliability and representativeness of the data generally appear to be good. However, FL9 had to be excluded because waves overtopped the instruments.

For the spectra (Figure 7.2b), the same remarks as for case IJA apply, but the FL25-spectrum now is closer to a pure wind sea spectrum.

.....
Table 7.4: As Table 7.3, for case IJB (22/2/2002, 4-5 h MET).

loc.	wind_dir. (degN)	U ₁₀ m/s	SWL m_NAP	H _{m0} m	T _p s	T _{m-10} s	T _{m01} s	T _{m02} s
FL2	216°	18.8	+0.21	1.23	4.62	4.25	3.67	3.28
FL5	-	-	+0.28	1.32	5.37	4.28	3.43	2.98
FL25	-	-	-0.08	0.32	1.77	1.99	1.69	1.61
FL26	211°	18.3	-0.09	1.07	3.34	3.03	2.78	2.61

Case IJC (Table 7.5) ; 27/10/2002, 14h20-15h20 h MET (WSW 10 Bft)

Until 18/1/2007, this used to be the strongest wind case for several years, probably since early 1990. The case is worth retaining because the lake level differences between 27/10/2002 and 18/1/2007. The wind field was fairly uniform, although FL25 probably had roughly 10% less wind than FL2. The stationarity just before the storm peak was somewhat less with a wind change of +7° and +5% per hour. Also, the air was about 4°C warmer than the water. The reliability of the wave data seems good; the representativeness is hard to judge by lack of similar cases. However, the FL25 data are definitely not representative as H_{m0} (~0.2 m) is 60% smaller than it can be at similar cases, while the spectral energy is very low for all frequencies (Figure 7.2c). This phenomenon of strong wave height and steepness reduction during storm is uncommon, but not totally unique; it also occurred at 20/3/2004 (Ruijter and Boomgaard, 2005). As the reason for this incidentally occurring wave flattening is unclear, it is decided to omit the FL25-data from table 7.5. At the other locations, the spectral shapes were consistent with those of case IJA and IJB.

.....
Table 7.5: As Table 7.3, for case IJC (27/10/2002, 14h20 h MET).

loc.	wind_dir. (degN)	U ₁₀ m/s	SWL m_NAP	H _{m0} m	T _p s	T _{m-10} s	T _{m01} s	T _{m02} s
FL2	249°	23.2	+0.25	1.61	5.26	5.01	4.26	3.75
FL5	-	-	+0.23	1.17	5.27	4.42	3.33	2.82
FL9	-	-	+0.14	1.52	5.17	4.53	3.81	3.37
FL26	-	22.7	-0.38	1.36	3.90	3.66	3.33	3.08

Case IJD (Table 7.6) ; 12/11/2002, 13-14 h MET (S-SSW 5 Beaufort)

Good deep water benchmark with a nice uniform wind field (except FL25, where wind may have been order 10% less). Stationarity is slightly less with -0.4 to +0.8 m/s wind variations at FL26 during the preceding two hours. The reliability and representativeness of the wave data seem to be good, although the FL2 wave heights perhaps are slightly higher than in similar cases. In these milder conditions, the spectra (Figure 7.4a) show no longer a combination of enhanced peaks, and humps at the right-hand flank. The FL25-spectrum seems rather broad, possibly due to mixed wave fields.

.....
Table 7.6: As Table 7.3, for case IJD (12/11/2002, 13-14 h MET).

loc.	wind_dir. (degN)	U ₁₀ m/s	SWL m_NAP	H _{m0} m	T _p s	T _{m-10} s	T _{m01} s	T _{m02} s
FL2	192°	9.7	-0.11	0.66	3.38	2.92	2.49	2.29
FL5	-	-	-0.11	0.63	3.41	2.88	2.54	2.32
FL9	-	-	-0.09	0.61	3.10	2.84	2.50	2.31
FL25	-	-	-0.20	0.22	2.27	2.00	1.63	1.52
FL26	194°	9.7	-0.17	0.51	2.73	2.28	2.07	1.95

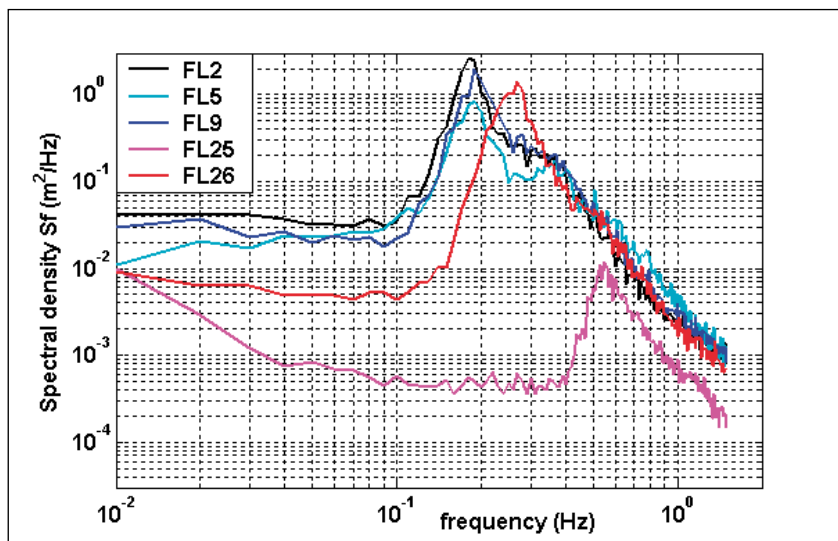
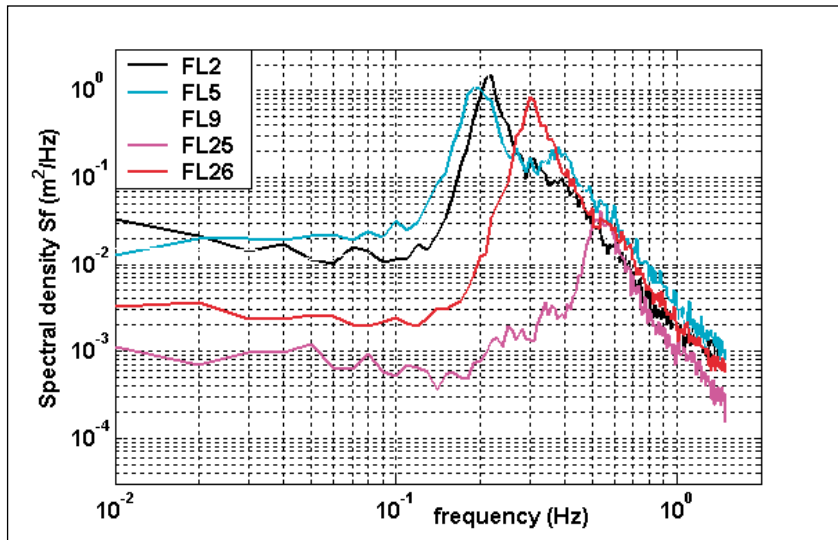
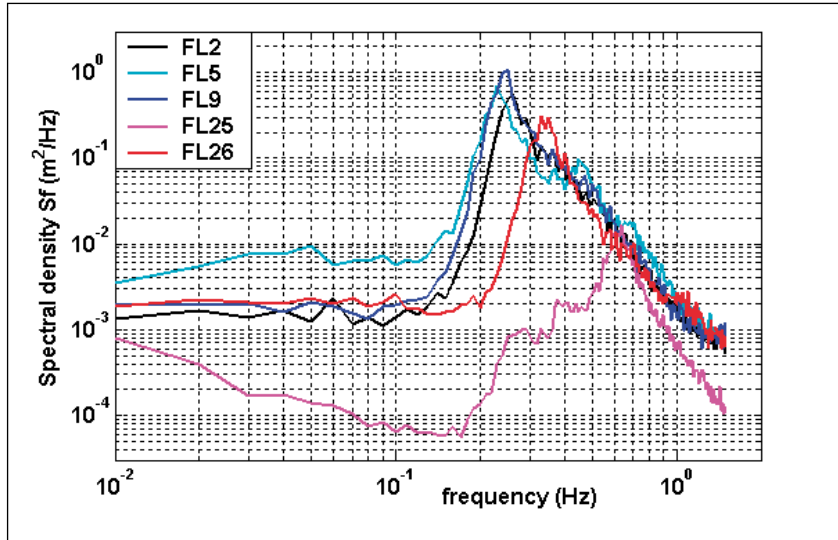
Case IJE (Table 7.7) ; 2/4/2003, 14-15 h MET (NW-NNW 7 Beaufort)

Case with strongest NW-NNW wind until 1/11/2006; at present one could consider replacing it by the two cases IJI and IJJ. Uniformity and stationarity of the wind are good, with +0.3 m/s and 3° wind change per hour. The reliability and representativeness of the wave data is good to excellent, but FL25 has a 10% smaller H_{m0} than would be expected in similar wind conditions. Still, this deviation is well within the experimental scatter and the 1σ-limit. The wave spectra (Figure 7.3b) look quite normal, although the somewhat broader spectra of FL5 and FL25 may be an indication of mixed wave fields.

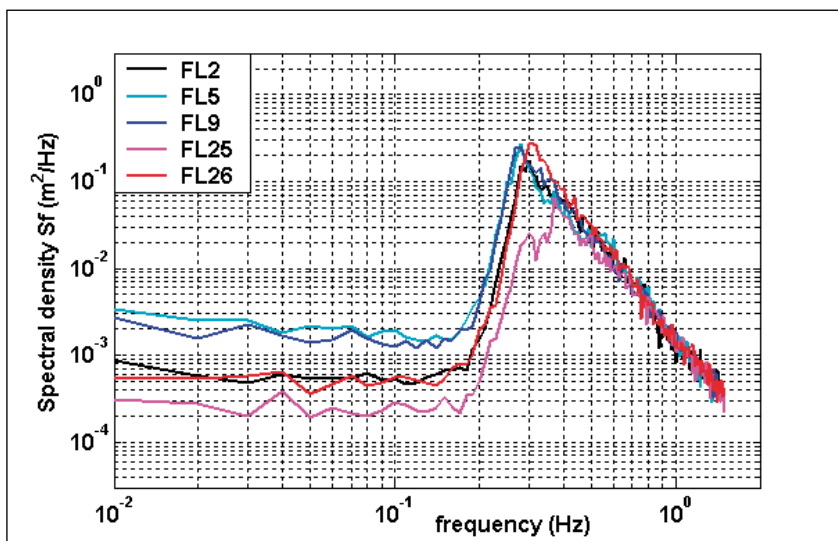
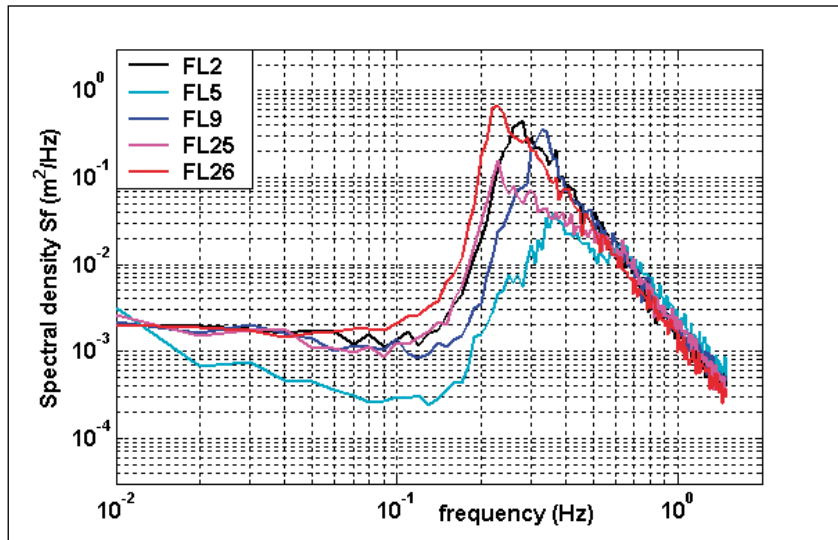
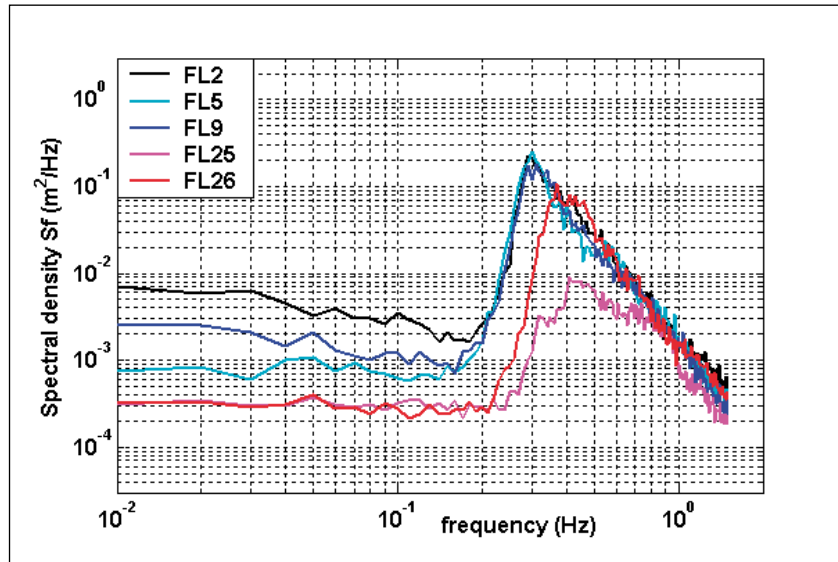
.....
Table 7.7: As Table 7.3, for case IJE (2/4/2003, 14-15 h MET).

loc.	wind_dir. (degN)	U ₁₀ m/s	SWL m_NAP	H _{m0} m	T _p s	T _{m-10} s	T _{m01} s	T _{m02} s
FL2	327°	14.6	-0.18	0.90	3.61	3.18	2.86	2.66
FL5	-	-	-0.29	0.40	2.75	2.15	1.79	1.65
FL9	-	-	-0.24	0.77	2.97	2.82	2.55	2.38
FL25	-	-	-0.21	0.57	4.35	3.08	2.48	2.20
FL26	330°	14.5	-0.20	0.98	4.42	3.67	3.28	3.02

.....
Figure 7.2: Wave spectra (on double logarithmic scale) for the Lake IJssel test cases IJA (top), IJB (middle) and IJC (below).



.....
Figure 7.3: Wave spectra (on double logarithmic scale) for the Lake IJssel test cases IJD (top), IJE (middle) and IJF (below).



Case IJF (Table 7.8) ; 18/4/2004, 14h20-15h20 (SSE-S 6 Beaufort)
 First case with near-uniform winds at FL2, FL26 and FL25. Stationary in two preceding hours; before that, the wind is 4% stronger and 9° backed. The representativeness of all wave data is excellent, with less than 5% H_{m0} -difference from the averages for similar wind conditions. All locations have neat spectra (Figure 7.3c) with shapes typical for mild wind conditions. However, FL25 has a small secondary maximum at about 0.8 times the peak frequency, possibly due to mixed wave fields.

.....
Table 7.8: As Table 7.3, for case IJF (18/4/2004, 14h20 MET).

loc.	wind_dir. (degN)	U_{10} m/s	SWL m_NAP	H_{m0} m	T_p s	T_{m-10} s	T_{m01} s	T_{m02} s
FL2	167°	11.5	-0.24	0.59	3.40	2.75	2.44	2.25
FL5	-	-	-0.12	0.63	3.57	2.99	2.57	2.33
FL9	-	-	-0.15	0.68	3.57	3.01	2.65	2.43
FL25	-	11.7	-0.23	0.40	2.57	2.30	2.01	1.86
FL26	172°	11.9	-0.23	0.70	3.23	2.81	2.53	2.36

Case IJG (Table 7.9) ; 8/1/2005, 13-14 h (WSW 8 Beaufort)

First suitable 8 Beaufort test case with FL25 wind measurements. Wind reduction at FL25 and FL26 with respect to FL2 is 14% and 4% respectively. Stationarity is not perfect with a 6° veering rate per hour. In addition, the air is substantially warmer than the water (+4°C). Despite all this, both the reliability and representativeness of the wave data appear to be good. For the latter however, FL25 is an exception since H_{m0} for these conditions usually is about 0.45 m, whereas it was only 0.32 m for this case. Despite this low H_{m0} -value, no deviations were detected in the FL25-spectrum (Figure 7.4a). Elsewhere, spectra were also OK.

.....
Table 7.9: As Table 7.3, for case IJG (8/1/2005, 13-14 h MET).

loc.	wind_dir. (degN)	U_{10} m/s	SWL m_NAP	H_{m0} m	T_p s	T_{m-10} s	T_{m01} s	T_{m02} s
FL2	247°	19.9	+0.11	1.44	4.92	4.41	3.82	3.45
FL5	-	-	+0.34	0.94	5.19	4.35	3.27	2.79
FL9	-	-	+0.08	1.46	4.82	4.28	3.65	3.26
FL25	-	17.2	-0.45	0.32	1.80	1.81	1.58	1.51
FL26	245°	19.1	-0.32	1.18	3.54	3.33	3.05	2.86

Case IJH (Table 7.10) ; 12/2/2005, 15-16 h (WNW 8 Beaufort)

The case is selected for its near-uniform wind field, although the air is somewhat warmer than the water. Stationarity is good from 14h on; before that, winds are backed by 10° and 4% weaker. All wave data appear to be reliable and representative. The wave spectra of FL5 and especially FL25 (Figure 7.4b) seem very broad, probably due to the presence of mixed wave fields.

.....
Table 7.10: As Table 7.3, for case IJH (12/2/2005, 15-16 h MET).

loc.	wind_dir. (degN)	U ₁₀ m/s	SWL m_NAP	H _{m0} m	T _p s	T _{m-10} s	T _{m01} s	T _{m02} s
FL2	285°	17.9	-0.01	1.29	5.00	4.23	3.65	3.29
FL5	-	-	-0.03	0.74	4.42	3.54	2.71	2.37
FL9	-	-	-0.16	1.09	4.62	3.80	3.25	2.91
FL25	-	17.8	-0.38	0.44	1.81	2.27	1.85	1.72
FL26	287°	18.7	-0.31	1.14	4.82	3.80	3.34	3.03

Case IJI (Table 7.11) ; 13/2/2005, 14-15 h (NW 6 Beaufort)

Nice NW-wind case with near-uniform wind and negligible air-water temperature difference. The stationarity is good from 12h MET on; before that, winds are about 12% weaker.

The wave data seem reliable and representative, although H_{m0} for FL9 and FL25 may be 10% higher than the average for similar winds. Again, the spectra of FL5 and FL25 (Figure 7.4c) are broad, suggesting the presence of mixed wave fields.

.....
Table 7.11: As Table 7.3, for case IJI (23/2/2005, 14-15 h MET).

loc.	wind_dir. (degN)	U ₁₀ m/s	SWL m_NAP	H _{m0} m	T _p s	T _{m-10} s	T _{m01} s	T _{m02} s
FL2	313°	11.8	-0.17	0.68	3.27	2.87	2.57	2.39
FL5	-	-	-0.16	0.35	2.64	2.17	1.85	1.69
FL9	-	-	-0.24	0.62	2.92	2.68	2.36	2.20
FL25	-	11.8	-0.24	0.39	3.70	2.40	1.99	1.82
FL26	315°	11.4	-0.24	0.78	3.75	3.20	2.88	2.66

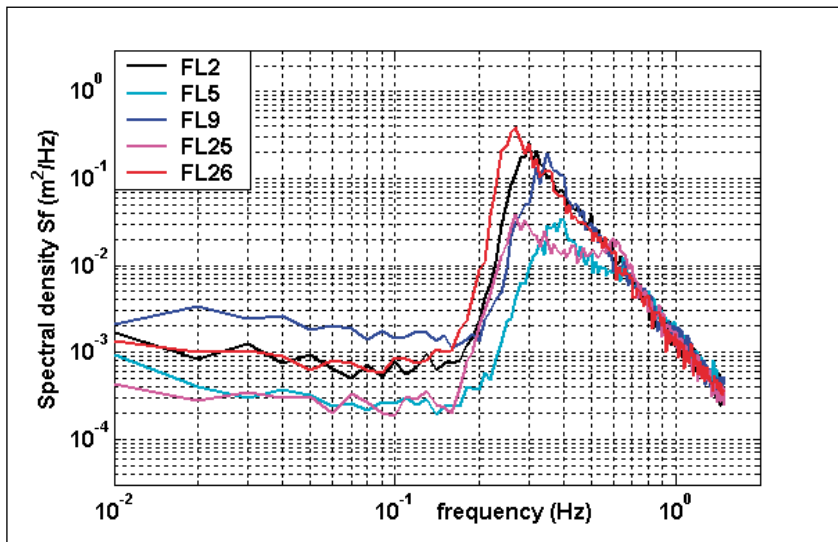
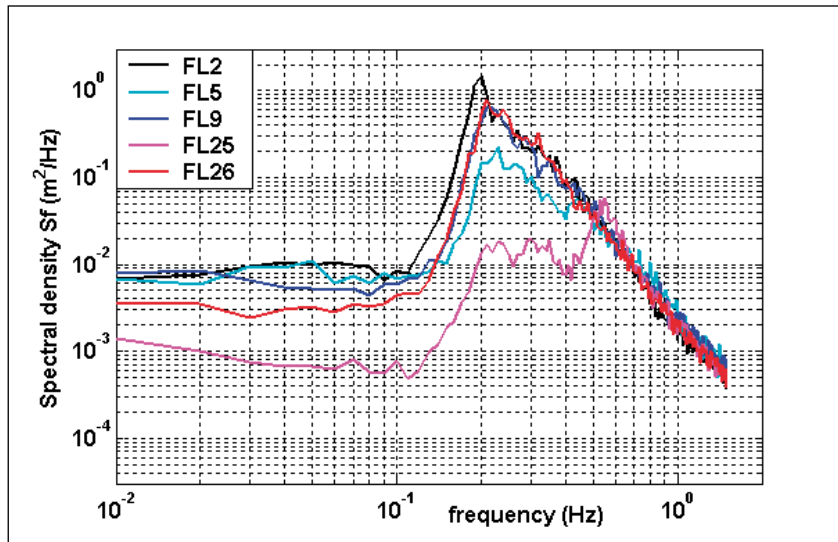
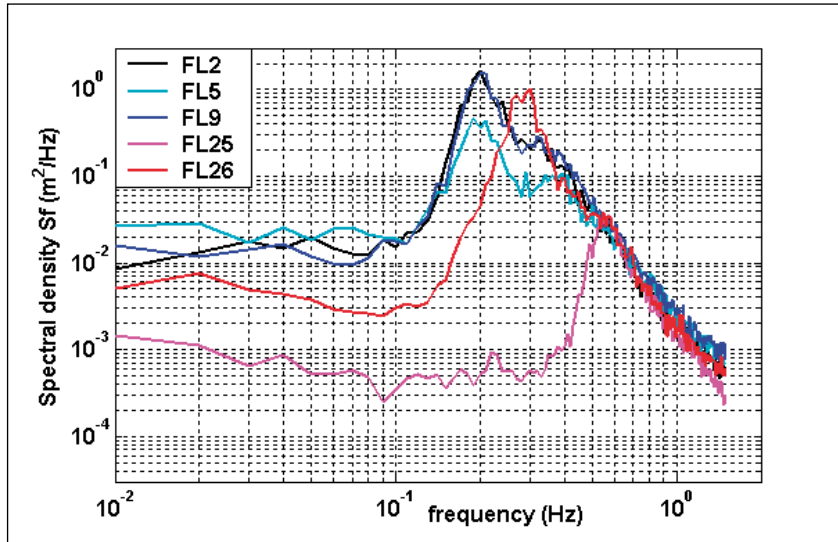
Case IJJ (Table 7.12) ; 1/11/2006, 7-8 h (NW 8 Beaufort)

Unique case in present data set: nearly 9 Beaufort wind from NW and slightly unstable atmosphere. The wind seemed quite stationary (-0.5 and +1.0 m/s hourly wind speed change at FL2 and FL37 and +3° veering) and uniform. Still, the SW-moving band with strong winds was quite narrow: SL29 already had 20% wind decrease between 6-7 h MET. The reliability of the wave data seems good, but FL26 suffered instrument damage shortly after the present time interval. The FL5-fetch is possibly ill-defined as part of the foreshore may have fallen dry. The wave spectra (Figure 7.5b) do not show any remarkable features, except the pronounced secondary peak (mixed wave field?) at FL5.

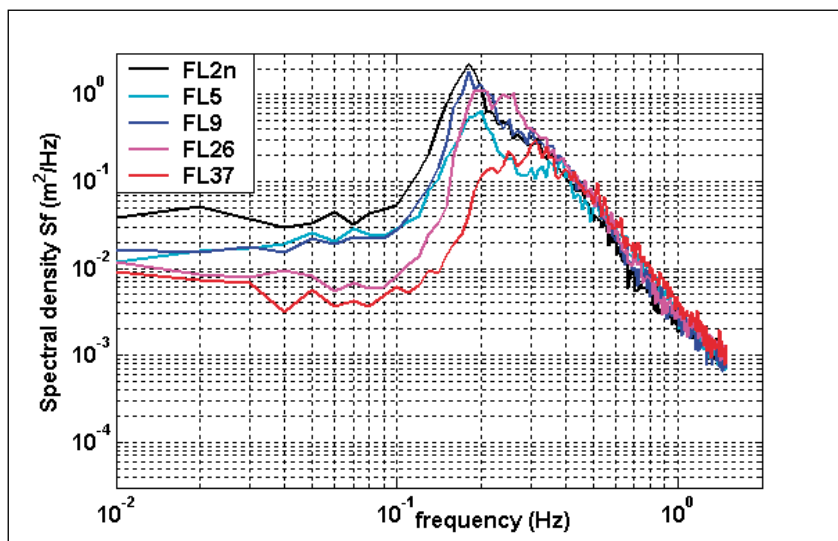
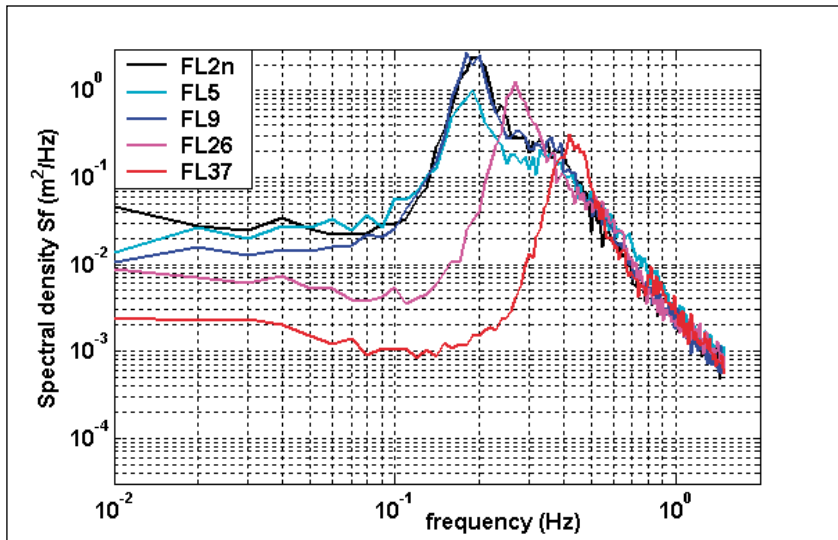
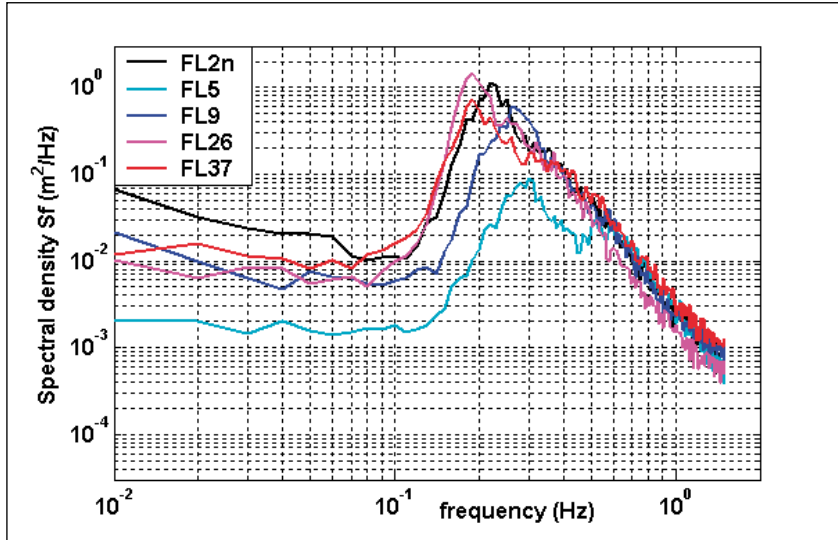
.....
Table 7.12: As Table 7.3, for case IJJ (1/11/2006, 7-8 h MET).

loc.	wind_dir. (degN)	U ₁₀ m/s	SWL m_NAP	H _{m0} m	T _p s	T _{m-10} s	T _{m01} s	T _{m02} s
FL2n	324°	19.5	+0.12	1.32	4.55	4.11	3.49	3.13
FL5	-	-	-0.19	0.54	3.38	2.77	2.18	1.99
FL9	-	-	-0.12	1.09	3.71	3.45	3.01	2.75
FL26	320°	19.7	-0.01	1.39	5.27	4.50	3.96	3.58
FL37	-	20.1	+0.06	1.15	5.27	4.08	3.25	2.81

.....
Figure 7.4: Wave spectra (on double logarithmic scale) for the Lake IJssel test cases IJG (top), IJH (middle) and IJI (below).



.....
Figure 7.5: Wave spectra (on double logarithmic scale) for the Lake IJssel test cases IJ (top), IJK (middle) and IJL (below). Please note change in locations and legend.



Case IJK (Table 7.13) ; 18/1/2007, 12-13 h (SW 9 Beaufort)

Rare combination of 9 Beaufort and elevated lake levels.

Rapid wind changes (+5m/s and +30° per hour) between 8h and 10h30 MET, followed by near-perfect stationarity and uniformity of the wind. Thermal conditions were not fully neutral: the air was 4°C warmer than the water. The representativeness of the wave data is hard to judge by lack of similar data. Some H_{m0} -underestimations are possible for FL5 and FL9 (wave overtopping, order -3% error), as well as FL26 (disturbance of mounting, possibly -8% error). The spectra (Figure 7.5c) show features of a strongly forced wind sea with enhanced peaks; FL2 and FL9 also show humps to the right of the peak. FL5 has a secondary maximum at twice the peak frequency, probably due to wave asymmetry.

.....
Table 7.13: As Table 7.3, for case IJK (18/1/2007, 12-13 h MET).

loc.	wind_dir. (degN)	U_{10} m/s	SWL m_NAP	H_{m0} m	T_p s	T_{m-10} s	T_{m01} s	T_{m02} s
FL2n	234°	22.1	+0.36	1.75	5.09	4.69	4.08	3.68
FL5	-	-	+0.50	1.27	5.43	4.53	3.51	3.02
FL9	-	-	+0.33	1.74	5.19	4.68	4.07	3.66
FL26	230°	22.8	+0.01	1.25	3.66	3.39	3.06	2.83
FL37	-	22.4	-0.24	0.75	2.33	2.29	2.11	2.01

Case IJL (Table 7.14) ; 18/1/2007, 19-20 h (W; nearly 10 Beaufort)

Very rare combination of West 9 Beaufort and elevated lake levels.

Winds reasonably uniform and stationary (+2 m/s and up to +10° change in preceding hour) except for some strong and prolonged gusts: at FL2 one 10-minute average was 3 m/s above the maximum hourly average of 23.8 m/s (just before the logger stopped storing wind data). Wave data were fairly reliable, but FL2/FL26 possibly had some (1-5%?) H_{m0} -underestimation due to disturbance of mountings. The spectra (Figure 7.5c) suggest that the waves were not as strongly forced as the previous case (less peak enhancement). Moreover, the presence of broad maxima at FL26 and FL37 suggests the presence of mixed wave fields at those locations. The secondary maximum at FL5 may be both due to wave breaking and mixed wave fields.

.....
Table 7.14: As Table 7.3, for case IJL (18/1/2007, 19-20 h MET).

loc.	wind_dir. (degN)	U_{10} m/s	SWL m_NAP	H_{m0} m	T_p s	T_{m-10} s	T_{m01} s	T_{m02} s
FL2n	-	-	+0.78	1.68	5.46	4.99	4.20	3.70
FL5	-	-	+0.52	1.13	5.09	4.29	3.29	2.83
FL9	-	-	+0.41	1.60	5.37	4.48	3.79	3.38
FL26	267°	23.0	+0.24	1.59	4.70	4.01	3.51	3.19
FL37	-	24.0	+0.16	0.98	3.23	3.07	2.53	2.32

Trends in SWAN model results

Evaluating the performance of the SWAN calculations is outside the scope of this study, so only previously published results from (Bottema, 2006c) are used here. As a result, test cases based on recent data (IJ, IJK and IJL) will not be considered. The key features of these SWAN simulations were a 80 m spatial resolution, uniform wind field, uniform water levels (matched to FL5 where depth-limitation of the waves was strongest), and neglect of any currents.

The results of the SWAN-validation of (Bottema, 2006c) were not fully unambiguous. By and large, the following error trends resulted if the default physics of SWAN was used:

- H_{m0} -overestimations between +40% for fetches of 1 km and +5% for 5 km fetch, but underestimations up to -20% in situations with depth-limited waves ($H_{m0}/d > 0.3$). The latter trend is similar to the trend in the Lake Sloten data of section 7.1;
- T_p 6-15% too low; largest errors in depth-limited conditions;
- T_{m-10} and T_{m01} : same trends as for T_p , but -10 to -17% error.
- T_{m02} : about 25% too low without clear trend
- In the wave spectra: peak too low and too far to the right; high frequency tail too high. In depth-limited conditions: SWAN fails to predict the enhanced main spectral peak and the hump at the right-hand flank of the spectrum.

All these trends are similar to those published by (Bottema et al., 2002, 2003).

It should be noted that the SWAN overestimations for short fetches ($x \sim 1$ km) are not caused by the default physics. Rather, the overestimations are the result of the wind assumptions and – to a lesser extent – discretisation errors due to too coarse a numerical grid.

With the new (Westhuysen et al, 2007) physics, SWAN suffers from spurious low-frequency energy propagating upwind (Bottema, 2006c). In the above Lake IJssel simulations, this results in severe H_{m0} -estimations for short fetches x . Compared with the default physics, H_{m0} increases about 7% for $x \sim 10$ km and about 20% for $x \sim 1$ km. For fetches well above 1-3 km, the new physics strongly improved the predictions of wave periods and wave spectra. However, even with the new physics, SWAN was not able to reproduce the enhanced peaks and humps that are typical of measured wave spectra in strongly forced and/or depth-limited conditions.

7.3 Time-dependent test cases

In a first approximation, time-dependent wind fields over Lake Sloten can be considered to be uniform as weather systems generally move much quicker over Lake Sloten than the waves do. Weather systems pass with speeds of order 5-20 m/s; the wave group velocities relevant for wave energy transport are order 2 m/s. For Lake IJssel, both speeds are likely to be (nearly) of the same order, which implies that one needs the actual spatial wind fields for time-dependent wave modelling.

For the present work, simplicity is preferred, which implies that time-dependent cases will only be presented for Lake Sloten.

The wind conditions, wave height and wave steepness for the four selected time-dependent test cases for Lake Sloten (SL29) are presented in Figure 7.6.

Case 1, 26/4/2002, time = zero at 21h10 (green line in Figure 7.6)

In the evening, a trough passed with showers and a very sharp increase and veering of the wind. The wind changes for this case are among the most rapid ones observed, except for thunderstorm gust fronts. Mean water levels were generally about -50 cm NAP.

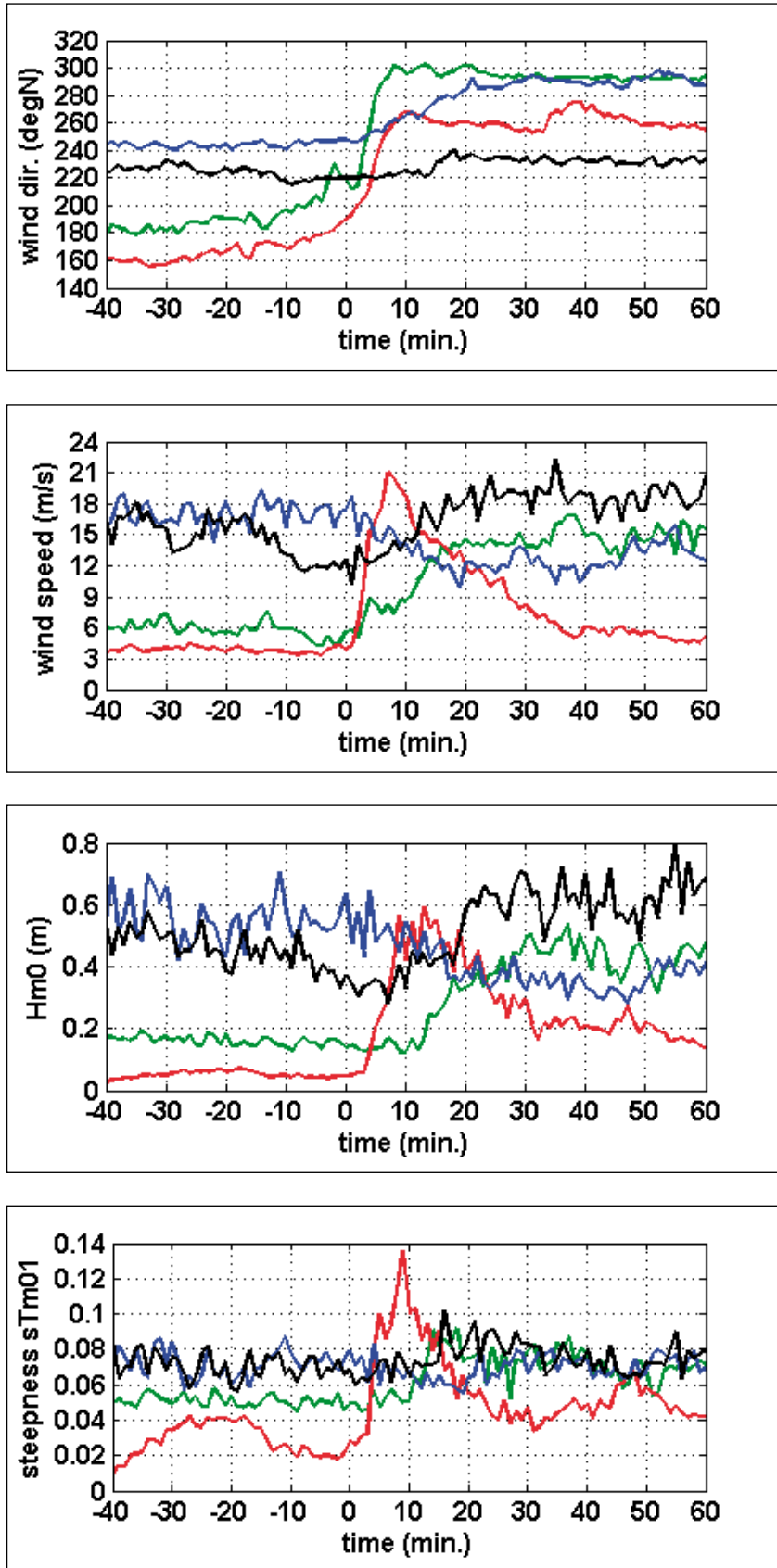
The actual wind change was from South 4 Beaufort to WNW 6-7 Beaufort within half an hour. The wind change started with a slow wind speed increase and a fairly rapid veering which resulted in a combination of increasing wind and decreasing fetch. This may explain the apparent 10-minute time lag in wave growth. After this initial stage, only 20 minutes are needed to reach an H_{m0} -value in apparent equilibrium with the wind. The adaptation of the wave period T_{m01} appears to be slightly slower, as is indicated by the slight overshoot in the wave steepness (first 0.09, then 0.07).

Case 2, 2/5/2003, time = zero at 20h25 (red line in Figure 7.6)

Passage of a thunderstorm gust front with extremely sharp wind increase and exceptionally rapid wave growth. Because the atmospheric boundary-layer structure may be non-standard for this case, it is maybe not a perfect model calibration case. Three water level minima of -60 cm NAP occurred at times of -40, -5 and +35 minutes, a maximum of +38 cm occurred at 15 minutes.

Waves started to grow a few minutes after the wind picked up, and then grew from 5 to 50 cm in just 6 minutes. Even more remarkable was the steepness of the waves, which overshooted to *twice* the value for equilibrium conditions. By contrast, the wave decaying phase had relatively low steepnesses. The wave steepnesses before the wind increase were also very small, but this is partly caused by the finite integration range (0.01-1.5 Hz) for calculating H_{m0} and T_{m01} .

Figure 7.6: Wind conditions, wave height and wave steepness for time-dependent test cases SL29. Green/red/blue/black lines correspond with 26/4/02, 2/5/03, 21/12/03 and 20/3/04. Main wind change starts at time = zero.



Case 3 21/12/2003, time = zero at 8h25 (blue line in Figure 7.6)

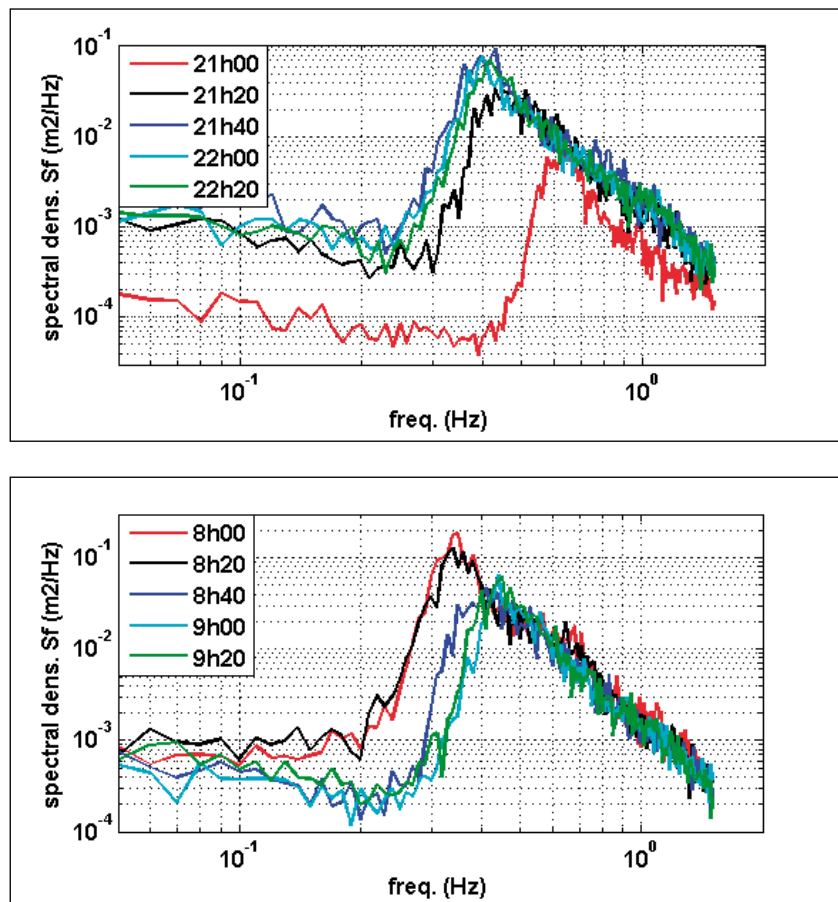
On of the few cases with a rapid wind speed decrease, accompanied by a decrease in fetch as the wind veered to WNW. Water levels were about -42 cm NAP until $t=+10$ minutes, and then fluctuated around -48 cm NAP.

In the first 20 minutes, winds decreased about 30% while wave heights only decreased by about 20%. In the next 20 minutes however, wind speeds remained constant while H_{m0} decreased another 10%. Surprisingly, the wave steepness changed little which suggests that the waves still were more or less in equilibrium with the wind (and not converting to swell).

Case 4, 20/3/2004, time = zero at 14h40 (black line in Figure 7.6)

For Lake Sloten, this was a remarkable case where the wind suddenly picked up to 9 Beaufort. Compared to the previous cases however, only the trends in the water levels are worth mentioning; initially levels were about -53 cm NAP but they reached a peak of -43 cm NAP at $t=43$ minutes.

.....
Figure 7.7: Evolution of wave spectra (double logarithmic scale) at SL29 for the time-dependent test cases of 26/4/02 (top panel) and 21/12/03 (lower panel)



Wave spectra for time-dependent cases

Figure 7.7 shows the wave spectra for the time-dependent cases 1 and 3 that were discussed above.

The spectra for 26/4/2002 are shown in the top panel; the corresponding H_{m0} -values are 0.15 m at 21h and 0.4 m from 22h on. The low-lying high-frequency tail at 21h may be due to wind decrease and wave decay in the preceding hours. Otherwise, the above spectra for growing waves look quite similar to the (presumed equilibrium) spectra of Figure 7.1-7.5, at least when the subset without mixed wave fields, strongly forced and/or depth-limited conditions is considered.

The lower panel shows the spectra of 21/12/2003 for a situation with decaying waves, where H_{m0} decreases from 0.55 m at 8h MET to 0.35 m at 9h. In fact, these spectra too seem to be close to their equilibrium shape. However, closer inspection shows two interesting features:

- As H_{m0} decreases below a value between 0.5 and 0.37 m (H_{m0}/d then is between 0.3 and 0.22), the depth-limited features of the spectrum disappear, i.e. the pronounced main peak, as well as the hump at the right flank.
- For some time, the main energy is lost in the spectral peak while energy levels in the tail remain unchanged. This is the opposite of what would be expected during the formation of swell.

In fact, some Lake IJssel measurements are more suitable to investigate the latter phenomenon than the SL29-spectra of Figure 7.7b. Some interesting Lake IJssel cases with decaying wave spectra are 29/9/2005 and 24/5/2006. Both cases are presented in (Bottema, 2006b).

Further possibilities for time-dependent test cases

If reliable spatial wind fields become available, it is recommended to extend the above set of time-dependent calibration cases for Lake Sloten with a set of model test cases for Lake IJssel.

When time-dependent simulations with the SWAN wave model are considered, it is strongly recommended to use both sets of test cases for model validation, especially since early time-dependent SWAN tests (Claessens et al., 2002) suggested that extremely small time steps are needed before the time-dependent SWAN output becomes independent of the model (time step) settings.

.....
Figure 7.8: Time evolution of wave height H_{m0} at the five Lake IJssel platforms, 26/4/2002

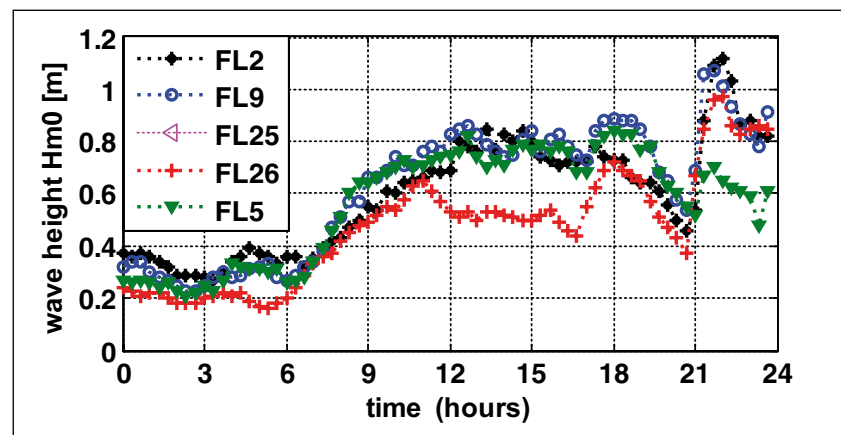


Figure 7.8 shows the wave height evolution at Lake IJssel for 26/4/2002, one of the rapid-wind-change cases presented in Figure 7.6. The wave height changes around 21 h MET are not as rapid as the SL29-changes in Figure 7.6 but still, wave evolution is very rapid. In fact, waves at Lake IJssel need hardly an hour to approximate their new equilibrium. This is even the case at FL2, with its order 20 km of fetch.

It is worth looking for other Lake IJssel test cases as Lake IJssel has another feature of interest: partly sheltered locations like FL25 often have 'swell' from neighbouring parts of Lake IJssel, both in stationary and time-dependent conditions.

A final subject of interest is the modulation of wind waves by seiches on Lake Sloten. If wave and water level modulations are in phase, and if the waves are large enough to be depth-limited, the waves are probably modulated by water depth variations. However, some cases have wave and water level modulations that are not in phase. This may be caused by different response times to the wind, but wave-current interactions may also be a cause of phase differences between wave height and water level modulations. Actually, such situations are one of the few cases where wave-current interaction might be investigated without the need to invest in a lot of current measuring equipment.

Some potentially interesting cases for this type of study are 28/12/2001, 23/2/2002 and 22/12/2003. Unfortunately, these cases have no winds parallel to the lake axis but from the W-NW (like many cases with showery weather and gusty wind causing seiches). By consequence, it was difficult to reach an unambiguous interpretation of the result. Therefore, these cases will not be presented in this report.

8. Wave run-up against dikes

In this chapter, the main results and main trends of the wave run-up measurements at the Rotterdamse Hoek site (see Figure 2.1) will be discussed.

8.1 Available data

The presence of analysable run-up data not only depends on the availability of wind and wave data at FL2 and run-up data at the Rotterdamse Hoek (RDH) site; it also depends strongly on the ambient conditions like wave height, wave direction and still water level (SWL). Within the measuring period 1997-2002, this results in the presence of extended periods with hardly any run-up data (even during storms). On the other hand, nearly 65% of the 3058 20-minute-runs with suitable run-up data originate from a 6-week period from 26/1 to 11/3/2002 with strongly elevated lake levels. Other significant periods were 3-9 January 1998 (183 runs) and 14-18 September 1998 (220 runs). The main storms with suitable run-up data were 26 February and 9 March 2002, when lake levels were much higher than usual.

In terms of the absolute run-up-level $h_{2\%}$, i.e. the absolute level which for a given 20-minute sample is reached by 2% of the waves which run up onto the dike at the RDH site, run-up did not exceed a level +1.4 m NAP until 2002. However, the storms of 26/2/2002 and 9/3/2002 yielded much higher run-up levels with $h_{2\%} = +2.4$ to +2.5 m NAP, about half a metre above the middle berm of the dike. The relative run-up levels, with reference to the SWL, remained below $Z_{2\%} \sim 1.8$ m for the latter two storms; for the remaining cases, $Z_{2\%}$ was 1.4 m or less.

Of the ambient conditions, the still water levels (SWLs) at FL2 were of the order of +0.2 m NAP, with a range of about -0.2 to 0.6 m NAP. The other ambient conditions strongly depended on the SWL at FL2. For a SWL below NAP, analysable run-up events only occurred with wave heights H_{m0} and peak wave periods T_p greater than 0.7 m and 3.5 s respectively (at FL2). The severest ambient wave conditions in this data set had H_{m0} - and T_p -values of 1.5 m and 5.5 s. As for the wind, the lowest recorded value during run-up events depended quite strongly on wind direction. For shore-normal wind directions, at least 6 Beaufort wind was required for run-up, for oblique (southwesterly) winds this lower limit even was as high as 8 Beaufort. On the other hand, the recorded run-up events with a SWL over +0.3 m NAP could pretty much happen with any ambient wind or wave condition.

All the in all, the run-up events for low SWL-values often had strong shore-normal winds and wave heights in excess of 0.7 m, where the events with high SWL-values had both high and low winds, with directions ranging from shore-normal to nearly shore-parallel (i.e. from 200-250°).

Finally, it has to be mentioned that the run-up data presented in this chapter are increased by + 7 cm with respect to the underlying original data. This correction is proposed by Wouters et al. (2003) to account for the vertical run-up gauge sensor position with respect to the dike surface.

8.2 Conceptual model framework

For modelling and parametrisation of wave run-up against dikes, the following formula is commonly used in the Netherlands:

$$(8.1) \quad Z_{2\%} / H_{m0} = 1.65 \gamma_b \gamma_\beta \gamma_f \xi_o$$

where:

- $Z_{2\%}$ is the run-up level that is reached by 2% of the waves in a finite time sample, measured with respect to the still water level rather than an absolute datum.
- H_{m0} is the spectral significant wave height at the toe of the dike
- γ_b a reduction factor accounting for berms in/before the dike profile
- γ_β a reduction factor accounting for oblique wave attack
- γ_f a reduction factor accounting for the roughness of the dike slope
- ξ_o a wave breaking parameter = $\tan(\alpha) / s_o^{0.5}$ with
 - α the (mean or equivalent) dike slope
 - $s_o = H_{m0} / 1.56 * T_{m-10}^2$ an equivalent deep water steepness (in the remainder of this report denoted as $s_{T_{m-10,o}}$)

The above formula is proposed by (TAW, 2002) and is the basis of the Dutch software package 'PC-overslag'. The description and validation of 'PC-overslag' is not within the scope of this report, so the reader is referred to (TAW, 2002) for the expressions of γ_b and γ_f , which are rather complex. By contrast, the expression for γ_β is rather simple as long as the angle β between the wave direction and the shore-normal is less than 80°: γ_β then equals $1 - 0.0022 * \beta$ (with β in degrees).

8.3 A few words about wave run up model applications

For the present measuring locations, the application of the above model is not straightforward in all respects. This will be illustrated in the following. In addition some conclusions of an earlier published model validation (Wouters et al., 2003) will be mentioned.

The first issue is mainly related to the use of wave parameters at the toe of the dike. At present, the required wave height and wave period (H_{m0} and T_{m-10}) are measured at FL2, whereas the required wave direction is not measured at all. For the latter, SWAN wave model simulations as presented in (Bottema, 2006c) suggest that wind and wave directions at FL2 differ less than 5° for winds between SSW and WNW. For shore-parallel southerly winds however, the SWAN mean wave direction is 12° larger than that of the wind, whereas it is about 10° smaller for north-westerly winds.

The above wave conditions at FL2 still have to be converted to those at the toe of the dike. Whereas FL2 is about 1.2 km offshore with a lake bed of -4.2 m NAP, the toe of the dike is, according to Wouters et al. (2003), within a few metres of the shore with a lake bed of -2.4 m NAP. Their SWAN wave model calculations suggest that the H_{m0} of FL2 has to be reduced by 0.94 for normal wave incidence and by 0.84 for waves coming in from the NW or SW. For the latter case, the wave direction at the toe differs 22° from that at FL2. Both these wave direction and H_{m0} -transformations are quite sensitive to the actual lake bed position and water depth, and to the SWAN model settings for depth-induced breaking. As a result the conversion of FL2 wave data to wave data at the toe of the dike is far from straightforward.

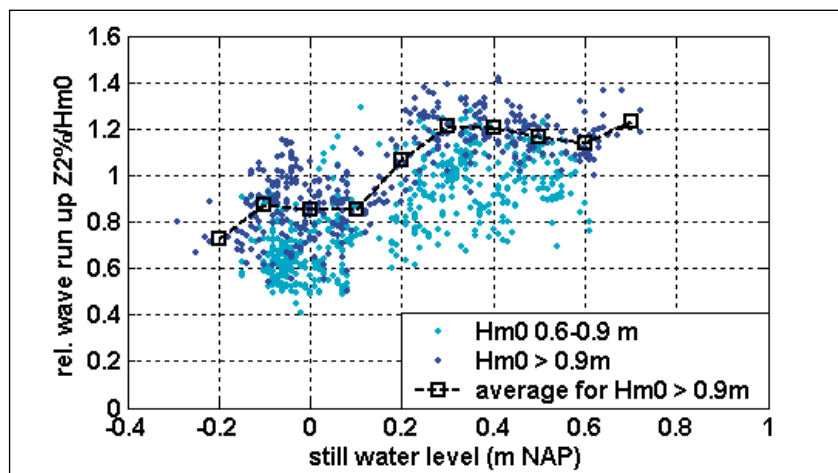
As it turns out, the application of 'PC-overslag' itself is not straightforward either, at least for the lower berm which the model can either deal with as a berm, or as a foreland, depending on the water level (Wouters et al., 2003).

As for the model results, Wouters et al. (2003) report that their model values are on average about 15% higher than the measured run-up values, with a range of -13% to $+52\%$. The largest model overestimations appear to occur for low water levels and oblique wave incidence. However, one should not be too quick in generalising this conclusion because only a limited data set was used (the 1997-1998 and 2000-2001 seasons), which only include water levels below the lower rubble berm. Moreover, as discussed above, the necessary modelling steps are far from straightforward. Therefore, a general model validation is not within the scope of this study. Instead, only some general experimental trends will be discussed in the next section.

8.4 Effect of berms and oblique wave attack

With the framework of Eq. (8.1), the ratio $Z_{2\%} / (\xi_o H_{m0})$ should be constant, except for a set of reduction factors related to berms, oblique wave attack and dike surface roughness. The trends in the measured ratio $Z_{2\%} / H_{m0}$ reflect the trends in the reduction factors γ_b , γ_β and γ_t , provided that ξ_o is constant. With a typical dike slope of 1/3 outside the berms (Figure 2.2) and a so-steepness of 0.05 (see Figure 6.9a), ξ_o is typically about 1.48. This implies that the total reduction factor $\gamma_b \gamma_\beta \gamma_t$ should be less than one if the ratio $Z_{2\%} / H_{m0}$ is less than about 2.4. In practice however, the ratio $Z_{2\%} / (1.65 \xi_o H_{m0})$ is only an approximation of the total reduction factor because the wave parameters of FL2 are taken as a reference, not the (unknown) wave parameters at the actual toe of the dike.

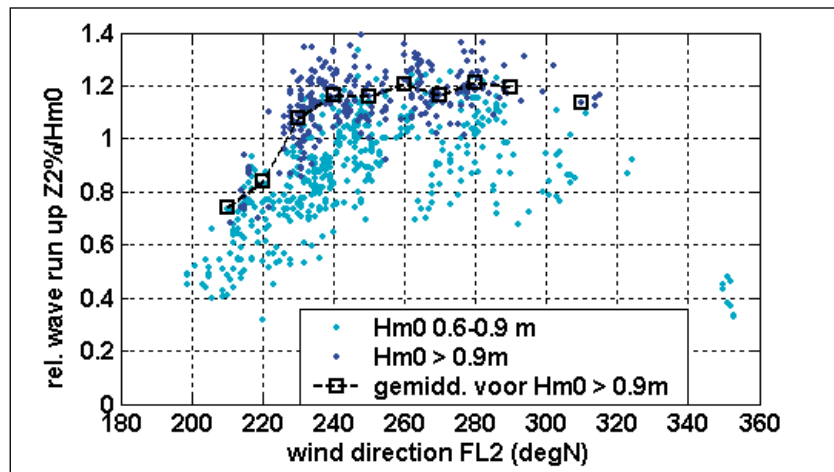
.....
Figure 8.1: Normalised relative wave run up $Z_{2\%}/H_{m0}$ at Rotterdamse Hoek as a function of still water level for westerly winds (240-300°), for two classes of FL2 wave height H_{m0} .



Firstly, to illustrate the effect of berms, Figure 8.1 shows the normalised relative wave run up $Z_{2\%} / H_{m0}$ as a function of the still water level, for approximately shore-normal wave attack. Two clusters can be identified in the graph. For still water levels below + 10 cm NAP, i.e. below the lower rubble berm, the ratio $Z_{2\%}/H_{m0}$ is about 0.8, provided the ambient waves are sufficiently high (0.9-1.5 m). For still water levels well above this lower berm the ratio $Z_{2\%}/H_{m0}$ is about 1.15. The slight dip for water levels of +0.6 m NAP is probably related to the influence of the near-horizontal middle berm which interrupts the otherwise fairly uniform dike profile. Another feature worth noting is the fact that the results depend quite strongly on the actual value of H_{m0} , even though this should not be the case if the scaling of Eq. (8.1) applies. This seems to suggest that either the effect of berms or the effect of surface roughness depends – in reality – quite strongly on the actual value of the ambient H_{m0} .

Figure 8.2 shows the normalised relative wave run up $Z_{2\%}/H_{m0}$ as a function of wind direction (at FL2), for water levels high enough to strongly reduce (or even fully remove) the effect of the lower rubble berm. For wind directions within 45° of shore-normal, the wind direction only appears to have little effect ($<10\%$) on the actual run up. For larger deviations from shore-normal however, the actual run-up quickly decreases. For a wind direction of 210° , the actual run-up reduction is as large as 40% , whereas the 'PC-overslag' expression of section 8.2 only yields 13% reduction. In practice, this model reduction will be still smaller because for this wind direction, the waves at the toe of the dike will be at least 20° closer to shore-normal than the wind (see Wouters et al., 2003). A possible explanation for these apparent model overestimations is the combined (synergetic) effect of berms, roughness and oblique wave attack in practice, whereas the model approach probably considers each effect separately.

.....
Figure 8.2: Normalised relative wave run up $Z_{2\%}/H_{m0}$ at Rotterdamse Hoek as a function of FL2 wind direction, for still water levels greater than $+0.25$ m NAP. Results are shown for two classes of FL2 wave height H_{m0} .



A final point of interest is the scatter in the data in Figure 8.1 and Figure 8.2. This scatter was also noticed by Wouters et al. (2003), who remarked that the scatter even occurred within a given storm, with near-constant ambient wave conditions. This suggests that much of the scatter reflects sampling variability and that a single 20-minute value of $Z_{2\%}$ is not an accurate run-up estimator. In the present data, this sampling variability in $Z_{2\%}$ was investigated for a few data subsets. It appears that the sampling variability is largest for water levels below NAP (about 20%) and smallest for water levels well above NAP and for large waves. In the latter case, the variability is about 5% for large waves and 10% for small waves. This trend is somewhat surprising because for small waves, the sample sizes tend to be larger because of the smaller waves periods. When the above numbers are compared to the actual scatter and differences between data subsets in Figure 8.1, one must conclude that random and systematic (H_{m0} -dependent) variability are roughly equal for low water levels, but that systematic H_{m0} -dependent trends clearly dominate the random scatter for water levels well above NAP.

9. Conclusions and recommendations

9.1 Conclusions

The general aim of the present wave measuring campaign is :

- *To gather and analyse well-documented wind and wave measurements of high quality, for various locations and various (strong wind) conditions, both for Lake IJssel and Lake Sloten.*

This aim has largely been reached, as is shown in Chapter 3 (range and availability of data). Some key results include the wind climatology of section 4.2-4.3, the wave climatology of section 6.2-6.3 (see also Appendix G) and a fairly large set of stationary and time-dependent cases to calibrate and validate wave models (Chapter 7). In addition, several aspects of wind, temperatures, water levels, storm surge, waves, wave run-up and wave instrumentation are investigated throughout Chapter 4 to 8, as well as Appendix A-C (for wave instrumentation).

In one significant aspect however, the present measuring campaign did not produce the desired result. For dike design purposes, measurements during 10-12 Beaufort winds are especially valuable. However, Lake IJssel has not experienced any sustained 10 Beaufort winds for an exceptionally long period that lasts now over 17 years, and started in March 1990. In order to enhance the probability on measuring such conditions, Rijkswaterstaat has recently started a wave measuring campaign in Lake Tai-Hu in China, in co-operation with the Chinese Tai-Hu Basin Authority.

Some further general conclusions are:

1. At some occasions and locations, the measured wave periods were as large as the design values for nearby dikes (Chapter 3, Table 3.2). This is remarkable as the design conditions are typical for 12 Beaufort winds while the measurements took place in 9 Beaufort winds. On the other hand observed wave heights and – more importantly – run-up heights against dikes still were 30-50% below their design levels.
2. Wind is poorly understood with respect to: evaluation of extremes, time-evolution and duration of storms, spatial wind transformation and wind drag. The first issue is not in the scope of this study, about the remainder the following can be said.
 - The number of measured storms is too small to evaluate reliable storm evolution statistics.
 - The present observations and official KNMI observations show that during several (severe) gales, winds over open water are *lower* than over land (section 4.4). This trend is unexpected and can not yet be reproduced by any model since all models make use of the fact that land surfaces are rougher (and

-
- have less wind) than water surfaces. Typically, this results in order 15-30% overestimation of the open-water winds by the models. Caution is needed when translating this into dike design because it is not clear why and when this phenomenon occurs.
- The present data (section 4.5) show that the drag coefficient C_D , which defines the wind drag force on the water, increases with wind speed up to at least 9 Beaufort. By lack of storms, no data were obtained for the interesting range of 10-12 Beaufort. This is unfortunate as scientific literature suggests that C_D might strongly decrease in the (near-) hurricane wind speeds used for Dutch dike design. In this respect, one should note that C_D influences wind, storm surge and waves: 30% change in C_D may yield up to 6% (or some decimetres) change in required dike height.
3. For wind-induced set-up of the mean water level (*storm surge*), not only the steady behaviour is important but also the *unsteady* behaviour. On time scales of 0.5 – 3 hours, the storm surge response to wind on Lake IJssel generally has an unsteady and resonant character (section 5.3). At Lelystad-Houtrib, an overshoot of a metre above the regular water level was observed after a sudden wind drop during the 9 Beaufort gale of 18/1/2007. At Lemmer, oscillations of 0.5-1 m are relatively common during 6-8 Beaufort winds near sharp weather fronts, or during periods with gusty winds.
 4. It is not advised to use directly measured wave climatologies of Lake IJssel for dike design purposes, as their extrapolation tends to produce physically unrealistic trends (section 6.1).
 5. Nearly all advanced wave models are calibrated with semi-empiric parametric wave growth curves. It is not yet clear whether these should be scaled with the wind speed or the wind *drag force* (section 6.5). During the Lake IJssel design winds of 35-40 m/s, there is about 50% wave height difference between either option, at least for deep water. Less important, but still significant, is the finding that several parametric curves are affected by hidden fetch assumptions and the fact that not all situations can be modelled with a single effective fetch (section 6.7.1).
 6. For Lake IJssel, design wave heights are order 40% lower than they would have been over deep water. Hence, knowledge of depth-limited wave growth over nearly flat bottoms is crucial. In the default SWAN and HISWA models, the ratio of significant wave height to water depth - H_{m0}/d - remains below 0.38, regardless of wind speed. For Lake Sloten and Lake George, the measured H_{m0}/d ratio reaches up to 0.44-0.45. By lack of (10+ Beaufort) storm conditions in either data set, it is not yet clear whether still higher values (above 0.45) are possible over flat lake bottoms.
 7. It is expected that probably, many findings of the present wave measurements will not find directly their way into dike design

conditions, but through successive improvements of wave models. The test and calibration cases in Chapter 7 may fulfill an important role in this.

8. For bad-weather warnings (for ship traffic as well as for dike monitoring), it is important to note that waves on Lake IJssel can grow fast, sometimes at a rate over 50 cm per hour.
9. For the present run-up measurements, the estimated run-up reduction by berms, dike surface roughness and oblique wave attack at the RDH location is order 50-75%. There appear to be some synergetic (reduction-enhancing) effects between these three mechanisms.
10. It is no easy task to find suitable wave instruments for Lake IJssel (Appendix A-B): many instruments have insufficient high-frequency response for the generally rather short waves. Acoustic log-a-levels may suffer from wind deflection of their sound beams; conventional step gauges and capa probes are prone to ice damage and – in summer - soiling by algae.

The detailed conclusions for each of the main chapters and appendices are given below.

Chapter 1 and 2 (Introduction / Measurements and data)

Although these chapters contain few real conclusions, they contain important background information. Chapter 1, focusses on the relevance and aim of the present measurements, and on the relations with other projects. Chapter 2 is important as it provides background information on the measuring locations, the instrumentation, and the procedures for acquisition, processing and validation of the data. For the latter it is important to note that for the present data set, it is not sufficient to fully rely on a software package detecting suspect cases. As it turned out during the last decade, in-depth analyses and interpretations had an indispensable role in the validation of the present data set.

Chapter 3: Availability and range of experimental data

- 3.1) For the period 1997-2000, data availability generally was below 40-70%. From 2001 on, it was 75-90% for most months. During days with at least 15 m/s wind (8-46 per year), the availability was slightly better.
- 3.2) The main sources of data loss were, in decreasing order of importance:
 - interruptions due to ice periods (7% overall data loss)
 - discarded data due to negligible wind and waves (about 10% data loss at sheltered locations to 5% elsewhere)
 - PC-problems at shore station or RWS office; damaged backups in early years: overall roughly 5%
 - malfunctioning instruments, energy problems, damaged platforms, absence of spare instruments: roughly 5%
 - communication problems (modems etc.) : about 4%

-
- 3.3) From mid-1997 to 1/2/2007, 16 cases occurred with at least 20 m/s wind. In seven of these cases, wind speeds reached 21-24 m/s (9 Beaufort). From 2001 on, data availability for these cases is (well) above 70%.
 - 3.4) Analysable run-up data are concentrated in a few windy periods with high water levels; two thirds of all suitable run-up data is measured between 26/1/02 and 10/3/02.
 - 3.5) Measured wind speeds during this campaign typically range up to 10-14 m/s for easterly winds and up to 20-24 m/s for westerly winds (S-NNW). In 1978 and 1990, KNMI measured wind speeds of 28 m/s, but no wave data are available for these cases. All measured wind speeds are far below the wind speeds used for dike design, which are typically 35-40 m/s.
 - 3.6) The severest waves that are measured so far have a significant wave height H_{m0} of 1.4-1.8 m and a peak period T_p of 5-6 s. The highest individual waves reached 3.1 m; still water levels during these conditions were -25 cm to + 80 cm NAP.
 - 3.7) The highest run-up levels measured so far are +240 cm NAP. This is above the middle berm of the dike at the Rotterdamse Hoek (RDH) site, but still two metres below the top of the dike.
 - 3.8) Measured still water levels, wave heights and run-up levels are still well below the design values (see Table 3.2 and general conclusions). By contrast, some measured T_p values are already as large as the intended design values.

Chapter 4: Wind and temperatures

- 4.1) Wind is a crucial factor in dike design, wave modelling and the interpretation of the present wave data (section 4.1). Wind speed changes as small as 7% may cause 10% change in wave height and required dike height. For fetches of a few km, wind direction changes of 6° may cause up to 10% wave height change.
- 4.2) The wind climate for Lake IJssel has the following general trends (section 4.2):
 - no clear prevailing wind direction, except for strong winds of at least 5 Beaufort, when (south)-westerly winds prevail.
 - winter wind speeds are about 20% higher than during summer
 - day-night differences are small, except for (calm) summer nights on land, or within order 1 km of land.
- 4.3) For all locations (including land-based KNMI-stations), Weibull fits have similar trends as in (Wieringa and Rijkoort, 1983) but higher values for both the 'a' and 'k' parameter in Eq. (4.1). Hence, the 1997-2006 period seems to differ from previous periods by a prevalence of moderately strong winds at the cost of extremes on either side.
- 4.4) Extrapolation of Weibull distributions (Eq. 4.1) outside the fitted range of 4-16 m/s may lead to implausible results.
- 4.5) The present estimates of extreme wind speeds appear to be

too low and should not be used for dike design purposes. Yet, some interesting trends can be derived from the results of section 4.3:

- The extrapolated wind extremes are higher over land than over water, which is physically implausible. The same trend is observed for some measured values (see conclusion 4.6).
- The period 1991-2007 has a remarkable absence of storms (of at least 10 Beaufort), which significantly influences the extremes from this period. Hence, a 16 year record length seems to be (far) too low to derive reliable wind extremes.
- Storm (duration) characteristics are quite variable. The rate of wind speed change is typically order 1.5 m/s per hour but can be as large as 5-6 m/s per hour. The rate of wind veering during storms is typically order 5° per hour, but may range from near-zero to 25° per hour and possibly more.

4.6) Spatial wind transformation methods (section 4.4) are essential to convert land-based wind statistics to open-water locations. Of the many available methods (Appendix E), two simple and verifiable methods are introduced in section 4.4.1: a meso-transformation method assuming *partially* adapted open-water wind and a macro-transformation assuming *fully* adapted wind. The main results from analysis of these models and the available wind data are:

- Open-water wind speeds are often unexpectedly low with respect to wind over land. Especially in strong winds, open-water winds are at various times *lower* than wind speeds over land, although the opposite is expected because of the larger surface roughness over land. *None* of the available wind transformation models reproduces this experimental trend.
- Meteorological textbooks (e.g. Wieringa and Rijkoort, 1983) often state that thermal influences of the wind are restricted to weak winds of less than 6 m/s. In the present case, air-water temperature differences turn out to have a strongly significant influence on land-water wind speed differences for wind speeds up to at least 7 Beaufort (14 m/s).

4.7) The aerodynamic roughness of the (wavy) water surface is a key factor in the meteorological and hydraulic models used for dike design (section 4.7). The key results for this subject are:

- The present measuring campaign is not designed to accurately measure roughness parameters. The wind-profile and turbulence-based methods that can be applied to the present data all yield rather inaccurate roughness parameters. Wieringa's (1986) gust method is particularly inaccurate for this case, while theoretical objections (Verkaik, 2000) have been brought forward as well.
- As far as can be judged, most measured roughnesses agree quite well with Wu's (1982) parametrisation given in Eq. 4.7. However, from 9 Beaufort on, wind-profile derived roughnesses seem to be larger than those of (Wu, 1982).

-
- The ratio of roughness length to wave height, z_0/H_{m0} , appears to strongly influenced by the relative wave age parameter c_p/U_{10} , where c_p is the phase propagation speed of the waves.
- 4.8) For the water temperatures (section 4.6), the main results are:
- In the period 1959-1992, 20°C temperatures were reached in 75% of the years. Ice also occurred in 75% of the years, with a 25% daily probability in the end of January and near-zero probabilities towards late November and late March.
 - The present measuring campaign took place in an exceptionally mild period that started in 1988. Typical water temperatures were 0-8°C in winter to 16-24°C in summer. All summers in the period 2001-2006 reached water temperatures of 22-24°C.
- 4.9) The main results for the air temperatures (section 4.6) are:
- Air-water temperature differences can be up to 4-9°C to either side; day-night air temperature differences over open water are generally small.
 - On average, air temperatures tend to be below the water temperatures for all seasons and wind directions, probably due to evaporation effects. The average differences are largest (2-3°C) for NW-winds in spring/summer and NE-winds in winter.
 - A 5°C air-water temperature difference with 10 m/s wind typically leads either to about 1°C water temperature decrease, or 0.7°C increase. In summer, rapid warming can also occur in calm conditions due to solar radiation.

Chapter 5: Water levels, storm surge, seiches

- 5.1) Target mean lake levels for Lake IJssel are –20 cm NAP from mid-April to end September and –40 cm in the remainder of the year (section 5.1). Actual lake levels are on average –20 to –30 cm NAP, with little variation in summer. In late winter however, actual lake levels can be up to a metre above the target levels.
- 5.2) Water levels for Lake Sloten are typically about -50 ± 8 cm; in one very rainy period, they did reach –20 cm NAP.
- 5.3) Wind-induced set-up of the mean water level (*storm surge*) is highly relevant for dike loading and the daily water management of Lake IJssel (section 5.2).
- 5.4) Storm surges Δz for wind speeds U_{10} of 17-19 m/s (8 Beaufort) are typically up to 15-30 cm for the present locations, and up to 30-50 cm for the nearshore locations of the Monitoring System Water. Typically, storm surge and wind speed are related as $\Delta z \sim U_{10}^{2.2}$.
- 5.5) For most of the scatter in the storm surge data, no explanation could yet be found.
- 5.6) Water level oscillations (section 5.3) with periods of order 1 hour occur quite regularly; at Lemmer, they can measure 0.5 – 1 m from trough to crest. This oscillations typically occur during 6-8 Beaufort gusty winds or near sharp weather fronts. At Lelystad-Houtrib however, a 1 metre oscillation (or rather

-
- overshoot) occurred after a sharp wind decrease during the 9 Beaufort gale of 18/1/2007. By lack of data, the probability on similar oscillations during dike design conditions (typically 12 Beaufort winds that have not yet been measured) can not yet be assessed.
- 5.7) The unsteady response of storm surge to wind is relevant for data analysis and for model validation. For Lake IJssel, it can be divided into three different regimes:
- Time scales over 2 hours (for Lemmer over 5 hours): quasi-steady reponse of storm surge to wind forcing;
 - Time scales of order 0.5 – 3 hours: Storm surge response to wind up to about three times larger than in steady winds due to resonant phenomena. The actual resonant time scales and amplification factors are strongly location dependent;
 - Time scales of order 1 h and less: Reduced response of storm surge to wind due to finite spatial extent of wind fluctuations and due to finite reponse time of Lake IJssel
- 5.8) For backwaters (e.g., Lake Ketel) that are separated from Lake IJssel by narrow channels, the above response and resonance time scales are expected to be considerably larger.

Chapter 6: Wave properties and wave climate

- 6.1) The long term average (section 6.1) of the significant wave height H_{m0} is 0.15 m at Lake Sloten and 0.23-0.39 m at the Lake IJssel locations FL25 and FL26 respectively. The highest H_{m0} -values recorded so far are typically a factor 4-5 higher.
- 6.2) It is not advised to use directly measured wave climatologies of Lake IJssel for dike design purposes, as their extrapolation tends to produce physically unrealistic trends, like higher extremes at the depth-limited location FL5 than at the more exposed deep-water location FL26. In practice, wave climatology usually must be evaluated from a continuous land-based wind climatology, together with methods to account for spatial wind variations and climatological wind-wave relations (section 6.2-6.3).
- 6.3) When averaged over a large number of cases, the wave conditions (H_{m0} , T_{m01}) at each location display a clear relation as a function of wind speed and wind direction (Figure 6.3-6.7).
- 6.4) The relative scatter (one standard deviation divided by mean) in H_{m0} is typically 10-15% for moderate winds and 5% for very strong winds. In cases with very strong winds and fetches of order 1 km, this scatter can be much larger. This applies especially to FL25 (Figure 6.2b) and to a lesser extent to SL29 (Figure 6.15). The scatter in the wave period T_{m01} is generally smaller than for H_{m0} .
- 6.5) Generally, the scatter reflects case-to-case variability, rather than variations within cases (like in very gusty winds). The similar scatter trends in the wave height H_{m0} and wave period T_{m01} suggest that case-to-case variability may well be related to

-
- atmospheric conditions.
- 6.6) The wave period ratios T_p/T_{m01} and T_{m-10}/T_{m01} are typically 1.13-1.33 and 1.07-1.17 respectively; for standard JONSWAP spectra these ratios are about 1.15 and 1.06 (section 6.3). In about 10 cases, the measured wave period ratios deviate from the above-specified ranges. These special cases are related to depth-limited breaking waves, shore-parallel winds, or offshore winds with fetches less than order 1 km. Results for the zero-crossing period T_{m02} are not presented as they are too sensitive to the spectral integration range used (see Appendix B.1).
 - 6.7) The peak period T_p often has ambiguous behaviour at the edges of sheltered wind sectors, when it may cluster around two or even three different values. In situations where very low waves ($H_{m0} < 0.1$ m; occurring roughly one third of the time at SL29 and FL25) are included in a data set for wave model validation, one should be aware of the fact that for these low-wave cases, both T_p and T_{m-10} may be a few times larger than expected due to residual low-frequency wave energy.
 - 6.8) The natural variations of the wave steepness are small, so that wave steepnesses (section 6.4) are a useful benchmark parameter to validate model results, statistical extrapolations and experimental data.
 - 6.9) Deep water steepnesses $s_{T_{m-10,o}}$ (Eq. 6.2a) are generally in the range of 0.04-0.06. Lower steepnesses may occur in mixed seas with some non-locally generated 'swell'. Steepnesses up to 0.08 are observed in situations with strong winds and fetches less than about 5 km, but enhanced wave steepnesses may also occur during sudden wind increases (section 7.3; Figure 7.6).
 - 6.10) In situations where H_{m0} is less than about 20% of the water depth, the steepness parameter s_{T_p} agrees well with a deep-water parametrisation (Eq. 6.3) that was derived from Kahma and Calkoen (1992).
 - 6.11) There is an ongoing scientific debate about the question whether the wave should scale with a wind speed parameter (U_{10}) or a wind force parameter (the friction velocity u^* ; section 6.5). During winds that are typical for Dutch dike design (35-40 m/s) the difference between either approach may be as large as 25-50% (for T_p and H_{m0} respectively).
 - 6.12) Clarity about the scaling to be used is essential as nearly every wave model, however advanced, is ultimately tuned to a U_{10} -based or u^* -based parametric wave growth formula.
 - 6.13) Analysis of the present FL26 data suggests that over deep water, wave heights and peak periods scale as $H_{m0} \sim U_{10}^{1.25}$ and $T_p \sim U_{10}^{0.5}$ respectively. However, it remains unclear whether U_{10} - or u^* scaling has to be used; rather it seems that the actual scaling might be between these two alternatives.
 - 6.14) The direct effect of air-water temperature differences on wave growth is also related to the above. Direct effects mainly occur

-
- for winds below 5 Beaufort (Figure 6.13). For higher wind speeds, thermal effects are mainly indirect through spatial wind variations (section 4.4).
- 6.15) The modelling of depth-limited waves is crucial for Lake IJssel as during design winds of 35-40 m/s, the actual design waves (section 3.3) are 30-50% lower than the wave conditions that are to be expected in deep-water conditions (section 6.5).
 - 6.16) The measured wave-height-over-depth ratios H_{m0}/d over nearly flat bottoms (section 6.6.1) reach values of nearly 0.38 (FL2; 18/1/07) up to 0.41-0.45 (SL29 and Lake George). The latter value is well above the 'hard' maximum H_{m0}/d (0.38) that can be reached with default settings of the SWAN wave model.
 - 6.17) FL5 is the main location of interest for cases with sloping bottoms (section 6.6.2). Despite its 10% longer fetch for onshore winds, FL5 then has about 10% lower wave heights than FL9. This applies mild conditions and wave-breaking conditions with H_{m0}/d up to 0.7. For H_{m0}/d values around 0.5, wave shoaling appears to be dominant as FL5 H_{m0} -values then tend to be equal or slightly larger than those of FL9.
 - 6.18) The peak periods T_p of FL5 tend to be 0-5% larger than those of FL9. At FL5, the wave period ratios T_{m-10}/T_p and especially T_{m01}/T_p start to steadily decrease for H_{m0}/d ratios above 0.32, probably because the wave asymmetry increases as the waves becomes more depth-limited.
 - 6.19) Parametric wave growth curves, which are used to calibrate more advanced models, rely on the assumption that real direction-dependent fetch conditions can be simplified to a single effective fetch. The present analysis (section 6.7.1) and its extension in (Bottema and Vledder, 2006) suggest that this assumption does not always hold, especially not in the first kilometres off the coast during obliquely offshore winds. Also, some commonly used parametric wave growth curves seem to be prone to bias by the (fetch conditions or fetch definitions in) the underlying data set.
 - 6.20) Wave spectra are shown in Figures 6.21 and 7.1-7.5. In moderately depth-limited conditions (H_{m0}/d between 0.3 and 0.6), the spectral parametrisations of Young and Babanin (2006) perform quite well. However, their assumption that the parameter gd/U_{10}^2 is the main scaling parameter seems not fully in accordance with the present data (section 6.7.2).
 - 6.21) For individual waves, the frequency distribution is generally close to a Rayleigh distribution (section 6.7.3). Significant depth limitation of individual waves only occurs for H_{m0}/d values of about 0.5 and larger, a value that is only reached over sloping bottoms (FL5). This is surprising because the first signs of depth limitation in the overall wave height H_{m0} seem to occur for H_{m0}/d values as low as 0.1 (section 6.7.1) to 0.14 (section 6.6.1). Apparently, some depth-dependent wave

-
- damping mechanisms (bottom friction?) affect all waves at once, rather than just the highest waves.
- 6.22) The behaviour of wave period distributions is quite uniform, except in situations with strongly shoaling and breaking waves (Figure 6.23b).
 - 6.23) The joint distribution of individual wave heights and periods (section 6.7.3) can be an interesting validation tool: for waves with periods that are at least 30% below the peak period, the steepest waves are nearly always very close to the theoretical 1-to-7 steepness limit. Lower and especially higher steepness values for these short waves are often suspect.

Chapter 7: Wave model calibration and test cases

- 7.1) For wave model *calibration*, Lake Sloten seems the best subset of the present data. This is because depth-limited wave growth is considered to a crucial feature for dike design applications. Nine calibration cases are presented in section 7.1; they are selected to be error-free, stationary and representative. Wind, fetch and water depth for these SL29-cases are about 10-23 m/s, 1-3 km and 1.65-1.83 m respectively.
- 7.2) In mild conditions, the standard SWAN wave model underestimates the wave periods by about 15%. In windy and strongly depth-limited conditions, wave heights and wave periods are underestimated by about 20-35%. The humps in the real spectra (Figure 6.21) then are also poorly predicted. For all cases that are just mentioned, recent improvements in the SWAN physics yield significantly smaller errors, that end up in the range of 10-20% (see Bottema, 2006c for all results).
- 7.3) For wave model *validation*, twelve Lake IJssel test cases are defined (section 7.2), with wind directions, wind speeds and mean lake levels in the range 169°-328° (SSE-NNW), 9.7-23.5 m/s (5-9 Beaufort) and -0.4 to 0.1 m NAP respectively. In the test case selection, uniformity of the wind field played a key role. Representativeness and air-water temperature differences were also considered where possible.
- 7.4) A few data were rejected because of measuring errors or lack of representativeness. The latter is most likely to occur for a combination of short (~1 km) fetch and gale force winds, for example at the FL25-location in the 9-Beaufort case IJC, where wave heights were as much as 60% (!) lower than usual.
- 7.5) The Lake IJssel error trends of the SWAN model (Bottema, 2006c) are similar to the Lake Sloten trends mentioned above. Model wave heights H_{m0} for fetches of 1 km and less were 40% too large, but not as a result of errors in model physics. With improved SWAN model physics, the short fetch overestimations even become order 60%. Elsewhere however, the new *physics* clearly yield improvements. In all cases, SWAN has some difficulty in predicting the correct shape of the wave spectrum, especially in depth-limited conditions.

-
- 7.6) Time-dependent test cases for Lake Sloten (section 7.3) show that the wave height H_{m0} may increase from 0.15 m to an equilibrium of 0.45 m within 20 minutes. Near thunderstorm gust fronts, even larger H_{m0} -increases occurred within 6 minutes. As wave period growth lags somewhat behind, wave steepnesses may be up to twice as large as in steady conditions with similar wind.
 - 7.7) Cases with rapid wind decrease are rare; the available data (see Bottema, 2006b) suggest that most wave decay at Lake IJssel takes place in the spectral peak rather than the high-frequency tail, contrary to what is expected during swell formation.
 - 7.8) In strong winds, time scales for wave adaptation at Lake IJssel seem to be about 1 hour, even at FL2 with its 20 km of fetch. This is much quicker than in some preliminary SWAN-calculation of Claessens et al. (2002).

Chapter 8: Wave run-up against dikes

- 8.1) Events with analysable wave run-up at the RDH dike location typically occur for still water levels above +0.3 m NAP, or during (very) strong onshore winds. The highest run-up recorded so far is in absolute terms +2.4 m NAP, in relative terms about 1.8 m above the still water level.
- 8.2) The actual validation of run-up models is outside the scope of this study. With a limited data set and some assumptions, Wouters (2003) concludes that modelled run-up tends to be order 15% too high.
- 8.3) At the RDH location and for the present data set, the combined effect of berms and dike surface roughness (and sometimes oblique wave attack) yields typically order 50-75% run-up reduction in comparison with a hypothetical situation without berms and with a smooth dike surface and shore-normal wave attack.
- 8.4) As opposed to commonly accepted scaling principles (as used in Eq. 8.1), the measured $Z_{2\%}/H_{m0}$ -values depend quite strongly on the actual H_{m0} -values at FL2. This suggests that some of the above run-up reduction mechanisms depend on the actual wave (run-up) height rather than a dimensionless parameter.
- 8.5) Run-up reduction seems to be stronger than expected when waves approach at angles over 40° from shore-normal. This may be due to combined (synergetic) run-up reduction effects due to berms, surface roughness and oblique wave attack.

Appendix A: Alternatives for present instrumentation

The present instruments are sensitive to ice and soiling. Some key considerations for alternatives of the present instruments are:

- A.1) Remote sensing is useful to measure wave fields but the resolution is often too coarse for wind waves on Lake IJssel.
- A.2) Buoys are commonly used for marine applications. For this campaign, their limited high-frequency response is a limitation.

-
- A.3) Downward looking instruments with too wide a signal beam suffer from high frequency losses; too narrow a beam increases the risk of interception and interruption of the signal.
 - A.4) High frequency loss and signal conversions can be problems when measuring below the water surface. ADCPs are an exception but do not yet seem accurate enough for Lake IJssel.

Appendix B: Wave measuring errors

- B.1) The spectral integration range (Appendix B.1) can be a major error source in especially T_{m02} . With integration up to 1 Hz, T_{m02} -biases generally are above +10% for wave heights H_{m0} below 0.7 m. For FL25 and SL29 this is effectively always the case. For H_{m0} and T_{m-10} , biases are less than -5% and +5% for H_{m0} above 0.4 m (or 0.2 m with integration up to 1.5 Hz).
- B.2) Out of range values are generally rejected. Outliers *within* the measurement range are hard to filter but generally have limited effects. In a few cases, the data contain too many staggers with respect to the benchmark given in Appendix B.2.
- B.3) If wave overtopping over the instruments occurs, it mainly affects the wave heights: especially H_{max} and $H_{1/10}$. In practice, the errors in H_{m0} are a few percent at most (Appendix B.3).
- B.4) Step gauges are preferably not used if H_{m0} is less than twice the sensor interspacing (10 cm) as errors then tend to be over 10% (Appendix B.4).
- B.5) Soiling of step gauges and capa probes is difficult to detect reliably, but it can easily cause order 30% underestimation of H_{m0} , even in strong winds (Appendix B.5). Most soiling problems occur from May to October.
- B.6) For capa probes, disturbances due to the instrument supports (Appendix B.6) seem to be the main error source. The error mechanism is not fully clear and the exact errors are hard to predict. The H_{m0} -errors can be as large as -20% for $H_{m0} = 0.55$ m and -60% for $H_{m0} = 0.23$ m; in the latter case, T_{m-10} errors can be over +100%. Potential problem periods can be recognised by pronounced preferential values near the still water level. Also, the skewness and kurtosis of the raw signal are quite good error estimators (Figure B.10).
- B.7) Capa probe drift (Appendix B.7) is hard to reliably assess but it is no crucial error source; it mainly occurs in the zero-offsets.
- B.8) Early log-a-level types that were used before mid-January 2007 suffered from an instrument software error that caused strong signal distortion (jagged wave crests) and strong wave height underestimations for all cases with H_{m0} larger than about 0.6 m (Appendix B.8). On some occasions, false reflections and outliers were also a problem.
- B.9) Two expected error sources of the log-a-level are footprint errors and wind deflection (Appendix B.9). For wave heights above 15 cm, footprint effects are expected to be less than 5%. Signal loss due to wind deflection may become quite

significant if wind speeds are higher than order 7-8 m/s.

Appendix C: Intercomparison of wave instruments

- C.1) Comparison of the present capa probe data with step gauge data of earlier years suggests that the integral wave parameters of both instruments agree within a few percent for a wide range of conditions (Appendix C.1).
- C.2) Wave flume tests (Kuiper, 2005) suggest that log-a-levels (after outlier removal) and step gauges perform best for Lake IJssel applications (Appendix C.2). A capa probe, radar sensor, ADCP and pressure sensor all ended up lower in the ranking.
- C.3) A preliminary comparison between of capa probes and recently improved log-a-levels suggests that wave heights and periods of both instruments generally agree(well) within 10% during mild and moderate conditions; wave spectra then also agree well (Appendix C.3).
- C.4) Log-a-levels seem less suitable for strong winds as for wind speeds above 12 m/s, all locations show a steady increase in the number of out-of-range data. Data blocks without out-of-range data then also tend to contain (outliers causing) large amounts of spurious scatter and low-frequency noise related to this.

Appendix D: Applied offsets and corrections

This appendix specifies the offsets and corrections to be applied to wind speeds, wind directions and the wave signal. Also, unreliable periods are specified for these variables, as well as for the temperatures and the SL29 pressure sensor. Over the last 10 years, there are:

- about 40 special cases related to failing wind sensor(s)
- about 60 different wind corrections, with 8 wind direction corrections of more than 20°
- about 100 different wave data offsets, plus 11 special cases related to failing amplifiers and/or data logger software errors.
- over 30 special cases with wave measuring problems other than those already discussed in Appendix B6 and B8.

Appendix E: Cornerstones of spatial wind modelling

This appendix discusses some key assumptions of common modelling approaches, so that non-experts can get an impression about do's, do not's, applicability and limitations. This is done because suitable textbooks about spatial wind modelling appear to be rare, especially if one looks for books that are complete from a theoretical and practical viewpoint.

In general, it is found that the approaches with the best theoretical basis seem to have the smallest application range, and vice versa. In addition, there are significant parameter uncertainties, especially in the estimation of the aerodynamic roughness of water surfaces and non-homogeneous land surfaces.

9.2 Recommendations

The recommendations that follow from the present analyses will be structured along the following topics:

- knowledge gaps related to wind over open water, water waves and storm surge, in particular in relation to flood protection;
- measuring and research needs from the above;
- measuring locations and instrumentation;
- application of the present work; dissemination of data.

Knowledge gaps:

The present measurements have clarified a lot about wind and waves over Lake IJssel during wind conditions of 4-9 Beaufort. Most remaining knowledge gaps are related to the extrapolation of these data to the 12 Beaufort conditions required for dike design, or to the application of the present findings to other water bodies, where key phenomena may be different from those over Lake IJssel.

The dike-design related knowledge gaps for wind (see also Waal, 2003), storm surge and waves on Lake IJssel (or similar lakes) are mainly related to conclusions 2-6 of the previous section:

1. *Evaluation of extreme wind speeds from measured time series of hourly wind data.* In fact not a result of this study but a conclusion of Lammers and Kok (2006).
2. *Spatial wind field and time evolution of wind during storms.* Too much variability in wind fields and wind evolution during storms, and too small a storm data base.
3. *Spatial wind transformation.* There is yet no model with acceptable theoretical basis that can reproduce our measured tendency for negligible land-water wind differences during storms.
4. *Drag force of wind on the water surface.* Drag force might suddenly start to decrease from 10-12 Beaufort on, due to wind-water decoupling as a result of massive foam formation.
5. *Unsteady and resonant storm surge behaviour.* Major source of uncertainty for some storms, but by lack of unsteady storm data, there has been little opportunity to investigate this issue.
6. *Scaling of parametric wave growth curves.* Still a major source of uncertainty (conclusion 5).
7. *Depth-limited wave growth.* This remains a significant source of uncertainty (conclusion 6), especially as a wave growth limit might be reached from 10 Beaufort on.
8. *Wave growth in the first kilometres offshore during storms.* Figure 6.2b shows that these conditions may yield extreme – and so far unexplained – data scatter.
9. *Wave conditions on foreshores and forelands.* The present data provide specific results, but generic knowledge is preferred as there are often foreshores and forelands in front of dikes.

The perceived knowledge gaps for other water bodies are:

10. *Time-evolution of waves*. The present data mainly provide specific rather than generic knowledge about this topic. However, knowledge about the wave growth rate is highly useful for various wave- and weather-related warnings.
11. *Waves in narrow fetch geometries*. Relevant for estuaries, rivers and other water bodies of which the width is much smaller than the length. Wave models tend to have difficulties with this kind of geometry (Kahma and Petterson, 2004). Air photographs and advanced models (like SWAN) suggest that in such cases, waves are often channelled so much that wave directions are not primarily steered by the wind, but by the shoreline.
12. *Wave-current interaction*. Especially relevant for rivers and marine applications; probably also relevant to wind driven systems like Lake IJssel (Vledder, 2005).
13. *Wave run-up in mild conditions*. Waves and wave run-up are significant factors in dike design for especially the Dutch Waal river. The results of Chapter 8 suggest that mechanisms for wave run-up may act synergetically and that for small waves, actual run-up may be smaller than model predictions.

Finally, one knowledge gap should be mentioned that is not related to the above-mentioned physical processes but rather to the Hydraulic Boundary conditions: It would be desirable to investigate why one of the main run-up forcings near the Rotterdamse Hoek site has been close to the design value of that dike (the peak period T_p reached values of nearly 6 seconds during ordinary 8-9 Beaufort gales), whereas the actual wave run-up level remained over 2 metres below the actual dike crest (see section 3.3).

Measuring and research needs

1. When deciding on further research and measurements on wind, waves and storm surge, one ideally considers all related applications and research needs (see section 1.2), not only on a regional/national level, but also internationally. Some flood-protection related entries to the latter are www.crue-eranet.net and www.safecoast.org. Such an integral analysis is far beyond the scope of this study. Hence, the remaining measuring and research needs are given from the perspective of this study only. Still, it is important to note that many answers to policy and operational questions are (and often have to be) given by models rather than experimental data sets. Therefore, a key role should be assigned to the measurement needs as defined by (wind and wave) model developers.
2. The evaluation of reliable extremes of open water winds (for dike design) requires representative open water measurements because of the problems in spatial wind transformation mentioned in this report. A homogeneous time series is essential to obtain unbiased extremes (Wieringa, 1996). For many land stations, it turns out

that this aim can not be achieved. In addition, the sudden absence of major storms during a 17-year period (1990-present) suggests that at least 20-30 years of data is desirable. As this is difficult to achieve as well, one might consider using the time series of climate models as an alternative.

3. One representative location with suitable instrumentation would also serve to fill the other wind-related knowledge gaps, provided that the KNMI station network remains at least in its present state. In the case of time evolution of storms, one could also use different (distant) locations in the same climate zone to enhance the present data set. As for the knowledge gap on unsteady storm surges, one can deal with these by using data of the existing MSW network (Monitoring System Water).
4. The drag coefficient knowledge gap requires accurate wind profile or turbulence measurements; solving the wind scaling knowledge gap also requires simultaneous wave measurements at the same location. The depth-limited wave growth knowledge gap can be dealt with if a location of the above type is placed in a lake of about 1-1.5 m deep and at least 2 km large, provided the wind climate is comparable with that of Lake IJssel. Perhaps, one would need yet another location to investigate the extreme wave data scatter that tends to occur during storms in the first kilometre(s) offshore.
5. For all the above issues, it is essential that location and measuring period are chosen in such a way that a few events with at least 10 Beaufort winds are measured. This requirement does not apply for the remaining items given below.
6. Wave current interactions and foreshore effects are a knowledge gap of some importance for the Lake IJssel area and other areas. Lake IJssel is not necessarily the best area to study these effects; possibly, one can make use of the SBW project mentioned in section 1.5. Time evolution of waves is also an issue that could be investigated in the SBW project. For the topic of wave run-up in mild conditions, it is not even certain whether new measurements are needed; additional analyses of existing data may suffice in this case.
7. Finally, there remains the issue of waves in narrow fetch geometries. A complicating factor in this case is the wish to measure wave directions. On the other hand, it does not seem necessary to measure during storms, so that the duration of such an experiment can remain limited.

How and where to measure

1. Continuation of some of the Lake IJssel measurements would have a number advantages:
 - allowing for a homogeneous open-water wind time series of reasonable continuity and length, so that a fairly reliable direct estimation of wind extremes from these data will become possible in about five years;

-
- possibility of measuring a 10-12 Beaufort event (if the present storm-free anomaly stops), whilst assuring comparability with the present data set.;
 - continued availability of representative wind and wave data for various operational purposes (flood warnings, ship traffic,)
2. It is not recommended to retain the full present network because of the efforts involved in maintenance and – to a lesser extent – data analysis. Rather, it is recommended to look for ways of achieving coordination between the present measurements and those of related projects (e.g., SBW Wadden Sea), as well as permanent national water monitoring networks like the Rijkswaterstaat LMW-network, that will be operational in the course of 2007. Finally, it may be useful to spread risks by trying to measure the same feature at different locations, as is done in the Chinese Lake Tai Hu experiment that aims to supplement the Lake Sloten data.
 3. The above-mentioned reduction of the present measuring network should coincide with a qualitative upgrading and an increase in flexibility. For example, using sonic anemometers for high-frequency measurements of turbulent momentum and heat flux is expected to be a key factor in obtaining reliable drag coefficient measurements. Furthermore, the use of moveable platforms with flexible instrumentation is recommended to investigate specific features (narrow fetch problems, wave current interaction) for a limited amount of time. The latter is a general recommendation that does not only apply to the present project, which is limited to the Lake IJssel area.
 4. It is not easy to answer the question ‘how to measure’ in a few words, also because the answer strongly depends on the intended application. General guidelines for instrumentation are given in (Bottema, 2006d); see also Appendix A-C of this report. Now that log-a-levels seem to be too wind-sensitive, step gauges appear to be the best alternatives for the present capa probes. Like capa probes however, step gauges are sensitive to soiling by algae in summer.
 5. It is recommended to organise a way of exchanging experiences related to large wave measuring campaigns as the present one, the Scheldt measurements, the Wadden Sea measurements and the SBW project in general (section 1.5), and projects abroad like the Norderney measurements of the German Coastal Research station. Enhancing such exchanges should help to clarify the do’s and do not’s of such a project, the critical success factors, as well as the main threats to the success of such projects.

Application of the measurements and dissemination of the data

1. During this campaign, a very large amount of effort has gone into assuring the availability and quality of the data. Due to lack of time, the application and dissemination of data has perhaps received slightly less attention than it should have.

-
2. For future work, it is strongly recommended that there is intensive interaction with model developers and operational and policy-oriented stakeholders. This is expected to be a key factor in assuring the applicability of the data. Moreover, interaction with model developers is an important incentive to assure the availability and quality of the experimental data. Model developers are recommended to look further than the output of their Test Bed analysis tools, and to have a close look at issues like spectral model response (especially when considering seiches), the causes of any discrepancies between experimental and model results, and the validity of underlying model assumptions (like the validity of parametric wave growth curves).
 3. In projects of this type, there should be more emphasis on English publications, especially conference papers. These are an essential for establishing international networks, which are a key factor when it comes to assuring that the present data are used for model validation and model development.
 4. It is recommended to give some attention to standardisation of data presentation and data processing, as this may facilitate data exchange within the Netherlands as well as abroad. Moreover, standardisation may enhance the confidence in data and thereby its applicability.
 5. It is recommended to make the data of the present measuring campaign publicly available, preferably by means of Internet (using www.waterbase.nl and/or other means). It remains to be seen how the data should best be made available: the amount of processed data is order 3 GigaByte; the estimated amount of raw data order 120 GigaByte (or nearly twice this amount if both the raw data logger output and the 20-minute data blocks are considered). The latter is especially valuable for all test cases of Chapter 7, and any case with rapid changes in wind, wave and water level conditions.

References

- Bak, C.I., D.P. Vlag, 1999, Achtergronden Hydraulische Belastingen Dijken IJsselmeergebied, deelrapport 5, Modelling waterbeweging (WAQUA), RWS RIZA, Lelystad, NL, Report 99.042 (in Dutch)
- Beyer, D., E.R.F. van der Goes, 2000, Golfmetingen IJsselmeergebied – verslag meetseizoen 1997-1998, RWS RIZA, Lelystad, NL, werkdocument 2000.158X (in Dutch)
- Bidlot, J.R., M.W. Holt, 1999, Numerical wave modelling at operational weather centres, Coastal Engineering 37, p. 409-429
- Witteveen and Bos, 2006, Wave measurements lake IJsselmeer and Sloterneer – extra analyses 2006 ; part 1-3: Advice for field tests / Optimisation measuring location Lake Sloten / Fitting and analysis of wave spectra and wave distributions, Report RW1518-1-boej3/013, Witteveen & Bos, Rotterdam, NL
- Blaakman, E.J., R. Lisman, 1999, Achtergronden Hydraulische Belastingen Dijken IJsselmeergebied, deelrapport 1, Gebruikershandleiding HYDRA_M, RWS RIZA, Lelystad, NL, Report 99.038 (in Dutch)
- Booij, N., R.C. Ris, en L.H. Holthuijsen, 1999, A third-generation wave model for coastal regions, Part I, Model description and validation, *J. Geophys. Res.* 104, C4, 7649-7666
- Bottema, M., 1992, Wind Climate and Urban Geometry, Proefschrift, technische Universiteit Eindhoven, Fac. Bouwkunde, 212 p., <http://alexandria.tue.nl/extra3/proefschrift/PREF9A/9321101.pdf>
- Bottema, M., 1996, Turbulence closure model 'constants' and the problems of 'inactive' atmospheric turbulence, *J. Wind Engng. Ind. Aerodyn.*, 67/68, p. 897-908
- Bottema, M., 2002a, rapportage golfmetingen IJsselmeergebied 2000-2001, RWS RIZA, Lelystad, NL, werkdocument 2002.063X (in Dutch)
- Bottema, M., 2002b, rapportage golfmetingen IJsselmeergebied 2001-2002, RWS RIZA, Lelystad, NL, werkdocument 2002.191X (in Dutch)

-
- Bottema, M., 2003a, rapportage golfmetingen IJsselmeergebied 1998-1999, RWS RIZA, Lelystad, NL, werkdocument 2003.143X (in Dutch)
- Bottema, M., 2003b, rapportage golfmetingen IJsselmeergebied 2002-2003, RWS RIZA, Lelystad, NL, werkdocument 2003.144X (in Dutch)
- Bottema, M., 2004, Verrassend snelle golfgroei op het IJsselmeer, *Meteorologica*, maart 2004, p. 15-19 (in Dutch)
- Bottema, M., 2005, Golfmetingen IJsselmeergebied – vergelijking stappenbaak- en capstaafmetingen 1997-2005, RWS RIZA, Lelystad, NL, werkdocument 2003.144X (in Dutch)
- Bottema, M., 2006a, rapportage golfmetingen IJsselmeergebied 2004-2005, RWS RIZA, Lelystad, NL, werkdocument 2006.056X (in Dutch)
- Bottema, M., 2006b, rapportage golfmetingen IJsselmeergebied 2005-2006, RWS RIZA, Lelystad, NL, werkdocument 2006.058X (in Dutch)
- Bottema, M., 2006c, Gedrag van het SWAN-golfmodel met en zonder nieuwe diepwaterfysica, met nadruk op korte strijklengtes, RWS RIZA, Lelystad, NL, werkdocument 2006.057X (in Dutch)
- Bottema, M., 2006d, Leidraad monitoring – golfcondities zoete Rijkswateren, 19p. (in Dutch)
<http://www.rijkswaterstaat.nl/rws/riza/leidraad/home.html>.
- Bottema, M., W. Klaassen, W.P. Hopwood, 1998, Landscape roughness parameters for Sherwood Forest, experimental results (part 1) & validation of aggregation models (part 2), *Boundary-Layer Meteorology*, 89, 285-347
- Bottema, M., D. Beyer, 2002, Evaluation of the SWAN wave model for the Dutch IJsselmeer area, Proc. 4th Int. Conf. on Ocean Waves (WAVES2001), Ed. B.L. Edge, 2-6 sept. 2001, San Francisco, 560-569
- Bottema, M., J.P. de Waal, H.J. Regeling, 2003, Some applications of the Lake IJssel / Lake Sloten wave data set, Proc. 28th Int. Conf. Coastal Engineering, Ed. J. McKee Smith, 9-13 juli 2002, Cardiff, UK, 413-425
- Bottema, M., H.J. Regeling, 2005a, Wachten op een superstorm, *Land + Water*, Sept. 2005, p. 28-29 (in Dutch)

-
- Bottema, M., H.J. Regeling, 2005b, Meetcampagne IJsselmeer vergroot inzicht in golfploopproductie, *Land + Water*, Oct. 2005, p. 14-15 (in Dutch)
- Bottema, M., H.J. Regeling, 2005c, Tyfoons helpen bij voorspelling extreme golfslag op IJsselmeer, *Land + Water*, Nov. 2005, p. 24-25 (in Dutch)
- Bottema, M., G.Ph. van Vledder, 2005, Evaluation of the SWAN wave model in slanting fetch conditions, Proc. 5th Int Symp on Meas. and Analysis of ocean Waves, WAVES2005, Madrid, paper No 165
- Bottema, M., G.Ph. van Vledder, 2006, Effective fetch and non-linear four-wave interactions during wave growth in slanting fetch conditions, RWS RIZA, manuscript, submitted to *Coastal Engineering*; also available as RWS RIZA werkdocument 2005.142x (original 2005 version revised in 2006)
- Bouws, E., 1986, Provisional results of a wind wave experiment in a shallow lake (Lake Marken, The Netherlands), unpublished Document, KNMI De Bilt, NL, www.knmi.nl/~bouws/en/mark-memo.pdf
- CERC, 1973, Shore Protection Manual, U.S. Army Coastal Engineering Research Center, Fort Belvoir, Virginia, USA
- Charnock, H., 1955, Wind stress on a water surface, *Quart. J. Royal Meteor. Soc.* 81, 639-640
- Claessens, E.C., J.P. de Waal, H.C. van Twuiver, M. Bottema, 2002, The application of a coupled wind, water level and wave model in a warning system against flooding, Proc. 7th Int. Conf. on Wave Hindcasting and Forecasting, Banff, Canada, 21-25 Oct 2002, 410-421
- Doorn, N., W. Eysink, 2004, Golfmetingen met drukopnemers, Report H4318, WL I Delft Hydraulics (in Dutch)
- ECE, 1997, Recommendations on Technical Requirements for Inland Navigation Vessels, addendum 2, TRANS/sc.3/104/add. 2; www.unece.org/trans/doc/finaldocs/sc3/TRANS-SC3-104a2e.pdf
- Foristall, G.Z., S.F. Barstow, H.E. Krogstad, M. Prevosto, P.H. Taylor, P.S. Tromans, 2004, Wave crest sensor intercomparison study, an overview of WACSIS, *J. of Offshore Mech. and Arctic Engng.* 126, 26-34

-
- Groeneweg, J. , A.R. van Dongeren, 2002, Measuring Campaign Wadden Sea, Module What to measure, Report H4174, WLI Delft Hydraulics, Delft, NL
- Hoekstra, P. , T. Hoitink, 2002, Design measuring campaign wave conditions Wadden Sea, Module Where to measure, IMAU Report R 02-01, Univ. Utrecht, Inst. for Marine and Atm. Research & Dept. of Physical Geography, 34.p.
- Hoitink, A.J.F, B.G. Ruessink, P. Hoekstra, 2004, Intercomparison of wave parameters and spectra from ADCP and wave buoy measurements, IMAU Report 04-03, Univ. Utrecht
- Holthuijsen, L.H., 1980, Methoden voor golfvoorspelling deel 1 / deel 2, Technische Adviescommissie Waterkeringen, Delft, NL (in Dutch)
- Holthuijsen, L.H., N. Booij en T.H.C. Herbers, 1989, A prediction model for stationary, short-crested waves in shallow water with ambient currents, *Coastal Engineering* 13, p. 23-54
- Holtslag, A.A.M., 1987, Surface fluxes and boundary-layer scaling, PhD Thesis Wageningen Agricultural University, also available as Scientific Report 87-02, KNMI, De Bilt, NL
- Jacobs en Van Vledder, 2003, Rapportage golfmetingen IJsselmeergebied 1999-2000, Report A972, Alkyon, Emmeloord, NL (in Dutch; also available as werkdocument 2002.190X, RWS RIZA, Lelystad, NL)
- Janssen, T.T., 2006, Nonlinear surface waves over topography, PhD Thesis, Delft University of technology, Delft, NL, 223 p.
- Jensen, N.O., 1978, Change of roughness and the planetary boundary layer, *Quart. J. Royal Meteor. Soc.*, 104, 351-356
- Jensen, N.O., E.L. Petersen, I. Troen, 1984, Extrapolation of mean wind statistics with special regard to wind energy applications, WMO, Geneva, CH, WMO Technical Note 15, 85 p.
- Jong, M.P.C., M. Bottema, R.J. Labeur, J.A. Battjes, C. Stolker, 2006, Atmospherically generated large-scale water-level fluctuations in a closed basin, Proc. 29th Int. Conf. Coastal Engineering, Sept 2006, San Diego, CA, USA, paper 37
- Kahma, K.K., C.J. Calkoen, 1992, Reconciling discrepancies in the observed growth rate of waves, *J. Phys. Oceanogr.* 22, p. 1271-1285

-
- Kahma, K.K., C.J. Calkoen, 1994, Growth curve observations, chapter II-8 in(p. 174-182) in Komen et al., 1994, Dynamics and Modelling of Ocean Waves, Cambridge Univ. Press, 532 p.
- Kahma, K.K., H. Petterson, 1994, Wave growth in a narrow fetch geometry, *The Global Atmosphere and Ocean System 2*, p. 253-263
- Kaimal, J.C, J.J. Finnigan, 1994, Atmospheric Boundary-layer Flows, their measurement and structure, Oxford Univ. Press, New York, 288 p.
- Komen, G.J., L. Cavaleri, M. Donelan, K. Hasselmann, S. Hasselmann, P.A.E.M. Janssen, 1994, Dynamics and Modelling of Ocean Waves, Cambridge Univ. Press, 532 p.
- Kudryavtsev, V.N., V.K. Makin, A.M.G. Klein Tank, J.W. Verkaik, 2000, A model of wind transformation over water-land surfaces, Scientific Report WR-2000-01, KNMI, De Bilt, NL
- Kuiper. C., 2005, Golfhoogtemetingen in de deltagoot – vergelijking tussen 5 golfhoogtemeters, Report H4617, WL | Delft Hydraulics (in Dutch)
- Lammers, I.B.M., M. Kok, 2006, Belang van windmodellering voor Hydraulische Randvoorwaarden, Report PR1072.10, HKV Lijn in Water, Lelystad, NL (in Dutch)
- Makin, V.K. , 2003, A note on the parameterization of the sea drag, *Boundary-Layer Meteorology* 106-3, 593-600
- McIlveen, 1992, Fundamentals of weather and climate, Chapman and Hall, London, UK, 497 p.
- Oost, W.A., 1998, The KNMI HEXMAX stress data – a reanalysis, *Boundary-Layer Meteorology* 86, 447-468
- Oost, W.A., C.M.J. Jacobs, C. van Oort, 2000, Stability effects on heat and moisture fluxes at sea, *Boundary-Layer Meteorology* 95-2, 271-302
- Panofsky, H.A., J.A. Dutton, 1984, Atmospheric Turbulence. Models and Methods for Engineering Applications, John Wiley & Sons, New York, 389 pp
- Reitsma, T., 1997, Een beschrijving van de berichtendienst Waarschuwingsdienst Dijken IJsselmeer en Markermeer, RWS RIZA, Lelystad, NL, Report 97.059 (in Dutch)

-
- Rijkswaterstaat, 2002, Hydraulische Randvoorwaarden 2001 voor het toetsen van primaire waterkeringen, DG Rijkswaterstaat, RWS RIKZ & RWS DWW & RWS RIZA, NL (in Dutch)
- RIKZ, 2003, Weten wat te meten – Evaluatie Landelijke Fysische Monitoring, RWS RIKZ Report 2003.053 (in Dutch)
- RIVM, 2004, Risico's in bedijkte termen (eds. W.B.M. ten Brinke and B.A. Bannink), Report 500799002, RIVM, Bilthoven, NL (in Dutch); <http://www.rivm.nl/bibliotheek/rapporten/500799002.html>
- Ruijter, M.N., M.J.C. van den Boomgaard, 2005, Rapportage Golfmetingen IJsselmeergebied 2003-2004, Report MB/05370/1336, SVASEK, Rotterdam, NL (in Dutch; also available as werkdocument 2005.116x, RWS RIZA, Lelystad, NL)
- Ruijter, M.N., M. Bottema, M.J.C. van den Boomgaard, 2005, Desk study to optimise wave instrumentation in large and shallow waters, Proc. 5th Int Symp on Meas. and Analysis of ocean Waves, WAVES2005, Madrid, paper No 8
- RVTV, 2001, Onderzoek naar een tiental scheepvaartongevallen op het Marker- en IJsselmeer, Report (in Dutch), www.rvtv.nl or www.onderzoeksraad.nl
- Schaik, M.P.J. van, 2004, Vertaling windsnelheid naar open water voor bepaling overstromingsrisico's buitendijks, RWS RIZA werkdocument 2004.139x (in Dutch)
- Simiu, E., R.H. Scanlan, 1986, Wind effects on structures, John Wiley and Sons New York, 590 p.
- Stb, 1971, Organiek Besluit Rijkswaterstaat, 14/1/71, Staatsblad 1971-42 (in Dutch)
- Stelwagen, U., 2002, Measurement Campaign Wadden Sea Module 3 – How to Measure, TNO-TPD, Rapport I&I-RPT-02007
- Stull, R.B., 1988, An Introduction to Boundary Layer Meteorology, Kluwer, Ac. Publ., 666 p.
- Taminiau, C.J., 2004, Wind(extremen) in het IJsselmeergebied – analyse van de Houtrib-meetreeks, RWS RIZA, Lelystad, NL, werkdocument 2004.138X (in Dutch)
- TAW, 2002, Technisch Rapport Golfoploop en Golfoverslag bij Dijken, Report, Technische Adviescommissie Waterkeringen and Rijkswaterstaat, RWS DWW, Delft, NL (in Dutch), www.tawinfo.nl/publicaties/download/TR%20Golfoploop%20Golfoverslag.pdf

-
- Tennekes, H., 1973, The logarithmic wind profile, *J. Atm. Sci.* 30, 234-238
- Tennekes, H. and J.L. Lumley, 1972, *A First course in turbulence*, MIT Press New York, 300 p.
- Troen, I., E.L. Petersen, 1989, *European Wind Atlas*, Risoe National Institute, DK, 656 p.
- Twuijver, H.C. van, C.P.M. Geerse, 1999, *Achtergronden Hydraulische Belastingen Dijken IJsselmeergebied, deelrapport 3, Windstatistiek*, RWS RIZA, Lelystad, NL, Report 99.040 (in Dutch)
- Verkaik, J.W., 2000, Evaluation of two gustiness models for exposure correction calculations, *Journal of applied meteorology*, 39-9., p. 1613-1626
- Verkaik, J.W., A. Smits and J. Ettema, 2003, *Wind statistics of the Netherlands including the coastal zone*, Report, KNMI, De Bilt, NL, see also the underlying phase reports at www.knmi.nl/samenw/hydra/documents/phasereports and www.knmi.nl/samenw/hydra/cgi-bin/phase14.cgi
- Vledder, G.Ph. van, 2005, *SWAN acceptance tests for RWS RIZA in 2005, wave-current interactions*, ALKYON Hydraulic Consultancy and research, Emmeloord, NL rapport A1477
- Waal, J.P. de, D. Beyer, J.H. Andorka Gal, L.H. Holthuisen, G.Ph. van Vledder, J.P.F.M. Janssen, D.P. Hurdle, 1997, *Instellingen golfmodel HISWA toe te passen bij productiesommen in het IJsselmeergebied*, RWS RIZA werkdokument 97.183X (in Dutch)
- Waal, J.P. de, 2002, *Wave growth limit in shallow water*, Proc. 4th Int. Conf. on Ocean Waves (WAVES2001), Ed. B.L. Edge, 2-6 sept. 2001, San Francisco, 580-589
- Waal, J.P. de, 2003, *Windmodellering voor bepaling waterstanden en golven*, RWS RIZA-werkdocument 2003.118X (in Dutch)
- Wenneker, I., 2007, *Validation instrument for SWAN, selection and assessment of data sets for validation of SWAN for the Wadden Sea*, Report H4803.80, WL I Delft Hydraulics, Delft, NL.
- Van der Westhuysen, A.J., M. Zijlema and J.A. Battjes, 2007, *Nonlinear saturation-based whitcapping dissipation in SWAN for deep and shallow water*, *Coastal Engineering*, 54, 151-170.

-
- Westphal, R., J. Hartman, 1999, Achtergronden Hydraulische Belastingen Dijken IJsselmeergebied, deelrapport 1, Een ontwerpmethodiek, RWS RIZA, Lelystad, NL, Report 99.037 (in Dutch)
- WFD, 2000, European Water Framework Directive, Water Framework Directive 2000/60/EC, Official Journal L 327 , 22/12/2000 p. 0001 - 0073.
- Wieringa, J., 1973, Gust factors over open water and built-up country, *Boundary-Layer Meteorology*, 3-4, p. 424-441
- Wieringa, J., 1986, Roughness-dependent geographical interpolation of surface wind speed averages, *Quart. J. Royal Meteor. Soc.* 112, 867-889
- Wieringa, J., 1993, Representative roughness parameters for homogeneous terrain, *Boundary-Layer Meteorology*, 63-4, p. 323-363
- Wieringa, J., 1996, Representativity of extreme wind data, Chapter 2 in 'Hydrology of Disasters' (ed. V.P. Singh), Kluwer, p. 19-40
- Wieringa, J. en P.J. Rijkoort, 1983, Windklimaat van Nederland, Staatsuitgeverij Den Haag, Den Haag, NL, 264 p. (in Dutch)
- WMO, 1998, Guide to wave analysis and forecasting, WMO, Geneve, WMO-no. 702
- Wouters, J., 2003, Verificatie oplooppformulering met veldmetingen bij de Rotterdamse Hoek, Infram, Marknesse, NL, Report I612 (in Dutch)
- WOW, 1996, Wet op de Waterkering, 21/12/1995, Staatsblad 1996-8, 1-12 (in Dutch)
- Wu, J., 1982, Wind stress coefficients for sea breeze to hurricane, *J. Geophys. Res.*, 87-C12, p. 9704-9706
- Xi, 2004, Manual for WAVES2004 wave processing software, www.xi-advies.nl, Xi advies, Delft, NL (in Dutch)
- Young, I.R., 1998, An experimental investigation of the role of atmospheric stability in wind wave growth, *Coastal Engineering* 34, p. 23-33

Young, I.R. and L.A. Verhagen, 1996, The growth of fetch limited waves in water of finite depth, part I Total energy and peak frequency, part II Spectral evolution, part III (with S.K. Khatri as 3rd author) Directional spectra, *Coastal Engineering* 28, p. 47-78, 79-100 and 101-122

Young, I.R. and A.V. Babanin, 2006, The growth of fetch limited The form of the asymptotic depth-limited wind wave frequency spectrum, *J. Geophys. Res.*, 111, C06031

Zijlema, M. and A.J. van der Westhuysen, 2005, On convergence behaviour and numerical accuracy in stationary SWAN simulations of nearshore wind wave spectra, *Coastal Engineering*, 52, 237-256.

Appendix A Alternatives for present instrumentation

In (Bottema, 2006d), an extensive inventory of potentially suitable instrumentation for wave measurements on lakes and rivers was presented. A condensed translation follows below.

Measuring methods – general points

For wave measurements on lakes and rivers, various methods can be considered, like (e.g. WMO, 1998; RIKZ, 2003) :

- remote sensing from the shore or from the air
- using floating instruments
- using fixed instruments, either:
 - under water: pressure or velocity sensor, Acoustic Doppler profiler (ADCP)
 - partly in the water: step gauge, inductive gauge, capacitance probe.
 - above the water: using reflections from either acoustic radar or laser beams

The choice for a measuring technique (and between measuring or modelling) strongly depends on the intended application, where one might consider the following:

- If wave fields are preferred over point measurements, remote sensing or even wave modelling might be an option.
- One should verify whether wave direction measurements are needed.
- One should verify whether continuity has priority (e.g. for warning systems) or accuracy (for model validation and development, like in the present case).
- The optimal choice between instruments strongly depends on the expected wave conditions, and thereby on the expected wind, wave and water depth.
- For the present campaign, one needs an instrument with the range and robustness of an instrument for shelf seas, but a response speed and resolution typical of laboratory instruments; a combination that is difficult to reconcile.

A *very rough* indication of the relative wave height inaccuracy of various instruments, based on various intercomparisons, is:

- fixed and floating instruments: about 10%
- remote sensing: about 20%

These numbers are only applied if the instruments are applied within their range of applicability; in breaking waves the inaccuracies are expected to be larger.

Remote sensing from the shore or from the air - general

Potentially, this is a valuable set of techniques because it allows for

the measurement of wave *fields*. Another advantage is the possibility to directly measure the wavelengths, instead of using various assumptions to evaluate them from measured wave periods. Also, remote sensing often gives information about wave directions and the directional spreading in a wave field; the latter is often difficult to measure with in-situ techniques. There are two main classes of remote sensing: from the shore and from satellites or air planes.

Little is yet known about the accuracy and suitability of remote sensing for wave measurements on inland waters, but the following can be said:

- Often, complex algorithms are needed to convert remotely sensed images to wave information.
- Often, remote sensing yields only wave length and wave period information, while wave heights are indirectly derived (often using site-specific calibrations using in-situ instruments).
- Continuity may be a problem as airplane measurements are often restricted to fair weather, while nearby satellites are often non-stationary. For the ocean, SAR (Synthetic Aperture Radar) is often used, but its pixel size (~20 m) is too large with respect to the wave lengths to be measured, even during storm conditions on Lake IJssel.
- Both shore- and ship navigation radar seem to be suitable to measure waves with lengths from 10-20 m and periods from 3 seconds on. On Lake IJssel, such conditions can be expected for at least 7 Beaufort winds, and fetches greater than 3 km. The radars are expensive and use lots of energy, but they give a wealth of data and seem to be relatively robust.

Using floating instruments - buoys

On the sea, buoys have set the standard, they are quite accurate, do not depend on platforms, and can measure continuously for a long time. The following measuring principles are used:

- Common buoy: measure vertical acceleration, integrate this twice to water level time series, process this to wave parameters and send data to shore.
- Directional buoy: measures also the horizontal accelerations, from which directional properties of the wave field can be evaluated.
- GPS buoy: Uses Global Positioning System to evaluate 3-dimensional time series of buoy position

The latter buoy is especially useful if long waves and/or still water levels are to be measured. In a more general sense, the advantages of buoys are:

- relatively free choice of measuring location
- little maintenance needed
- much experience has been gained with buoys
- measuring directional wave properties (with advanced buoys)

Rijkswaterstaat RIKZ has two types of buoys on stock, with diameters of 70 and 90 cm and suitable for wave frequencies (from 0.03 Hz) up to 0.5 – 0.9 Hz. For the present campaign however, the following must be considered:

-
- Expert advice on the mooring is generally needed, but especially in the presence of currents or near shallow foreshores.
 - Buoys tend to avoid (float around rather than over) short wave crests, and thereby tend to underestimate wave asymmetry.
 - The main reason why buoys were not selected at the start of this measuring campaign: the high-frequency response is not ideal. A standard 0.8 m diameter wave rider has only a correct response from 0.07-0.5 Hz, then overshoots due to resonance, following by a strongly decreasing response above 1 Hz. In addition, one can argue that wave lengths must be at least 5-10 times the buoy diameter to accurately measure the wave crests and troughs. All in all, in our case, significant response corrections can only be avoided if the wind is at least 6 Beaufort and if the fetch is over about 3 km. Recently, miniature buoys were proposed as an alternative, but they need more maintenance (or replacement) since they have less room for batteries.

Fixed instruments near the still water level

The advantage of this approach is the fact that besides short wind waves, long waves, still water levels, currents and wind can all be easily measured. The disadvantages are:

- the need to mount a platform (and to remove it during ice periods!)
- relatively large risk on damage by ice and driftwood
- risk of soiling by algae

Step gauges and capacitance probes are quite commonly used in the Netherlands. A description is given in section 2.2; here only some advantages and limitations are mentioned. Inductive probes (as used for Lake George, Young and Verhagen, 1996) seem to be a suitable alternative, but no manufacturer appears to be available at present.

Step gauges used to be the main alternative for shallow water and short fetch locations where buoys did not seem to be the optimal instrument. In the Netherlands, they have been both used near the coast (Petten) and in Lake IJssel.

Advantages are :

- High sample frequency (may be increased up to 10 Hz) and quick instrument response
- No drift, so no recalibrations needed

Disadvantages are:

- Soiling by algae (in the summer half year)
- For wave heights < 10-15 cm: over 5-10% error due to the 5 cm distance between the individual step gauge sensors.
- Sometimes prone to disturbances, especially older types like the Marine-300 (Foristall et al., 2004; Bottema, 2005).
- The probe length (3 m) is somewhat too short to reliably measure during all Lake IJssel conditions, without having to adjust the measuring height from time to time.

Capacitance probes have been frequently used on Lake IJssel since at least 1995. The advantages are:

- the price (about 1000-2000 Euro)
- quick response (as for step gauge)
- potentially suitable to measure waves smaller than 10 cm (unlike step gauge)

However, capacitance probes have some additional disadvantages in comparison with step gauges:

- Supports between the teflon coated wire and the mass tube can disturb the signal to such an extent that wave height errors may increase to 20-50%, especially with supports near the still water line and waves smaller than 20-50 cm. Hence, it is crucial to remove such critical supports.
- Drift may cause errors in the wave height (up to 5%) and water levels (up to 10 cm), and even more if the teflon coating is damaged. Frequent recalibrations and field checks are therefore needed.
- Capacitance probes appear to be more vulnerable than step gauges in cases with floating ice (Lake IJssel/Sloten) and/or driftwood (North Sea Coast, Petten).

Downward-looking instruments above the water

This type of instruments sends a signal beam to the wavy water surface, and measures the time between emitting the signal and receiving the reflection. In practice, the signal is often deflected by the wavy water surface and – for acoustic instruments – by the wind. This may cause signal loss with too narrow a signal beam, and measuring errors (due to false reflections) with too broad a beam. The energy consumption for instruments of this type is 1-5 Watt, which can be supported by the present energy supply, unless one wants an array of the instruments for directional wave measurements.

The main advantage of downward-looking instruments with respect to step gauges is the fact that the former type is generally rather insensitive to soiling and ice. The disadvantages depend to some extent on the type of instrument.

In the Dutch coastal waters, radar sensors are now considered as a suitable alternative for the step gauge: the sampling rate (up to 5.12 Hz) has increased sufficiently, while the energy consumption is now below 5 W. The experience of Rijkswaterstaat RIKZ suggests that radar sensors are suitable for wave frequencies up to 0.5 Hz; for higher frequencies the instrument has not yet been tested sufficiently. Yet, one must be aware of potential measuring errors :

- Isolated outliers (Foristall et al., 2004; RIKZ, 2004; Kuiper, 2005).
- Wave height and wave period biases due to high noise levels, especially for waves smaller than 50 cm (Kuiper, 2005)
- Errors for asymmetric and/or breaking waves (Kuiper, 2005; RIKZ, 2004)

-
- Either exaggeration or missing of wave tops (Foristall et al. 2004; Kuiper, 2005)

Recent developments and experience of Rijkswaterstaat RIKZ suggests that many of those errors might be something of the past. Yet one still must be aware that the finite radar beam width (order 5°) leads to a non-negligible footprint area over which the wave signal is spatially averaged; especially wave components which are not an order of magnitude larger than the footprint size (for 3 m mounting height and 5° beam width typically 30 cm) may be underestimated in this way.

Acoustic instruments appear to be a good alternative for radar and they are quite cheap (roughly 5000 Euro). The acoustic Log_a level scored quite well in a recent desk study (Ruijter et al., 2005) and wave flume test. Therefore, Rijkswaterstaat IJsselmeergebied bought some instruments and started a field intercomparison study from September 2006 on. The first results of this field pilot were contrary to prior expectations unfavourable, with strong signal distortions and wave height underestimations for waves greater than about 0.5 m. At present, the manufacturer is optimising his instrument (and especially its software) to avoid this type of errors. After this optimisation, the following remains to be tested before one can accept the instrument:

- the footprint effects as discussed in the previous paragraph
- the effect of wind on signal deflection, possibly resulting in partial or full signal loss during storms
- the effect of rain and spray (performance in breaking waves) on the performance of the instrument.

In the above, the effect of temperature and moisture on the sound speed (and measured wave signal) is not mentioned because the instrument compensates for this by an autocalibration facility. Still, the acoustic measuring principle appears to be far more sensitive to the ambient (weather) conditions than the radar.

The latter also applies to laser, where the beam may be intercepted or deflected by fog, rain spray and also by steep wave flanks. Moreover, reflection of sound and radar beams from a water surface is better than reflection of (laser) light beams. Still, the few available experiences (Foristall et al., 2004) are quite positive. Also, one of the laser disadvantages can also turn into an advantage: its narrow beam – though easily intercepted – yields a small footprint which increases the effective high-frequency response of this measuring principle.

Upward-looking instruments in the water

Like buoys, upward looking instruments in the water have the advantage that no fixed platform is needed. Commonly used measuring principles are pressure- or current based or acoustic, the Acoustic Doppler Current Profiler (ADCP) combines all three of them.

Pressure sensors are cheap (a few thousand Euros) and are quite commonly used. Using a number of assumptions, the measured

pressure spectrum is converted to a wave spectrum. Disadvantages are:

- Only spectral information and no information about individual wave unless all wave phase information is stored and processed.
- The required assumptions to convert pressure to wave spectra may be inaccurate for non-linear (steep or nearly breaking) waves, and in situations with strong density stratification (estuaria!).
- Currents in excess of order 0.3 m/s may significantly influence both the pressure signal itself and its amplitude-depth relation.
- The sensor may be sensitive to drift (note that errors in still-water-level significantly bias the amplitude-depth-relation).
- Short waves tend to be restricted to a thin surface layer. Doorn and Eysink (2004) recommend not to place the sensor below a depth where the signal damping is a factor 10. For wave components with periods of 0.5-1.5 s, this corresponds to a depth of about 0.15-0.3 m. In practice, with varying water levels and wave heights, one often needs a whole set of pressure sensors to meet this requirement while avoiding sensors to fall dry in the wave troughs.

For current meters, many of the limitations are similar to those of the pressure sensors. An obvious advantage over pressure sensors is the fact that current effects can now be reasonably corrected for, since the currents (in wind driven systems often an unknown factor!) are measured at at least one level. A disadvantage is the fact that the still water level is not measured, while this is an important variable to calculate the damping of the wave current amplitude with depth.

ADCP's typically use three measuring principles:

- a pressure sensor (as discussed above)
- acoustic current measurements at various levels
- acoustic surface tracking (similar to upward sounding)

An important asset of ADCP is the fact that it allows to measure directional wave information. However, there are also potential limitations:

- Measurements are frequently interrupted for some minutes because of storage and transfer of the great amount of data.
- For short waves (as often occurs on inland waters), Acoustic Surface Tracking (AST) seems the most suitable option because of the small footprint.
- Two independent investigations on two different ADCP-types (Hoitink et al., 2004; Kuiper, 2005) yielded quite a lot of noise and outliers in the measured signal.
- A recent North Sea field pilot (Hoitink et al., 2004) shows there are problems in measuring short waves (above 0.4 Hz, rather the rule than the exception in inland waters) and wave directions.
- Moreover, the results of this field pilot show that different instrument settings were needed to accurately measure either short waves or wave directions; hence it seems not yet feasible to measure the direction of short waves.

Appendix B Wave measuring errors

In (Bottema, 2005), an extensive analysis was made of experimental step gauge (including run-up) and capa probe errors. A condensed summary follows below. This summary is supplemented with a short description of some log-a-level errors.

First some errors of all instruments will be discussed, next some errors that are typical for each type of instrument (step gauge, capa probe and log-a-level). In section B.6, some possibilities for indicative quality labelling will also be briefly discussed.

B.1 All instruments: effect of spectral integration range

For validation of spectral wave models, one often uses spectral wave height and wave period measures like H_{m0} , T_{m-10} , T_{m01} en T_{m02} . Often the underlying spectral moments are evaluated from a semi-infinite spectral integration range $[0, \infty]$ in the model, and a *finite* range $[f_{min}, f_{max}]$ in the measurements. The latter is related to the finite sample length and sample frequency. Inadequate and/or undocumented choices for $[f_{min}, f_{max}]$ can lead to strongly biased results. Some error estimates will be given below.

Some first error estimates are made with a simplified spectrum $S(f)$: $S(f)$ is f^{-N} for frequencies f above the peak frequency $f_p (=1/T_p)$, and $S(f)$ is zero for $f < f_p$. The high frequency slope (power) N is typically between 4 and 4.3 (see figures in Chapter 7). Table B.1 shows, for a given error level in a given parameter, the minimum relative length of the spectral integration range.

Table B.1 Estimate of required maximum integration frequency f_{max} (relative to peak frequency f_p), for a given wave parameter and a given error level

relative error	Rel. minimum length of spectral integration range: f_{max}/f_p							
	for f^{-4} - spectrum				for $f^{-4.3}$ - spectrum			
	H_{m0}	T_{m-10}	T_{m01}	T_{m02}	H_{m0}	T_{m-10}	T_{m01}	T_{m02}
<2%	3	3	>5	>5	2.8	2.8	5	>5
<5%	2.2	2.2	1.8	>5	2.2	2.2	3.1	>5
<10%	1.7	1.7	2.7	>5	1.6	1.6	2.3	3.7
<20%	1.4	1.2	1.8	3	1.3	1.1	1.6	2.2

It can be noticed that:

- the error levels strongly depend on the chosen f_{max} -value
- T_{m01} and T_{m02} are sensitive to the chosen f_{max} -value.

The minimum T_p -values to guarantee a given accuracy in H_{m0} and various spectral wave period parameters is given in Table B.2. These minimum T_p -values are evaluated from experimental data of the winter

2001-2002 (see Bottema, 2002b) because the estimates of Table B.1 are too sensitive to the actual spectral slope. It is assumed that the upper limit of the spectral integration range is 1.0 Hz. Table B.2 also gives an indication of the minimum required H_{m0} to reach given accuracy levels, assuming conditions with pure wind sea in deep water.

Table B.2 Estimate of minimum H_{m0} and T_p to guarantee a given accuracy in H_{m0} and the spectral wave periods, for $f_{max} = 1.0$ Hz and pure wind sea.

for errors :	required H_{m0} (m)				required T_p (s)			
	H_{m0}	T_{m-10}	T_{m01}	T_{m02}	H_{m0}	T_{m-10}	T_{m01}	T_{m02}
<2%	0.55	0.6	>0.7	>0.7	2.5	2.7	>3	>3
<5%	0.35	0.4	0.7	>0.7	2.0	2.1	3.0	>3
<10%	0.22	0.25	0.4	0.7	1.5	1.6	2.1	3.0
<20%	0.15	0.15	0.17	0.25	1.15	1.2	1.3	1.6

For T_{m02} , less than 10% bias can only be attained for H_{m0} -values above 0.7 m. For FL25 and especially SL29, this is just not feasible. Therefore, f_{max} has always been 1.5 Hz for FL25 and SL29. The required H_{m0} and T_p then are roughly a factor 2.0 and 1.5 lower. Even then, at least 7 Beaufort wind is needed to keep the T_{m02} error near or below 10%. The biases for H_{m0} and T_{m-10} are much smaller and can be kept below 5% if H_{m0} is over 0.2 to 0.4 m (for f_{max} is 1.5 and 1.0 Hz respectively). The former occurs for onshore winds from 4-6 Beaufort on, the latter also for offshore (short-fetch) winds from 6 Beaufort on.

All in all, a f_{max} of 1.0 to 1.5 Hz is quite suitable for the present applications, as long as no accurate T_{m02} -values are required. If the latter is the case, one probably needs a larger sampling frequency. This is because a f_{max} greater than 0.4 times the sampling frequency is undesirable because of spectral aliasing effects.

The lower limit of the spectral integration range, f_{min} , is fixed at 0.03 Hz. No wind wave energy is expected here, but low frequency energy may sometimes be present. If a 100-second average water level differs more than 3 cm from the 20-minute average, a moving (or rather step-wise) 100-second average is subtracted from the raw signal, rather than the 20-minute average. This removes nearly all low-frequency biases in the spectral wave parameters; only T_{m-10} can still become up to 10% too large if much low-frequency energy is present.

B.2 All instruments: outliers and stagers

Especially in early years, step gauge registrations sometimes suffered from outliers. Capa probe outliers are rare, and often related to data logger or file manipulation errors. On the other hand, outliers seem to be relatively common for many alternative instruments (Kuiper, 2005), like the log-a-level that is presently tested (and already used in China).

Outliers can be identified by :

- out-of-range values of the instrument
- using the g (gravitational) criterion
- using the so-called σ -criterion

At present, 20-minute blocks with out-of-range data are generally rejected. For step gauges, the definition of out-of-range values is straightforward because the data can only equal one of the sensor numbers. For capa probes, only negative values are generally checked for as the upper limit of the measurement range is generally not exactly known due to drift, non-linearities in the calibration and - sometimes – errors in the calibration function.

For the log-a-levels, outliers are far more common. If less than 2% of the data is outlier, outliers are replaced by the previous sample.

Typically, data are labelled as outlier if:

- raw signal is above -0.1 m (less than 10 cm below sensor)
- raw signal is below -4.4 m (over 4.4 m below sensor)
- raw signal is more than 1.3 m below still water level
- raw signal is more than 2.2 m above still water level

For SL29, these figures are -0.8 , -3.0 , 0.7 and 1.4 m respectively.

Jacobs and Van Vledder (2003) proposed using the g -criterion, i.e. rejecting data where the vertical water surface acceleration is greater than the gravity acceleration g . It turned out that most cases that violate the above g -criterion would already have been an out-of-range value. In fact, the g -criterion only has substantial added value with measurement ranges greater than 3-5 m and/or sampling frequencies above 4-8 Hz.

Jacobs and Van Vledder (2003) also recommended using the σ -criterion, rejecting samples that are more than N standard deviations ($N\sigma$) from the mean. However, as wave signals are typically slightly non-Gaussian. Even signals without apparent errors have a significant fraction of samples that violate 4σ -criterion (Bottema, 2003a). For winds above 5 Beaufort, this is the case for 5-10% of the data, for weaker winds even for 10-30% of the data. With the more lenient 5σ -criterion, the above numbers typically reduce with a factor 2. In all cases however, applying the above criteria may significantly bias the remaining data set, especially when one is interested in non-linear wave properties to describe depth-limited wave conditions. This non-linear information can be quite important to estimate extreme wave (run-up) heights and the validity range of various models and model approaches. A better way of finding outliers, without rejecting many correct but non-linear data, may be to apply a 5σ -criterion to both the raw signal and its first derivative, but this approach has not yet been fully tested.

Unremoved outliers *within* the measurement range mainly need consideration if there are many of them, or of the wave heights are

low. For example, a single outlier of less than 1.5 metre may bias H_{m0} by about 4-10% if H_{m0} is 0.3 and 0.2 m respectively. For H_{m0} above 0.5 m, even five of such outliers (on 5/2/1999; see Bottema, 2003a) have no noticeable effect on most wave parameters.

Staggers are cases where subsequent sample values are identical. Staggers have not been much of a concern until the second half of 2006, when it was noticed that the use of CR1000 data loggers and/or log-a-levels seemed to cause too high a number of staggers in the wave and wind registrations. Numerical experiments on undisturbed data with a near-Gaussian distribution (FL26 capa probe data of 3/4/2006) suggested that the fraction of staggers $\text{frac}_{\text{STAG}}$ in a sample is related to the standard deviation SD and the resolution RES of the raw signal, and that the following empirical relation can be used to predict $\text{frac}_{\text{STAG}}$:

$$(B.1) \quad \text{frac}_{\text{STAG}} \sim 0.8 * \text{RES} / \text{SD}$$

It should be noted that this relation is highly approximate. Typical resolutions (RES) for the waves and wind direction are 1 mm and 1.4° respectively. For the wind speeds, the resolution is often about 0.06 m/s, but it is 0.2-0.25 m/s in periods where DA-converters are placed between the anemometers and data loggers (from mid-2006 on; for FL2 also from early 2000 to 23/4/2002, for FL26 also from 1999 to Dec. 2001). From mid 2006 to early 2007 on (when log-a-levels and CR1000 data loggers are used), the fraction of staggers seems to be roughly a factor two too high in the log-a-level and wind data, at least when compared to Eq. (B.1). The former typically have order 1% of staggers, the latter order 10%. From February 2007 on, there seems to be some decrease in the fraction of staggers. On the other hand, the fraction of wind staggers in the FL37 data of June-Oct. 2006 is about 60%, which is exceptionally large.

In all cases, the resulting errors are hard to estimate because it is not clear *which* samples tend to become (one of the extra) staggers.

B.3 All instruments: overtopping

During stormy conditions, wave overtopping over the instruments may occur, especially if lake levels are much higher than usual (like in autumn 1998, early 2002 and January 2007).

The resulting errors can be parameterised fairly well as function of the overtopping parameter Y_{top} / H_{m0} , where Y_{top} is the vertical distance between the still water level and the top of the wave instrument. Note that if $Y_{\text{top}} = 0$, the still water level reaches right up to the instrument top. Table B.3 gives a summary of the errors as a function of Y_{top}/H_{m0} . The actual errors will probably be smaller in strongly asymmetric waves (skewness larger than 0.4) and larger in highly linear waves (near-zero skewness).

Wave heights tend to be more sensitive to overtopping than wave periods. For the former, the largest errors occur (not surprisingly) in H_{\max} and ratios containing H_{\max} . For the latter, wave period errors are mainly restricted to T_{m-10} .

As for H_{m0} , a fair amount of overtopping can occur before H_{m0} -errors exceed 5%. Y_{top}/H_{m0} then has to be 0.7, the lowest value measured so far (FL9, during two storms in February-March 2002). However, such situations are still better avoided as overtopping is likely to have caused damage both in 2002 (failure of FL9 capa probe some time later) and on 18/1/2007 (mounting of log-a-level FL2 loose).

Table B.3 Wave overtopping over the instrument, typical errors as a function of Y_{top}/H_{m0} .

Y_{top} / H_{m0}	Description of errors
< 0.25	<ul style="list-style-type: none"> • all wave height at least 20-30% too low • T_{m-10} 5-30% too high, oother period up to +3% • skewness suspect (< 0)
0.25 – 0.5	<ul style="list-style-type: none"> • still water level too low (abs. bias up to $0.1 * H_{m0}$) • error H_{m0}, $H_{1/3}$ en T_{m-10} up to -20%, -30% en +5% ; • H_{\max}/H_{m0} and $H_{1/3}/H_{m0}$ strongly biased ; • skewness about 0.3 too low, kurtosis about 1.0 too low
0.5 – 0.7	H_{m0} , $H_{1/3}$, $H_{1/10}$, H_{\max} up to +5%, +9%, +16%, +27% too low; H_{\max}/H_{m0} 15-22% too low; $H_{1/3}/H_{m0}$ up to 10% too low
0.7 – 0.9	H_{m0} , $H_{1/3}$, $H_{1/10}$, H_{\max} up to +1%, +2%, +5%, +16% too low; ratio H_{\max}/H_{m0} up to 15% too low
0.9 – 1.1	H_{\max} , $H_{1/10}$ up to 7% and 1% too low respectively; slight flattening of top wave height distribution
> 1.1	none

Finally, it is important that efforts to avoid wave overtopping do not lead to instruments that are mounted so high that the instrument get fully out of the water. Many capa probe calibrations are strongly non-linear in the lowest decimetres, so that (nearly) dry instruments are likely to suffer from biases up to – in the worst case – a few decimetres.

B.4 Step gauge: effect of finite resolution

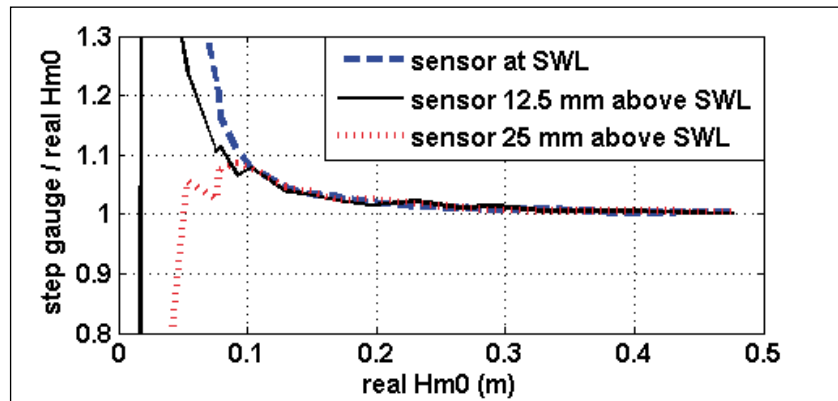
If the wave height is less than 2-3 times the present step gauge sensor spacing Δy (which is 5 cm), significant errors may occur.

For H_{m0} , the errors increase from 2% to 10% at $H_{m0} = 0.2$ and 0.1 m respectively. For smaller H_{m0} , the actual error strongly depends on the sensor position with respect to the still water level (Figure B.1). If the ratio $H_{m0}/\Delta y$ is less than 1.0-1.4, both H_{m0} -overestimations and underestimations in excess of 30% are possible.

For H_{m0} above 0.1 m, the T_{m-10} -errors are typically twice as large as those shown in Figure B.1. For H_{m0} below 0.1 m, the T_{m-10} error trends are less ambiguous than those of H_{m0} , typically, T_{m-10} is overestimated by at least 20-30%. The error trends in T_{m01} and T_{m02} are similar to

those in T_{m-10} but roughly a factor 4 and 6 smaller; the T_p -errors are small anyway. The errors in the time domain wave parameters need further investigation but the first impression is that their trends are more ambiguous than for the spectral wave parameters.

.....
Figure B.1 Ratio of step gauge and real H_{m0} , as a function of H_{m0} and a number of sensor positions (sensor spacing 5 cm).



All in all, one should preferably not use a step gauge when H_{m0} is less than twice the sensor distance. In the present case, one should therefore restrict to cases with H_{m0} above 0.1 m; which implies that step gauge data tend to be unreliable if – for fetches of order 1 km and less – there is less than 5-6 Beaufort wind. Hence, step gauges are not suitable to investigate wave in mild to moderate conditions if the fetch is order 1 km or less. Finally, it is noted that the above described errors do not show up in the instrument intercomparison of (Kuiper, 2005) as he restricted his investigation to cases with H_{m0} greater than 0.22 m.

B.5 Step gauge and capa probe: algae

Soiling by algae is perhaps the most serious source of experimental errors for step gauge and capa probe wave measurements during the summer months. In addition, soiling effects are often difficult to detect because there is only a poor correlation between the actual measuring errors, and both visual assessments of soiling and field verifications of the calibration of the capa probe. The latter is done by moving the probe over a fixed vertical distance while verifying that the measured water level by the same amount.

All in all, the only option left is to inspect the measured data for soiling effects.

.....
Figure B.2 Example registration with soiling effects: SL29, 21/7/2005, 12h.

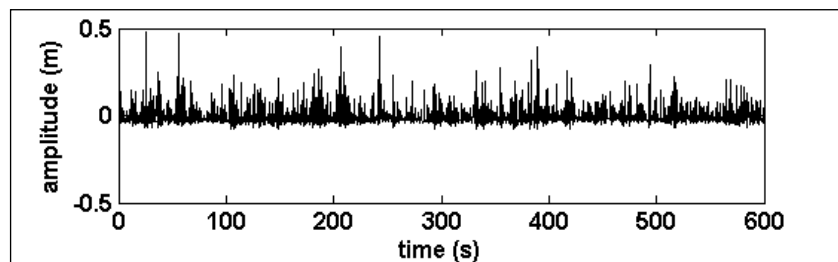
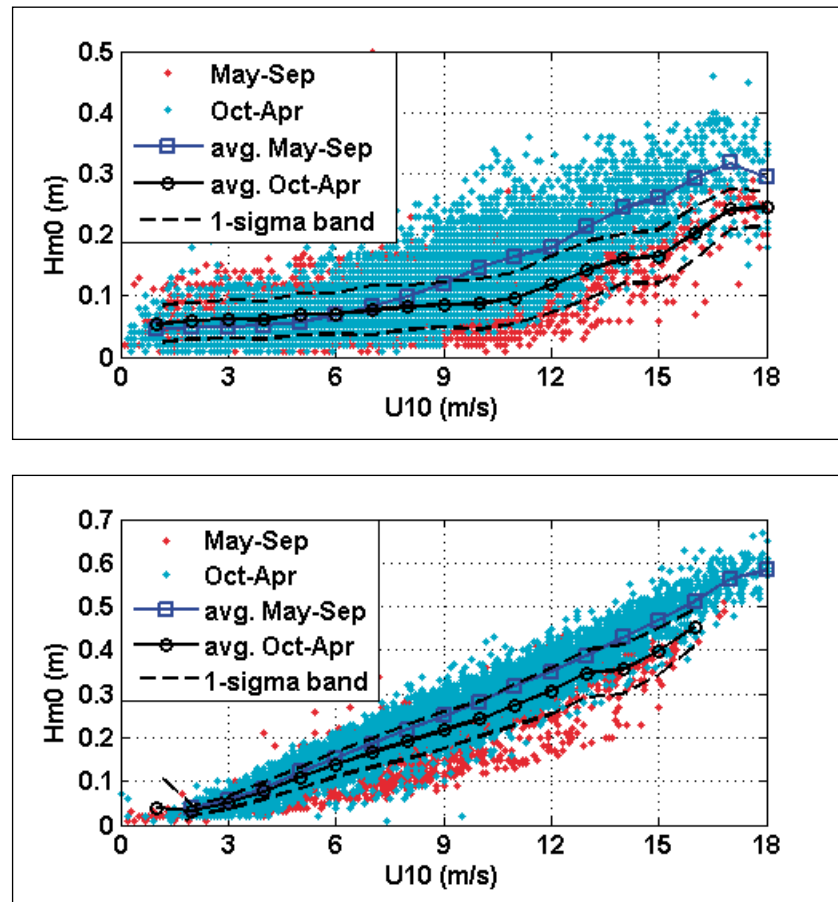


Figure B.2 shows an example registration with soiling effects, where the y-axis coincides with the still water level. One can clearly see that in this registration, the wave troughs near coincide with the still water level. In other cases, many of the wave crests are also suppressed so that the signal is nearly flat, except for some spikes where the wave signal is temporarily undamped.

Figure B.3 Wave height as a function of wind speed for WSW-winds, for summer and winter subsets of data. Top panel shows FL25-data with FL2-wind, lower panel SL29-data with SL29-wind. Both individual data and averages are shown, dashed lines indicate scatter (plus and minus one standard deviation) of the summer data.



Some typical features of the registration in Figure B.2 are:

- small H_{m0} -value (0.22 m, while about 0.32 m was expected with the 12 m/s WNW wind of that moment)
- increased T_{m-10} value (2.6 s while 2.0 s was expected)
- strongly increased skewness and kurtosis of the raw signal (about 2.5 and 10-12, where 0.5 and 3-4 were expected) as frequently occurring waves are damped more than the extremes.
- increased H_{max}/H_{m0} -ratio (2.5 where 1.5-2.0 was expected)

Further features that may occur are:

- still water level increases of up to 10-20 cm
- increased ratio of $T_{H1/3}/T_{m01}$
- concave wave height distribution as small waves are suppressed more strongly than the large waves

Several of these features were considered as possible detection criteria in (Ruijter and Boomgaard, 2004) and earlier publications. Finally, the

most reliable (though not perfect) criterion appeared to be one based on the skewness and kurtosis of the raw signal, where values above 1.25 and 6 were mentioned as an indication for soiling. See section B.8 for some further considerations on skewness and kurtosis.

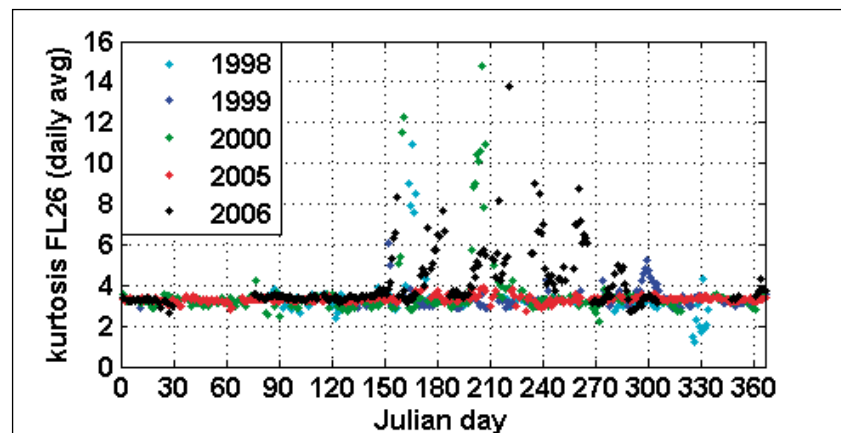
Similar analyses for the other locations are given in (Bottema, 2005). The results for FL26 are comparable with those of SL29. For the other locations, the difference between summer and winter data was generally less than 10%.

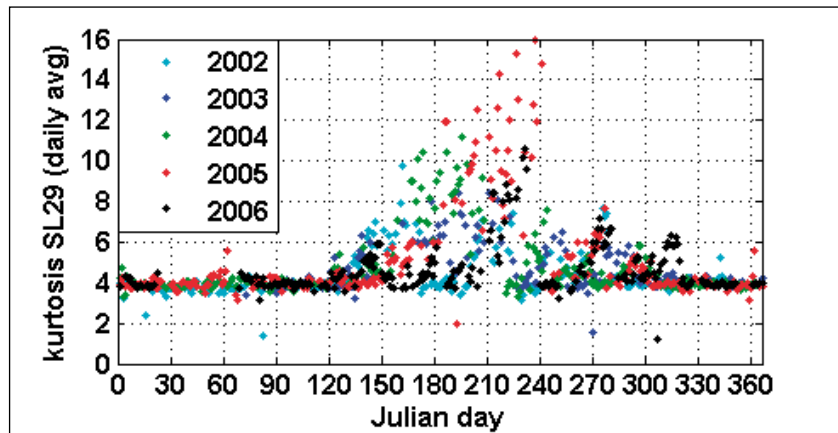
By considering the kurtosis of the raw signal, one can also get an impression about the periods in which soiling occurs. For FL26 and SL29, this is illustrated in Figure B.4. Note that daily averaged values are plotted to reduce scatter, and that only cases with at least 4 Beaufort winds are considered.

For FL26 (top panel), both step gauge results of 1998-2000 and capa probe results of 2005 and 2006 are shown. In both cases, the kurtosis is generally about 3.3 in the winter half year. Between late May (day 150) and the end of September (day 270), part of the data has strongly elevated kurtosis values, presumably due to soiling. This is most clearly seen in the late spring of 2006, where gradual kurtosis increases are followed by sudden drops at days where maintenance and probe cleaning takes place.

The results for SL29 are shown in the lower panel. The main difference compared to FL26 is the fact that at SL29, soiling appears to occur in nearly all summer periods, rather than just some of them. Also, the season with soiling appears to be relatively long at SL29. Soiling effects at SL29 typically start in early May (near day 120), and they may well persist into October, occasionally even into November. Once again, the 2006 data clearly show the gradual build-up of soiling, and the sudden drops due to cleaning.

.....
Figure B.4 Daily averaged kurtosis of raw wave signal, plotted as function Julian day number, for days with at least 4 Beaufort wind. Top and lower panel: FL26 and SL29.





For the other locations, results are similar, but they are more ambiguous because of disturbances by the capa probe supports in certain periods. This error source will be considered in the next section. Finally, it is interesting to note that most soiling seems to occur in periods with with water temperatures above 12-16°C.

B.6 Capa probe: preferential values

Besides soiling, the main error source for capa probe measurements is probably related to disturbances by the probe supports, resulting in preferential values. Especially during mild low-wave conditions, these errors can be very large. Interestingly, the errors due to preferential values happen to have qualitative similarities with soiling errors.

.....
Figure B.5 Histogram of raw capa probe samples (FL2, 8/1/2005 from 13-14 h MET, with $H_{m0} \sim 1.4$ m).

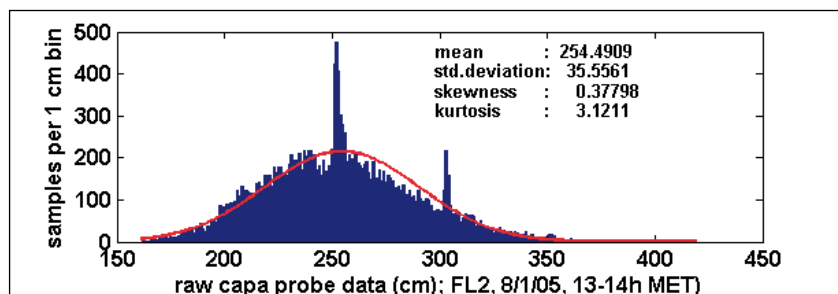
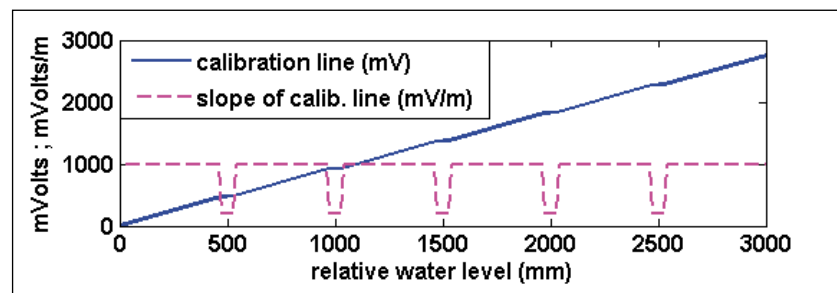


Figure B.5 shows an example histogram of the raw capa probe signal of FL2, during the storm of 8/1/2005, with an H_{m0} slightly above 1.4 m. The raw sample values range from about 140 to 420 cm, both measured from the lower end of the capa probe. Two clear preferential values can be seen near 250 and 300 cm, a third and weaker one can be seen near 350 cm. Since the preferential values generally occur at regular intervals equal to the probe support distance, it was logical to attribute the preferential values to some disturbance by the probe supports. This is all the more so because the preferential values disappear when supports are removed, like is done for the 200 cm support.

For a long time, it was believed that the (errors due to) preferential values, were related to disturbances in the static calibration function at the locations of the probe supports. This principle is illustrated in Figure B.6. The actual calibration function is simply the relation between capa probe output voltage and the water level as measured from the lower end of the capa probe. The calibration functions in the data loggers are in all cases linear fits to the actual calibration function. When the latter is plotted as output voltage as a function of water level (blue line in Figure B.6), the hiccups caused by the probe supports can be hardly seen. However, the slope of the calibration line (purple line) reveals clear dips at the location of the probe supports.

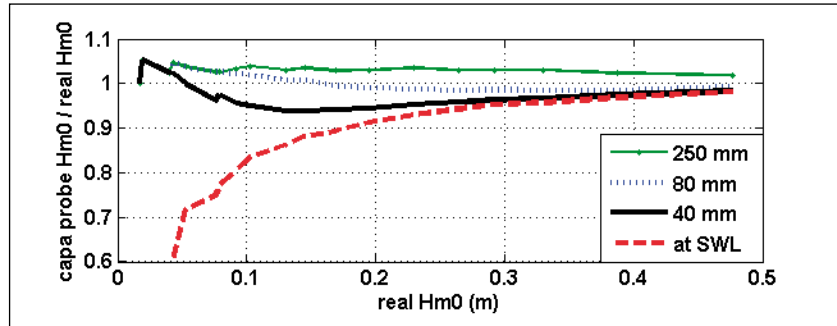
.....
Figure B.6 Schematic example representation of calibration line (in milliVolts) and slope of calibration line (mVolt per metre) as a function of relative water level.



The disturbed calibration function of the type of Figure B.6 can be applied to an undisturbed signal (signal of capa probe where supports are removed) to estimate the errors due to the disturbed calibration. This is done by (Bottema, 2005) for the only capa probe where a sufficiently detailed calibration was available. It turns out that the main errors occur in H_{m0} , especially when one of the capa probe supports is right at the still water level. Figure B.7 shows that in that situation, H_{m0} is underestimated by about 9% for $H_{m0} \sim 0.2$ m, and 18% for $H_{m0} \sim 0.1$ m. In these cases, the errors in the wave period T_{m-10} are about +5%. For probe supports at some distance from the still water level, all errors quickly decrease. However, with small waves and water levels between the probe supports, H_{m0} is often overestimated by 2-8% (depending on the probe). This is because then, the local calibration slope is slightly steeper than the overall slope used in the data logger, which is slightly reduced by the dips in Figure B.6.

An extensive comparison of step gauge and capa probe data (Bottema, 2005) showed that in practice, the H_{m0} errors can be as much as two to six times as large as the above estimates. In addition, two probes had T_{m-10} errors that much larger than expected: T_{m-10} -errors ranged from +20% for $H_{m0} \sim 0.5$ m to +120% (!) for $H_{m0} \sim 0.2$ m. Both errors only apply for probe supports near the still water levels.

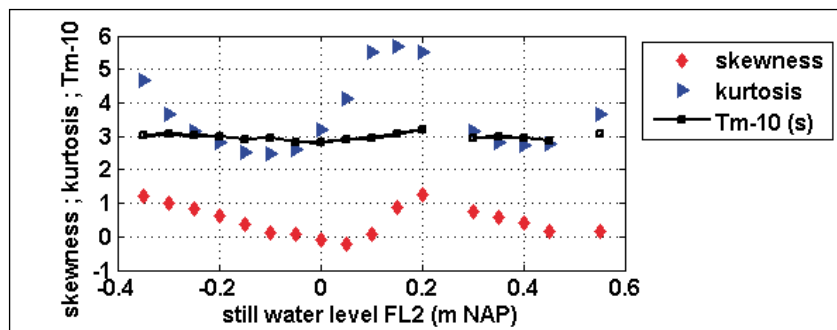
.....
Figure B.7 Estimated ratio of capa probe H_{m0} divided by real H_{m0} (after Bottema, 2005), as a function of real H_{m0} for a number of capa probe support positions with respect to the still water level (SWL).



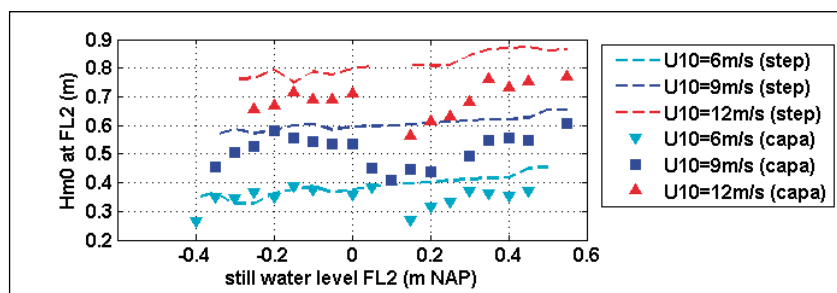
The extreme differences between the calibration-based error estimate and the real errors do strongly suggest that in the field, the capa probe does not behave according to the disturbed but static calibration of the type of Figure B.6. Rather, it is believed that the actual errors related to the probe supports are caused by some quick and dynamic wetting and drying process.

Figure B.8 gives as first impression of disturbances by capa probe supports in the field during moderately strong westerly winds at FL2. The kurtosis seems to have a clear repetitive pattern, with kurtosis maxima below -40 , near $+15$ and above $+60$ cm NAP. At the same water levels, the skewness quickly jumps from values near -0.2 to $+1.2$, while undisturbed skewness and kurtosis values ideally are about 0.5 and 3.3 respectively. Both trends can be explained by the location of preferential values related to the probe supports. At still water levels of $+5$ cm NAP, such a preferential values apparently is just above the water (explaining the negative skewness), at $+20$ cm NAP it is just below it (explaining the very high skewness). The wave period T_{m-10} shows a slight increase at still water levels of about $+20$ cm NAP, but H_{m0} (~ 0.6 m) is too large for substantial effects

.....
Figure B.8 Skewness, kurtosis and T_{m-10} wave period as a function of still water level, for FL2-data of winter 2001-2002; only W-wind ($240-300^\circ$) of $8-10$ m/s)



.....
Figure B.9 Step gauge H_{m0} -values of FL2 (winter data of 1997-1999) and capa probe data of FL2 (winter 2001-2002) as a function of still water level, for westerly winds ($240-300^\circ$) and wind speeds of $6, 9$ and 12 m/s.



In Figure B.9, step gauge H_{m0} -data of FL2 are compared with the capa probe data from the winter 2001-2002, for three different wind speeds and westerly winds (240-300°). At strong winds however, the capa probe data seem somewhat biased, possibly because these coincided with stable atmospheric stratification (warm air over cold water). As a result, Figure B.9 only allows for an approximate error estimate: roughly -30% to -20% H_{m0} -error for H_{m0} -values of about 0.4-0.7 m.

Some further error estimates were given in (Bottema, 2006b), based on plots of (Bottema, 2005):

.....
Table B.4 Errors when capa probe supports are at the still water level.

H_{m0} (m)	reg. number of capa probe; location	H_{m0} -error	T_{m-10} -error
0.55	ANM2882; FL2	-20%	+20%
0.50	ANM156; FL25, FL5 from 2001-2004	-10%	<10%
0.35	ANM3705; FL26	-12%	<10%
0.28	ANM3671; FL9	-18%	+20%
0.23	ANM2882; FL2	-60%	+115%
0.20	ANM2308; FL25; in 2004 FL5	-40%	+100%

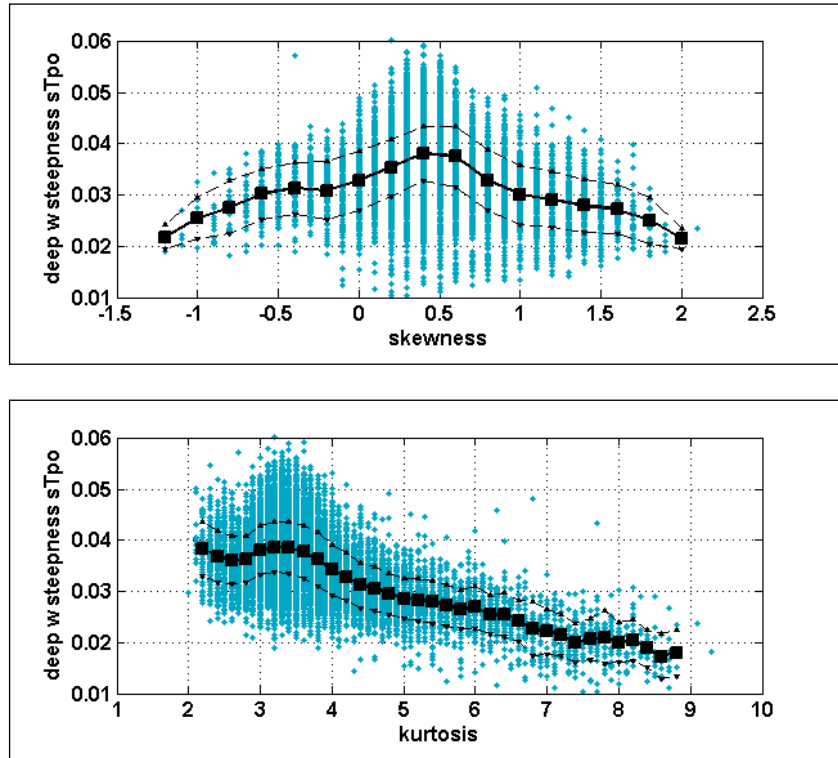
All in all, these field errors are much larger than the estimated errors of Figure B.7. Moreover, the errors are not limited to small waves; they are also significant for waves with H_{m0} -values of 0.5-0.8 m. On the other, one should note that several probe supports are removed in the season 2001-2002. As a result, capa probe data before 2002 are much more likely to have this type of error than later data.

The fact that the errors are no longer related to the calibrations also makes it difficult to make any reliable error estimates. Moreover, probes and probe (support) positions have changed quite frequently, so that it is quite cumbersome to find and list all cases where capa probe supports are close to the still water level. Luckily, both soiling errors and errors by preferential values happen to correlate quite well with the skewness and kurtosis of the raw measured signal.

These correlations are investigated in Figure B.10, where the deep water steepness s_{Tpo} of FL2 is plotted as a function of skewness and kurtosis. Only data with wind speeds above 8 m/s and wind directions of 210-300° are considered, as without errors, s_{Tpo} is approximately constant for these conditions. For the remainder, the full FL2 data set is considered, with summer and winter data, and step gauge and capa probe data.

The top panel of Figure B.10 shows that both very high and very low skewnesses lead to underestimations of s_{Tpo} with respect to its normal value of 0.035-0.040. Average underestimations are over 20% when the skewness is outside the range of -0.2 to +1.0. For kurtosis-values above 4.5, nearly all sample values of s_{Tpo} are too low, while the average underestimation is 20%. For kurtosis-values of order 10, the steepness is even reduced to half its original value.

.....
Figure B.10 Deep water steepness s_{Tpo} at FL2 as a function of skewness and kurtosis (summer and winter data from 1997-2006, with winds from 210-300° above 8 m/s).



For the other locations, the error trends are similar, although for FL5, the normal skewness and kurtosis values are somewhat higher (up to 1.2 and 4.5) than for locations without very large wave-height-over-depth ratios. This implies that skewness- and kurtosis-based quality labels must be somewhat on the lenient side to avoid rejecting correct data. For the present quality codes on a 0-10 scale, the following reductions are applied for suspect values of the skewness Sk and kurtosis Ku :

- no reduction if $-0.5 < Sk < 1.5$ or $2.2 < Ku < 5$
- Sk -based reduction: $\text{floor}[\text{abs}(Sk-0.5)^3]$
- Ku -based reduction: $\text{floor}[\text{abs}(0.7*(Ku-3.6)^{1.5})]$

Note that these quality labels are quite appropriate for the main error sources of both step gauges and capa probes: summer soiling and preferential values (by capa probe supports or by malfunctioning step gauge sensors).

B.7 Capa probe: drift

The present data set has several indications for *possible* capa probe drift, but unambiguous indications for drift are rare.

Indications for drift typically result from:

- field tests during maintenance visits, when the probe is temporarily put at a different height (may indicate drift, but in practice more useful to detect cases with wrongly implemented calibration data in the data loggers)
- drift in the preferential values of the capa probe

-
- drift in the offset to relate raw data to the NAP datum
 - drift in relatively stable wave parameters, like wave steepnesses
 - recalibrations

In most cases with apparent drift, the zero offset of the capa probe has changed. This change is most clearly visible in the preferential values and the offsets to relate the raw data to the NAP datum; the change can be up to 10-20 cm. In some late summers, *all* lake IJssel capa probes have a simultaneous offset dip of order 10 cm; an explanation is not yet known.

Drift in the calibration factor can rarely be reliably detected, especially when the drift is below 10%, which is nearly always the cases. In fact, drift as derived from recalibrations is generally (well) below 3%. The only indication of drift with some consistence is for the FL2, where the capa probe response may have been order 7-10% too low in 2001 and 2002. Besides this, the FL26 capa probe response is possibly 4% too high from 2002-2005 as a wrong calibration factor may have been implemented in this period.

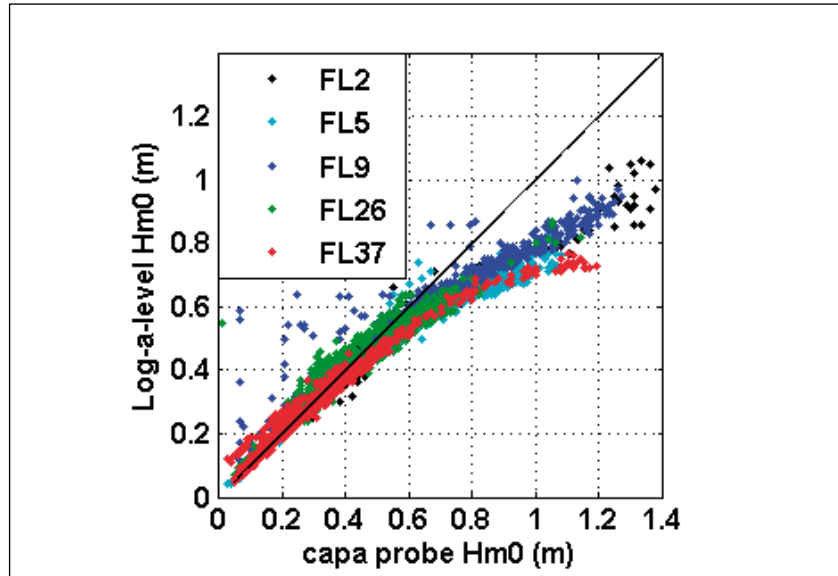
B.8 Log-a-level: errors of early types

During the wave flume tests of 2005 (Kuiper, 2005), the log-a-level suffered from incidental outliers, during which the instantaneous surface elevation was close to the maximum instrument range (6 m) rather than the actual water level (3 m). Kuiper also reported that most outliers appeared to occur during wave breaking. Therefore, he concluded that the raw log-a-level signal should be repaired before further processing.

In response to this, a new version of the log-a-level was developed with *two* adjacent (and closely spaced) sensors: if one sensor produced an outlier, the signal of the other sensor was chosen. In the summer of 2006, this sensor type was installed on all Lake IJssel and Lake Sloten platforms. In early June, the first sensor was attached to the FL37-platform. Initially, some extended periods occurred in which the raw signal was about 3 m off its expected value. This was attributed to reflections from the platform; indeed this problem was solved when (on 7/6/2006) the sensor was attached to the end of a boom extending about 1 metre out of the platform. In the autumn of 2006, some styrofoam was taped or glued to most booms to avoid any remaining reflections.

Despite the above measures, the performance of the log-a-levels still was not as good as expected. In fact, strong wave height underestimations occurred for *all* locations as soon as the wave height H_{m0} was about 0.6 m or more. See Figure B.11.

Figure B.11 H_{m0} as measured by log-a-level as a function of capa probe H_{m0} ; all Lake IJssel locations, 16/10 - 15/12/06.



Further suspect trends for wave heights H_{m0} over 0.6 m were:

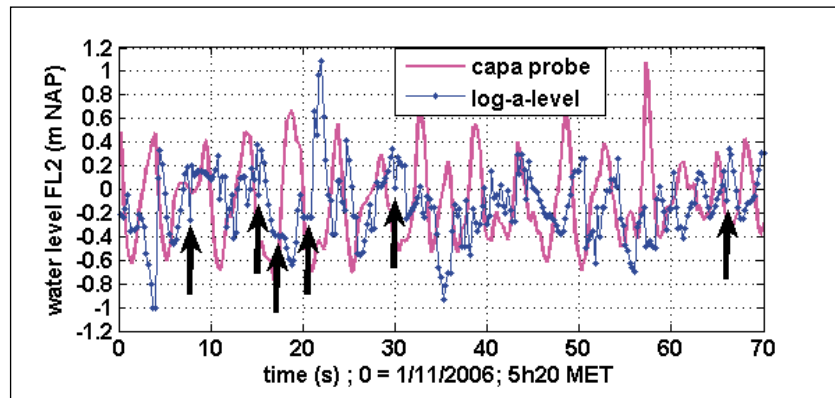
- H_{max}/H_{m0} – ratios of about 1.2, while normally, values are 1.6-2.0 unless waves are *strongly* depth-limited (like at FL5).
- $H_{1/3}/H_{m0}$ -ratio decreasing to 0.85, while theoretically, the ratio should be within a few percent of 0.95.
- Skewness values *decreasing* to about -0.2 ; they should have an increasing trend with values between 0 to $+0.7$ (theory) and $+0.4$ to $+1.2$ (step gauge and capa probe data).
- Distorted wave spectra:
 - wide and flat peaks
 - elevated low frequency energy
 - elevated high frequency energy: spectral slope less than the expected f^{-4} – relation; spectrum veering up above about 0.9 Hz.
- Presence of several individual waves with periods below 1.5 s and heights of order 0.4-0.8 m, *far* above the theoretical steepness limit.

Inspections of the raw measured signal gave an indication of the cause of all the above features. In several registrations with H_{m0} -values of order 0.5 m or more, as in Figure B.12, the log-a-level registrations did not show the smooth wave crest profile of the capa probe registrations, but rather a *jagged* wave crest shape. In addition, the log-a-level signal sometimes remained constant for a number of samples. In Figure B.12, both problems are indicated by red arrows. In a more general sense, one can note that the log-a-level signal looks much more irregular than the capa probe signal.

It is important to note that the aforementioned jagged wave crests often do not contain real outliers, but rather to water levels *within* the measurement range, often corresponding to some point near a wave *trough*. This suggests that these signal dips are probably related

to some unintended reflection of either the main signal beam or the backup-beam.

.....
Figure B.12 Raw signal (except for zero-offset correction) of capa probe and log-a-level, 1/11/2006, from 5h20 MET on.



After considering the above described errors, the log-a-level manufacturer offered to change the internal software (settings) of the log-a-level. These improved log-a-levels were installed between 15 January 2007 (FL2, SL29) and 30/31 January 2007 (remaining locations). Since then, the performance of the log-a-levels has significantly improved.

B.9 Log-a-level: expected errors

Prior to the present experiments, the following log-a-level error sources were anticipated:

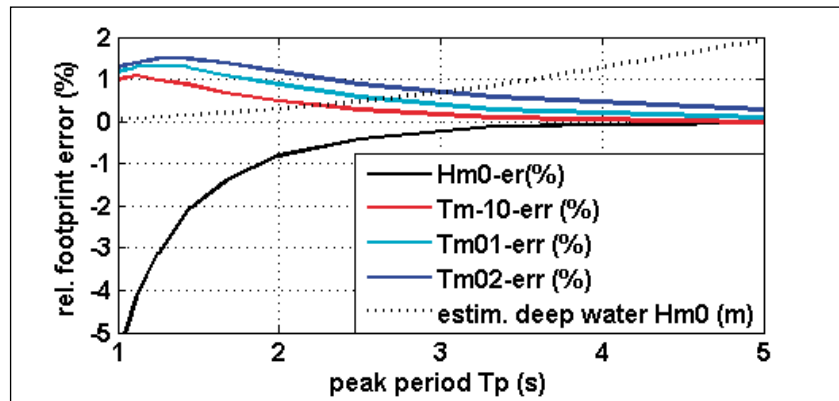
- finite footprint effects
- false reflections
- drift
- signal loss by a range of effects
 - wind deflection of sound beam
 - steep waves deflecting the sound beam away from the receptor
 - breaking waves (insufficient reflection of sound beam)
 - beam interception (on rain/spray drops)

The first error source to be considered is related to the finite footprint effect. Only for this error source, a quantitative error estimate is available; see (Witteveen and Bos, 2006). They considered the effect of five footprint diameters (0.2, 0.3, 0.4, 0.5 and 0.7 m) on the wave height H_{m0} and the wave periods T_{m-10} , T_{m01} , T_{m02} , each of them based on a spectral integration range up to 1.5 Hz. All error estimates are based on circular footprints, and a standard deep water (JONSWAP) spectrum with random wave phases.

The estimated finite-footprint errors are shown as a function of the peak period T_p in Figure B.13, together with a wave height estimate (H_{m0}) for deep water, assuming a wave steepness s_{Tp} of 0.05. For a 20 cm diameter footprint, T_p -values below 2 s and H_{m0} -values below 0.4

m, wave periods are typically overestimated by about 1%, while H_{m0} is underestimated by 1-5%.

Figure B.13 Effect of a finite log-a-level footprint (20 cm diameter) on H_{m0} , T_{m-10} , T_{m01} and T_{m02} as a function of peak period T_p , together with an estimate of the deep water H_{m0} that would occur with this T_p .



In the absence of strong storm surge effects, the Lake IJssel log-a-levels are typically 2.5 – 3 m above the still-water level; for Lake Sloten this height is typically about 1.7 m. With a 5° sound beam width, this yields footprint sizes of 22-26 cm for Lake IJssel and about 17 cm for Lake Sloten. The estimated footprint error in Witteveen and Bos, 2006a) roughly scales with the squared footprint size. This implies that in practice, the expected footprint errors at SL29 are 25-30% lower than in Figure B.13, while the expected errors for Lake IJssel are typically 20-70% larger. These largest errors are expected to occur when the still water levels are about –30 cm NAP or less. But even then, footprint effects are only expected to be significant (> 5%) for wave heights H_{m0} below 15-20 cm.

Another error source is related to false reflections, either from the platform, from parts of the water surface one does not intend to measure, or from rain and spray drops. The former two types of error are already discussed in the previous section. As for the false reflections on rain drops, no obvious correlation was found between rainy periods and malfunctioning of the log-a-levels.

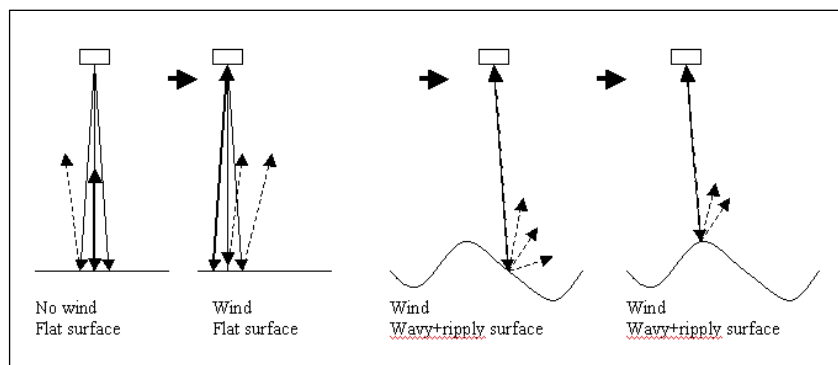
An potential source of drift is the dependence of sound speed on temperature (and to a lesser extent air moisture). The present log-a-levels automatically correct for these effects by measuring the transit time of a reference sound beam along a given length. Errors may occur if conditions along this reference beam are not representative, for example due to strong insolation of the sensor or due to vertical temperature gradients. However, no obvious drift effects were detected during any of the field tests, not even on calm and sunny summer days.

A last type of problem is signal loss, which can occur due to a range of effects. Depending on the instrument settings, it typically results in a missing sample, or in an outlier sample.

Interception or deflection of the sound signal by rain or spray is a possible source of signal loss, although there are no clear indications

that such problems have occurred in the present measurements. Breaking waves may also be a source of signal loss as in such conditions, the water surface may become too diffuse to allow for a sufficiently strong (and focussed) reflected sound beam. Hence, it is worthwhile to investigate the log-a-level performance as a function of a parameter that indicates the breaking probability of the waves, for example the wave-height-over-depth ratio H_{m0}/d . For perfectly smooth waves, signal loss will occur if the local wave slope is larger than the half-width of the log-a-level sound beam, which is about 2.5° . In practice, the wave steepness of short ripple waves is (at least) of the same order as the steepness of the dominant waves. This implies that without wind effects, always some part of the log-a-level sound beam will be reflected back to the receptor part of the sensor.

.....
Figure B.14 Sketches illustrating wind deflection of sound beams.



Wind deflection of the log-a-level sound beam may be a significant source of errors and signal loss, especially during storms when the wind speed can be order 5-10% of the sound speed. The latter is typically about 340 m/s. Figure B.14 illustrates some of the deflection effects; signal loss will occur if no part of the emitted sound beam is reflected back to the instrument. With geometrical reasoning and some further assumptions (as given below), the following can be concluded:

- For a flat and smooth surface, signal loss will occur if the wind deflection is larger than a quarter (1.25°) of the sound beam width, this is the case for wind speeds over 7-8 m/s.
- If short ripples and dominant waves are equally steep, the water surface at the centre of the downwind wave slopes either points downwind or upwards, the latter only if the sound beam hits the *upwind* slope of a wave ripple. One can then apply the arguments for the smooth and flat surface to argue that the first signal loss will occur in the middle of the downwind wave slope, starting at a 7-8 m/s wind speed. A small wind increase on top of this may cause about 15% signal loss as for a sinus-shaped wave profile, the overall wave slope changes little over the central 30% of the downwind wave slope (which itself is half of the wave).
- If the maximum ripple slope angle is assumed to be 9° , and the beam width is 5° , one can argue that for wind deflections over about 7° , signal loss will occur for the full downwind wave flank

including the wave crests and wave troughs. This requires wind speeds of order 40 m/s, which may be reached in typhoons, or during gusts in extratropical storms.

The above arguments are highly approximate and rather conservative, the latter due to the fact that short wave ripples appear to be steeper than the dominant waves (see section 6.7.3; Figure 6.24). Still, signal loss due to wind deflection is potentially an important error source, which should be taken into account in acceptance tests for this instrument.

Appendix C Intercomparison of wave instruments

In this appendix, the results of a number of instrument intercomparisons will be presented. The first intercomparison is an indirect one, considering the step gauge and capa probe measurements of Lake IJssel. The second intercomparison (Kuiper, 2005) includes several instruments and is done in a wave flume. Finally, the third intercomparison is based on simultaneous capa probe and log-a-level measurements in Lake IJssel and Lake Sloten.

C.1 Indirect comparison step gauge and capa probe

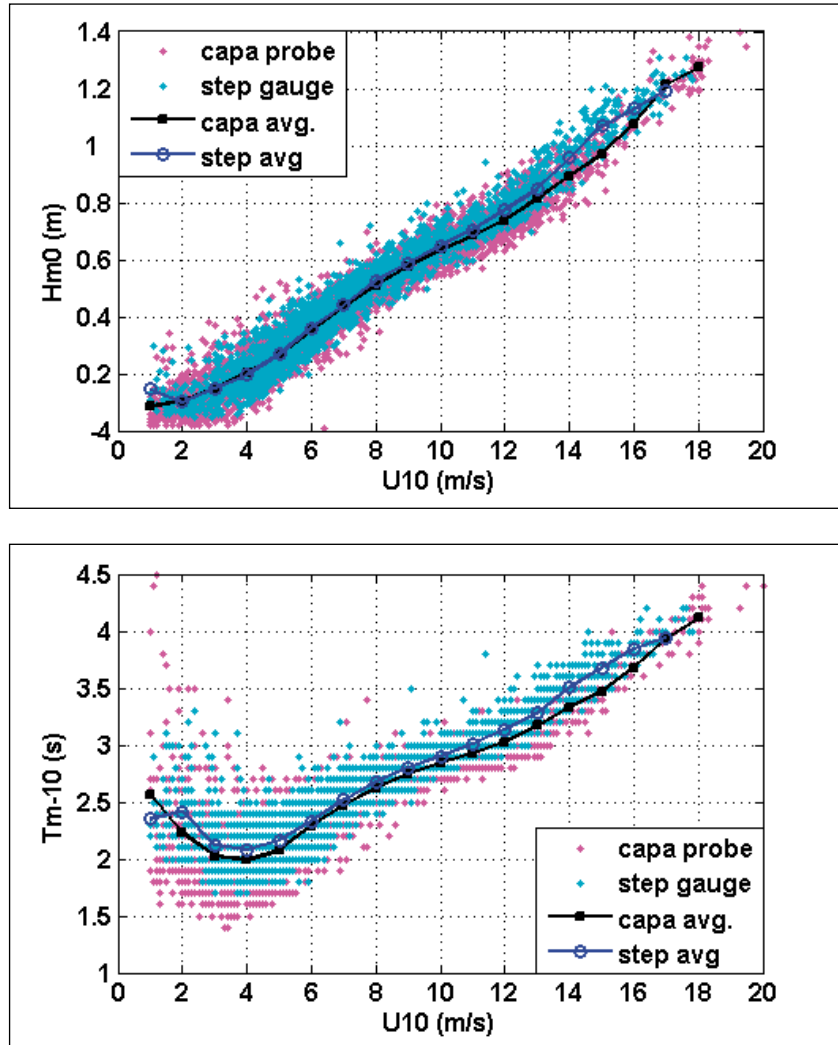
Until recently, the only experimental benchmark for the present capa probe data was a set of step gauge measurements done in the early years of this measuring campaign. Unfortunately, no simultaneous measurements were carried out. Therefore, the intercomparison focussed mainly on wind-related wave climatologies like the ones presented in section 6.2-6.4 of this report. A detailed analysis is reported in (Bottema, 2005). Unfortunately, an erroneous wind offset in the data logger software was discovered a few months after publication of that report. As a result, many wind-dependent results, including the apparent integral wave parameter differences between step gauge and capa probe, were biased by order 5%. Therefore, the main revised results are summarised in the present report.

The upper panel of Figure 3.1 shows the step gauge and capa probe H_{m0} at FL2 as a function of wind speed, for westerly winds, considering winter half year data only. On average, the step gauge and capa probe results are nearly indistinguishable, except for wind speeds of about 14 m/s. As the latter difference also occurs in T_{m-10} (lower) panel but not in the wave steepness, the difference is probably not related to the wave instruments but to a difference in the wave forcing (e.g. in atmospheric conditions). For the remainder, the step gauge and capa probe T_{m-10} -values agree well, although closer inspection shows that the capa probe values tend to be 1-5% lower. As the H_{m0} -values are nearly identical, this yields a slightly larger wave steepness $s_{T_{m-10}}$ for the capa probe data.

For other locations where step gauge and capa probe measurements were done at the same location (FL9 and FL26), a comparison for southwesterly winds yields the same trends as above. In some details, the agreement for these locations is even slightly better:

- for FL9, the capa probe wave periods are nearly identical to the step gauge data, instead of a few percent lower
- for FL26, the small dip in the strong wind data (with $U_{10} \sim 14$ m/s) of the capa probe data is missing

Figure C.1 Wave height H_{m0} (top panel) and wave period T_{m-10} (lower panel) at FL2 as a function of FL2 wind speed U_{10} , for westerly wind (240-300°), comparing winter half data of Oct97-Oct99 (step gauge) and Mar03-Apr05 (capa probe).



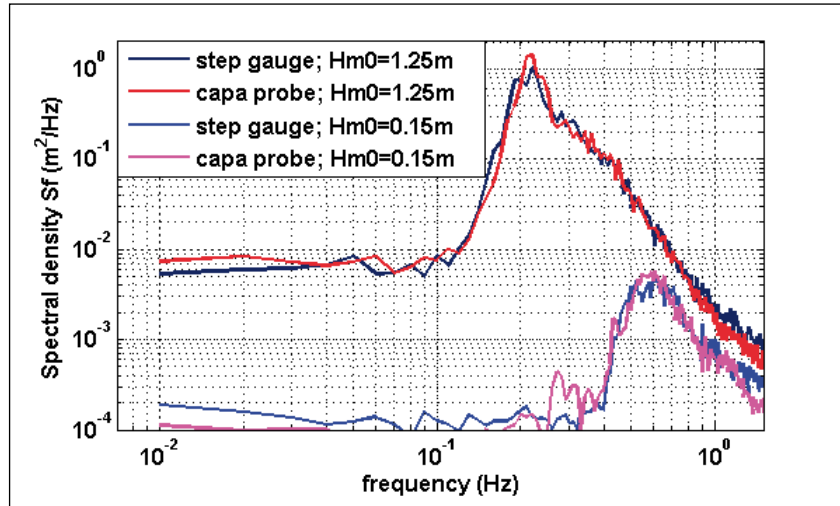
In Figure C.2, the FL2 wave spectra of four cases are compared:

- 5/2/1999, 6-7 h MET (step gauge)
- 12/2/2005, 12-13h MET (capa probe)
- 31/1/1999, 19h40-20h40 MET (step gauge)
- 3/12/2004, 14-15h MET (capa probe)

The former two cases have a WNW wind of about 18 m/s, a H_{m0} of 1.24, a peak period T_p of about 4.7 s and a mean wave period T_{m01} of 3.6 s. The latter two cases have a (W)SW wind of 4-5 m/s with a H_{m0} of 0.15 m, while T_p and T_{m01} both are 1.6 s.

With these nearly identical integral wave parameters, the capa probe and step gauge wave spectra (see Figure C.2) also agree excellently. At frequencies above 1 Hz, both spectra slightly veer up, which is not to be expected from a physical viewpoint. For the step gauge spectra, this veering up is slightly stronger. For FL5, FL9 and FL26, some additional cases are defined in section 4.2 of (Bottema, 2005). For these additional cases, the comparison results are virtually the same as above.

Figure C.2 Comparison of step gauge and capa probe wave spectra, based on 1h of data with H_{m0} wave height of 1.25 and 0.15 m.



After the comparison of integral wave parameters and wave spectra, the last issue that remains to be considered is the time domain signal. However, no direct comparisons are possible here by lack of simultaneous data. Still, it is interesting to investigate the skewness of the raw signal, as this is a useful indicator for the non-linearity of the waves and the shape (see section 6.7.3) of the wave height distribution. Moreover, the skewness of downward-looking instruments may – due to focussing effects of their signal beam – well deviate from that of fixed instrument. Therefore, it is useful to verify whether the capa probe data agree sufficiently well with the step gauge data to be a suitable benchmark.

Figure C.3 Step gauge and capa probe skewness at FL5 (all winter season data) as a function of wave height over depth ratio H_{m0}/d .

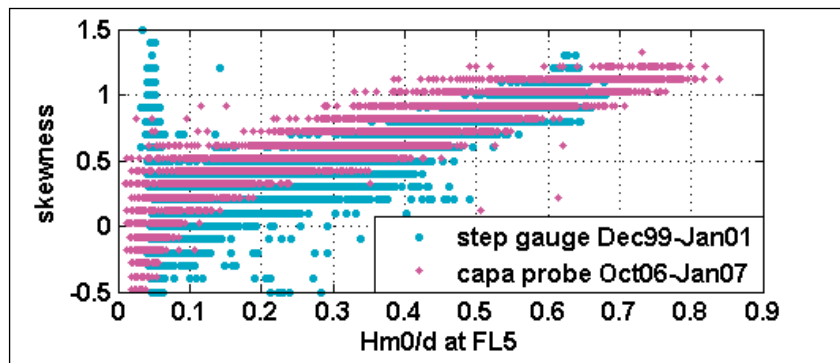


Figure C.3 shows the FL5-skewness data as a function of the wave-height-over-depth ratio H_{m0}/d , for all winter data mentioned in the figure legend. The FL5 is chosen for this comparison because the range in skewness and H_{m0}/d values is by far the largest for this location. Strictly speaking however, the step gauge FL5-location differs slightly from the capa probe FL5-location. Except for a very small fraction of outliers, the agreement between both data sets is excellent, with skewnesses gradually increasing from near-zero for very small waves to about 1.0 for H_{m0}/d of about 0.65. Closer inspection suggests that the capa probe are slightly higher, but the difference is small (0.1-0.2).

Finally, it should be noted that the above comparison is based on a slightly idealised data sets, where errors due to soiling and due to capa probe preferential values are excluded as much as possible. This makes sense, because one wishes to avoid such errors anyway. For these situations one can summarise the above results as follows:

- *step gauge and capa probe results agree within a few percent in terms of integral wave parameters; the wave spectra agree excellently as well.*
- *step gauges and capa probes yield largely the same amount of wave asymmetry (skewness) in situations with depth-limited waves, although the skewness from the capa probe may be slightly (0.1-0.2) larger than for the step gauges.*

C.2 Wave flume instrument comparisons

The choice for the log-a-level as a possible alternative for the present capa probe measurements originates from a desk study (Ruijter et al., 2005), followed by an intercomparison (Kuiper, 2005) in a wave flume with 4 m water depth. In this wave flume test, five instruments were compared with the fast-response wave flume reference meter:

- one of the current capa probes
- an Etrometa step gauge
- a downward looking Miros 'Range Finder' radar sensor
- an upward looking AWAC Acoustic Doppler Profiler
- a downward looking acoustic Log-a-level sensor

Eight wave conditions were tested with wave height H_{m0} ranging from 0.25 to 1.45 m, peak periods T_p ranging from 1.8 to 11 seconds, and wave steepnesses stop ranging from 0.003 to 0.05. In one case ($H_{m0} \sim 0.65$ m, $T_p \sim 11$ s), asymmetric waves with sharp crests and shallow troughs were generated.

Prior to this experiment, a set of pressure sensors was tested separately in the same flume (Doorn and Eysink, 2004), with H_{m0} , T_p and stop in the range of 0.16-1.45 m, 2.5-5.2 s and 0.016-0.037 respectively.

The *log-a-level* (after removal of outliers) and step gauge received the best ratings in these tests. The capa probe rating was somewhat lower, probably due to disturbances by one of the probe supports.

For each of the instruments tested, a brief summary of the key results is given below. For sake of brevity, differences with respect to the reference meter are indicated as 'errors'.

all instruments

- peak period errors were nearly always negligible (less than 1%)

capa probe

- H_{m0} -errors are between -1% and +3%, except for the test with $H_{m0} = 0.25$ where the error is -9%.
- T_{m-10} -errors are between -6% and +3%, except for the test

with $H_{m0} = 0.25$ where the error is +67%, probably related to disturbance by one of the probe supports (see Appendix B.6).

- spectra agreed excellently with the reference sensor except for enhanced low-frequency noise in the test with $H_{m0} = 0.25$ m.
- $H_{2\%}$ tended to be somewhat too low (-12% to +1% error) as was the upper part of the wave height distribution.

step gauge

- H_{m0} -errors were between -1% for mild conditions and about +4% for the severest conditions tested.
- T_{m-10} had an opposite trend with errors between -2% and +5%
- $H_{2\%}$ tended to be somewhat too high (-3% to +12% error), possibly because some waves were seen to 'slosh' up against the probe (pers. comm. R. Kleine, RWS IJG).
- Spectra agree excellently with reference sensor up to 0.5 - 1 Hz; above it, the high frequency tails often flattens off too much (a trend also seen in Figure C.2).

'Range Finder' radar sensor

- H_{m0} -errors in two case -5% and +10%, else 2% or less.
- T_{m-10} -errors in two cases +20% and +50%, else +1% to +5%.
- $H_{2\%}$: -9% to +1% error but -22% during asymmetric waves, top of wave height distribution often flattens off too soon.
- Spectra: tendency for high noise levels above 0.5-1 Hz, during mild conditions also for low frequencies.

'AWAC' acoustic doppler profiler

- H_{m0} -errors in two case +8% and +18%, else 2% or less.
- T_{m-10} -errors in two cases about +15%, else up to +5%.
- $H_{2\%}$: -2% to +61% error; top wave height distribution often too high (near-outliers).
- Spectra: in some cases even noisier than radar, sometimes quite good.

Log-a-level

- H_{m0} -errors -4% to +1%, the latter in mild conditions
- T_{m-10} -errors -1% to +8%, in one case ($H_{m0} \sim 0.25$ m) +35%.
- $H_{2\%}$: -8% to +2% error.
- Spectra: rather noisy when $H_{m0} = 0.25$; else very similar to step gauge spectra.

Pressure sensor

- H_{m0} -errors -7% to +12% (both in mild conditions, with sensor 0.5 and 1.5 m below surface respectively)
- T_{m-10} -errors: -15% (shallow sensor, high waves) to +16% (deep sensor, low waves); T_{m02} -error -24% and +19% in same conditions.
- reported estimated error by neglecting non-linear terms: 5-10%.

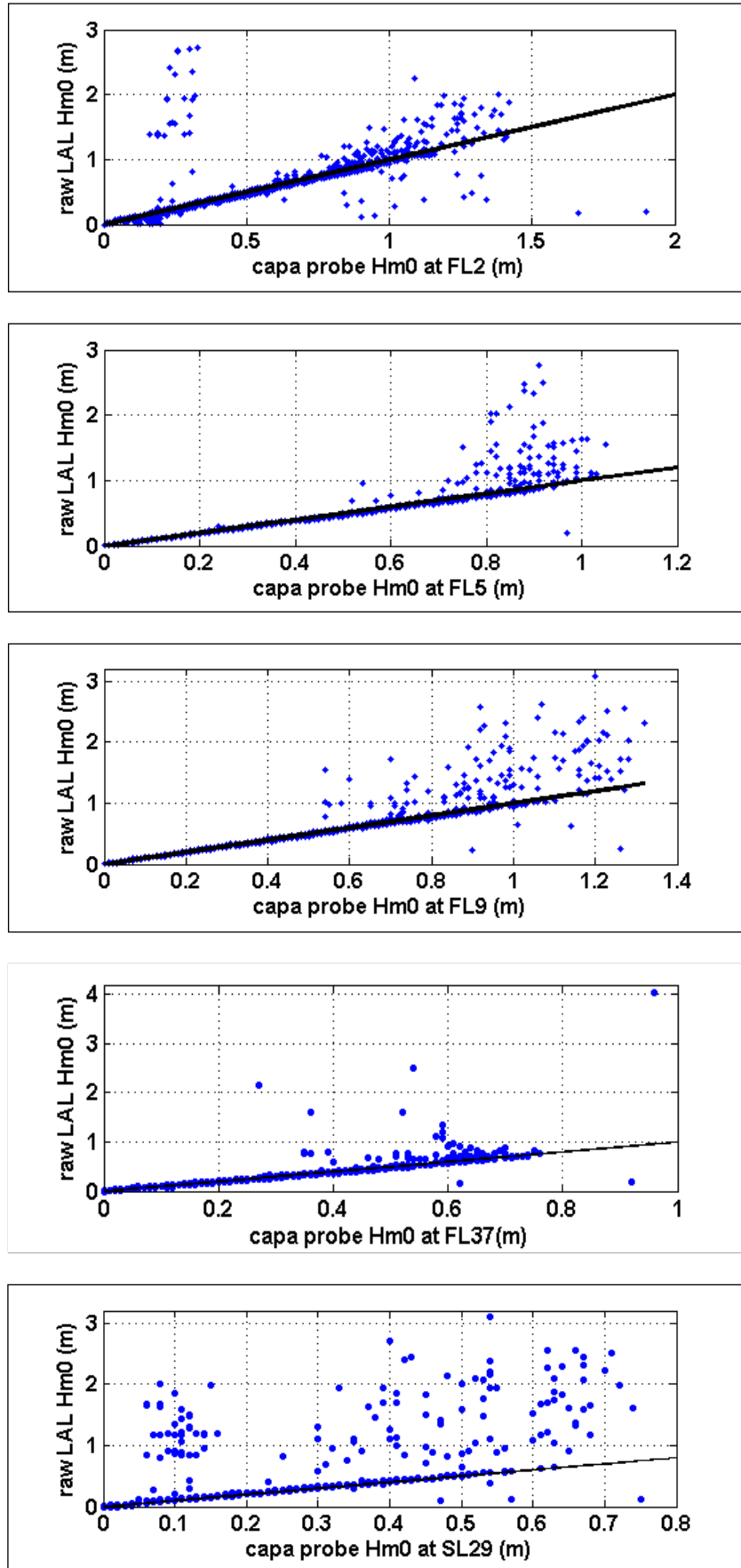
Furthermore, it must be noted that the advised measuring height requirements are rather restrictive. On one hand, the sensor should remain below about $0.5 H_{m0}$ to remain in the water. On the other hand, good spectral response up to 0.7-2 Hz can only be obtained if the sensor is within 30-15 cm of the surface. For deeper sensors, the damping for waves of these frequencies is reported to be over a factor 10, so that noise is likely to significantly influence the measured signal.

C.3 Field comparison of capa probe and log-a-level

On 15 January 2007, an improved version of the log-a-levels is installed at FL2 and SL29. By 1 February, the other locations were also provided with these instruments. This section presents a comparison between these log-a-level data and capa probe data for a period of about 8 weeks, until 18 March 2007. Note that one week of FL2 data had to be rejected as the log-a-level fixings were hit loose by a high wave in the evening of 18 January. In the following, it will be shown that the log-a-level performs quite good, but that its weak point is related to windy conditions.

Figure C.4 compares the H_{m0} wave height data from the *uncorrected* log-a-level signal with the capa probe H_{m0} . A few outliers below the black line are related to unreliable capa probe data, for example due to maintenance. From the FL2- and SL29-log-a-level data, some data for mild conditions are *much* too high. Further inspection of the data reveals that this is related to outliers in the raw data. Essentially these outliers can have any value between 0.2-0.6 m and 10 m (in terms of position below the instrument). For FL2 and SL29, these outliers may occur both during very mild and during windy conditions; elsewhere the outliers mainly occur during conditions with relatively high waves. This can also be seen in Figure C.4, where nearly all locations have increased scatter above the black reference line that indicates equal log-a-level and capa-probe results. In fact, most locations have increased scatter for wave height H_{m0} above about 0.7 m. However, for SL29 this limit is about 0.3 m and for FL37 probably too. Wave breaking does not seem to be the main cause, as the outliers at FL5 and SL29 start at strongly different wave heights although the water depths for both locations are quite the same. On the other hand, Figure 6.3-6.5 shows that for southwesterly winds of 12 m/s, all locations have a H_{m0} of about 0.7 m, except FL37 and SL29 where H_{m0} is about 0.3 m. This suggests that wind speeds above 12 m/s may be an important source of outliers.

.....
Figure C.4 H_{m0} from uncorrected log-a-level data as a function of capa probe H_{m0} , Jan-Mar 2007, for FL2 (top), FL5, FL9, FL37 and SL29 (below). Black line indicates 1:1 relation (equal H_{m0} 's).



In the present study, 20-minute data blocks with more than 2% outliers are rejected, where samples are considered to be outlier if they are outside a predefined and location-dependent range of physically realistic values. It is interesting to extend the analysis of Figure C.4 by considering the percentage of rejected data, as this determines the suitability of the log-a-levels in practice.

Overall, the percentage of rejected data blocks is less than 3% for all locations. For the data subset with H_{m0} greater than 0.5, this percentage increases to 6-13% for the Lake IJssel locations and 64% for the SL29-location in Lake Sloten. The subset for H_{m0} greater than 0.8 m is only relevant for Lake IJssel. The percentage rejected data ranged from 17-51%; for FL37 no percentage can be given as no H_{m0} values above 0.8 m occurred for the period under consideration. All in all, one can conclude that during conditions with strong winds and high waves, a significant fraction of the log-a-level data blocks contains so many outliers that the data have to be rejected.

In the remainder of this section, log-a-level data blocks with over 2% outliers are not considered at all. For the retained data blocks, outliers were first removed before further processing.

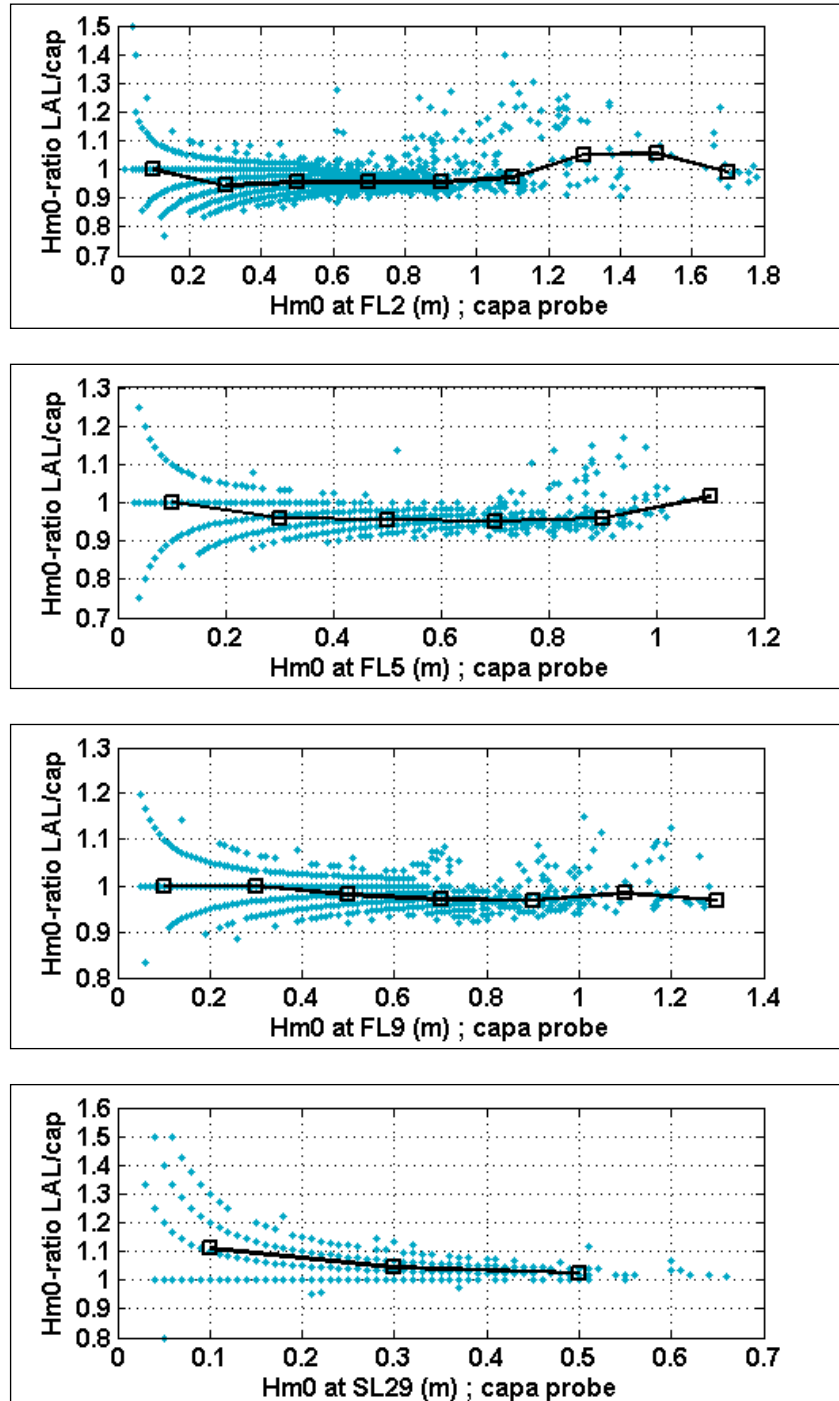
Figure C.5 compares these corrected log-a-level data with capa probe data: it shows the ratio of log-a-level and capa probe H_{m0} as a function of the H_{m0} measured by the capa probe. For all locations, both scatter and average bias are less than 5%, at least during mild conditions. For larger wave heights (and winds above 12 m/s), the log-a-level data have increased scatter while they tend to be higher than the capa probe data. Apparently, there is still some influence of outliers for these conditions. This is not entirely surprising as only samples outside a predefined physically realistic range were rejected. In practice however, the suspect log-a-level values are not restricted to values outside this physical range. This applies especially for Lake IJssel. For Lake Sloten, the remaining data set seems quite reliable, although strong wind and high wave cases are hardly included in these remaining data.

A final point of interest is the fact that for all Lake IJssel locations, the log-a-level H_{m0} -values tend to be a few percent lower than the capa probe values, while the opposite is the case for Lake Sloten. The reason for this is not clear, although it can be noted that at Lake Sloten, the sensor is about 1.5 m above the water while this is 2.5-3 m for all Lake IJssel locations.

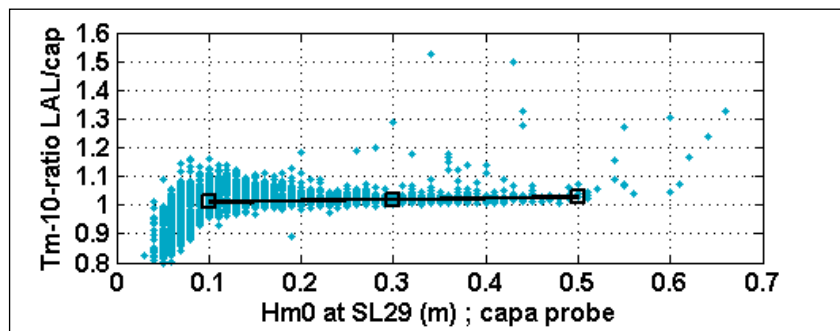
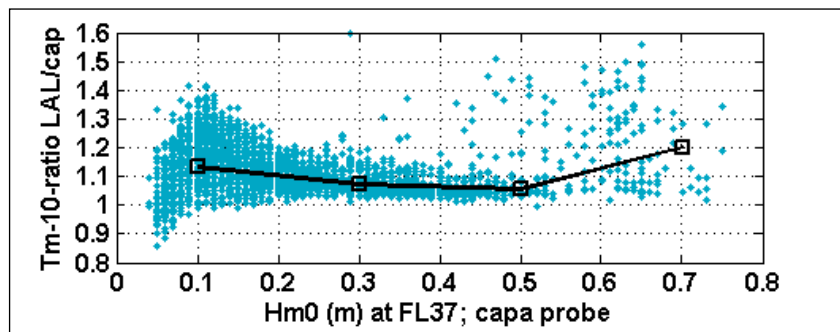
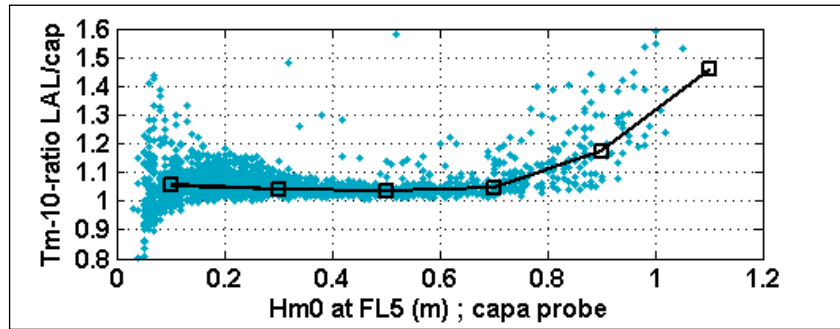
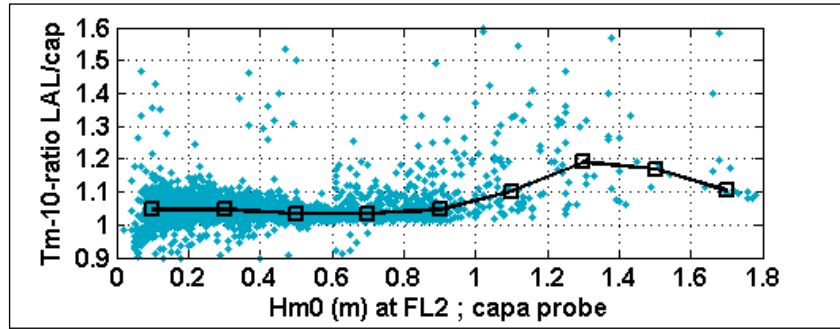
The results for the T_{m-10} wave period are shown in Figure 3.6. It can be seen that for wave heights above 0.7 m (0.3 m for FL37 and SL29), the log-a-level T_{m-10} values are often too high. This is probably related to the same outliers that cause the H_{m0} -overestimations on Figure C.5. For the remainder, the log-a-level T_{m-10} value is typically 2-10% higher than the capa probe value. In a qualitative sense, this combination of small H_{m0} -underestimations and small wave period

overestimations is consistent with the finite-footprint effects of section B.9. Quantitatively however, the present data and trends do not agree with those of section B.9. Finally, there is once a again a significant difference in the apparent errors of the log-a-levels of SL29 and Lake IJssel respectively.

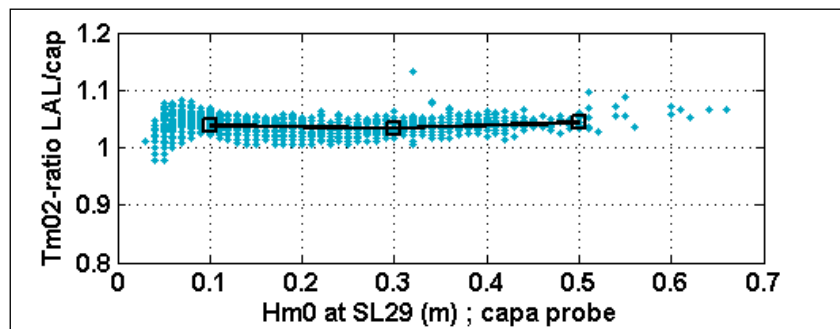
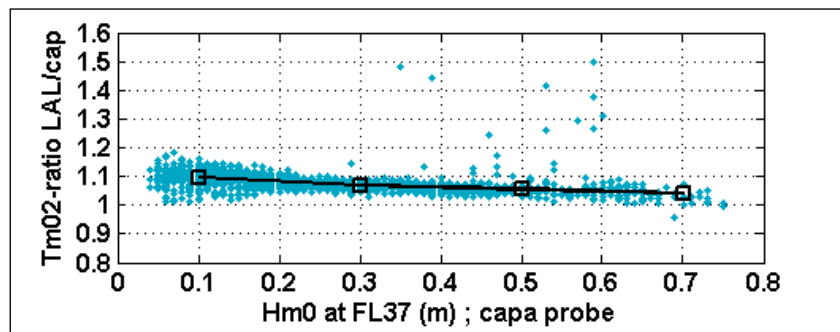
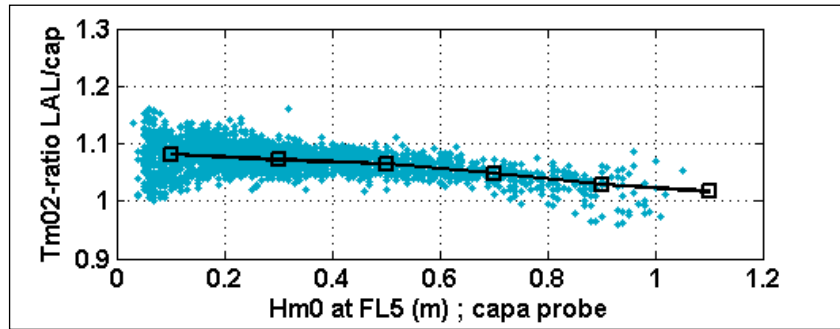
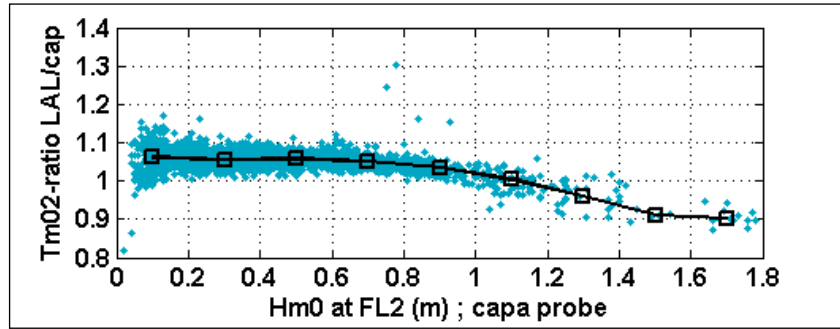
Figure C.5 Ratio of log-a-level H_{m0} (after outlier filtering) and capa probe H_{m0} as a function of the latter; Jan-Mar 2007, for FL2 (top), FL5, FL9 and SL29 (below). Median of data is indicated by black squares and line.



.....
Figure C.6 As Figure C.5 but for
 T_{m-10} ratio and the locations FL2,
FL5, FL37 and SL29.



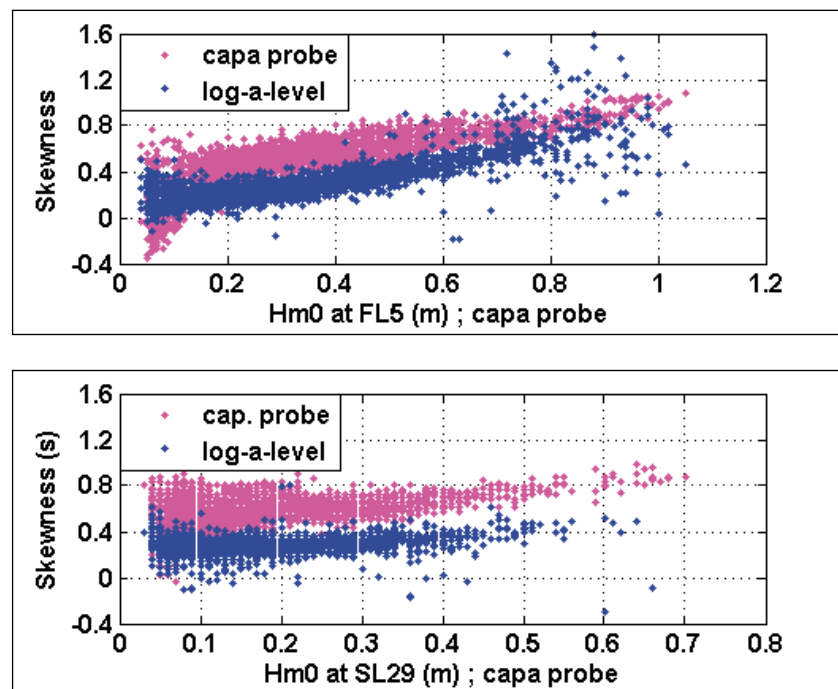
.....
Figure C.7 As Figure C.6 but for
 T_{m02} ratio.



In Figure C.7, the T_{m02} wave periods of the capa probe and log-a-level are compared. The trends are largely the same as those in Figure B.6, but the aforementioned outliers appear to have less effect on T_{m02} than on T_{m-10} (as shown in Figure B.6). In severe wave conditions, the log-a-level T_{m02} -values tend to become about 10% lower than the capa probe values; this trend can best be seen in the top panel for FL2 (which includes the storm data of 18/1/2007).

In Figure C.8, the capa probe and log-a-level skewnesses are compared for the FL5 and SL29. Outliers in the raw signal clearly affect the log-a-level skewness of FL5 at high H_{m0} -values. For the remainder the log-a-level data have largely the same trends as the capa probe data, although the absolute values are about 0.3 lower. This implies that the log-a-levels reasonably predict the trends in non-linearity and asymmetry of the waves, but that the log-a-level registrations still yield somewhat too linear and symmetric waves with respect to the capa probe, and the step gauge which only slightly differs from the latter (Figure C.3).

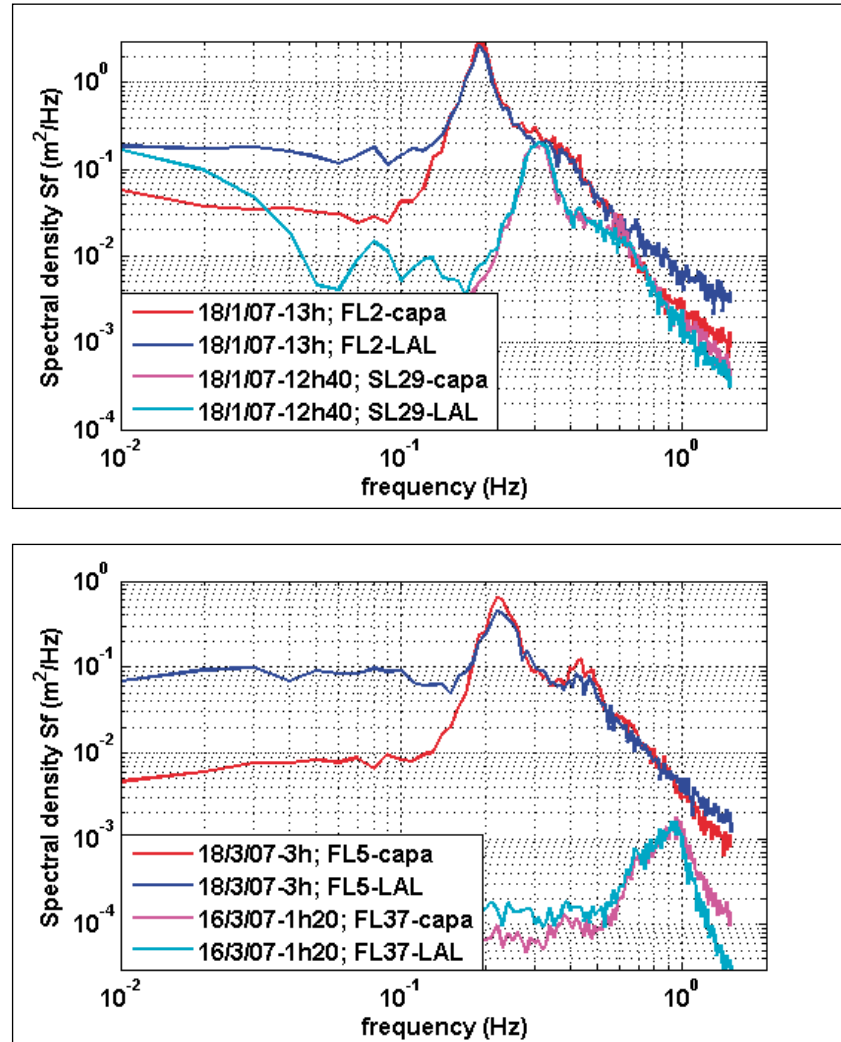
.....
Figure C.8 Capa probe and log-a-level skewness as a function of capa probe H_{m0} ; Jan-Mar 2007, for FL5 (top) and SL29 (below).



Some wave spectra of the capa probe and log-a-level are shown in Figure C.9. For the major part of the spectra, the agreement between both instruments is excellent. This is not totally surprising as for most (though not all) cases, the integral wave parameters of both instruments agree excellently, as shown in Figure C5-C7. For low frequencies however, the log-a-levels often seem to suffer from high noise levels. For frequencies above 0.5-1 Hz, the picture is rather inconsistent. For high waves, the log-a-level tends towards too high energy levels compared to the capa probe, in accordance with the wave flume test result of Kuiper (2005). For the very low waves at FL37 however, the high frequency energy levels of the log-a-level

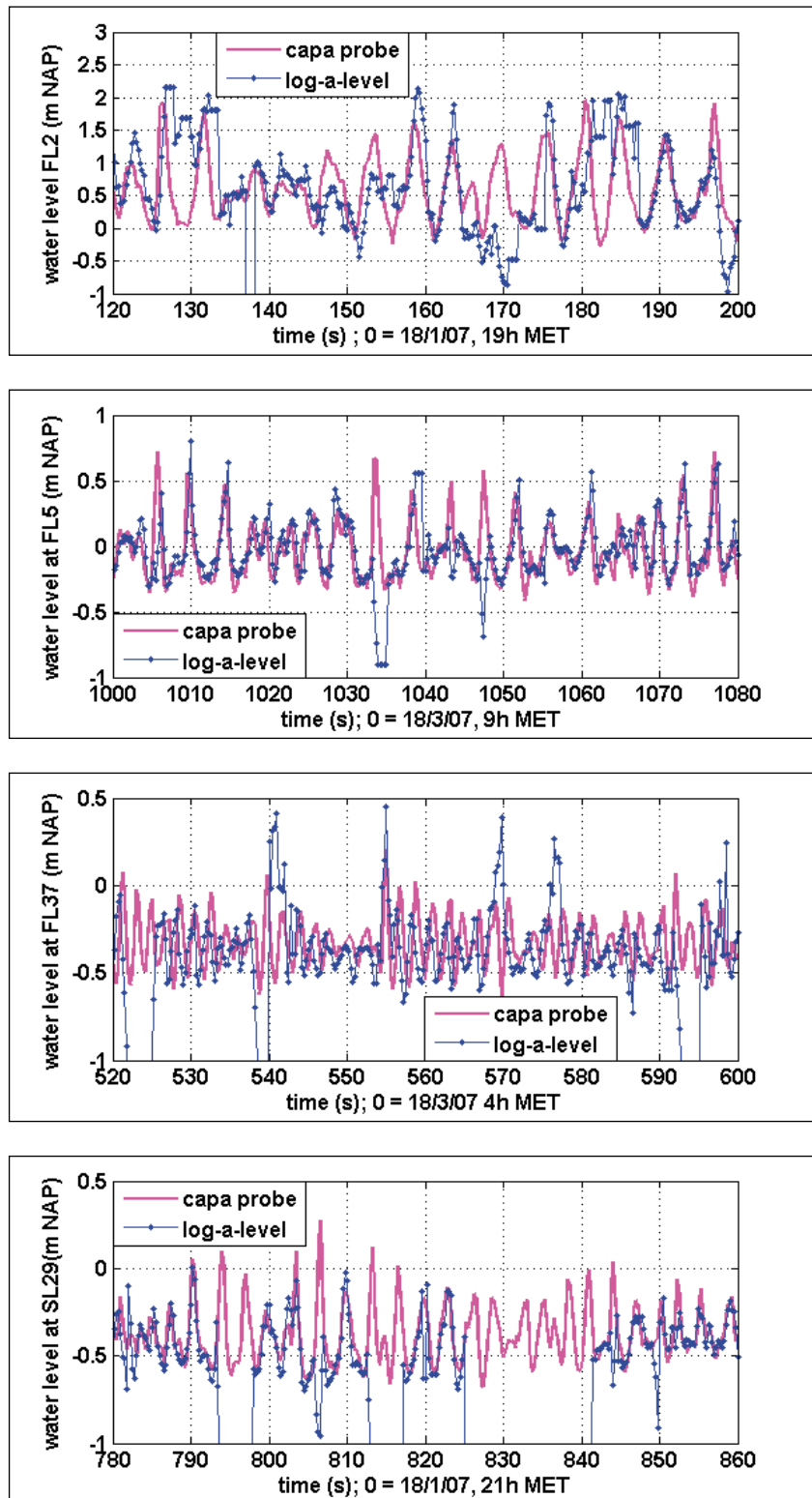
seem to be too low. This may well be due to the finite-footprint effect of section B.9. This is confirmed by the fact that the effect is much weaker in a simultaneous registration at SL29, where wave conditions were similar but where the log-a-level was much closer to the water surface.

Figure C.9 Comparison capa probe and log-a-level wave spectra. Top panel: Spectra during storm for FL2 ($H_{m0} \sim 1.7$ m) and SL29 ($H_{m0} \sim 0.6$ m). Spectrum during strong wind for FL5 ($H_{m0} \sim 1.0$ m) and during weak wind for FL37 ($H_{m0} \sim 0.1$ m).



Finally, some registrations of the instantaneous water level (as measured by both instrument) are shown in Figure B.10. From time to time, the agreement between both instruments is excellent, even on the level of individual waves. However, the log-a-level signal also has some sudden jumps, peaks and dips, as well as some staggers where the signal stays constant for some samples. By times, the latter was especially a nuisance at FL26 (not shown) where apparently, the log-a-level and data-logger settings had a far from optimal matching; it is important that both are definitely not ready-to-use in this respect. As for the outliers, one can note that these typically last a few samples. At SL29 however, the log-a-level outliers tend to cluster during several seconds. It is not clear whether this is related to the fact that the SL29-sensor is much closer to the water than for the Lake IJssel locations.

.....
Figure C.10 Instantaneous water level of capa probe and log-a-level during the storm of 18/1/07 (FL2 in top panel, SL29 in lowest panel) and the near-gale of 18/3/07 (FL5 and FL37, middle panels).



Finally, it is interesting to revisit the effect of wind on the log-a-level registrations. In section B.9, it was argued that signal outliers, as caused by wind deflection effects, will predominantly occur at the downwind wave slope. In a time registration, this slope passes before the wave crest. In Figure C.10 however, there is no clear preference for outliers in these downwind wave slopes. Rather, there is slight preference for dips in the wave signal to occur at the wave crests, while the opposite (peaks at wave troughs) sometimes occurs as well. This suggests that the wind effects as described in Section B.9 are either absent in the registrations, or more complex than anticipated. Still, it is important to bear in mind that the observed number of log-a-level outliers strongly increased from winds of order 12 m/s on.

All in all, the following can be concluded :

- in many mild and moderate wind cases, the agreement between log-a-level and capa probe is excellent ;
- above wave heights corresponding with 12 m/s winds, the log-a-level data contain so many outliers that many (and sometimes most) 20-minute data blocks must be rejected ;
- log-a-levels are not ready-to-use for inexperienced users as one requires often optimisation of the combined log-a-level and data logger settings.

Appendix D Applied offsets and corrections

In the following, an overview is given of the offsets and corrections that must be applied to the raw data for four key variables:

- wind direction and wind speed
- air and water temperatures
- water levels as derived from the SL29 pressure sensor
- raw wave signal of the step gauge, capa probe and log-a-level.

D.1 Offsets and corrections wind

Nearly all wind direction measurements need some kind of offset correction because in the field, it is difficult to point the wind vanes exactly to the North. Besides this, offset corrections also need to be applied to some wind speed data. Finally, exception values need to be assigned to some periods with unreliable wind data.

The simplest case is that of the wind speed corrections as it only involves two locations (FL2 and FL26) and a few – albeit long – periods. The corrections are needed because during these periods, a wrong zero-offset (+0.5 m/s or –0.5 m/s instead of –0.1 m/s) is applied in the data-logger software, see Bottema (2006ab).

The corrections to be applied are given in Table D.1:

Table D.1 Corrections that should be applied to the raw wind speed data.

location	period	required correction
FL2 (3m wind)	1/1/00 – 6/4/06	-0.6 m/s
FL2 (10 m wind)	23/4/02 – 8/8/02	+0.4 m/s
FL2 (10 m wind)	8/8/02 – 6/4/06	-0.6 m/s
FL26 (10 m wind)	1/1/02 – 16/3/05	-0.6 m/s

Table D.2 gives the cases for which exception values should be assigned: -999 for the wind direction and –99 for the wind speed. In the table, wind direction and wind speed are denoted as ‘dir.’ and ‘U₁₀’ respectively, except for 3-metre-wind at FL2, which is denoted as U₃. In some cases, unreliable wind directions may lead to biased (vectorial) averages of U₁₀, while the samples are still correct. For these cases, the U₁₀-indicator is placed between brackets.

Table D.2 Cases where (unreliable) wind data should be replaced by exception values.

loc.	period	variable	remarks
FL2	1/7/97 – 2/8/97	dir.	no documentation available
FL2	11/4/99 – 4/5/99	dir. + U ₁₀	wind speed sensor defect
FL2	18/11/99 – 11/1/00	dir, U ₃ , U ₁₀	instruments not installed
FL2	12/1/00 – 24/2/00	dir.	vane not available
FL2	9/3/00 – 27/6/00	dir. (U ₁₀)	vane unreliable
FL2	27/7/01 – 20/8/01	dir. + U ₁₀	fuse defect
FL2	5/12/01 – 21/1/02	U ₁₀	often ~2x too high, except 28/12/01
FL2	12/2/02 – 16/2/02	U ₁₀	often 2-3 x too high
FL2	5-12, 17, 20/7/02 27/7-12/8/02 29-25 + 29/8/02 2+3/9/02	U ₁₀	cable problem
FL2	20-26/8; 2+3/9/02	dir.	(fuse of?) wind vane defect
FL2	21/12/04-11/1/05	U ₃	U ₃ disconnected from battery
FL2	3/6/05 – 13/6/05	dir. (U ₁₀)	vane unreliable
FL2n	2/8/05 – 9/8/05	dir. + U ₁₀	sensors connected in wrong way
FL2n	31/8/05 – 8/9/05	dir. + U ₁₀	sensors dismantled
FL2n	1/9/06 – 27/9/06	U ₃	U ₁₀ data at U ₃ position ?
FL25	1/7/03 - 11/7/03	U ₁₀	zero dummies only
FL25	11/7/03 – 31/1/06	U ₁₀	files contain some zeros = dummy value; no vane available
FL26	22/7/98 – 19/11/98	dir. (+ U ₁₀)	U ₁₀ unrel. from 6/8/98 - 7/10/98
FL26	11/1/99	U ₁₀	unexpectedly high
FL26	1/5/99 – 9/6/99	dir.	unreliable data
FL26	1/7/99 – 24/8/99	dir. + U ₁₀	cable problem?
FL26	30/11/99 – 6/12/99	dir. + U ₁₀	fuse problem?
FL26	18/12/00 – 18/5/01	dir. + U ₁₀	U ₁₀ OK from 1-12/4/2001
FL26	19/5/01 – 30/6/01	U ₁₀	U ₁₀ often 2-3 x too high
FL26	16/9/01 – 27/9/01	U ₁₀	U ₁₀ often 2-3 x too high
FL26	23/10/01 – 21/1/02	U ₁₀	U ₁₀ often 2-3 x too high
FL26	24/10/02-30/10/02	dir.	fuse problem
FL26	3/9 + 16-28/9/03	dir.	unreliable data
FL26	20-25/11/03 & 5-10/12/03 & 3-14/1/04	dir.	unreliable data
FL26	29/1 – 17/2/04 & 4/4 - 14/4/04 & 24/6 – 29/6/04 & 8 + 9/7/04	dir. + U ₁₀	(near-) constant values
FL26	19/7/05 – 29/8/05	dir. + U ₁₀	fuse problem ?
FL26	17/3/06 – 11/4/06	dir. + U ₁₀	fuse problem ?
FL26	17/7/06 – 20/8/06	dir.	vane problem
FL26	21/8/06 – 25/9/06	dir.	spurious 239.1 if battery is low
FL26	1/11/06 – 29/11/06	dir.	cable problem ?
FL26	27/2/07	dir. + U ₁₀	problem data logger software?
FL37	9/6/06 – 23/8/06	U ₁₀	time stamp bias up to several hours
FL37	9/6/06 – 30/10/06	U ₁₀	many (~60%) staggers in samples
SL29	19/12/00 – 13/1/00	dir. + U ₁₀	fuse problem
SL29	25/1/01 – 3/4/01	dir. (U ₁₀)	vane damaged
SL29	8/8/01 – 22/8/01	dir. + U ₁₀	fuse problem
SL29	29/4/02 – 21/6/02	dir. (U ₁₀)	vane damaged
SL29	2/3/06 – 9/3/06	dir.	fuse problem?

The zero-offset correction for wind direction are given in Table D.3. In all cases, the assignment of exception values (Table D.2) should have priority over the assignment of ordinary offset corrections (Table D.3).

Table D.3 Corrections to be applied to raw wind direction data for FL2, FL26 and SL29, with start date of each correction period.

year	correction to be applied and start date, for locations..		
	FL2(n)	FL26	SL29
1997	+2° (3/8/97)	-	-
1998	+4° (1/7/98)	+12° (1/3/98)	-
	-11° (20/11/98)	-
1999	-3° (5/5/99)	+5° (10/6/99)	-
	+9° (25/8/99)	+3° (1/9/99)
2000	0° (25/2/00)	+5° (25/2/00)	+4° (12/1/00)
	+12° (28/6/00)	+10° (15/6/00)	+6° (1/7/00)
	+70° (17/8/00)
	+9° (28/9/00)	-2° (17/10/00)
	-5° (18/12/00)	-8° (13/12/00)
2001	-27° (1/3/01)	+7° (4/4/01)
	-12° (19/3/01)	-7° (19/5/01)	+11° (1/7/01)
	-5° (21/8/01)	+24° (23/8/01)
	+5° (25/9/01)
2002	+2° (22/1/02)	+2° (10/1/02)
	0° (8/8/02)	0° (8/8/02)	+6° (22/6/02)
2003	+4° (1/7/03)	-4° (1/1/03)	-3° (1/1/03)
	-25° (24/8/03)
	+3° (9/10/03)	+13° (22/10/03)
2004	+4° (1/7/04)	+15° (17/4/03)
2005	-4° (15/2/05)	+22° (4/3/05)
	0° (14/6/05)
	+22° (20/6/05)
	-4° (10/8/05)
	-11° (9/9/05)	0° (6/9/05)	-7° (20/10/05)
2006	-34° (10/5/06)	+4° (12/4/06)	-5° (10/3/06)
	0° (1/6/06)
	-19° (1/9/06)	-39° (30/11/06)	-7° (3/11/06)
	+5° (10/11/06)	+4° (13/12/06)

Before leaving the issue of wind, a number of points should be noted:

- FL25 and FL37 are not included in table D.3 because no wind vanes have been installed at these locations;
- Required corrections for SL29 are generally small and do not change very often.
- Required corrections above 20° often indicate periods in which the data logger software contains erroneous offsets;
- Until 2002, required corrections of about +10° are quite common because the reference vane of one of the maintenance ships had a similar error in its zero offset.

D.2 Temperature data to be labelled as unreliable

The main modification that (can and) should be applied to the raw air and water temperatures is the assignment of exception values to unreliable data. These unreliable data occur in the following cases:

- air temperature FL2
 - all data before 23/3/2005
 - 22/12/2005 – 5/1/2006
 - 1/9/2006 – 5/10/2006
- water temperature FL2
 - all data before 9/8/2002
 - 26/8/2002 – 23/9/2002
 - 21/12/2004 – 11/1/2005
 - 2/8/2005 – 10/8/2005
 - 1/9/2006 – 27/9/2006
 - 19/1/2007 – 8/2/2007
- air temperature FL26
 - all data before 22/10/2003
 - 5/2/2004 – 17/2/2004
 - 21/8/2006 – 12/9/2006
- water temperature FL26
 - all data before june 2001
 - 4/3/2005 – 9/3/2005
 - 16/3/2005 – 30/3/2005
 - 15/7/2006 – 9/8/2006
 - 30/1/2007 – 8/2/2007

Only part of the above cases is related to real instrument problems; other causes of unreliable data are programming errors in the data logger software and periods in which instruments were temporarily disconnected.

Besides this, one might occasionally find data logger exception values (± 6999 or ± 7999) amongst the water temperature data. A small fraction of the air temperature data also consists of *random* outliers.

These outliers are most likely to occur in the following cases:

- FL2, April 2003 – April 2004 (malfunctioning data logger)
- FL2, 10/8/2005 – 30/8/2005
- FL26, 19/5/2006 – 14/6/2006

D.3 Offsets and corrections water level pressure sensor

The Lake Sloten location SL29 is equipped with a pressure sensor which provides reference values for the still water level. Ideally, this sensor is calibrated in such a way that the data logger directly outputs the still water level with respect to the NAP datum. However, there remain still some cases where corrections need to be applied to the

pressure sensor output. These cases, and their corrections, are:

- until 23/5/2000: unreliable data, assign exception value
- 23/5/00 – 16/8/00: apply correction of -1.35 m
- 17/8/00 – 19/12/00: apply correction of -1.50 m
- 15/9/02 – 28/11/02: apply correction of +0.08 m? (drift)
- 12/8/03 – 11/11/03: unreliable (20-25 cm too high)
- ~3/7/04 – 3/9/04: unreliable (~10 too low, sensor pulled up)
- Oct-Dec 2006: unreliable (either constant at -47 cm NAP or 10-20 cm too high)

Besides this, the pressure sensor tends to become unreliable during frosty conditions. In some cases with stormy conditions, the pressure sensor may also become less reliable. The pressure sensor water levels then may become about 5-10 cm lower than the capa probe and log-a-level values, while all three are normally virtually the same during calm conditions.

D.4 Offsets and corrections of wave signal

For each location, the last 10 years can be split up in several sub-periods, each with a unique zero offset and – sometimes – calibration factor correction to be applied to the raw wave signal. In the following, these offsets and corrections will be considered for the log-a-level, step gauge and capa probe measurements respectively.

The raw log-a-level signal Z_{LAL} is given in metres, water levels Z_{NAP} in metres with respect to NAP can be calculated as $Z_{NAP} = Z_{LAL} + \text{offset}_{LAL}$. The offsets are given in Table D.4.

Table D.4 Preliminary offset corrections (m), to be applied to raw log-a-level signal.

location	start date	offset to be applied (m)
FL2n	1/9/2006	2.77
FL2n	16/1/2007	2.64
FL5	21/8/2006	2.50
FL9	21/8/2006	2.57
FL26	21/8/2006	2.14
FL26	6/11/2006	2.72
FL37	9/6/2006	2.60
FL37	21/9/2006	2.70
SL29	8/9/2006	1.23
SL29	1/1/2007	1.18

The reliability of log-a-level data is discussed in section B.9 and C.3. The following additional remarks can be made:

- at FL2n, no log-a-level was present from 10/11/06 – 16/1/07
- the log-a-level data of FL2n are less reliable from 18/1/07 to 24/1/07 as the sensor was hit loose in the evening of the 18th.
- at SL29, no log-a-level was present from 22/11/06 – 16/1/07

Like for the log-a-levels, the step gauge measurements of early years (until 2001) typically only need zero-offset corrections. There is one exception to this:

- until 6/8/1998, the FL26 step gauge sensors 32-39 were skipped, so that a correction of –8 had to be applied to each sensor number in the range of 40-60.

In the remaining cases, where only offset corrections are needed, Z_{NAP} is calculated as $Z_{NAP} = 0.05 * (STEP_{no} - 1) - offset_{STEP}$, where $STEP_{no}$ is the raw data output (step gauge sensor number) and $offset_{STEP}$ the offset to be applied. The offsets to be applied are listed in Table D.5.

Table D.5 Zero offset corrections (m), to be applied to raw step gauge signal, with start date of each sub-period in brackets.

year	offsets to be applied and start date, for locations ...			
	FL2	FL5	FL9	FL26
1997	1.71 (1/7)	1.69 (1/7)	1.75 (1/7)	-
	1.39 (17/7)	-
1998	...	1.38 (20/6)	1.69 (6/5)	1.64 (1/3)
	...	1.69 (27/7)	1.39 (19/6)	...
	...	1.20 (1/11)
1999	1.76 (1/7)	1.22 (28/6)	1.44 (1/7)	1.68 (1/7)
	until Dec'99
2000	-	1.13 (1/7)	1.36 (1/7)	1.60 (1/7)
	-	until Feb'01	until Feb'01	until Feb'01

Note that some offset changes take place at 1/7 because data of neighbouring seasons were either not available or – for early reports – not considered.

The capa probe offsets are given in Table D.6. Unless mentioned otherwise, the NAP water levels Z_{NAP} are calculated as $Z_{NAP} = 0.01 * Z_{capa} - offset_{capa}$, where Z_{capa} is the raw capa probe output (in cm). The table also specifies 11 special cases:

- sc02a (FL2): $Z_{NAP} = (z_2 - 140) / 100$; $z_2 = 0.103 * z_1 + 0.134$; $z_1 = (Z_{capa} - 6.79) / 0.204$
- sc02b (FL2): $Z_{NAP} = (z_1 - 244) / 100$; $z_1 = 0.844 * Z_{capa} + 67.0$;
- sc02c (FL2): $Z_{NAP} = (z_1 - 246) / 100$; $z_1 = Z_{capa} / 1.22 + 20$;
- sc02d (FL2): offset is 2.85 m instead of 2.35 m for 2-17/8/2005, 31/8 and 1/9/2005;
- sc05a (FL5): $Z_{NAP} = (8.7 * Z_{capa} - 160) / 100$;
- sc05b (FL5): $Z_{NAP} = (4.88 * Z_{capa} - 139) / 100$;
- sc05c (FL5): $Z_{NAP} = (Z_{capa} - 550) / 300$;
- sc25a (FL25): $Z_{NAP} = (z_2 - 151) / 100$; $z_2 = 0.586 * z_1 - 80.6$; $z_1 = 100 * Z_{capa} + 365$;
- sc25b (FL25): $Z_{NAP} = (z_2 - 130) / 100$; $z_2 = 0.566 * z_1 - 83.6$; $z_1 = 100 * Z_{capa} + 353$;
- sc25c (FL25): $Z_{NAP} = (Z_{capa} - 211) / 100$, but this does not include the overall signal correction of a factor 1.2-1.5 that is probably required;
- sc25d (FL25): $Z_{NAP} = (z_1 - 144) / 100$; $z_1 = 4 * Z_{capa}$;

In most cases, there is either a problem with the instrument electronics (amplifiers), or with the data logger software. Only the sc02d-case describes a number of real modifications in instrument position.

Table D.6 Zero offset corrections (m), to be applied to raw capa probe signal, with start date of each sub-period; special cases are indicated as 'sc'.

year	offsets to be applied and start date, for locations ...					
	FL2/FL2n	FL5	FL9	FL25/37	FL26	SL29
1997	-	-	-	1.00; 1/7	-	-
	-	-	-	sc25a; 28/9	-	-
1998	-	-	-	sc25b; 13/10	-	-
1999	-	-	-	1.41; 18/3	-	-
	1.41; 20/12	-	-	1.44; 1/7	-	1.90; 1/1
2000	sc02a; 6/4	-	-	sc25c; 6/4	-	...
	...	-	-	1.44; 7/5	-	...
	2.55; 18/12	-	-	sc25d; 10/7	-	...
2001	3.13; 1/3	1.29; 1/3	1.75; 1/3	1.50; 1/3	1.58; 1/3	1.41; 4/4
	2.95; 31/5	1.32; 29/11	1.51; 23/8	...
	3.04; 1/9	1.56; 29/11	1.58; 28/9	...
2002	1.57; 24/4	1.47; 9/8	...	1.71; 1/2
	1.65; 17/8	1.70; 9/8	1.96; 21/6
	2.44; 2/9	1.54; 24/9	1.58; 3/9	...
2003	2.99; 1/3	1.43; 1/3	1.31; 1/3	1.56; 1/3	1.53; 1/3	...
	2.44; 26/3
	sc02b; 26/8	...	1.32; 1/7	1.61; 8/9
	2.46; 9/10	1.62; 23/10	...
2004	sc02c; 28/1	sc05a; 3/1	1.82; 27/2	...
	2.46; 15/2	sc05b; 6/2
	...	1.32; 31/3
	...	sc05c; 29/12
2005	...	1.32; 7/1	1.13; 19/1	1.65; 4/3	1.63; 17/1	1.75; 18/3
	sc02d; 2/8	1.52; 4/3	1.17; 10/3	1.66; 1/7	1.82; 9/3	...
	2.35; 2/9	1.40; 20/8	1.21; 10/4	...	1.83; 1/7	...
	2.42; 24/10	1.64; 23/11	1.22; 1/7	...	2.01; 29/8	...
	1.83; 3/10	...
2006	2.75; 17/3	...	1.62; 21/3	...	1.49; 17/3	...
	2.30; 11/5	1.20; 12/5	1.23; 12/5	1.85; 28/8
	2.50; 11/11	1.39; 5/10	...	1.58; 21/9	1.07; 13/12	...
2007	2.66; 1/1	1.61; 22/1	1.20; 16/1	1.91; 1/1
	2.52; 13/2

Finally, it is useful to specify the main periods with unreliable data. Some of the main periods with unreliable wave data are given in Table D.7. It is important to note that Table D.7 only includes problem cases that can be assigned to specific periods. Measuring errors due to soiling (in summer) and due to preferential capa probe values can typically occur at any time and for any length. Hence, it is nearly impossible to summarise the latter type of problem cases in a table. On the other hand, Appendix B.6 provides some useful detection criteria for errors due to soiling and preferential values.

.....

Table D.7 List of the main periods with serious wave signal errors, other than the errors due to soiling and preferential values discussed in Appendix B.5-B.6.

location	period	type of error
FL2	25/2-4/4/00	near-total failure of electronic unit
FL2	6-23/3/01	capa probe voltage outside data logger range
FL2	23/4/03-29/3/04	some disturbances during data transfer
FL2	28/1-15/2/04	wave calibration factor correction uncertain
FL2n	16/1-1/2/06	some effects of ice accretion and ice fields
FL2n	17/3-6/4/06	capa probe voltage (partly) outside logger range
FL2n	20/4-17/5/06	signal disturbance by electric power unit
FL2n	3/4/07-...	offset capa probe strongly unreliable /variable
FL5	1/3-24/7/98	FL5 and FL9 data mixed up
FL5	5/1-30/3/04	malfunctioning amplifiers; corrections uncertain
FL5	21/12/04-6/1/05	frequent modifications data logger software
FL5	4/3/-23/3/05	ice damage
FL5	4/7-19/8/05	malfunctioning capa probe
FL5	16/1-1/2/06	some effects of ice accretion and ice fields
FL9	1/3-24/7/98	FL5 and FL9 data mixed up
FL9	15-19/11/98	malfunctioning step gauge
FL9	29/1-11/3/02	(+28/12/01) freq. wave overtopping over probe
FL9	1-9/3/05	ice damage
FL9	16/1-1/2/06	some effects of ice accretion and ice fields
FL25	1/7/97-17/3/99	capa probe used without accurate calibration
FL25	12/3/00-15/1/01	various disturbances, e.g. at 0.18 Hz most of time also data logger software errors
FL25	4-9/3/05	capa probe removed to prevent ice damage
FL25	16/1-1/2/06	some effects of ice accretion and ice fields
FL26	1/3/98-22/7/98	8 (out of 60) malfunctioning step gauge sensors
FL26	19-30/11/98	malfunctioning step gauge
FL26	4-9/3/05	capa probe removed to prevent ice damage
FL26	16/1-1/2/06	some effects of ice accretion and ice fields
FL26	1/11-13/12/06	failure of capa probe electronics unit
SL29	20/3-13/5/00 & 31/5-13/6/00	electronic disturbances on wave signal
SL29	22/12/00-3/4/01	ice damage
SL29	15/1-1/2/02	ice damage
SL29	2/2-20/6/02	provisional probe repair; reliability somewhat less
SL29	28/2-19/3/05	ice damage
SL29	27/12/05-22/1/06	until probe removal: ice fields / ice accretion

Finally, it is noted that Table D.7 only lists the main periods with wave signal errors. For a complete overview of all details, one still needs the previously published yearly reports of the Lake IJssel measurements.

Appendix E Cornerstones of spatial wind modelling

For Rijkswaterstaat users, no textbook is yet available with all ins and outs of spatial wind modelling. In many cases, either (Wieringa and Rijkoort, 1983) or (Wieringa, 1986) is used. However, these works are 20 years old, not sufficiently complete to compensate for all knowledge gaps about wind, and their term 'potential wind speed' is confusing because it is actually based on partial exposure corrections (for near field only). In the following, some cornerstones, certainties and uncertainties will be highlighted. Although common wind transformation techniques will be mentioned, the present approach is rather theoretical; for the role of wind modelling for dike design, the reader is referred to (Waal, 2003).

Uniform terrain - general

Uniform terrain is nearly the only situation in which analytical modelling is an option, so that theories and conceptual models can be developed. This implies that models for uniform terrain have the best theoretical framework. However, a disadvantage is that uniform terrain requires uniform fetches of at least 20-50 km, a situation that does not exist in the Netherlands.

Uniform terrain – logarithmic wind profile

Theoretical framework: (very) good

Empirical support: (very) good

Application range: fair

The logarithmic wind profile (Tennekes, 1973) can be considered as the cornerstone of the atmospheric boundary layer (ABL), a layer of order 0.2-2 km thick which is directly influenced by the earth's surface. Besides stationarity for order two hours, three assumptions are crucial in its derivation :

1. the vertical wind speed gradient is proportional to a wind speed scale divided by a length scale
2. the wind speed scale has a 1:1 coupling to the ABL-generated turbulence.
3. the log-profile is valid for an asymptotic limit where $L \ll z \ll z_{ABL}$ where L is the scale of the surface obstacles (trees, waves, ...), z the measuring height and z_{ABL} the ABL-depth

Note 2: Sometimes, turbulence is not only generated in the ABL but throughout the lowest 10 km of the atmosphere, especially during storms, heavy showers or foehn episodes.

Note 3: The result of these assumptions is that turbulent fluxes in the logarithmic height range are near-constant. Often, the latter result is presented as starting assumption, but this may lead to the wrong wind profile formulas (Tennekes, 1973).

The logarithmic wind profile can be written as:

$$(E.1) \quad U(z) = \frac{u^*}{\kappa} \ln\left(\frac{z-z_d}{z_0}\right) \quad \text{of:} \quad \frac{U(z_1)}{U(z_2)} = \frac{\ln((z_1-z_d)/z_0)}{\ln((z_2-z_d)/z_0)}$$

with : $U(z)$ the wind speed at height z
 u^* the so-called friction velocity
 κ the Von Kármán-constant (~ 0.4)
 z_0 the aerodynamic roughness length
 z_d a zero-plane displacement

The application range of (E.1) is only fair because of its underlying assumptions and because of the interpretation of its parameters.

The application range is:

- $z < 0.25 * z_{ABL}$ (no problem for present data)
- $z > 20 * z_0 + z_d$ See Wieringa and Rijkoort (1983)
- $z > 2-3$ times the significant wave height (over water)
- stationary conditions (for more than one hour)
- uniform terrain; in practice: fetch must be at least 20 times the largest measuring height.
- thermally neutral atmosphere

For the latter, no ready-to-use criterion is available. Over land, wind over 11 m/s tends to suffice for neutral conditions (Bottema, 1993); over water the required wind is probably stronger because of the larger heat fluxes. The assumption of negligible thermal stability effects for winds over 6 m/s, as published in (Wieringa and Rijkoort, 1983) and several other text books, is for the present purposes *certainly* incorrect.

Caution is also required in the interpretation of (E.1):

- z_0 and d are aerodynamic length scales and no hard surface properties. This implies that z_0 and d may depend on wind, temperature stratification, etc.
- u^* is a wind speed scale that is related to a turbulent shear stress $\tau = \rho u^{*2}$ (ρ being the air density) near the earth's surface. The interpretation of τ has some pitfalls and should preferably be done by experts.
- u^* , z_0 and z_d *only* have a physical meaning if all requirements for the validity of the logarithmic wind profile are satisfied.

Uniform terrain – logarithmic wind profile

Theoretical framework: good

Empirical support: reasonable

Application range: fair

In practice, the temperature stratification of the ABL over water surfaces, and to a lesser extent over land, is rarely neutral. The turbulence and the vertical profiles of average properties (wind, temperature, etc.) then are determined by three variables:

- measuring height z
- boundary-layer height z_{ABL}
- the so-called Monin-Obukhov length $L = -\theta_v u^{*3} / (g\kappa w'\theta_v')$, where g is the gravity acceleration, θ_v is de virtual potential temperature in Kelvin (temperature corrected for air pressure and water vapour content); $w'\theta_v'$ is a measure for the turbulent heat flux. With these variables, three scaling regimes can be defined, where each regime has its own formulas and validity range (see Holtslag, 1987). For the present work, it suffices to extend the logarithmic wind profile with a stability correction Ψ :

$$(E.2) \quad U(z) = \frac{u^*}{\kappa} \left[\ln\left(\frac{z-z_d}{z_0}\right) - \Psi\left(\frac{z}{L}\right) \right]$$

The application range of (E.2) is similar to that of (E.1) except for the requirement of a neutral ABL. However, caution is needed in very stable ABL's (with warm air flowing over a cold surface) as the ABL then is very shallow.

Several expressions for $\Psi(z/L)$ are mentioned in the literature, which suggests that the Ψ -expressions are relatively uncertain. Special care is needed in situations with large stability corrections, for example with large air-water temperature differences and/or weak winds. In such cases, the ABL-height often plays a role as well, which is unfortunate because it is not measured in the present campaign.

Another complication is that the calculation of $\Psi(z/L)$ over open water requires extremely accurate profile measurements; experimental errors of 1% may well be too large for this case. Direct flux measurements are a good alternative to evaluate $\Psi(z/L)$, but they require special equipment like sonic anemometers.

Also, wind profiles over open water are significantly modified by stability effects. In unstable situations over open water, the wind is nearly constant with height, but its drag on the water surface is quite strong. The opposite is true in stably stratified atmospheres.

Uniform terrain – coupling wind within and above the ABL

Theoretical framework: reasonable

Empirical support: fair

Application range: fair / poor

The mathematical derivation of the log-profile (Tennekes, 1973) also yield so-called resistance laws. The latter describe the relation between u^* and U_M , where U_M is the so-called macro wind above the ABL, i.e. at a height which is no longer directly influenced by the earth's surface, but only by various mesoscale and large scale weather systems. Resistance laws allow to link the wind within the ABL to the wind above the ABL. The formulas are somewhat more complex than the previous ones, and are given in most textbooks on boundary-layer meteorology.

Both the application range and empirical support of resistance laws are rather disappointing. the main reasons for this are:

- Rather ambiguous theoretical framework
 - The real ABL-height (height of thermal inversion, if present) and theoretical scale heights are often mixed up, as is done with the real macro wind and the so-called geostrophic wind (wind as calculated from frictionless balance between pressure gradient and earth's rotation).
- Limited application range
 - One can hardly satisfy all requirements at a time:
 - uniform terrain for at least 20-50 km
 - horizontally uniform pressure gradient
 - preferably no thermal stability effects
 - no horizontal temperature gradients on any vertical level
- Little empirical support
 - Because the above requirements can be hardly satisfied in practice, any estimate of the resistance law constants is rather inaccurate, errors of order 10% are easily made.

Wind formulas for uniform terrain – parameter uncertainties

Besides the resistance law constants mentioned above, there are three parameters that play a key role in wind modelling

- the friction velocity u^*
- the roughness length z_0 (assuming that z_d is known)
- the Obukhov length L

It is no easy job to obtain u^* , z_0 and L from a fit of experimental data to (E.2), because mathematically such a fit is often ill-posed (different parameters have too much of a similar effect). Special fitting techniques with pre-estimates of u^* , z_0 and L are often needed, especially over open water where vertical wind speed gradients are small. However, pre-estimates of turbulent fluxes often require special equipment, like sonic anemometers. Despite these problems (see for example Wieringa, 1993; Bottema et al., 1998), roughness lengths over often are often successfully measured, with an accuracy in z_0 of a factor 2 or better. Over sea, it is far from easy to get good roughness estimates. For ideal conditions (thermally neutral atmosphere, well developed waves, deep water without swell) the formulas of Charnock (1955) and Wu (1982) both are a good option:

$$(E.3) \quad z_0 = 0.0185 u^{*2} / g ; C_D = 0.8 + 0.065 * U_{10}^2$$

where the drag coefficient C_D is defined as $(u^*/U_{10})^2$.

For shallow water and/or young waves (which are slow with respect to the wind), there are indications that the roughness may be significantly larger than indicated by (E.3); for steep waves this may also be the

case because of their larger drag. On Lake IJssel and Lake Sloten, these effects can not be excluded. Besides this, there are indications that in extreme (near-hurricane) winds the roughness of the water surface increases at a reduced rate with wind speed; it might even decrease with increasing wind (Makin, 2003); possibly due to foam.

Non-uniform terrain - general

In practice, one can rarely speak of uniform terrain. For non-uniform terrain, an overall theoretical framework is lacking, and this lack of interpretative framework probably is one of the reasons that few empirical data are available.

Spatial wind modelling with resistance laws (wind fully adapted)

Theoretical framework: reasonable

Empirical support: fair

Application range: fair / poor

The above discussed resistance laws can also be used to link the ABL-winds for two different locations. Ideally, the implicit formulas of the original resistance laws are used. However, inaccuracies in the resistance laws (and their parameters) justify a simplified approximate approach (Simiu and Scanlan, 1986) :

$$(C4.a) \quad \text{area 1: } U(z_1) = \frac{u^*_{1}}{\kappa} \ln \left(\frac{z-z_{d1}}{z_1} \right)$$

$$(C4b) \quad \text{area 2: } U(z_2) = \frac{u^*_{2}}{\kappa} \ln \left(\frac{z-z_2}{z_{02}} \right)$$

$$(E.4c) \quad \frac{u^*_{1}}{u^*_{2}} = \left(\frac{z_{01}}{z_{02}} \right)^{0.0706}$$

Note that the use of (E.4a-E.4c) is only justified if the macro wind at both locations is equal, which generally implies that the formulas should not be used for areas larger than 50-100 km. In addition, all (restrictive) conditions for the use of resistance laws also apply to above formulas.

The empirical support of (E.4a-E.4c) is fair at best by lack of other data than of Simiu and Scanlan (1986). Still, the above equations are important because they describe the situation of full wind adaption to a new terrain type.

Non-uniform terrain – internal boundary-layer models

Theoretical framework: reasonable

Empirical support: fair / poor

Application range: fair / poor

Internal boundary-layer models describe the gradual adaptation of the flow to a new type of terrain. As a conceptual model, this approach is quite suitable; the practical applicability is rather disappointing. A

very large amount of different models has been published, but the model approach and the model constants differ from author to author. Besides this, there are two more aspects in which models differ :

- case-specific formulas (certainly no rarity, and often not indicated as such) versus formulas that are more universally applicable
- formulas for a change-in-roughness versus formulas for a change-in-surface-temperature or even moisture

Danish researchers (e.g., Jensen et al, 1984) mainly concentrated on roughness jumps in thermally neutral conditions; Australians (Garratt) mainly focussed on thermal internal boundary layers. Combinations of both approaches have rarely been considered.

By lack of measurements, little is known about internal boundary layer effects in the upper reaches of the ABL. Kudryavtsev et al (2000) have a complete internal boundary-layer model, but their model is very complex. Jensen et al (1984) proposed a much simpler model which is consistent with (a simplified version of) the Kudryavtsev model. Also, the Jensen model appears to agree quite well with measurements of the eighties as reported by Wood, Arya and Simiu and Scanlan. Jensen's model assumes that a roughness jump creates a disturbed sub-boundary-layer within the ABL. The slope of the disturbed interface is proportional to $\sigma_w/U(z)$ where σ_w is a measure for the vertical turbulent fluctuations, and $U(z)$ the time-averaged wind speed at height z . The slope of the interface then follows from $dh_{IBL}/dx \sim A / (\ln(z/z_0^+))$ with A a constant of order 0.5; this relation is used by various investigators. After some more approximations, Jensen et al. (1984) propose the following explicit formula for the height of the internal boundary layer, h_{IBL} :

$$(E.5) \quad \frac{h_{IBL}}{x} = 0.3 \left[\frac{x}{z_0^+} \right]^{0.8}$$

where x is the fetch over the new surface and z_0^+ the larger of the two roughness lengths (as the roughest terrain determines the level of turbulence near the interface). For the present applications, the slope of the internal boundary layer (h_{IBL}/x) is typically of the order of 20. The wind profile formulas to be used are those of (E.1) and (E.2), where the upstream roughness length is to be used for $z > h_{IBL}$, and the downstream roughness for $z < h_{IBL}$. This is a rather coarse approximation, which is mainly justified by the lack of more detailed data.

The following can be said about the applicability of this approach:

- Internal boundary-layer models, if necessary supplemented with resistance laws, turned out to be suitable tools to convert wind climates of one location to another (Troen et al, 1989).
- Simple models as (E.5) are quite suitable for first guesses of the wind field for short distances offshore, but their range of applicability is limited to the first kilometres offshore.

-
- Advanced models like (Kudryavtsev et al., 2000) are complex and may crash with multiple roughness changes (pers comm. J. Verkaik 2003, KNMI). Moreover, they are still unsuitable for modelling the three-dimensional roughness changes that are generally occur in practice. Finally, the use of complex models requires a lot of additional input (heat and moisture fluxes) that is not always available.

Non-uniform terrain – Two-layer model ; downscaling

Theoretical framework: fair

Empirical support: fair

Application range: fair / reasonable

A two-layer approach (e.g., Wieringa en Rijkoort, 1983; Verkaik et al., 2003) has some parallels with the previous two approaches. In the lower layer, once again a log-profile with a local roughness length is used. In the upper layer, a resistance law with a regional roughness length is used. The theoretical support for this approach is not perfect: although it is correct to distinguish local and regional effects, the separation between the two soon becomes rather arbitrary. In addition, it is far from trivial to evaluate regionally averaged roughnesses and fluxes (e.g., Bottema et al, 1998). For the Dutch situation, one should also realise that the Dutch landscape is strongly non-uniform, and that the gustiness-derived local roughnesses of KNMI have a far from straightforward interpretation. By contrast, many formulas for large-scale landscape roughness at least yield reproducible results, with formulas that allow for reasonable interpretations of the results. In practice, the two-layer approach seems to be quite suitable, even though the number of cases with errors over 10% (and sometimes even 20%) is far from negligible (Taminiau, 2004; Schaik, 2004). Despite these errors, the applicability of the method is quite good. This is because the method is quite flexible and easy to use; moreover no special assumptions about fetch and terrain uniformity need to be made.

Finally, some remarks must be made about the wind modelling approach that up to now has often been used by RWS RIZA (Bak en Vlag, 1999). The approach essentially assumed that the so-called potential wind speed is spatially uniform, or that it can be derived from linear interpolation. Note that the potential wind is a fictitious wind speed in which the actual local roughness for the log-profile section of 10-60 m height is replaced by a similar section with the roughness for an ideal meteorological site, which is $z_0 = 0.03$ m. In fact this potential wind speed only provides partial exposure corrections because the large-scale roughness (related to the wind profile above 60 m height) also yields significant shelter effects for rough landscapes. No surprise then that the yearly averaged potential wind speed over the Netherlands shows several small-scale variations (see the maps of Wieringa, 1986). It is also important to notice that the potential wind speed and so-called meso wind at 60 m only differ by a constant factor

(1.31; Wieringa and Rijkoort, 1983). Hence, the above assumption essentially prescribes a constant wind speed at 60 m height, whereas it only should be constant at the top of the ABL where all surface influences have disappeared. Note that this top is typically between 0.2 and 2 km height.

In mathematical terms, the above assumption corresponds to an internal boundary-layer model with a fixed internal boundary-layer height h_{IBL} of 60 m. By (E.5), it can be shown that $h_{IBL} \sim 60$ m corresponds to a fetch of 1 km or slightly larger. Since the framework for internal boundary-layer models is much more sturdy than the present assumption of spatially uniform U_{pot} , it must be concluded that the latter is only valid for fetches of (up to) about 1 km.

Non-uniform terrain – numerical models

Theoretical framework: fair / reasonable

Empirical support: fair

Application range: fair / reasonable

It seems to be a small step to move from a complex internal boundary-layer model (like Kudryavtsev et al., 2000) to a full numerical model. Both are complex, and both require an amount of input that is not necessarily available.

Because of the required input, weather forecasting models such as X-HIRLAM (the KNMI High-Resolution Limited Area Model) seems most suitable. However, its model assumptions do not seem suited for wind modelling over uniform terrain. This is not only because of the small vertical model resolution, but also because of the turbulence parametrisations (typically for uniform terrain) and the fact that the model is hydrostatic (so that pressure fields around roughness jumps are neglected).

Even for models with advanced turbulence assumptions, it turns out to be difficult or even impossible to find universally valid turbulence parametrisations (Bottema, 1996). In addition, there are hardly any well-documented full-scale data that allow for thorough model calibration and validation.

Large-Eddy-Simulation (LES) may be an option because of recently increased computer power. The strong point of LES is its explicit modelling of large turbulent structures; for small-scale turbulence, parametrisations (with the above-mentioned universality problems) are still needed. This may become a problem in situations where nearly all turbulence is small scale: close to the surface and in stably stratified boundary layers.

Appendix F Beaufort scale

At various locations in this report, wind speed indications are given in terms of Beaufort-scale classes. The relation between Beaufort scale and wind speed is given in Table F.1; the wind speeds are taken from (Wieringa and Rijkoort, 1983), the class names from (McIlveen, 1992). It should be noted that the Beaufort scale speed refer to wind speeds which are measured at 10 m height over land, and averaged over at least 10 minutes (Wieringa and Rijkoort, 1983); the scale should not be used to describe gusts. In this report, the Beaufort scale will also be used for open water because open-water alternatives for the Beaufort scale are not yet universally agreed upon. Moreover, the general public typically is not familiar with such alternative classes.

Table F.1 Wind speed range for each of the Beaufort scale classes.

Beaufort class number	Beaufort class name	range of mean wind speed U_{10} (m/s)
0	Calm	0 – 0.2
1	Light air	0.3 – 1.5
2	Light breeze	1.6 – 3.3
3	Gentle breeze	3.4 – 5.4
4	Moderate breeze	5.5 – 7.9
5	Fresh breeze	8.0 – 10.7
6	Strong breeze	10.8 – 13.8
7	Near gale	13.9 – 17.1
8	Gale	17.2 – 20.7
9	Strong gale	20.8 – 24.4
10	Storm	24.5 – 28.4
11	Violent storm	28.5 – 32.6
12	Hurricane	32.7 or more

Appendix G Wind and wave climate tables for information requests

From time to time, Rijkswaterstaat IJsselmeergebied (RWS IJG) receives information requests from third parties, relating to the wind and wave conditions over Lake IJssel, for example wind climate, wave climate, or wave parameters for given wind conditions.

For many requests, various parts of the main body of this report can be used:

- wind climate data can be obtained from section 4.2 (Figure 4.1-4.2, together with Eq. (4.1) and Table 4.1)
- water temperature data can be obtained from section 4.6 (Figure 4.18)
- water level and storm surge data can be obtained from section 5.1-5.2 (Figure 5.1-5.3; Table 5.1)
- wave climate data can be obtained from section 6.1 (Figure 6.1, as well as Table 6.1 with Eq. (4.1))
- wave data for given wind conditions can be obtained from section 6.2 and 6.3 (Figure 6.2-6.8)

Besides this mainly graphical information, RWS IJG finds it convenient to provide tabular output to third parties. To this end, some tables are made in which some key results of this report are summarised:

- the approximate wind climate at the FL2 location
- wave conditions at a number of Lake IJssel locations, for *given wind conditions at FL2*.

All wave conditions to be represented are representative for cases with still water levels in the range of –60 cm NAP to +20 cm NAP. The results are given for a limited number of wind speeds as interpolation as fairly straightforward (near-linear). No tables are provided for FL2n, FL5 and SL29 for a variety of reasons: FL2n is too similar to FL2; FL5 is representative of only a very small area and had too many location changes; SL29 is not located in the interest area of RWS IJG.

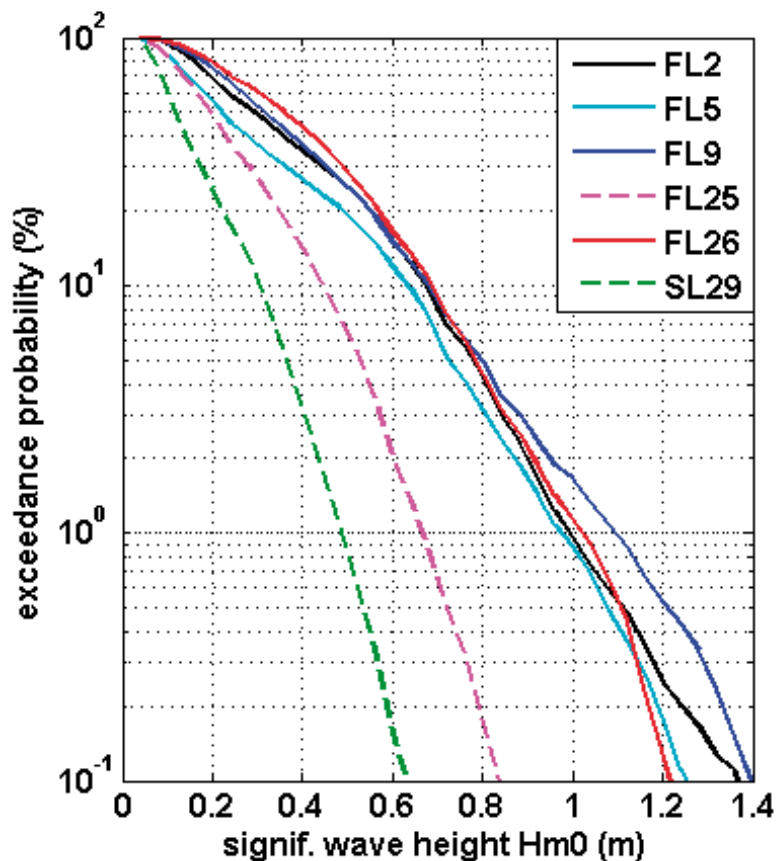
In practice, the first step in wave climate evaluation is often the definition of the *wind* climate at a reference location. In Table G.1 the approximate wind climate of the FL2 location is given.

Table G.1 Approximate percentage of time that a given combined class of wind speed and wind direction occurs at FL2.

wind dir. (deg N)	wind speed (m/s)									
	0-2	2-4	4-6	6-8	8-10	10-12	12-14	14-16	16-18	18-20
0-30	0.33	1.06	1.50	1.04	0.60	0.16	0.02	0.00	0.00	-
30-60	0.37	1.30	1.90	1.24	0.49	0.10	0.01	-	-	-
60-90	0.51	1.96	2.37	1.18	0.36	0.05	0.01	-	-	-
90-120	0.60	2.25	2.54	1.57	0.72	0.24	0.04	0.00	-	-
120-150	0.43	2.09	2.08	1.12	0.42	0.10	0.00	-	-	-
150-180	0.38	1.11	1.52	1.52	0.84	0.31	0.07	0.02	0.00	-
180-210	0.35	1.15	1.94	2.69	2.38	1.64	0.72	0.22	0.03	0.02
210-240	0.42	1.27	2.77	3.42	3.38	2.44	1.11	0.42	0.14	0.04
240-270	0.46	1.25	2.48	2.66	2.51	1.51	0.76	0.31	0.13	0.03
270-300	0.47	1.27	2.01	2.21	1.66	0.92	0.48	0.20	0.06	0.02
300-330	0.50	1.40	1.99	1.90	1.40	0.96	0.45	0.22	0.02	0.01
330-360	0.46	1.30	1.72	1.57	0.99	0.40	0.14	0.02	0.01	-

The easiest way to obtain an estimate of the climate of the significant wave height H_{m0} at a given location is to make use of Figure 6.1, which is reproduced below:

Figure G.1: Reproduction of Figure 6.1: Approximate 4-year (2001-2005) climatology for the wave height H_{m0} (all locations, Nov.-April only).



On can also rather easily describe the H_{m0} -climate in terms of a Weibull distribution, for convenience its formula (Eq. (4.1)) is repeated here:

$$(G.1) \quad P(U_{10} > U) = \exp\left(-\left(\frac{U}{a}\right)^k\right)$$

The Weibull fit can be used for the 0.5-90% probability interval; the Weibull parameters are given in Table G.2 (a copy of Table 6.1):

.....
Table G.2: Copy of Table 6.1:
 Parameters characterising the
 climatology of wave height H_{m0} ,
 as shown in Figure 6.1 / Figure
 G.1.

	FL2	FL5	FL9	FL25	FL26	SL29
long term mean of H_{m0} (m)	0.35	0.30	0.37	0.23	0.39	0.15
standard deviation H_{m0} (m)	0.22	0.22	0.22	0.15	0.21	0.10
Weibull scale parameter a (m)	0.38	0.32	0.41	0.25	0.44	0.16
Weibull shape parameter k	1.57	1.31	1.64	1.55	1.87	1.42

Once (the frequency distribution of) H_{m0} is known, one can also obtain an estimate of the wave period measure T_{m-10} , by making use of the fact that the deep water steepness $s_{T_{m-10},0}$ is close to 0.05 for most cases (see section 6.4). This wave steepness measure is related to H_{m0} by:

$$(G.2) \quad s_{T_{m-10},0} = \frac{2\pi H_{m0}}{gT_{m-10}^2}$$

The peak period T_p and the mean period T_{m-10} can generally be estimated from T_{m-10} by using the relations (see section 6.3):

- $T_p/T_{m-10} \sim 1.2$
- $T_{m01}/T_{m-10} \sim 0.9$

However, these ratios are not valid in a number of special cases related to offshore winds, shore-parallel winds and breaking waves (section 6.3).

In many cases, information requests are related to the expected wave conditions for *given wind*. For this type of request, some key results for FL2, FL9, FL25, FL26 and FL37 are summarised in Table G.3-G.7. It is noted once again that generally, linear interpolation between the table values is a reasonable first approximation.

Table G.3: Wave height H_{m0} and wave period measures T_p , T_{m-10} and T_{m01} at FL2, for given wind conditions at FL2.

wind dir.	wind speed (m/s)											
	6	6	6	6	12	12	12	12	18	18	18	18
	H_{m0} (m)	T_p (s)	T_{m-10} (s)	T_{m01} (s)	H_{m0} (m)	T_p (s)	T_{m-10} (s)	T_{m01} (s)	H_{m0} (m)	T_p (s)	T_{m-10} (s)	T_{m01} (s)
15°	0.28	2.19	2.13	1.91	0.58	3.02	2.84	2.55	-	-	-	-
45°	0.25	2.30	2.15	1.93	-	-	-	-	-	-	-	-
75°	0.19	2.16	2.01	1.76	0.41	2.71	2.35	2.15	-	-	-	-
105°	0.15	1.66	1.85	1.52	0.37	1.97	2.25	1.94	-	-	-	-
135°	0.18	2.10	2.06	1.75	0.43	2.81	2.47	2.22	-	-	-	-
165°	0.27	2.47	2.29	2.02	0.52	3.28	2.90	2.56	-	-	-	-
195°	0.33	2.54	2.36	2.10	0.65	3.43	3.00	2.70	1.07	4.36	3.73	3.32
225°	0.35	2.52	2.36	2.12	0.73	3.50	3.14	2.82	1.10	4.25	3.85	3.40
255°	0.36	2.59	2.39	2.13	0.73	3.59	3.13	2.80	1.26	4.66	4.05	3.59
285°	0.35	2.65	2.43	2.14	0.74	3.57	3.09	2.78	1.22	4.80	4.06	3.58
315°	0.35	2.63	2.40	2.14	0.69	3.43	3.02	2.72	-	-	-	-
345°	0.33	2.40	2.31	2.07	0.70	3.21	2.96	2.68	-	-	-	-

Table G.4: Wave height H_{m0} and wave period measures T_p , T_{m-10} and T_{m01} at FL9, for given wind conditions at FL2.

wind dir.	wind speed (m/s)											
	6	6	6	6	12	12	12	12	18	18	18	18
	H_{m0} (m)	T_p (s)	T_{m-10} (s)	T_{m01} (s)	H_{m0} (m)	T_p (s)	T_{m-10} (s)	T_{m01} (s)	H_{m0} (m)	T_p (s)	T_{m-10} (s)	T_{m01} (s)
15°	0.19	1.72	1.90	1.64	0.451	2.38	2.28	2.13	-	-	-	-
45°	0.23	1.93	1.99	1.73	-	-	-	-	-	-	-	-
75°	0.30	2.31	2.16	1.94	-	-	-	-	-	-	-	-
105°	0.33	2.29	2.23	2.01	0.61	3.00	2.89	2.53	-	-	-	-
135°	0.35	2.51	2.27	2.05	0.83	3.31	3.04	2.79	-	-	-	-
165°	0.36	2.64	2.36	2.13	0.69	3.44	2.97	2.67	-	-	-	-
195°	0.38	2.63	2.39	2.16	0.75	3.51	3.06	2.76	-	-	-	-
225°	0.33	2.48	2.30	2.07	0.79	3.53	3.10	2.80	1.41	4.69	4.18	3.64
255°	0.33	2.50	2.26	2.04	0.69	3.47	2.92	2.62	1.24	4.55	3.94	3.47
285°	0.30	2.41	2.20	1.98	0.65	3.31	2.86	2.58	1.06	4.58	3.76	3.28
315°	0.26	2.23	2.14	1.90	0.56	2.93	2.71	2.45	0.95	3.51	3.32	2.94
345°	0.23	1.97	2.03	1.79	0.54	2.71	2.55	2.34	-	-	-	-

Table G.5: Wave height H_{m0} and wave period measures T_p , T_{m-10} and T_{m01} at FL25, for given wind conditions at FL2.

wind dir.	wind speed (m/s)											
	6	6	6	6	12	12	12	12	18	18	18	18
	H_{m0} (m)	T_p (s)	T_{m-10} (s)	T_{m01} (s)	H_{m0} (m)	T_p (s)	T_{m-10} (s)	T_{m01} (s)	H_{m0} (m)	T_p (s)	T_{m-10} (s)	T_{m01} (s)
15°	0.30	2.69	2.36	2.01	0.66	3.74	3.25	2.72	-	-	-	-
45°	0.42	2.89	2.60	2.23	-	-	-	-	-	-	-	-
75°	0.43	2.95	2.59	2.26	0.79	3.84	3.32	2.92	-	-	-	-
105°	0.36	2.73	2.44	2.10	0.58	3.65	3.40	2.71	-	-	-	-
135°	0.27	2.53	2.28	1.91	-	-	-	-	-	-	-	-
165°	0.20	2.10	2.04	1.66	0.41	2.80	2.50	2.10	-	-	-	-
195°	0.13	1.85	1.89	1.43	0.27	2.20	2.06	1.71	-	-	-	-
225°	0.07	1.54	1.99	1.22	0.17	1.42	1.77	1.36	0.30	1.73	1.85	1.57
255°	0.07	1.80	2.10	1.28	0.19	1.46	1.76	1.38	0.33	1.77	1.95	1.60
285°	0.11	2.18	2.05	1.49	0.26	1.96	2.00	1.61	0.43	1.85	2.20	1.81
315°	0.18	2.67	2.23	1.78	0.34	3.64	2.79	2.16	-	-	-	-
345°	0.28	3.07	2.50	2.05	0.53	3.99	3.08	2.50	-	-	-	-

Table G.6: Wave height H_{m0} and wave period measures T_p , T_{m-10} and T_{m01} at FL26, for given wind conditions at FL2.

wind dir.	wind speed (m/s)											
	6	6	6	6	12	12	12	12	18	18	18	18
	H_{m0} (m)	T_p (s)	T_{m-10} (s)	T_{m01} (s)	H_{m0} (m)	T_p (s)	T_{m-10} (s)	T_{m01} (s)	H_{m0} (m)	T_p (s)	T_{m-10} (s)	T_{m01} (s)
15°	0.39	2.64	2.38	2.19	0.93	3.62	3.32	3.05	-	-	-	-
45°	0.48	2.81	2.53	2.33	-	-	-	-	-	-	-	-
75°	0.48	2.82	2.52	2.33	-	-	-	-	-	-	-	-
105°	0.40	2.66	2.43	2.22	0.80	3.54	3.17	2.90	-	-	-	-
135°	0.35	2.58	2.34	2.12	0.84	3.67	3.29	2.96	-	-	-	-
165°	0.31	2.39	2.18	1.97	0.69	3.20	2.87	2.61	-	-	-	-
195°	0.28	2.08	2.02	1.84	0.68	2.84	2.67	2.46	-	-	-	-
225°	0.22	1.81	1.87	1.69	0.53	2.62	2.44	2.25	0.97	3.32	3.06	2.83
255°	0.23	2.06	1.96	1.77	0.59	2.68	2.60	2.38	1.00	3.30	3.15	2.90
285°	0.27	2.53	2.20	2.00	0.68	3.65	3.09	2.80	1.09	4.40	3.68	3.29
315°	0.34	2.76	2.40	2.19	0.77	3.86	3.32	3.01	1.17	4.66	3.95	3.54
345°	0.47	3.03	2.66	2.42	0.87	3.99	3.54	3.11	-	-	-	-

.....
Table G.7: Wave height H_{m0} and wave period measures T_p , T_{m-10} and T_{m01} at FL37, for given wind conditions at FL2.

wind dir.	wind speed (m/s)											
	6	6	6	6	12	12	12	12	18	18	18	18
	H_{m0} (m)	T_p (s)	T_{m-10} (s)	T_{m01} (s)	H_{m0} (m)	T_p (s)	T_{m-10} (s)	T_{m01} (s)	H_{m0} (m)	T_p (s)	T_{m-10} (s)	T_{m01} (s)
15°	-	-	-	-	-	-	-	-	-	-	-	-
45°	-	-	-	-	-	-	-	-	-	-	-	-
75°	0.35	2.47	2.25	1.99	-	-	-	-	-	-	-	-
105°	0.31	2.39	2.14	1.88	-	-	-	-	-	-	-	-
135°	0.21	2.16	1.99	1.70	-	-	-	-	-	-	-	-
165°	0.17	1.95	1.85	1.54	0.37	2.17	2.03	1.80	-	-	-	-
195°	0.14	1.78	1.72	1.42	0.32	2.01	1.90	1.69	-	-	-	-
225°	0.11	1.28	1.71	1.23	0.29	1.71	1.78	1.58	-	-	-	-
255°	0.13	2.03	1.87	1.44	0.32	2.04	1.98	1.71	-	-	-	-
285°	0.18	2.36	1.98	1.66	0.42	2.60	2.43	2.07	-	-	-	-
315°	0.24	2.59	2.21	1.88	0.51	3.50	2.75	2.35	0.88	4.65	3.62	2.96
345°	0.37	3.09	2.49	2.16	-	-	-	-	-	-	-	-

As the implementing body of the Ministry of Transport, Public Works and Water Management, the Directorate-General for Public Works and Water Management ensures the smooth flow of traffic and water on the national networks, and works on keeping our feet dry and providing us with sufficient supplies of clean water. www.rijkswaterstaat.nl

